

**A COMBINED DIRECTED METALATION
CROSS-COUPPLING ROUTE TO A NEW SMECTIC
LIQUID CRYSTAL WITH A PHENANTHRENE CORE**

by

Wei Gan

A thesis submitted to the Department of Chemistry
in conformity with the requirements for
the degree of Doctor of Philosophy

Queen's University
Kingston, Ontario, Canada
August, 2009

copyright © Wei Gan, 2009

ABSTRACT

A series of phenanthrene and oxidized phenanthrene derivatives with typical substitution patterns, **1.31**, **1.32**, **2.30a-f**, **3.1a,b** and **(-)-4.1** have been synthesized as liquid crystal cores by a combined Directed *ortho* Metalation (DoM), cross coupling and Directed Remote Metalation (DreM) strategy. The synthetic methodology employed allowed variation of the tail and core structures, for the preparation of a new smectic liquid crystal compound (**1.32**), a homologous series of 9,10-dihydrophenanthrene-9,10-diones (**2.30a-f**), a diastereomeric *trans*-9,10-dihydrophenanthrene-9,10-diol (**1.31**), two enantiomeric 9,10-dihydrophenanthrene-9,10-diones (*R*)-**3.1a-b**) and an enantiomeric 9,10-dihydro-9,10-dimethylphenanthrene-9,10-diol ((-)-**4.1**).

Polarized microscopic and differential scanning calorimetric measurements suggest that **1.31** forms a large range of SmC phase, *ca.* 100 °C, followed by a small range of nematic phase, *ca.* 10 °C; the **2.30a-f** series show similar mesogenic properties, but with the extension of the length of a side chain from six carbons to eleven carbons, the nematic phase has disappeared (in the cases of **2.30a-c**).

Although (*R*)-**3.1a-b** and **(-)-4.1** are not liquid crystals, they show ferroelectric induction by doping, in the amount of *ca.* 5 mol%, into unchiral liquid crystal hosts **PhB**, **DFT**, **PhP1**, **NCB76** and **2.30f**. However, due to the detection limit of the instrument, i.e., *ca.* 0.5 nC/cm², the spontaneous polarizations (P_s) induced could not be measured.

ACKNOWLEDGEMENTS

I would like to thank my supervisors Victor Snieckus and Bob Lemieux for their guidance, enthusiasm and patience during the course of this work.

I am grateful to all members of the Snieckus groups, Lemieux groups, past and present, for helpful advice and for making my time here enjoyable. Special thanks go to Dr. Ruiyao Wang, Dr. Jianxin Wang, Dr. Toni Ratanen, Dr. Timothy Hurst, Sunny Lai, Yigang Zhou and Qian Cui.

I would like to thank my parents and sister for helping me to get to this far. Most of all I thank my wife Grace and my son Kevin for their support and understanding. I could not have done it without you.

For Grace Xia

STATEMENT OF CO-AUTHORSHIP AND ORIGINALITY

The work presented in this thesis was conducted by the author under the supervision of Professor V. Snieckus and Professor R. P. Lemieux in the Department of Chemistry at Queen's University. X-Ray experiments were performed by Dr. Ruiyao Wang in the Department of Chemistry at Queen's University.

The following is a list of new compounds prepared using new methodology in the course of this work: **2.5, 2.10b, 2.10c, 2.10e, 2.11a, 2.11b, 2.12a, 2.12b, 2.15, 2.16, 2.17, 2.18, 2.19, 2.20, 2.21, 2.22, 2.23, 2.24, 1.32, 2.28, 2.29, 2.30a-f, 1.31, 2.32, 2.33, 2.31, 3.7, 3.8, 3.9, 3.10, 3.11, 3.12, 3.13, 3.14, 3.16, 3.17, 3.1a, 3.18, 3.20, 3.22, 3.23, 3.24, 3.25, 3.26, 3.27, 3.28, 3.29, 3.1b, (-)-4.1.**

The following is a list of known compounds prepared using new methodology or existing methods in the course of this work: **2.2, 2.3, 2.6, 3.3, 3.4, 3.6.**

TABLE OF CONTENTS

ABSTRACT	ii
ACKNOWLEDGEMENTS	iii
STATEMENT OF CO-AUTHORSHIP AND ORIGINALITY	v
TABLE OF CONTENTS	vi
LIST OF TABLES	ix
LIST OF FIGURES	x
ABBREVIATIONS	xii
LIST OF EXPERIMENTAL PROCEDURES	xvi
CHAPTER 1 – INTRODUCTION	1
1.1 Liquid Crystals	1
1.1.1 Liquid Crystal Phases and Their Properties	1
1.1.2 Odd-Even Effect	7
1.1.3 The Chiral Smectic C phase (SmC*)	9
1.1.4 Hydrogen Bonding in Mesogens	19
1.1.4.1 Hydrogen Bonding in Non-amphiphilic Mesogens	20
1.1.4.2 Hydrogen Bonding in Amphiphilic Mesogens	26
1.1.5 Liquid Crystals Containing Phenanthrene Core Structures	30
1.1.6 Mesogen Design Considerations	33
1.2 Synthetic Methodology	36
1.2.1 The Directed <i>ortho</i> Metalation (DoM) Reaction	36
1.2.2 The Mechanism of the DoM Reaction	39
1.2.3 Other Bases Mediated DoM	46

1.2.4 Directed C-H Activation	51
1.2.5 The Combined DoM-Cross Coupling Reaction	53
1.2.6 The Directed remote Metalation (DreM) Reaction	55
1.3 The Synthesis of Phenanthrenes	59
1.3.1 Intermolecular Routes to Phenanthrenes	60
1.3.1.1 Diels-Alder Approach	60
1.3.1.2 Pd-Catalyzed Cyclization Approach	63
1.3.2 Intramolecular Cyclization Approaches to Phenanthrenes	65
1.3.2.1 Ring Expansion Reactions	65
1.3.2.2 Intramolecular Electrophilic Cyclization	66
1.3.2.3 Intramolecular Radical Cyclization	69
1.3.2.4 Intramolecular Photocyclization (Mallory Reaction)	71
1.3.2.5 Intramolecular Ring-Closing Olefin Metathesis (RCM)	74
1.3.2.6 Directed Remote Metalation (DreM) Approaches	74
1.4 Outline of Synthesis	76
CHAPTER 2 – PHENANTHRENE AND 9,10-DIHYDROPHENANTHRENE-9,10-DIOL LIQUID CRYSTALS	78
2.1 Synthesis of 7-(Octyloxy)phenanthren-2-yl 4-(undecyloxy)benzoate 1.32	78
2.2 Synthesis of 9,10-Dihydroxy-7-(octyloxy)-9,10-dihydrophenanthren-2-yl 4-(undecyloxy)benzoate 1.31	85
2.3 Mesophase Characterization of Phenanthrene Liquid Crystal 1.32	88
2.4 Synthesis of the Stable 9,10-Dihydroxy-9,10-dimethyl-7-(octyloxy)-9,10-dihydrophenanthren-2-yl 4-(undecyloxy)benzoate 2.31	91

2.5 Summary	93
CHAPTER 3 – PHENANTHRENE DIONE AND CHIRAL	
PHENANTHRENE DIONE LIQUID CRYSTALS	94
3.1 Synthesis of Phenanthrene dione Liquid Crystals 2.30a-f in a Modified Route	95
3.2 Mesophase Characterization	100
3.3 Synthesis of Chiral Phenanthrene-9,10-diones 3.1a-b	106
3.4 Summary	109
CHAPTER 4 – CHIRAL PHENANTHRENE DIONE 3.1a,b AND CHIRAL	
PHENANTHRENE-9,10-DIOL (-)-4.1 AS DOPANTS	110
4.1 Polarization Measurements	113
4.2 Summary	115
4.3 Conclusions	116
CHAPTER 5 – EXPERIMENTAL	118
5.1 General Methods	118
5.2 Materials	119
5.3 Specific Experimental Procedures	120

REFERENCES	171
APPENDICES	183
Appendix 1. Single Crystal X-ray Data for 1.31	183
Appendix 2. Resolution Analysis Data for 2.36	222
Appendix 3 The Texture of Compounds 3.30a-e in Polarized Microscopy	223

List of Tables

Table 1.1	Typical DMGs.	38
Table 1.2	The pKa of selected bases used in <i>D_oM</i>	47
Table 1.3	The half-lives of butyllithium reagents in typical solvents	48
Table 2.1	The phase transition temperatures of 1.32 on cooling by polarized microscopy	89
Table 2.2	The enthalpy changes of 1.32 at the transition temperature	90
Table 3.1	The phase transition temperatures of 2.30a-f during cooling in polarized microscopy	102
Table 3.2	The phase transition temperatures and enthalpy changes of 2.30a-f by DSC	105

List of Figures

Figure 1.1	Structures of some calamitic, discotic, and polycatenar mesogens	2
Figure 1.2	Schematic representation of three LC phases	4
Figure 1.3	Schlieren texture of the nematic phase observed by polarized microscopy	4
Figure 1.4	Photomicrographs of the typical textures of (a) SmA and (b) SmC phases	5
Figure 1.5	Schematic representation of the McMillan model for the origin of the tilt	6
Figure 1.6	Schematic representation of the Wulff model for the origin of the tilt	6
Figure 1.7	Representation of the Durand model showing the core is more tilted	7
Figure 1.8	Graph of transition temperature vs the number of carbon atoms in the chain	8
Figure 1.9	Schematic odd-even effect	9
Figure 1.10	Schematic representation of the helical SmC* phase and a SSFLC	10
Figure 1.11	Schematic representation of an electro-optical SSFLC switch	11
Figure 1.12	Meyer's symmetry argument for a SmC* phase	12
Figure 1.13	The binding site according to the Boulder model	13
Figure 1.14.	Conformational analysis of the (<i>S</i>)-2-octyloxy side chain and the resulting sign of Ps	15
Figure 1.15.	Schematic conformations for 1.1 and 1.2 and the sign of Ps for a (<i>S</i>)-2-octyloxy side chain <i>ortho</i> to (a) a nitro group and (b) to a pyridine nitrogen	16
Figure 1.16	The four AM1-minimized conformations by rotation of the atropisomeric biphenyl core about the two ester C-O bonds	18
Figure 1.17.	Liquid crystal host structures and phase transition temperatures in °C	19
Figure 1.18.	Model for chirality transfer <i>via</i> core-core interactions	19
Figure 1.19.	Two modes of hydrogen bonding in liquid crystals: (a) head-to-head; (b) side-to-side	20
Figure 1.20	The mesogenic dimer formed by hydrogen bonding	20
Figure 1.21	The suggested lamellar structure: (a) folded; (b) extended	23

Figure 1.22.	The carbohydrates forming only a SmA mesophase	27
Figure 1.23	The lamellar structures for two models: I and II	28
Figure 1.24.	The dithioacetal aldoses and the representation of the hexagonal columnar mesophase	29
Figure 1.25	Phenanthrene core liquid crystal compounds and the representation of a tilted chiral column	32
Figure 1.26	Molecular models (MM2) of 1.30 in relation to the mean-field potential according to the Boulder model. From left to right the fluorene core is rotated 180° with respect to the two side chains	34
Figure 2.1	Photomicrographs of 1.32 (a) in the nematic phase at 208 °C; (b) in the SmC phase at 183 °C; (c) in the crystalline at 94 °C.	88
Figure 2.2	DSC measurement of 1.32	90
Figure 3.1	Photomicrographs of 2.30f (a) in the N phase at 197 °C; (b) in the SmC phase at 185 °C	101
Figure 3.2	DSC measurement of 2.30 : (a) for 2.30a ; (b) for 2.30b ; (c) for 2.30c ; (d) for 2.30d ; (e) for 2.30e ; (f) for 2.30f	104

Abbreviations

δ	polarization power
δ	chemical shift
η	rotational viscosity
θ	tilt angle
δ_p	polarization power
τ_r	ferroelectric switching time
Ac	acetyl
aq	aqueous
Ar	aryl
Bu	butyl
calcd	calculated
CIPE	complex induced proximity effect
Col	columnar phase
Cr	crystalline
d	layer spacing
d	doublet
DCC	1,3-dicyclohexylcarbodiimide
DIAD	diisopropyl azodicarboxylate
DIPA	<i>N,N</i> -diisopropylamine
DMAP	4-(<i>N,N</i> -dimethylamino)pyridine
DMAD	dimethyl acetylenedicarboxylate
DME	1,2-dimethoxyethane

DMF	<i>N,N</i>-dimethylformamide
DMG	directed metalation group
DoM	directed <i>ortho</i> metalation
DreM	directed remote metalation
DSC	differential scanning calorimetry
E	electric field
E⁺	electrophile
EDG	electron donating group
equiv	equivalent
Et	ethyl
EWG	electron withdrawing group
EVL	α-ethoxyvinyl lithium
FLC	ferroelectric liquid crystal
FT	Fourier transform
g	gram(s)
GC	gas chromatograph
h	hour(s)
HMPA	hexamethylphosphoramide
HRMS	high resolution mass spectrum
Hz	Hertz
I	isotropic liquid
<i>i</i>-Pr	isopropyl
IR	infrared

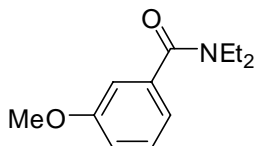
KEM	kinetically enhanced metalation
KIE	kinetic isotope effect
l	molecular lenth
L	ligand
LC	liquid crystal
LCD	liquid crystal display
LDA	lithium diisopropylamide
LG	leaving group
LRMS	low resolution mass spectrometry
LTMP	lithium 2,2,6,6-tetramethylpiperidin-1-ide
LUMO	lowest unoccupied molecular orbital
m	multiplet
M	molar
Me	methyl
min	minute(s)
mmol	millimole(s)
MOM	methoxymethyl
mp	melting point
MS	mass spectrum
mw	microwaves
N	nematic phase
n	director
NMR	nuclear magnetic resonance

NR	no reaction
P₀	reduced polarization
PCC	pyridinium chlorochromate
PG	protecting group
Ph	phenyl
PMDTA	<i>N,N,N',N'',N'''</i>-pentamethyldiethylenetriamine
PPA	polyphosphoric acid
P_S	spontaneous polarization
recov	recovered
rt	room temperature
s	singlet
satd	saturated
SmA	smectic A phase
SmC	smectic C phase
SmC*	chiral smectic C phase
SmX	unidentified smectic phase
SSFLC	surface stabilized ferroelectric liquid crystal
t	triplet
TBAF	tetrabutylammonium fluoride
TBDMS	<i>t</i>-butyldimethylsilyl
TBS	<i>t</i>-butyldimethylsilyl
T_C	critical temperature
Tf	trifluomethanesulfonyl

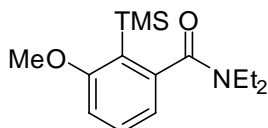
TFAA	trifluoroacetic anhydride
THF	tetrahydrofuran
TIPS	triisopropylsilyl
TMEDA	<i>N,N,N',N'</i>-tetramethylethylenediamine
TMP	2,2,6,6-tetramethylpiperidine
TMS	trimethylsilyl
x_d	mole fraction
z	layer normal

List of Experimental Procedures

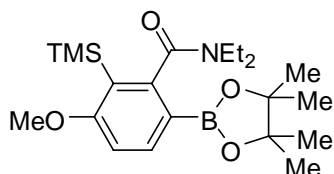
***N,N*-diethyl-3-methoxybenzamide (2.2).** 120



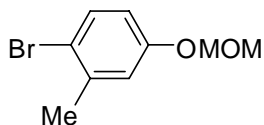
***N,N*-Diethyl-3-methoxy-2-trimethylsilylbenzamide (2.3).** 120



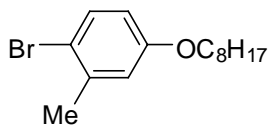
***N,N*-Diethyl-3-methoxy-6-(4,4,5,5-tetramethyl-1,3,2-dioxaborolan-2-yl)-2-(trimethylsilyl)benzamide (2.5)** 121



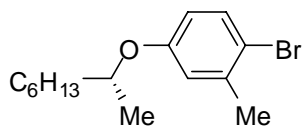
1-Bromo-4-(methoxymethoxy)-2-methylbenzene (2.10b) 122



1-Bromo-2-methyl-4-(octyloxy)benzene (2.10c) 123

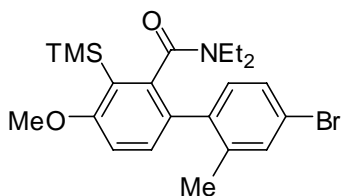


(*R*)-1-Bromo-2-methyl-4-(octan-2-yloxy)benzene (2.10e) 123



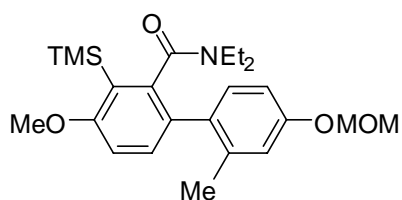
4'-Bromo-*N,N*-diethyl-4-methoxy-2'-methyl-3-(trimethylsilyl)biphenyl-2-carboxamide (2.11a).

124



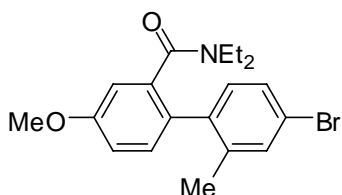
***N,N*-Diethyl-4-methoxy-4'-(methoxymethoxy)-2'-methyl-3-(trimethylsilyl)biphenyl-2-carboxamide (2.11b)**

125



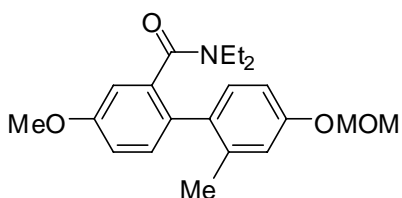
4'-Bromo-*N,N*-diethyl-4-methoxy-2'-methylbiphenyl-2-carboxamide (2.12a)

126



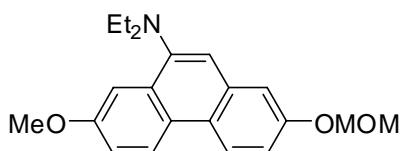
***N,N*-diethyl-4-methoxy-4'-(methoxymethoxy)-2'-methylbiphenyl-2-carboxamide (2.12b)**

127



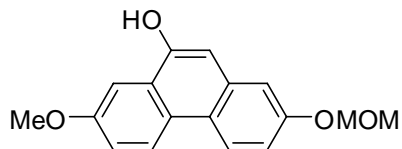
***N,N*-Diethyl-7-methoxy-2-(methoxymethoxy)phenanthren-9-amine (2.15)**

127



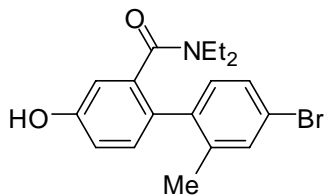
7-Methoxy-2-(methoxymethoxy)phenanthrene-9-ol (2.16)

128



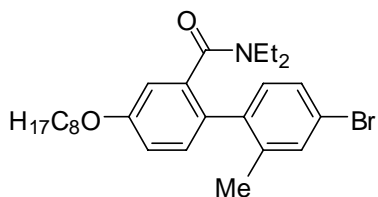
4'-Bromo-*N,N*-diethyl-4-hydroxy-2'-methylbiphenyl-2-carboxamide (2.17)

129



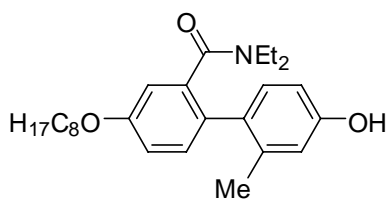
4'-Bromo-*N,N*-diethyl-2'-methyl-4-(octyloxy)biphenyl-2-carboxamide (2.18)

130



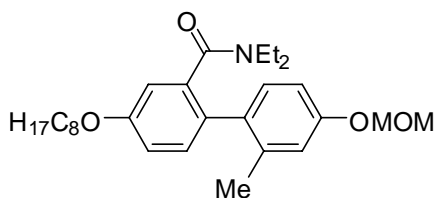
***N,N*-Diethyl-4'-(hydroxy)-2'-methyl-4-(octyloxy)biphenyl-2-carboxamide (2.19)**

130

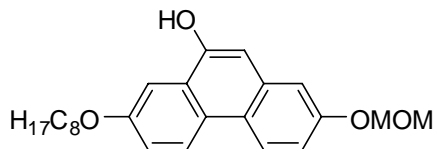


***N,N*-Diethyl-4'-(methoxymethoxy)-2'-methyl-4-(octyloxy)biphenyl-2-carboxamide (2.20)**

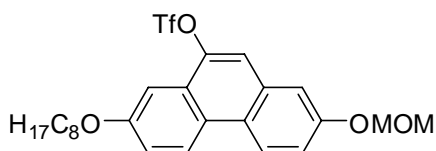
131



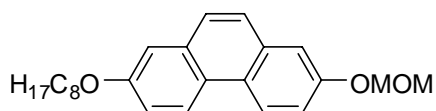
2-(Methoxymethoxy)-7-(octyloxy)phenanthren-9-ol (2.21) **132**



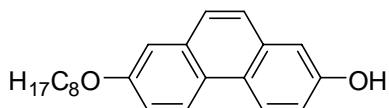
2-(Methoxymethoxy)-7-(octyloxy)phenanthren-9-yl trifluoromethanesulfonate (2.22). **133**



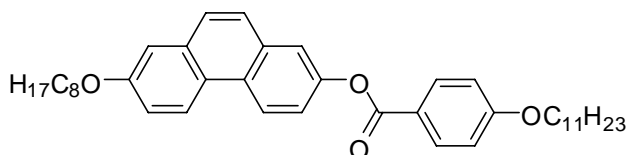
2-(Methoxymethoxy)-7-(octyloxy)phenanthrene (2.23) **134**



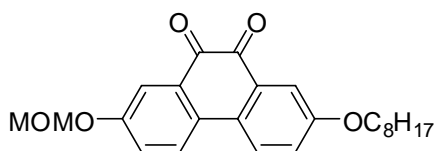
7-(Octyloxy)phenanthren-2-ol (2.24) **135**



7-(Octyloxy)phenanthren-2-yl 4-(undecyloxy)benzoate (1.32) **135**

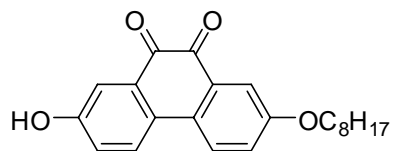


2-(Methoxymethoxy)-7-(octyloxy)phenanthrene-9,10-dione (2.28) **136**



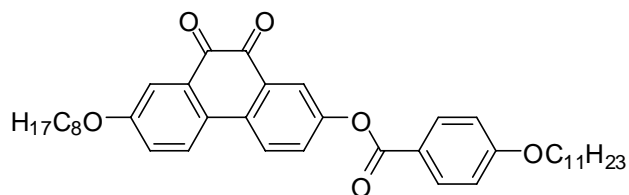
2-Hydroxy-7-(octyloxy)phenanthrene-9,10-dione (2.29)

137



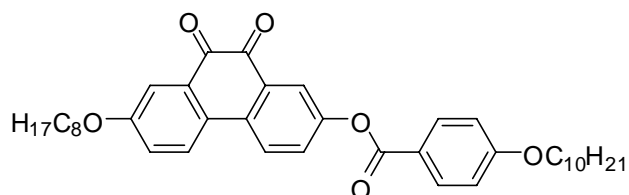
7-(Octyloxy)-9,10-dioxo-9,10-dihydrophenanthren-2-yl 4-(undecyloxy)benzoate (2.30a)

138



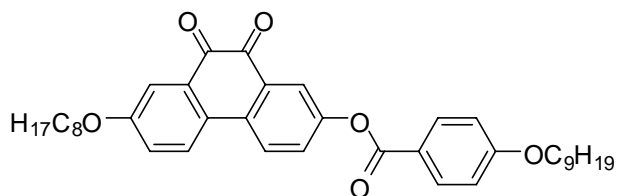
7-(Octyloxy)-9,10-dioxo-9,10-dihydrophenanthren-2-yl 4-(decyloxy)benzoate (2.30b)

138



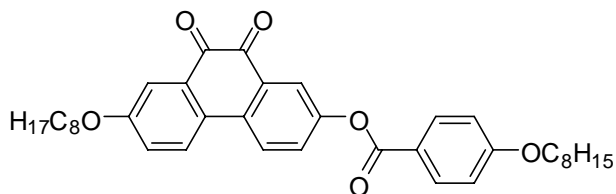
7-(Octyloxy)-9,10-dioxo-9,10-dihydrophenanthren-2-yl 4-(nonyloxy)benzoate (2.30c)

139



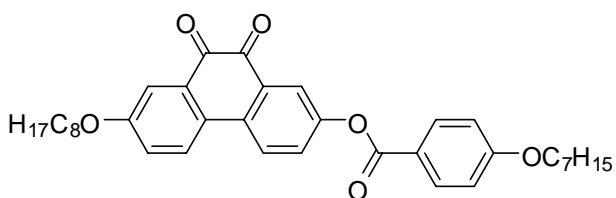
7-(Octyloxy)-9,10-dioxo-9,10-dihydrophenanthren-2-yl 4-(octyloxy)benzoate
(2.30d)

140



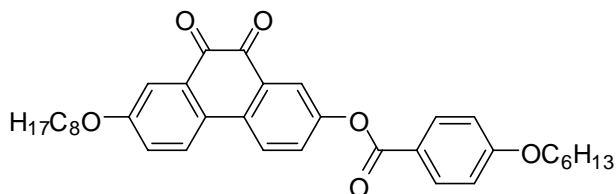
7-(Octyloxy)-9,10-dioxo-9,10-dihydrophenanthren-2-yl 4-(heptyloxy)benzoate
(2.30e)

141



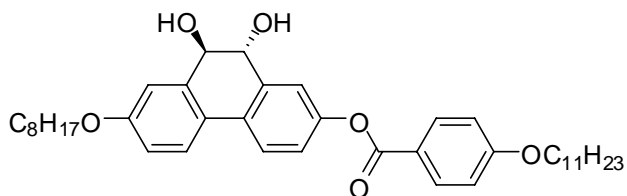
7-(Octyloxy)-9,10-dioxo-9,10-dihydrophenanthren-2-yl 4-(hexyloxy)benzoate
(2.30f)

142



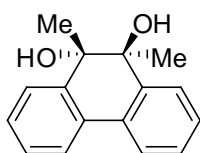
9,10-Dihydroxy-7-(octyloxy)-9,10-dihydrophenanthren-2-yl 4-(undecyloxy)benzoate
(1.31)

142

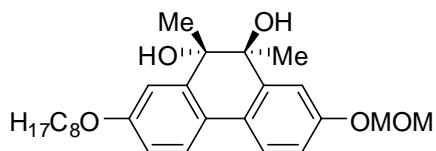


9,10-Dimethyl-9,10-dihydrophenanthrene-9,10-diol (2.36)

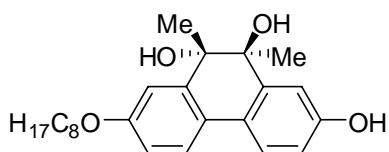
143



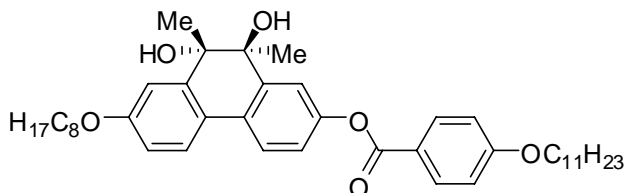
2-(Methoxymethoxy)-9,10-dimethyl-7-(octyloxy)-9,10-dihydrophenanthrene-9,10-diol (2.32) **144**



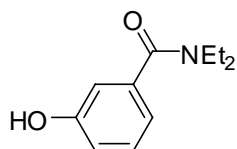
9,10-Dimethyl-7-(octyloxy)-9,10-dihydrophenanthrene-2,9,10-triol (2.33) **145**



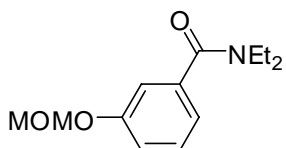
9,10-Dihydroxy-9,10-dimethyl-7-(octyloxy)-9,10-dihydrophenanthren-2-yl 4-undecyloxybenzoate (2.31) **145**



***N,N*-Diethyl-3-hydroxybenzamide (2.6)** **146**

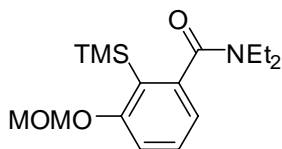


***N,N*-Diethyl-3-(methoxymethoxy)benzamide (3.3)** **147**



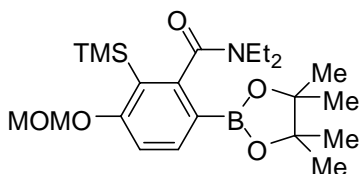
***N,N*-Diethyl-3-(methoxymethoxy)-2-(trimethylsilyl)benzamide (3.4)**

148



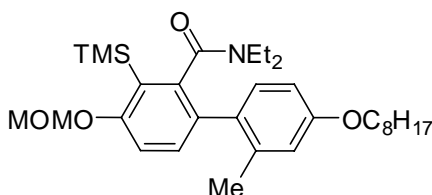
***N,N*-Diethyl-3-(methoxymethoxy)-6-(4,4,5,5-tetramethyl-1,3,2-dioxaborolan-2-yl)-2-(trimethylsilyl)benzamide (3.6)**

149



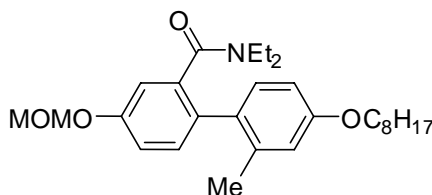
***N,N*-Diethyl-4-(methoxymethoxy)-2'-methyl-4'-(octyloxy)-3-(trimethylsilyl)biphenyl-2-carboxamide (3.7)**

149



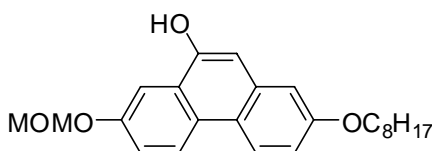
***N,N*-Diethyl-4-(methoxymethoxy)-2'-methyl-4'-(octyloxy)biphenyl-2-carboxamide (3.8)**

150, 155



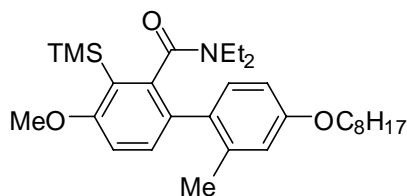
7-(Methoxymethoxy)-2-(octyloxy)phenanthren-9-ol (3.9)

151



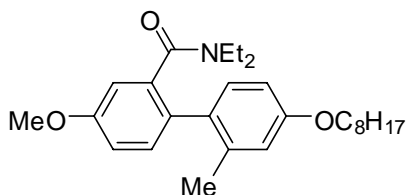
***N,N*-Diethyl-4-methoxy-2'-methyl-4'-(octyloxy)-3-(trimethylsilyl)biphenyl-2-carboxamide (3.10)**

152



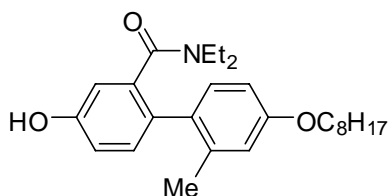
***N,N*-Diethyl-4-methoxy-2'-methyl-4'-(octyloxy)biphenyl-2-carboxamide (3.11)**

153



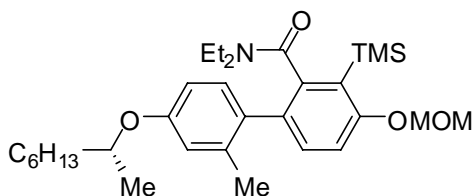
***N,N*-Diethyl-4-hydroxy-2'-methyl-4'-(octyloxy)biphenyl-2-carboxamide (3.12)**

154



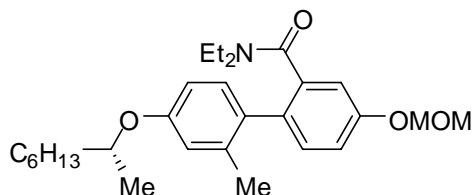
(*R*)-*N,N*-Diethyl-4-(methoxymethoxy)-2'-methyl-4'-(oct-2-yloxy)-3-(trimethylsilyl)biphenyl-2-carboxamide (3.13)

155

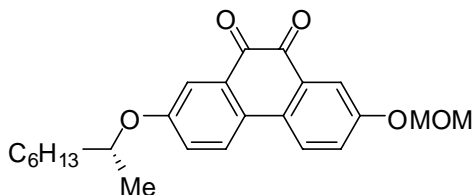


(*R*)-*N,N*-Diethyl-4-(methoxymethoxy)-2'-methyl-4'-(oct-2-yloxy)biphenyl-2-carboxamide (3.14)

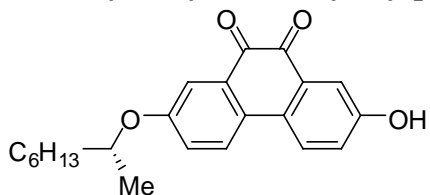
157



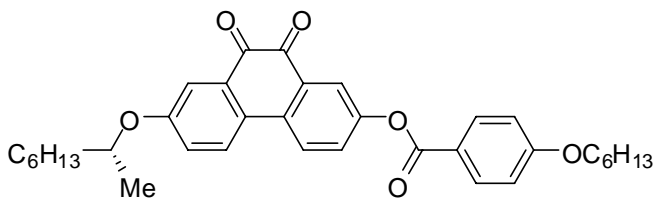
(R)-2-(Methoxymethoxy)-7-(oct-2-yloxy)phenanthrene-9,10-dione (3.16) 157



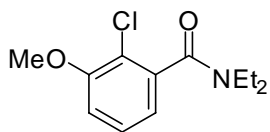
(R)-2-Hydroxy-7-(oct-2-yloxy)phenanthrene-9,10-dione (3.17) 159



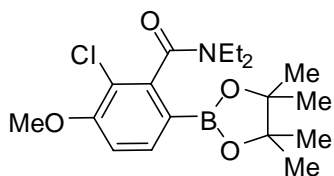
(R)-7-(Oct-2-yloxy)-9,10-dioxo-9,10-dihydrophenanthren-2-yl 4-hexyloxybenzoate (3.1a) 159



2-Chloro-N,N-diethyl-3-methoxybenzamide (3.18) 160

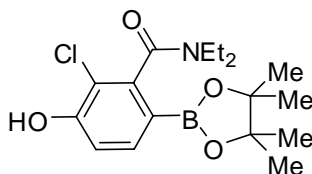


2-Chloro-N,N-diethyl-3-methoxy-6-(4,4,5,5-tetramethyl-1,3,2-dioxaborolan-2-yl)benzamide (3.20) 161



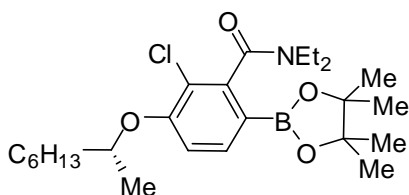
2-Chloro-*N,N*-diethyl-3-hydroxy-6-(4,4,5,5-tetramethyl-1,3,2-dioxaborolan-2-yl)benzamide (3.22)

162



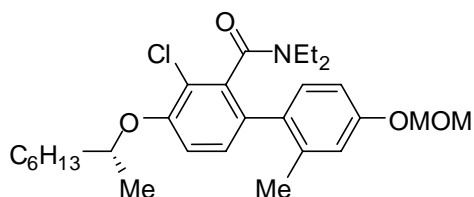
(*R*)-2-Chloro-*N,N*-diethyl-3-(oct-2-yloxy)-6-(4,4,5,5-tetramethyl-1,3,2-dioxaborolan-2-yl)benzamide (3.23)

163



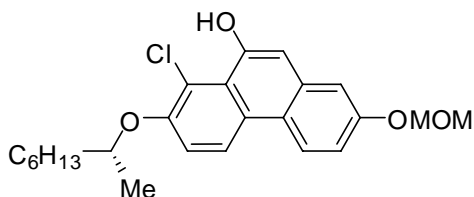
(*R*)-3-Chloro-*N,N*-diethyl-4'-(methoxymethoxy)-2'-methyl-4-(oct-2-yloxy)biphenyl-2-carboxamide (3.24)

163



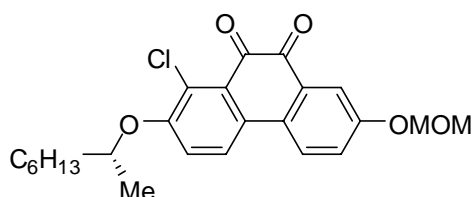
(*R*)-8-Chloro-2-(methoxymethoxy)-7-(oct-2-yloxy)phenanthren-9-ol (3.25)

164

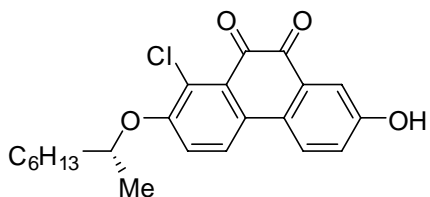


(*R*)-1-Chloro-7-(methoxymethoxy)-2-(oct-2-yloxy)phenanthrene-9,10-dione (3.26)

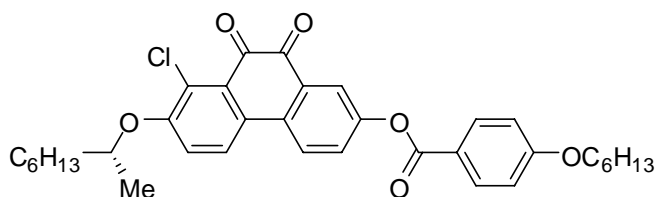
165



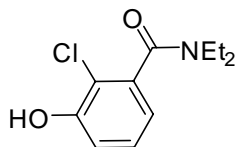
(R)-1-Chloro-7-hydroxy-2-(oct-2-yloxy)phenanthrene-9,10-dione (3.27) 166



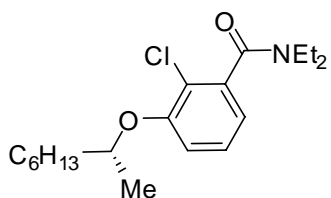
(R)-8-Chloro-7-(oct-2-yloxy)-9,10-dioxo-9,10-dihydrophenanthren-2-yl 4-(hexyloxy)benzoate (3.1b) 166



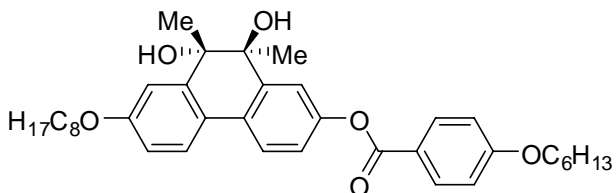
2-Chloro-N,N-diethyl-3-hydroxybenzamide (3.28) 167



(R)-2-Chloro-N,N-diethyl-3-(octan-2-yloxy)benzamide (3.29) 168



(-)-9,10-Dihydroxy-9,10-dimethyl-7-(octyloxy)-9,10-dihydrophenanthren-2-yl 4-(hexyloxy)benzoate ((-)-4.1) 169



CHAPTER 1–INTRODUCTION

1.1 Introduction: Liquid Crystals

Liquid crystals (LC) were first discovered by an Austrian botanical physiologist, Friedrich Reinitzer¹ in 1888, when he was examining the physico-chemical properties of cholesterol benzoate. Reinitzer found that, unlike normal compounds, cholesterol benzoate had two melting points on heating: at 145.5 °C, the compound melted to a cloudy fluid, and at 178.5 °C, it turned clear. He could not explain the phenomena and wrote letters to a physicist, Otto Lehmann² for help. After a systematic study by microscopy, Lehmann concluded that the compounds showing double-melting phenomena formed a phase intermediate between crystalline phase and isotropic liquid phase as the result of a combination of anisotropic intermolecular interactions with a fluidity. After this discovery, LCs remained dormant in the scientific literature until they found applications in liquid crystal displays (LCD) 80 years later.

1.1.1 Liquid Crystal Phases and Their Properties

Although LCs maintain the properties of both crystalline and liquid, they are more liquid than crystalline in nature because the ΔH of transition from Cr \rightarrow LC is significantly higher than that of LC \rightarrow liquid.

Compounds forming LCs are called mesogens. The LC phases formed by mesogens are called mesophases. LCs are broadly classified as thermotropic and lyotropic phases according to the presence or absence of solvent. Lyotropic phases are formed in polar or nonpolar solvents. They are usually composed of a hydrophobic head

and a hydrophilic tail. These amphiphilic molecules form mesophases of various kinds depending on the volume balances between the hydrophilic and hydrophobic parts in certain solvents as a result of the microsegregation of the two incompatible components. Soap is an everyday example of lyotropic LCs. Thermotropic phases appear as a function of temperature, either on heating and cooling (*enantiotropic*) or on cooling only (*monotropic*). The structure and stability of thermotropic phases do not depend on solvation, but are an intrinsic property of the material as a result of anisotropic van der Waal forces and packing interactions.

There are three kinds of thermotropic mesogens: calamitic mesogens, formed by rod-shaped molecules of which one molecular axis is much longer than other two; discotic mesogens, formed by disc-like molecules, namely molecules with one molecular axis much shorter than the other two; and polycatenar mesogens, formed by board-like molecules of which the shapes are something between rod and disc molecules (Figure 1.1)

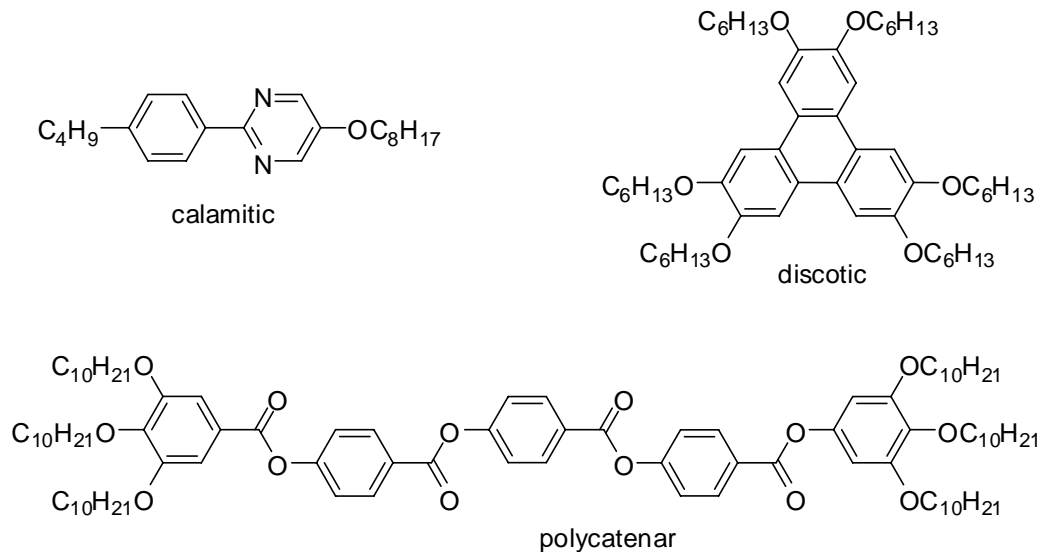


Figure 1.1 Structures of some calamitic, discotic, and polycatenar mesogens.

Discotic LCs are composed of a rigid core which is normally based on benzene, triphenylene, or truxene with six or eight flexible aliphatic side chains. The discotic molecules have a tendency to pack to form columns which may be organized into rectangular or hexagonal arrays. The most common type of LCs is calamitic. The molecules that form calamitic phases usually have a rigid core with one or two hydrocarbon chains at each end. The rigid core is important for the formation of calamitic LCs, since it maintains an elongated shape producing interactions that favour alignment. This thesis focuses on this type of LC.

The most common mesophases formed by calamitic mesogens are nematic (N) phases, smectic A (SmA) phases and smectic C (SmC) phases, which differ in the degrees of their orientational and translational/positional orders. The phase sequence is illustrated in Figure 1.2. In the isotropic liquid phase, the mesogens are randomly distributed throughout the sample. On cooling, the van der Waal forces and packing interactions between the mesogens align the mesogens such that the long axes of

mesogens are oriented, on the time average, in one direction while the molecules diffuse randomly, as in a liquid (Figure 1.2a). There is no translational/positional order in this phase. The word nematic comes from the Greek for thread, a term originated from “schlieren” texture of nematic phases observed in a polarized microscope (Figure 1.3).

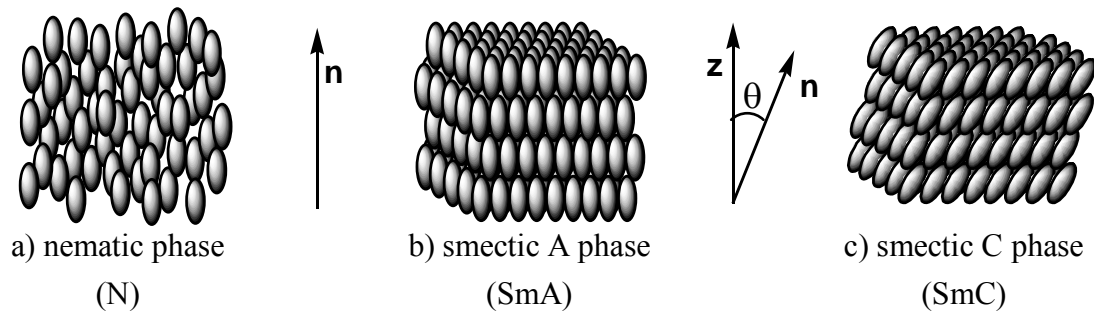


Figure 1.2 Schematic representation of three LC phases.

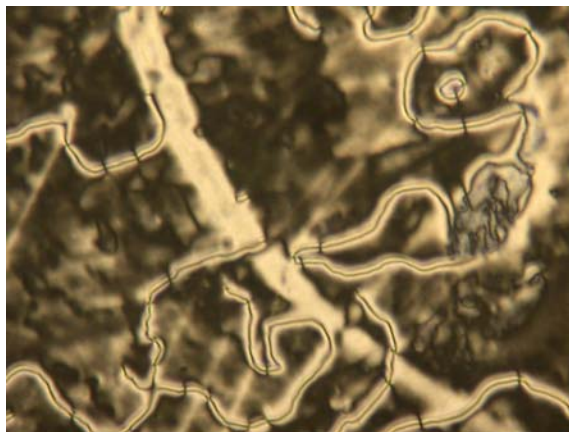


Figure 1.3 Schlieren texture of the nematic phase observed by polarized microscopy.

Upon further cooling, short-range positional order forming layers may be achieved. If the mesogens are oriented along the layer normal z , it is called a SmA phase (Figure

1.2b), in which there is no correlation between the layers, and the mesogens freely rotate along their long axes. The SmA phase typically exhibits a focal conic (fan) texture, as well as homeotropic regions (dark areas) in a polarized microscope (Figure 1.4a). The latter texture results from the mesogens being oriented perpendicular to the glass slides, i.e., along the optic axis direction of plane-polarized light, and therefore no birefringence is exhibited.

The SmC phase is formed either on cooling from the SmA phase or directly from the nematic phase. The SmC phase differs from SmA in that the mesogens are uniformly tilted away from the layer normal z at an angle (θ) (Figure 1.2c), which is temperature dependent and increases with decreasing temperature. In a polarized microscope, the fan texture of the SmA phase turns to a broken fan texture and the homeotropic regions turn to schlieren textures upon transition from the SmA to SmC phase (Figure 1.4).

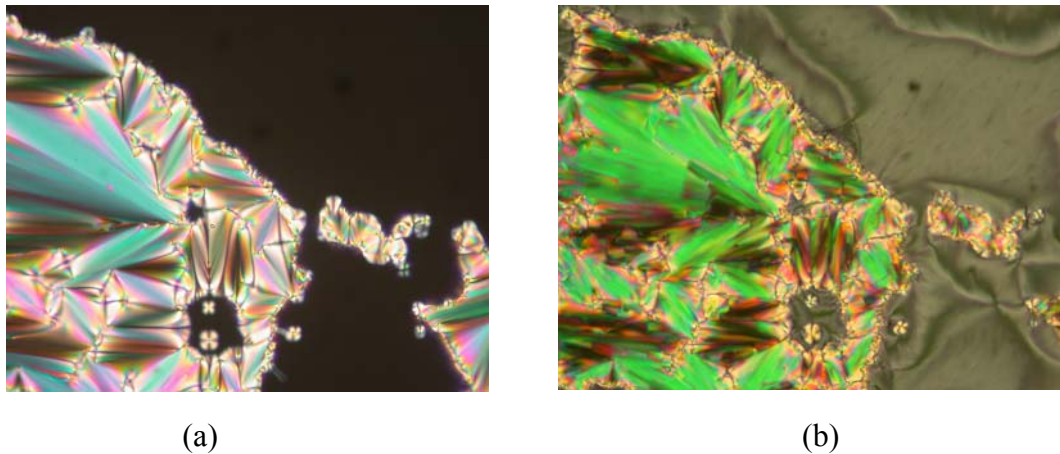


Figure 1.4 Photomicrographs of the typical textures of (a) SmA and (b) SmC phases.

The molecular origins of the tilt in the SmC phase have been explained by two models. McMillan proposed that the tilt is the result of a torque produced by the

coupling of outboard dipoles. With the decrease in temperature, the mesogen rotation around the long axis slows down, which leads to the coupling of outboard dipoles to give a macroscopic torque (Figure 1.5).³ On the other hand, Wulff postulated that packing forces lead to the tilt. The formation of the SmA or SmC phases depends on the balance between the rotational entropy and packing forces (Figure 1.6). Rotational entropy favours a perpendicular structure while the packing forces favour a tilted zig-zag conformation. As the mesogen rotation slows down, the packing forces become predominant at a lower temperature, which results in an overall molecular tilt.⁴

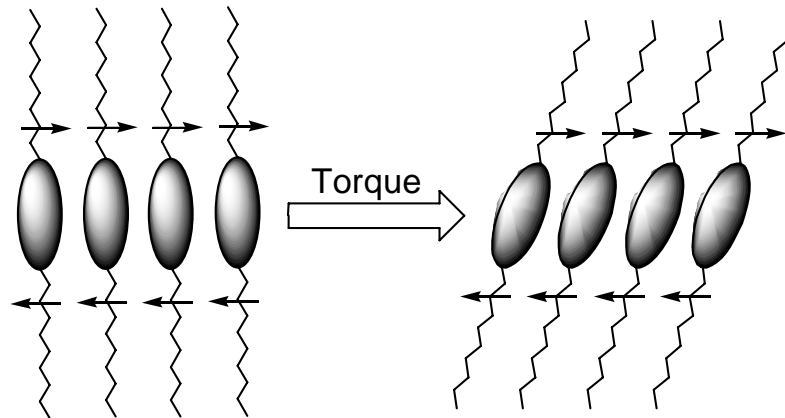


Figure 1.5 Schematic representation of the McMillan model for the origin of the tilt.

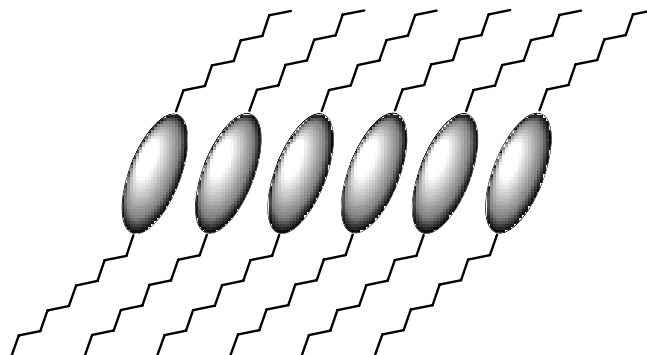


Figure 1.6 Schematic representation of the Wulff model for the origin of the tilt.

Wulff thought that the tails were more tilted than the core. But actually, as shown by Durand, the core is more tilted with respect to the layer normal than the tails based on a comparison of the optical tilt angle θ with the steric tilt angle α . The optical tilt angle θ is derived from polarizable anisotropy of mesogens. The aromatic core has the highest polarizability anisotropy, so the optical tilt angle θ measured by polarized microscopy is actually the tilt angle of the rigid core with respect to the layer normal. The steric angle α is determined from the actual length of layer spacing d measured by powder X-ray diffraction and the calculated molecular length l as $\cos \alpha = d/l$. It was found that the optical tilt angle is normally larger than the steric tilt angle, which indicates that the rigid core is more tilted than the flexible tails (Figure 1.7).⁵

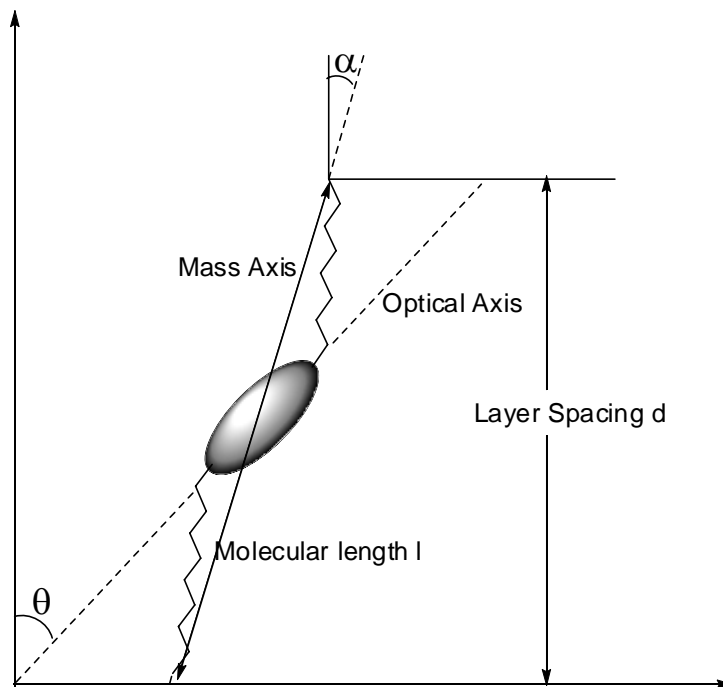


Figure 1.7. Representation of the Durand model showing the core is more tilted.

1.1.2 Odd-Even Effect

The odd-even effect was discovered by Gray⁶ in 1955 who measured the thermal stability of a series of mesogens based on benzylideneaminofluorenone **A**, and found that the clearing points (the transition temperature from a mesophase to liquid) of the series **A** lay on two well separated curves as a function of chain length. One was for the chains with odd numbers and the other was for the chain with even numbers (Figure 1.8). This effect on the thermal stability of mesophases was called odd-even effect.

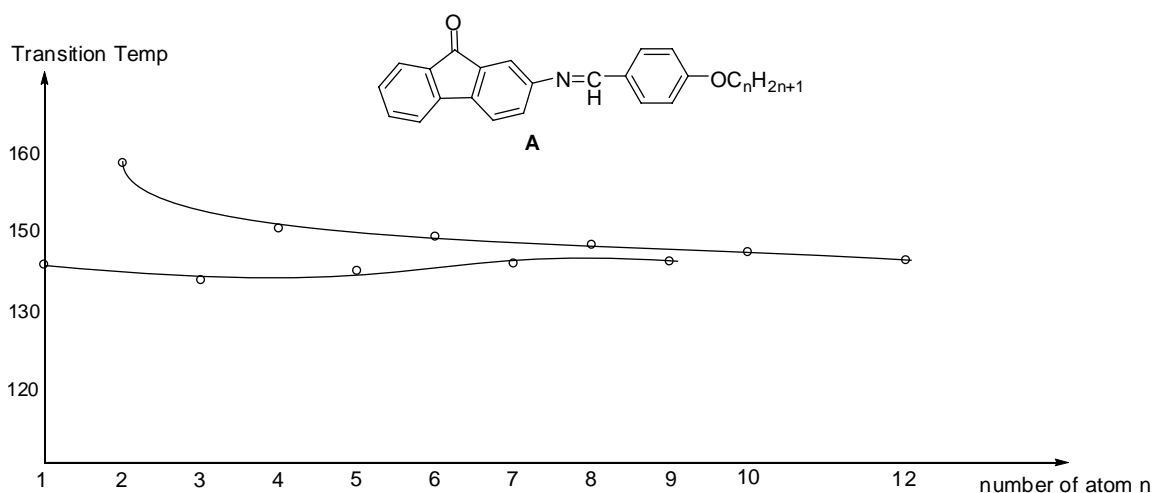


Figure 1.8 Graph of transition temperature vs the number of carbon atoms in the chain.

It was suggested that the odd-even effect is related to the molecular aspect ratio (the length over the width of the molecule). When adding one more carbon to the chain to make it even, the increase of the aspect ratio is more than that going from odd to even (Figure 1.9). With the increase of the chain length, the difference becomes less significant, so the odd-even effect tapers off.⁷

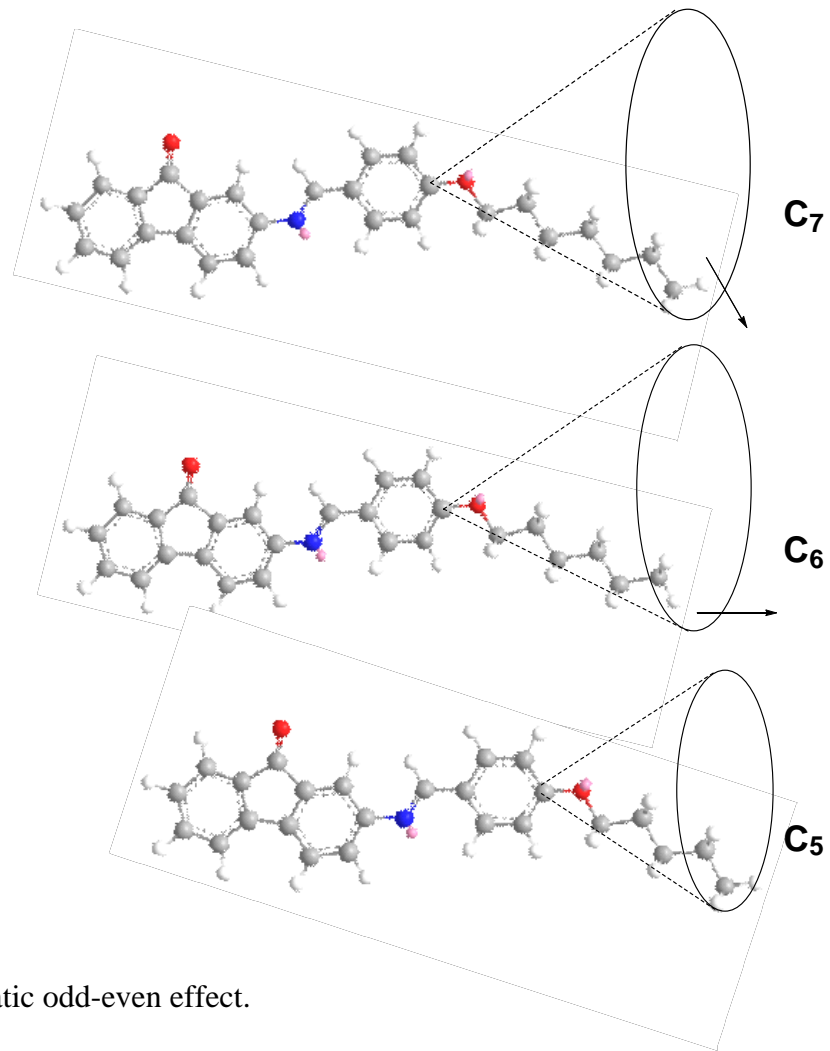


Figure 1.9 Schematic odd-even effect.

1.1.3 The Chiral Smectic C Phase (SmC^*)

The applications of LCs in industry are based on their optical property of birefringence, which is the ability to rotate plane-polarized light. For a LC film between two crossed polarizers, the birefringence is a function of angle formed between the plane of polarization and the average molecular orientation (director \mathbf{n}), which can be switched between two directions by applying an electrical field. Therefore, an aligned LC film can act as a light shutter by electrically switching the director orientation with respect to the polarized light. Currently, most of the liquid crystal display (LCD) devices on the market use nematic LCs as an electro-optical material. The chiral SmC^* phase has received

increasing consideration as a light shutter for the next generation of LCD devices because its switching time is 10^3 faster than that of the nematic phase.

In the SmC^* phase, molecular chirality induces a finite twist of the director about the layer normal from one layer to the next to form a supramolecular helical structure (Figure 1.10). Another characteristic of the SmC^* phase is that each smectic layer exhibits a spontaneous polarization (P_s) along its C_2 symmetry axis. But the helical form of the SmC^* phase does not exhibit a net macroscopic polarization because the P_s vector of each layer rotates about the layer normal from one layer to the next and the overall P_s of the helical SmC^* phase is cancelled out. However, it was discovered by Clark and Lagerwall⁸ in 1980 that the helical structure of the SmC^* unwinds between two polyimide-coated glass slides to form a uniformly tilted chiral smectic film (Figure 1.10). The slides must be rubbed in one direction and have a spacing on the order of the helical pitch (typically 1–5 μm). The resulting surface-stabilized ferroelectric liquid crystal (SSFLC) film exhibits a net P_s perpendicular to the glass slides.

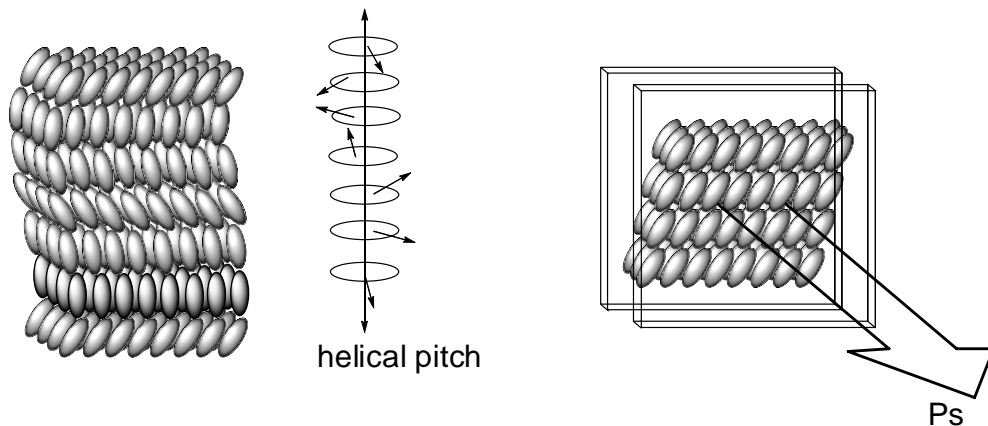


Figure 1.10 Schematic representation of the helical SmC^* phase and a SSFLC.

By coupling P_s with an electric field E , a SSFLC can be switched back and forth between two degenerate states with opposite tilt and P_s orientations to give an ON/OFF

light shutter between crossed polarizers (Figure 1.11). The switching time of a SSFLC shutter depends on the rotational viscosity (η), the applied voltage (E) as well as the P_s of the sample, as shown in eqn (1).

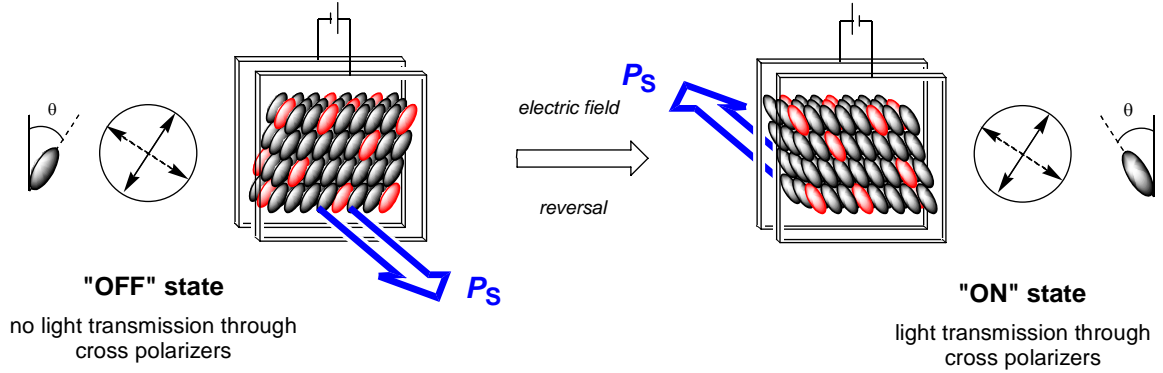


Figure 1.11 Schematic representation of an electro-optical SSFLC switch.

$$t \approx \frac{1.8 \eta}{P_s E} \quad (1)$$

Normally, a neat SmC* material has a high viscosity value which results in a slow switch time. Liquid crystal formulations for commercially available SmC* shutters are obtained by mixing a small amount of chiral dopant in an achiral SmC liquid crystal mixture with low viscosity and a broad temperature range. The chiral dopant may not be mesogenic, but should have a high polarization power (δ), i.e., the propensity of a chiral dopant to induce a P_s in an achiral host. The polarization power (δ) is expressed by eqn (2), where x_d is the dopant mole fraction, P_0 is the spontaneous polarization normalized for the tilt angle according to eqn (3).

$$\delta = \left(\frac{dP_0(x_d)}{dx_d} \right)_{x_d \rightarrow 0} \quad (2)$$

$$P_0 = P_s / \sin\theta \quad (3)$$

Several models have been developed to explain the molecular origins of spontaneous polarization. Meyer's symmetry model provides a simple and efficient argument. A SmC liquid crystal, on the time average, has C_{2h} symmetry with a C_2 axis element perpendicular to the tilt plane which is defined by the layer normal \mathbf{z} and the molecule director \mathbf{n} , and an σ_h plane element which is congruent with the tilt plane (Figure 1.12). Any dipole moment within the tilt plane and perpendicular to the plane cancels out upon application of the σ_h operation. If the chirality is introduced into the smectic liquid crystal, the C_2 operation is invariant, but the σ_h plane symmetry disappears, which results in a net dipole moment (a microscopic polarization) along the C_2 axis.⁹

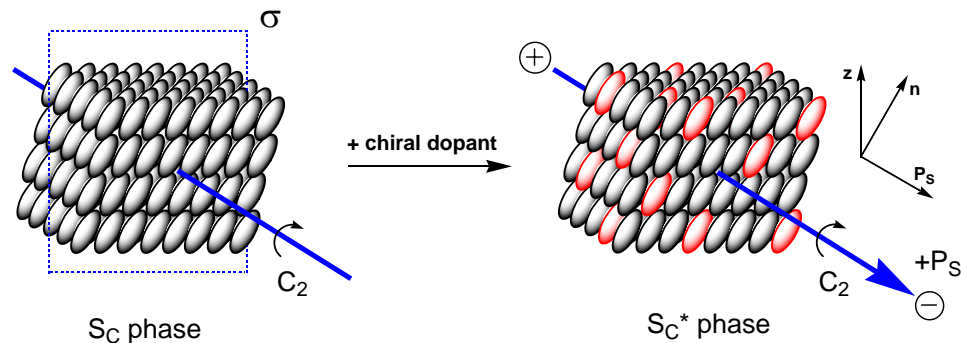


Figure 1.12 Meyer's symmetry argument for a SmC* phase.

The molecular origin of spontaneous polarization is also described by the Boulder model.¹⁰ According to this model, the SmC phase is considered to be a supramolecular

host and the ordering imposed by the host is modeled by a mean-field potential which qualitatively behaves like a receptor or binding site (Figure 1.13). The binding site is a bent cylinder with a C_{2h} symmetry and a zig-zag conformation with the core more tilted than the tails. When a chiral compound is confined to the binding site, the coupling of the chiral center with the polar functional groups (stereo-polar unit) produces an orientational bias along the polar C_2 axis to give a Ps.¹¹

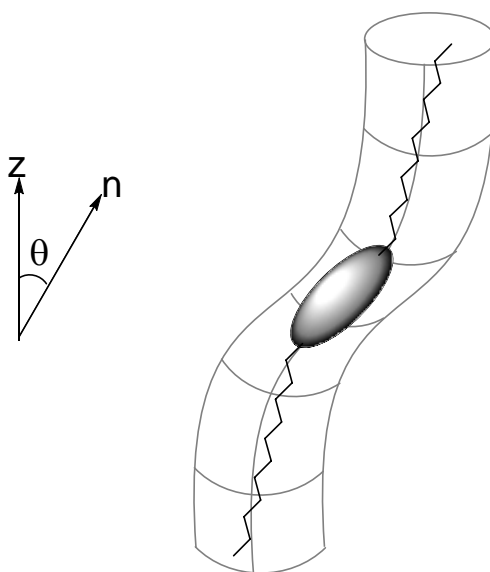


Figure 1.13 The binding site according to the Boulder model.

Conformational analysis of mesogens bearing a (*S*)-4-(oct-2-yloxy)phenyl 4-(octyloxy)benzoate reveals the origin of spontaneous polarization (Figure 1.14). There are three staggered conformations about the C2-C3 bond axis. For conformation **A**, the polar alkoxy group lies within the tilt plane and no dipole moment contributes to the Ps. The alkoxy group lies perpendicular to the tilt plane in conformations **B** and **C**, in which the alkoxy dipoles are opposite and oriented along the C_2 axis to contribute to Ps. The

conformations **B** and **C** are non-equivalent and conformation **B** is energetically favourable over conformation **C** by the *anti* relationship between methyl group and the C4 alkyl group. The magnitude of P_s is dependant on the energy difference between the two conformations.

The sign of the P_s is defined by the absolute configuration of the chiral constituent. According to the physics convention, a positive sign of P_s is defined by the cross-product of the P_s vector, which points from the negative to the positive end of a dipole (opposite to that used in chemistry) and the director. In this thesis, the sign of P_s is based on the chemistry convention (Figure 1.14).

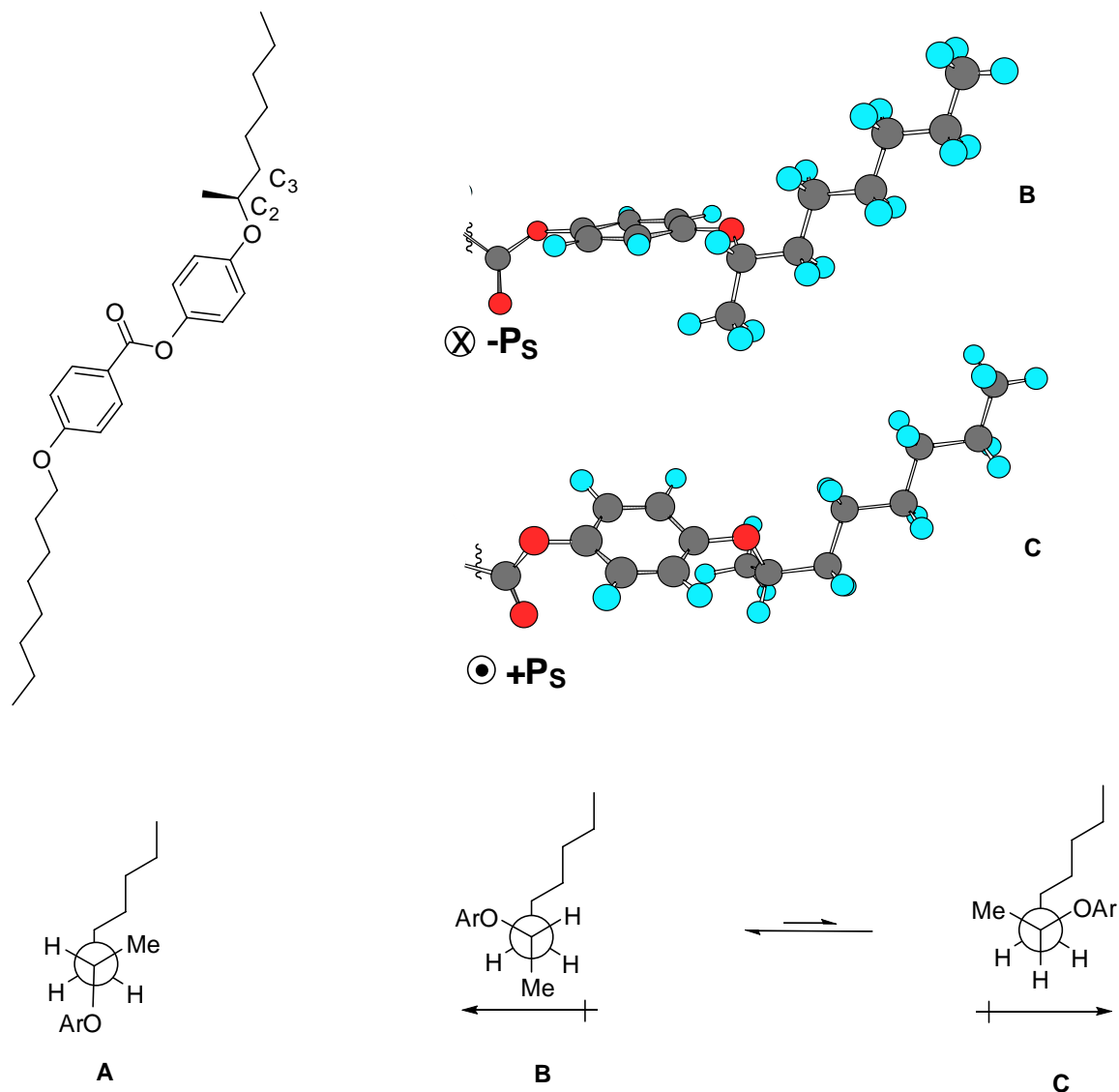


Figure 1.14 Conformational analysis of the (*S*)-2-octyloxy side chain and the resulting sign of Ps. A side-on view along the polar axis is shown on the top. An end-on view is shown as a Newman projection along the C₂-C₃ bond axis of the (*S*)-2-octyloxy side-chain on the bottom. The sign of Ps is negative according to the chemistry convention.

A substituent *ortho* to a chiral side chain may couple with the chiral center and lead to a dramatic change in Ps. For example, in compound biphenylcarboxylate **1.1**, a high Ps (negative) was observed due to the steric coupling between the nitro substituent and the (*S*)-2-octyloxy side chain causing their dipoles to align in the same direction to

contribute to Ps.¹² As shown in the Figure 1.15 (a), the conformation in which the nitro group is oriented *anti* to C2 is favoured because the nitro group is sterically more demanding than the *ortho* hydrogen. The resulting conformation combines the dipole moment of the nitro and alkoxy group to contribute to a negative Ps. However, in compound **1.2** (Figure 1.15 (b)), a high positive Ps was observed.¹¹ The pyridine nitrogen is oriented *syn* to C2 because the nitrogen lone pair is sterically less demanding than the *ortho* hydrogen. The pyridine nitrogen has an opposite and larger dipole moment to that of alkoxy group along the polar axis, which results in a positive Ps.

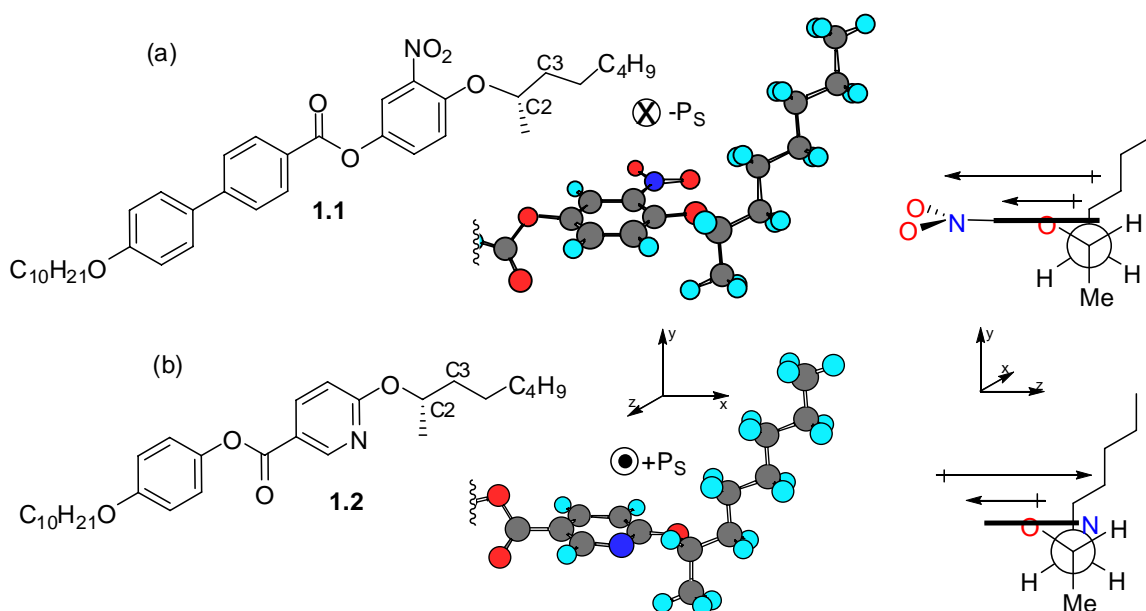


Figure 1.15 Schematic conformations for **1.1** and **1.2** and the sign of Ps for a (*S*)-2-octyloxy side chain *ortho* to (a) a nitro group and (b) to a pyridine nitrogen. Side-on views along the polar axis are shown on the left. End-on views are shown as Newman projections along the C2-C3 bond axis of the (*S*)-2-octyloxy side-chains on the right.

There are two types of dopants which induce a ferroelectric SmC* phase. One type has the stereo-polar unit located in the side chain and is classified as Type I dopant.^{13,14} The polarization power of a Type I dopant is, in general, invariant with the structure of

the SmC host. This is likely due to the fact that the side chains are conformationally more disordered in the diffuse lamellar structure of the SmC phase compared with their rigid aromatic core. Hence, the stereo-polar unit in the side chain does not, on the time average, interact with the host environment via effective molecular recognition. The dopant must simply adopt a particular conformation and orientation to fit the binding site of the SmC host. That is the reason a Type I dopant is also called a “passive guest”.

The other type of dopant is called Type II dopant, which is characterized by a stereo-polar unit located in the rigid core of the molecule. The polarization power of Type II dopants normally varies with the structure of the SmC host. This may be explained by assuming that the central part of the binding site changes shape from one host to the next, since the rigid aromatic core has a higher degree of conformational order. A small change in the topography of the binding site can have a large influence on the polarization power of Type II dopants due to the conformational asymmetry of the stereo-polar unit in the core. However, for atropisomeric dopants such as **1.3**, the Type II behaviour may also be due to chirality transfer via the core-core interactions between the dopant and host.¹⁵

Assuming a rigid zig-zag conformation as shown in Figure 1.16, one can identify four conformational minima in **1.3** corresponding to rotation of the core around the two ester C-O bonds according to AM1 calculations (Figure 1.16).^{16,17} Two of the minima **B** and **D** have no Ps since their transverse dipole moments lie in the tilt plane. Only **A** and **C** have transverse dipole along the polar axis to contribute to Ps but in opposite directions. The rotamers **C** have a favoured conformation with the carbonyl groups quasi

anti-periplanar with respect to the nitro groups relative to that of **A**, which has a quasi *syn*-periplanar relationship between the carbonyl and nitro groups.

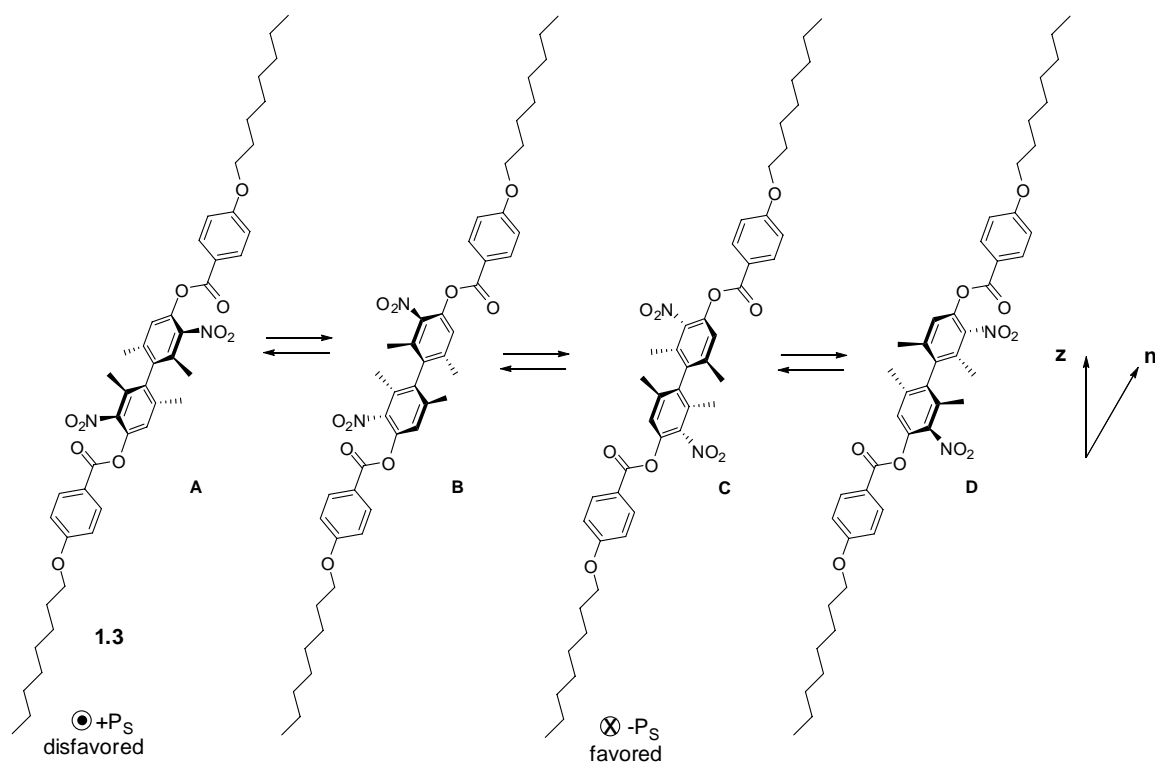


Figure 1.16 The four AM1-minimized conformations by rotation of the atropisomeric biphenyl core about the two ester C-O bonds. The tilt plane in the plane of the page.

Variations in polarization powers were observed when **1.3** was used as dopant in four different SmC hosts (Figure 1.17), among which the value of 1738 nC/cm² (the highest reported thus far) was measured for the SmC* mixture of **1.3** (up to 5 mol%) in **PhP1** while a value of 30 nC/cm² was given for the mixture of **1.3** (up to 5 mol%) in **PhB**. This pronounced Type II behaviour was explained by a chirality transfer feedback mechanism. In the ground state, the core structure of **PhP1** has a planar conformation, which may be distorted into an axially chiral form when **1.3** interacts with **PhP1** (Figure 1.18). Such interaction may result in a chiral perturbation of the host (chirality transfer)

and amplify the polarization power of the dopant as a feedback effect. Effective chirality transfer requires a good core-core structural match between the dopant and host. **PhP1** has a good structural match with **1.3** where **PhB** does not.

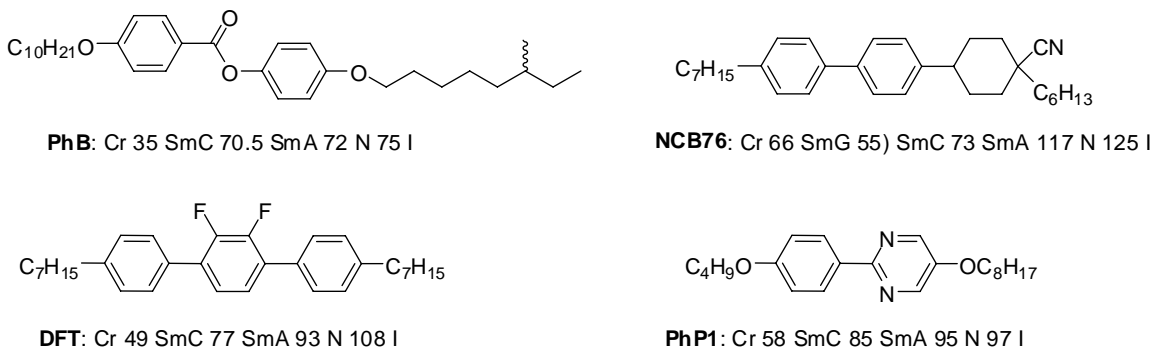


Figure 1.17 Liquid crystal host structures and phase transition temperatures in °C.

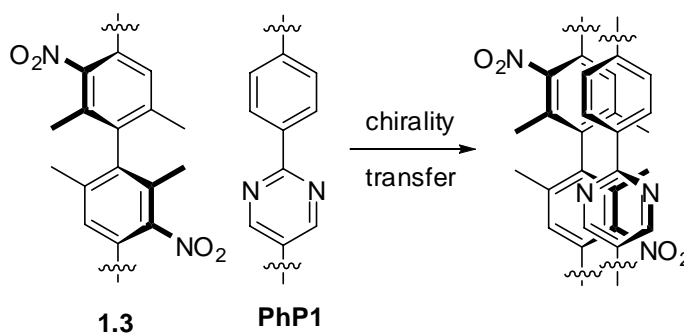


Figure 1.18 Model for chirality transfer *via* core-core interactions.

1.1.4 Hydrogen Bonding in Non-amphiphilic Mesogens

Liquid crystals can be viewed, to some degree, as a supramolecular assembly in which the mesogens are held together by intermolecular forces. In supramolecular chemistry, hydrogen bonding plays a crucial role in the formation and stabilization of a supramolecule, e.g. the double helical structure of nucleic acids held *via* hydrogen bonding between complementary nucleobases. Also in liquid crystals, whose formation

is attributed to intermolecular interactions, hydrogen bonding can play an important role in the stabilization of certain mesophases. Head-to-head hydrogen bonding promotes the microsegregation of molecules into a rod-like supramolecular structure that can exhibit mesogenicity. Side-to-side hydrogen bonding enhances positional ordering to promote and stabilize smectic phases (Figure 1.19) ¹⁸

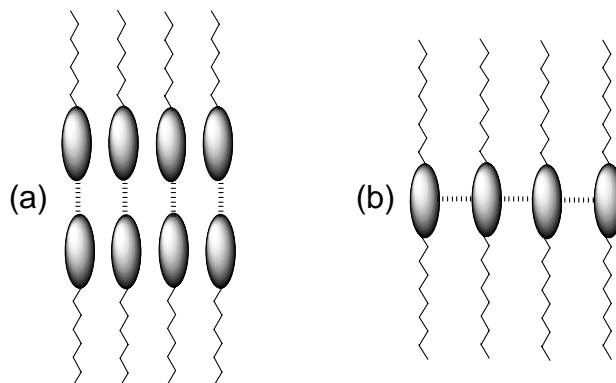


Figure 1.19 Two modes of hydrogen bonding in liquid crystals: (a) head-to-head; (b) side-to-side.

1.1.4.1 Hydrogen Bonding in Mesogens

Carboxylic acids were the first compounds discovered to exhibit liquid crystal behaviours due to hydrogen bonding. 4-Alkoxybenzoic and cinnamic acids are among those that form liquid crystal phases, while aliphatic carboxylic acids are usually not mesogenic. The mesogenicity of those compounds may be attributed to the hydrogen-bonded dimerization leading to a lengthening of the rigid core moiety which promotes liquid crystallinity (Figure 1.20).

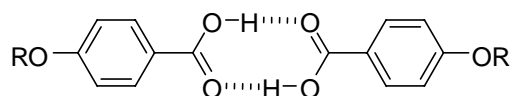
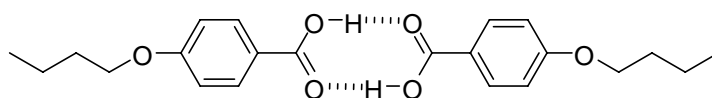
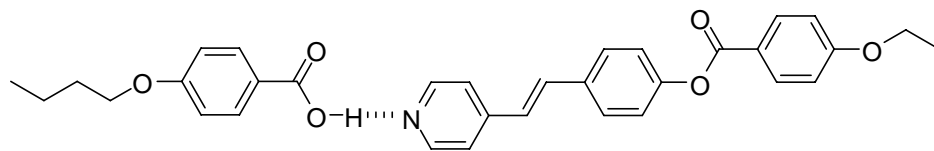


Figure 1.20 The mesogenic dimer formed by hydrogen bonding.

Pyridine and aromatic carboxylic acids are one of the most common pairs utilized to design new liquid crystals or to stabilize already existing liquid crystals. For example, 4-butoxybenzoic acid and *trans*-4-[(4-ethoxybenzoyl)oxy-4'-stilbazole only exhibit nematic phases between 147–160 °C and 165–213 °C respectively. But, when mixed together in a 1:1 ratio, gives an unspecified smectic phase. The newly formed mesogens exhibit a focal conic texture between 136–160 °C, followed by an increased nematic range between 160–238 °C. This was attributed to the formation of an elongated molecular structure via hydrogen bonding and supported by FTIR measurements which show evidence that the dimer of 4-butoxybenzoic acid was replaced by the complex **1.4**.¹⁹

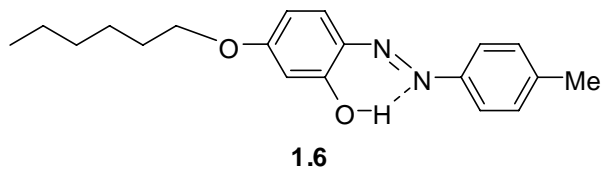
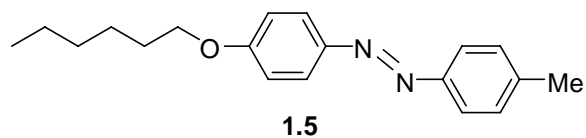


Cr 147 N 160 I

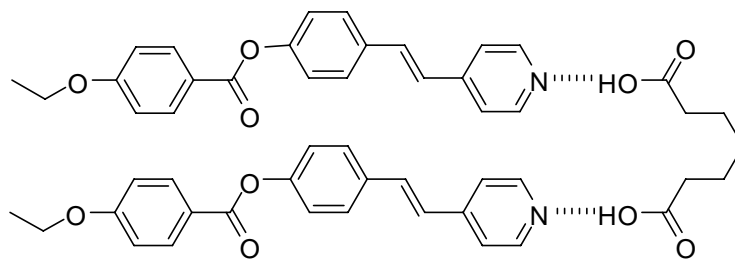


1.4 Cr 136 SmX 160 N 238 I

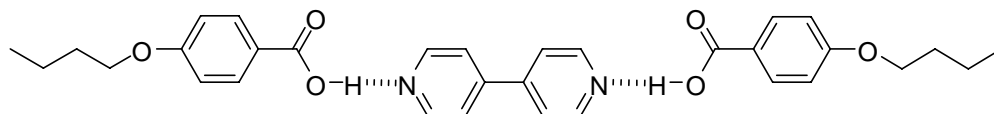
Mesophase stabilization can be achieved via intramolecular hydrogen bonding. A marked broadening of the nematic phase was observed when an OH group was inserted at the *ortho* position of **1.5** to give **1.6**. The N-to-I transition temperature of **1.6** is *ca* 15 °C higher than that of **1.5**. The broader mesophase is ascribed to intramolecular hydrogen bonding to increase the core rigidity. The evidence of intramolecular hydrogen bonding was provided by X-ray and IR spectral data.²⁰



Multiple-hydrogen bonding donors or acceptors may be used to form folded mesogens. Thus, an aliphatic dicarboxylic acid may form a twin-type liquid crystalline complex **1.7** with *trans*-4-[(4-ethoxybenzoyl)oxy-4'-stilbazole and exhibit both smectic and nematic phases with an odd-even effect.²¹ 4,4'-Bipyridine was used as a linking group to form an elongated complex **1.8** with 4-butoxybenzoic acid, which displays a sharp phase transition and smectic and nematic phases.²² In both cases, the end group monomers exhibit a nematic phase only.



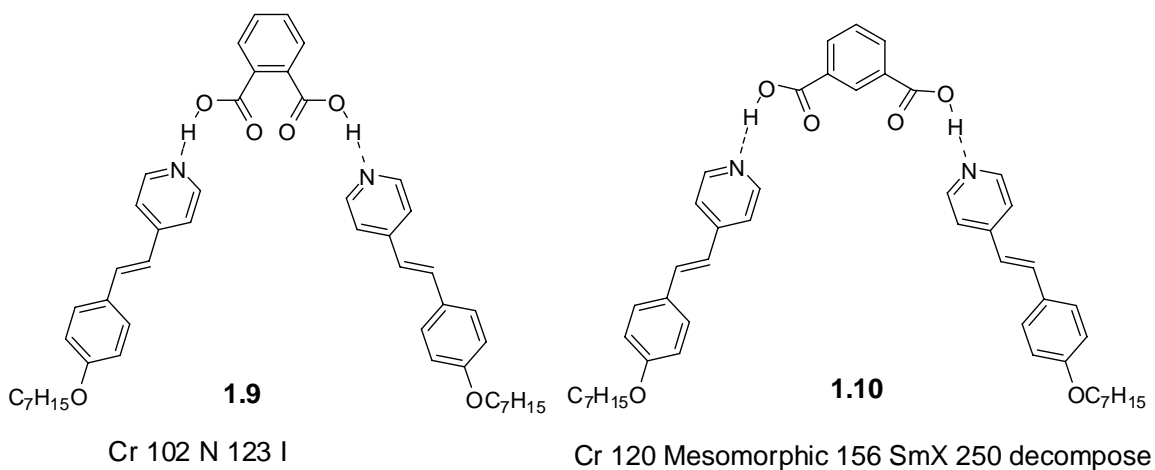
1.7: Cr 146 SmX 182 N 230 I



1.8: Cr 134 SmX 150 N 159 I

Phthalic or isophthalic acid can also be used as a linking group to form mesogenic complexes with *trans*-4-[(4-ethoxybenzoyl)oxy-4'-stilbazole via hydrogen bonding. The proposed structures for the complexes thus formed are banana-like bent shapes. Complex

1.9 displays a nematic phase only, while complex **1.10** exhibits a smectic phase between 156 °C and 250 °C, and decomposes above 250 °C.²³



Diacylhydrazine **B** forms supramolecules via lateral hydrogen bonding (Figure 1.21). A smectic phase is exhibited by **B** and the intermolecular hydrogen bonding is arranged in two possible forms: the overlap folded structure (a) and the staggered extended structure (b).²⁴

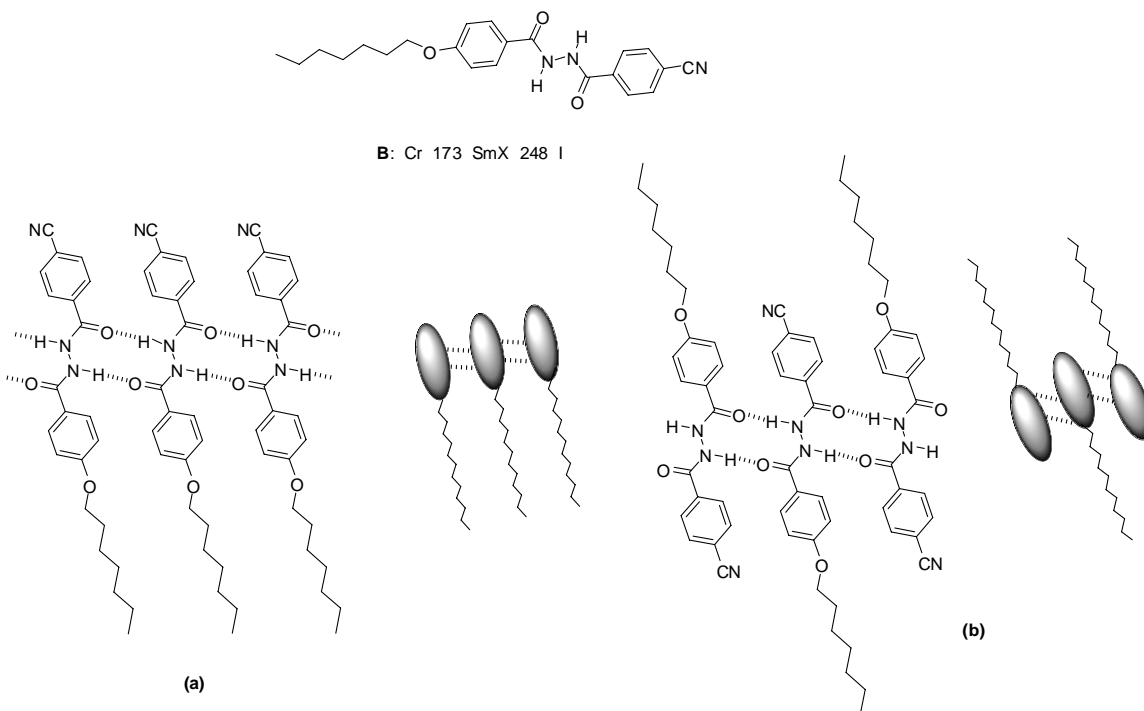
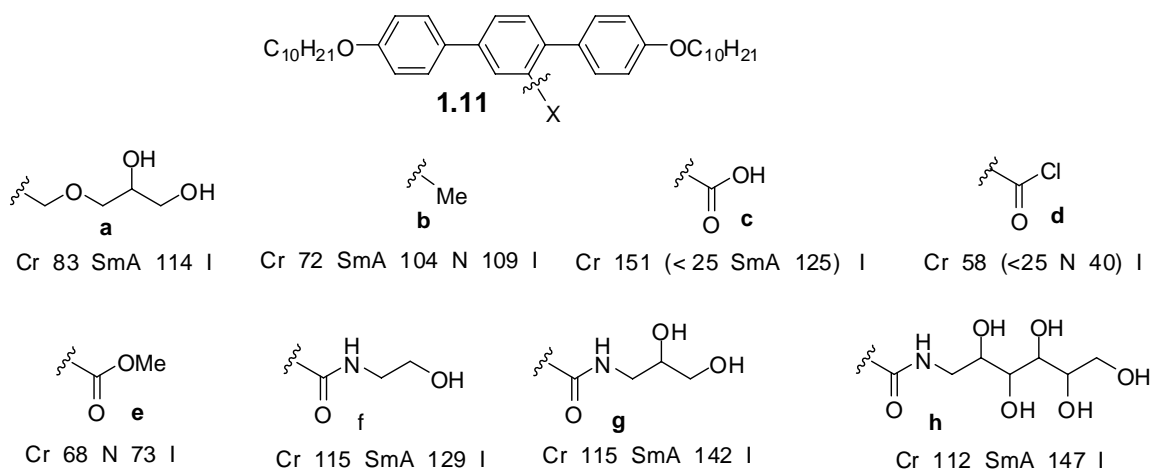
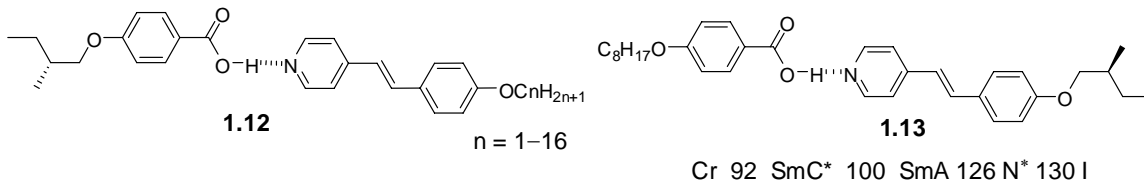


Figure 1.21 The suggested lamellar structure: (a) folded; (b) extended.

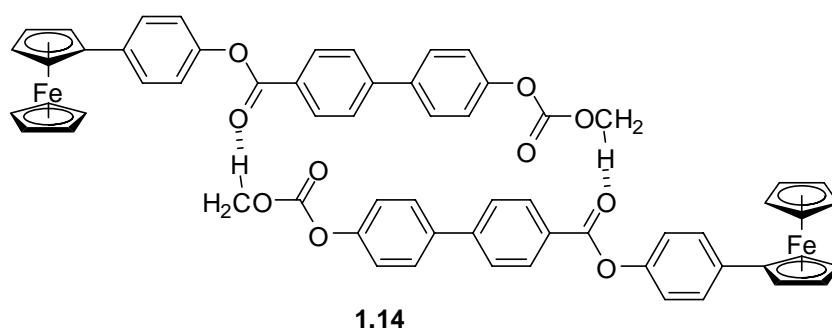
In order to test the stabilizing effect of lateral hydrogen bonding on the mesogenic behaviours of LCs, Tschierske designed a series of LCs with the general structure **1.11**. A comparison of compounds **1.11a** and **1.11b** reveals that the SmA phase formed by **1.11a** is more stable even though its lateral group X is bulkier, which may be ascribed to the formation of intermolecular lateral hydrogen bonding. In a comparison with the non-hydrogen bonding analogues **1.11d** and **1.11e**, compound **1.11c**, bearing a carboxylic acid group, was the only mesogen forming a SmA phase. From compound **1.11f** to **1.11h**, with an increasing number of OH groups, the SmA phase becomes more stable and the smectic temperature range become broader despite the increased lateral bulk.²⁵



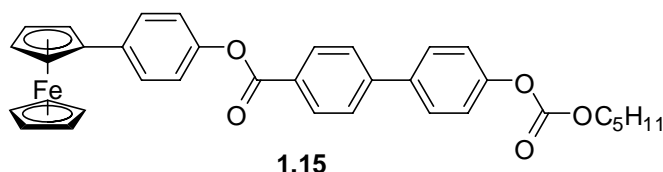
Ferroelectric LCs were reported based on the benzoic acid-pyridine hydrogen bonding pair. Complex **1.12** exhibits chiral nematic and blue phases with $n = 1, 2$ and chiral SmC* phases with $n \geq 5$,²⁶ while complex **1.13** shows a narrow SmC* phase with a maximum spontaneous polarization of 16 nC/cm^2 at $91 \text{ }^\circ\text{C}$.²⁷



LCs with a larger aspect ratio usually show more stable mesogenic behaviour. Interestingly, compound **1.14** with a shorter methyl carbonate tail forms a broader enantiotropic nematic phase than compound **1.15**, even though the latter has a longer tail and larger aspect ratio. It is proposed that hydrogen bonding between the ester methyl hydrogen and the ester carbonyl oxygen stabilizes the liquid crystalline phase by changing the overall L-shape topography to a more rod-like shape. Such dimerization cannot occur with **1.15** because the bulkier pentyl group prevents hydrogen bonding interactions. The evidence for hydrogen bonding in **1.14** is from X-Ray crystallographic analysis which reveals that the distance between the methyl carbonate hydrogen and the ester carbonyl oxygen in a neighbouring molecule is within the range of effective hydrogen bonding.²⁸



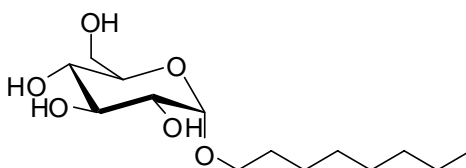
Cr 166 N 194 I



Cr (170 N) 187 I

1.1.4.2 Hydrogen Bonding in Amphiphilic Mesogens

The liquid crystalline behaviour exhibited by amphiphilic carbohydrates was first reported by Fischer and Helferich in 1911²⁹ and characterized by Noller and Rockwell³⁰ in 1938. Considering the variety of available structures, it is not surprising that numerous amphiphilic LCs have been synthesized. Hydrogen bonding is crucial for their mesogenicity. For example, α -D-glucopyranoside **1.16** is mesogenic while the fully acetylated carbohydrate is not.³¹ Normally, carbohydrate amphiphiles with one lipophilic chain form smectic phases, while carbohydrates with more than one lipophilic chain form columnar mesophases.¹⁸



1.16 Cr 72 SmA 116 I

Van Doren and coworkers investigated the liquid crystalline behaviors of six homologous series of D-glucose and 2-deoxy-D-glucose derivatives with an amino-linked alkyl chain (Figure 1.22). It was found that all the compounds exhibit only a SmA phase with layer spacing in a range of $l < d < 2l$, where l is the molecular length of the fully extended molecule and d is the calculated layer thickness.³²

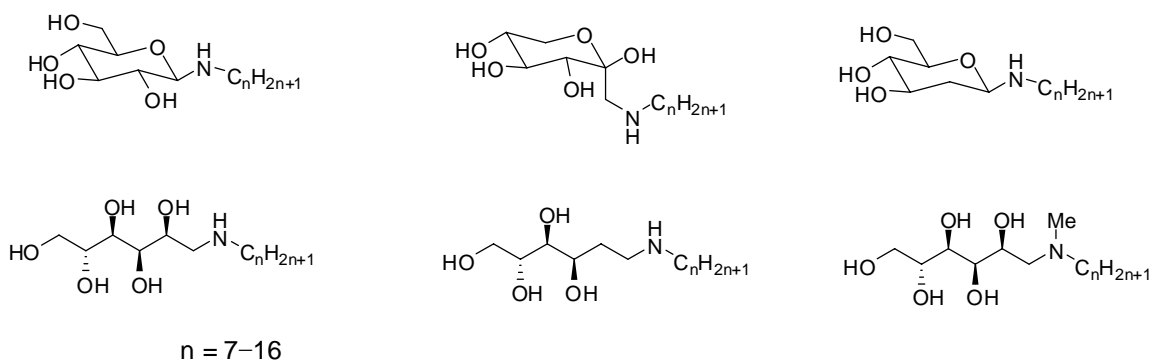


Figure 1.22 The carbohydrates forming only a SmA mesophase.

Two models were proposed for the arrangement of molecules within the layer (Figure 1.23). In model I, bilayers were formed with the carbohydrate moieties partially overlapped in a dynamic hydrogen bonding network and the alkyl chains pointing outwards. However, this model was questioned by Jeffery because the melting points of such amphiphilic carbohydrates change very little with lengthening of the chain while clearing points increase a lot. An alternate model II was proposed with an opposite layer structure. The extended alkyl chains form the core of the smectic layers with the carbohydrate moieties on the exterior as in lamellar lyotropic phases.³³ The rigid interdigitated packing model may explain why only a SmA phase formed.

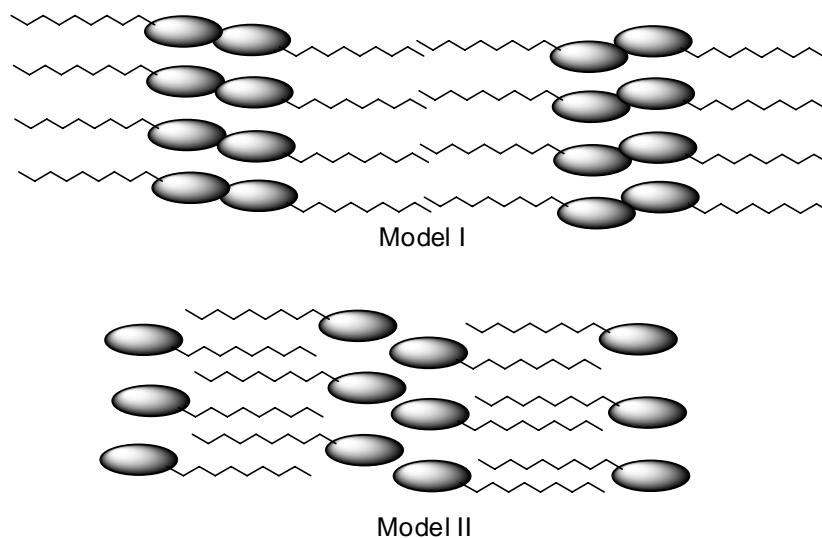


Figure 1.23 The lamellar structures for two models: I and II.

Dithioacetal aldoses (Figure 1.24) have been shown to form a columnar hexagonal mesophase. These compounds, although different in stereochemistry, form only one type of disc-shaped multimer by hydrogen bonding which was proved by X-ray diffraction. A mesophase structure was proposed with the sugar parts of the molecules forming the core of the column surrounded by thioalkyl groups in the periphery. However, an analogous 6-deoxy sugar dithioacetal did not show mesogenicity. This indicated that the terminal hydroxyl function is essential for this molecular arrangement.³⁴

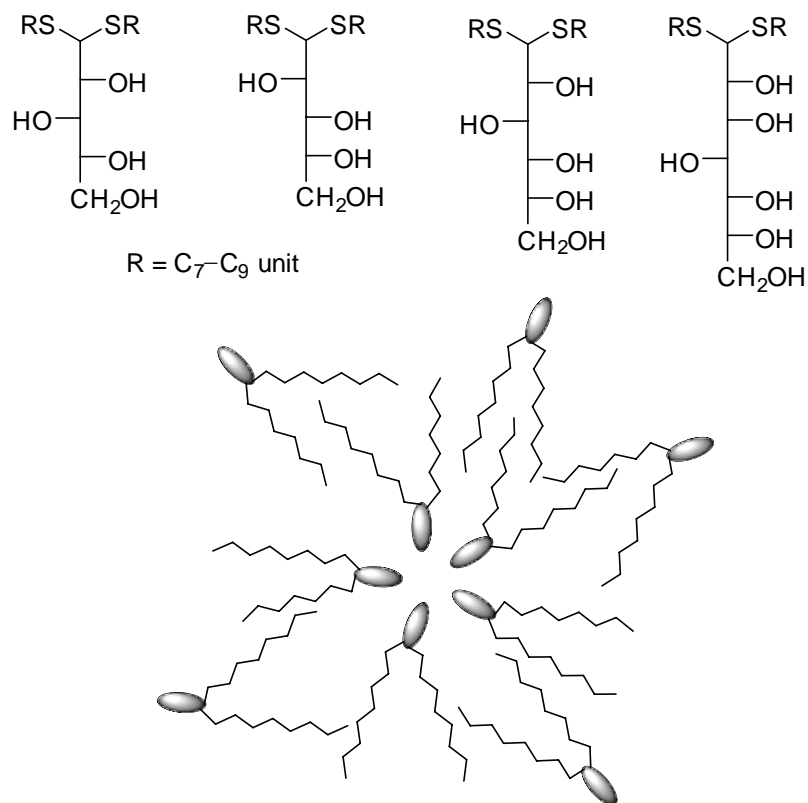
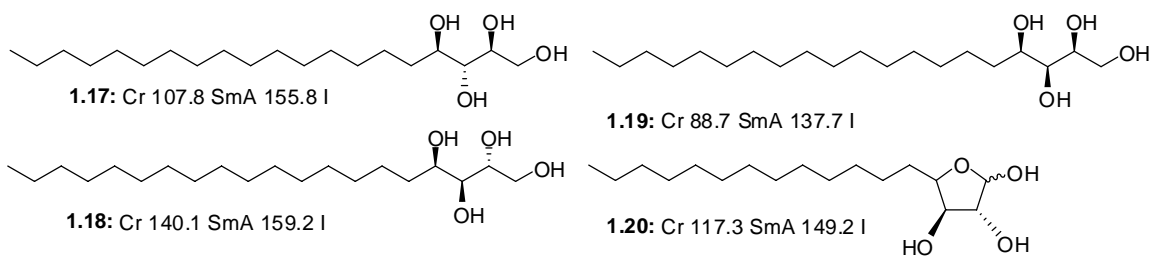


Figure 1.24 The dithioacetal aldoses and the representation of the hexagonal columnar mesophase.

Some polyols with one polar head may form thermotropic liquid crystals depending on the tendency of the hydroxyl groups to form a dynamic network via cooperative hydrogen bonding and on their location at the ends of lipophilic chains. For example, the four polyols **1.17**–**1.20** have been shown to form SmA phases.³⁵

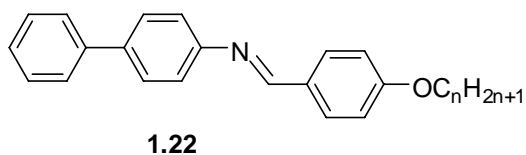
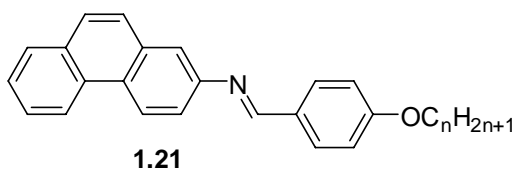


1.1.5 Liquid Crystals Containing Phenanthrene Core Structures

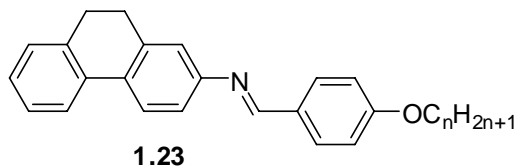
Liquid crystalline phenanthrene compounds are analogues of the more common biphenyl LCs. However, studies on such LC systems are comparatively few due, in part, to the difficulty in the synthesis of such systems with appropriate substitution patterns (almost exclusively 2- or 2,7-substituents) by classical routes.

The phenanthrene core is flat and fully conjugated. Therefore, it is more polarizable than the conventional biphenyl core, which is non-planar in the ground state. This favours $\pi-\pi$ stacking interactions and promotes the formation of smectic phases *via* microsegregation. Furthermore, the permanent transverse dipole moment of a phenanthrene core is likely to stabilize the SmC phase.³⁶ However, the lateral bulk of the bridging groups is considered to destabilize potential SmC phases.³⁷

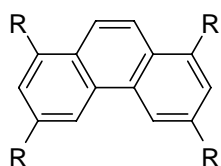
The first LCs with phenanthrene cores were reported by Gray in 1958. To investigate the effects of increasing the breadth and polarizability of molecules on their mesogenic behaviour, he prepared the mono-substituted phenanthrene aniline **1.21** to compare with the analogous biphenyl aniline **1.22**. Most compounds in these two series were shown to form a nematic phase and an unspecified smectic phase. Changing the core from biphenyl to phenanthrene destabilized the smectic phase by lowering the transition temperature by *ca* 16 °C (average value when $n = 6-10$), but stabilized the nematic phase by increasing the transition temperature by *ca* 26 °C (average value when $n = 1-10$).³⁸



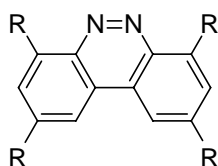
Further studies were carried out by Byron and coworkers in 1983 who compared the thermal behaviours of the analogous 9,10-dihydrophenanthrene LCs **1.23** with **1.21** and **1.22**. It was shown that the mesophases formed by **1.23** are less stable than those of **1.21** and **1.22**. This can be explained by that fact that **1.23** is laterally more bulky than **1.21** and **1.22** and less polarizable than **1.21**.³⁹



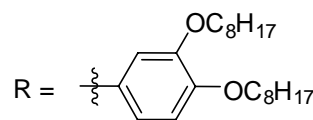
Recently, phenanthrene and its derivative cores have been investigated as discotic mesogens rather than as calamitic mesogens. In 2007, Kaszynski and coworkers synthesized and reported the mesogenic behaviours of 1,3,6,8-tetrasubstituted phenanthrene **1.24** and its diaza-derivative **1.25**. Compound **1.24** is not mesogenic and a columnar hexagonal phase is formed by **1.25** due to the presence of nitrogens whose sterically less hindered lone pairs are thought to lower the planarization barriers.⁴⁰



1.24



1.25: Cr₁ 19 Cr₂ 92 Col_h 168 I



The first report by Scherowsky and coworkers of ferroelectric liquid crystals with phenanthrene cores (type I) appeared in 1994. The disc-like 1,2,3,6,8,-pentasubstituted and 1,2,3,6,7,8-hexasubstituted phenanthrenes bearing (*R*)-2-(oct-2-yloxy) side chains **1.26a** and **1.27a** form a broad columnar phase.⁴¹ The disc plane is tilted with respect to the columnar axis (Figure **1.25**)⁴² and is switchable under an electric field. The 1:1 mixture of chiral **1.27b** and nonchiral **1.27c** shows a linear electrical switching property.

The switching angle for this mixture is $\pm 5^\circ$ under $\pm 5 \text{ V } \mu\text{m}^{-1}$ and rises to $\pm 20^\circ$ under $\pm 20 \text{ V } \mu\text{m}^{-1}$. The change of temperature has a weak influence on the switching angle.⁴²

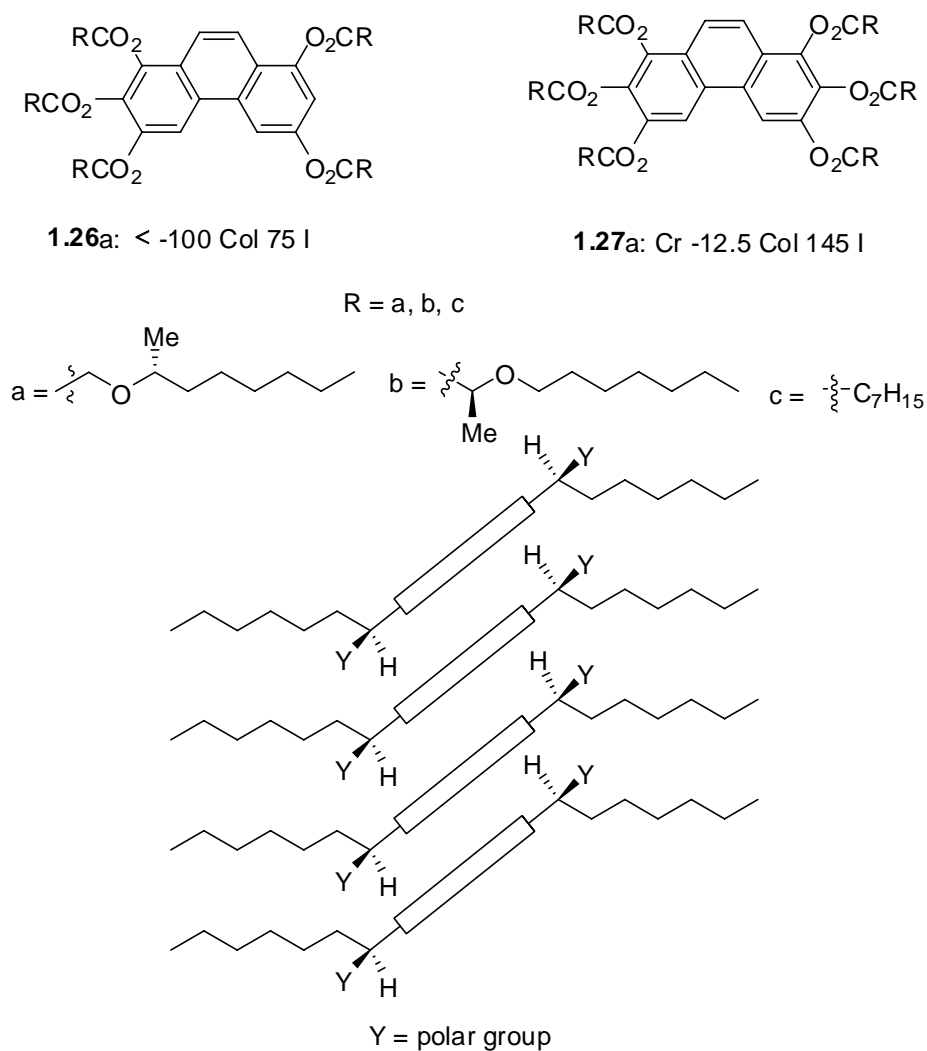
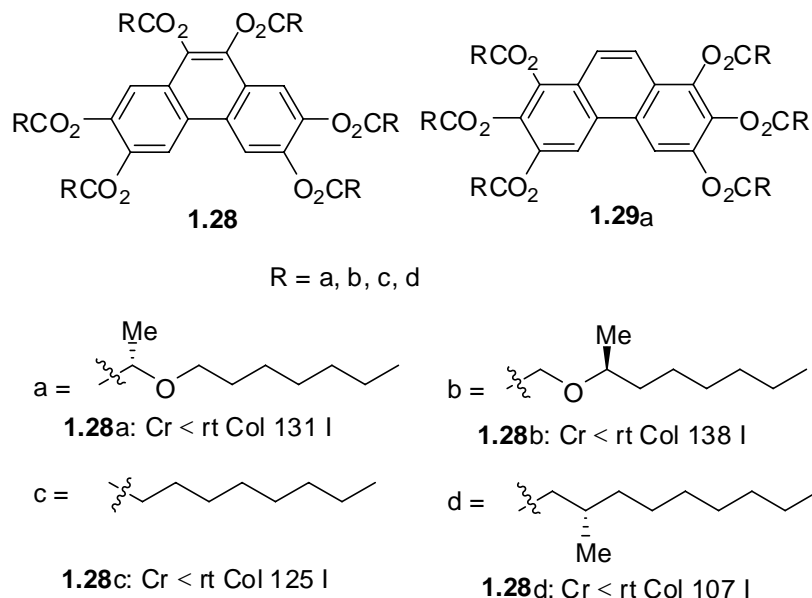


Figure 1.25 Phenanthrene core liquid crystal compounds and the representation of a tilted chiral column.

The modified version of phenanthrene derivatives **1.28a–d** appeared one year later with a discussion of spontaneous polarization. A very broad enantiotropic columnar phase is formed by the chiral derivatives **1.28a,b,d**. The columnar phase is stabilized by

the insertion of oxygen into the side-chain (compare **1.28b** and **1.28d**) and destabilized when the chiral center approaches the mesogenic core (compare **1.28a** and **1.28b**). No phase transition from the discotic to crystalline phase was observed by DSC measurements. Compound **1.29a** is not mesogenic, but a mixture of **1.28a** (15%) and **1.29a** (85%) exhibit a spontaneous polarization up to ca 54 nC/cm^{-1} at $42 \text{ }^\circ\text{C}$.⁴²



1.1.6 Mesogen Design Considerations

As discussed in the above review, intermolecular hydrogen bonding may be harnessed to promote the formation of liquid crystal phases and/or to modify their bulk properties. Extensive studies have focused on the effect of hydrogen bonding on the promotion of mesogenicity and the stabilization of mesophases. However, to date, knowledge about the relationship between hydrogen bonding and polar order of SmC^* mesophase is limited. In the work of a previous group member, Adam McCubbin, a chiral compound with a fluorenol core **1.30** was synthesized and shown to form a SmC^* phase with a negative spontaneous polarization of -10.7 nC/cm^{-1} at 10 K below the

I—SmC* transition point ($T-T_c = -10$ K). The measurable P_s is explained by the fact that fluorene cores are slightly bent (24° in the crystal structure), which limits their free rotation with respect to the side chains while maintain the zig-zag shape imposed by the smectic C* phase (Figure 1.26). Because of this rotational bias, the transverse dipole moment of the chiral fluorene may have a preferred orientation along the SmC* polar axis dependent on its absolute configuration, and may therefore contribute to the spontaneous polarization.

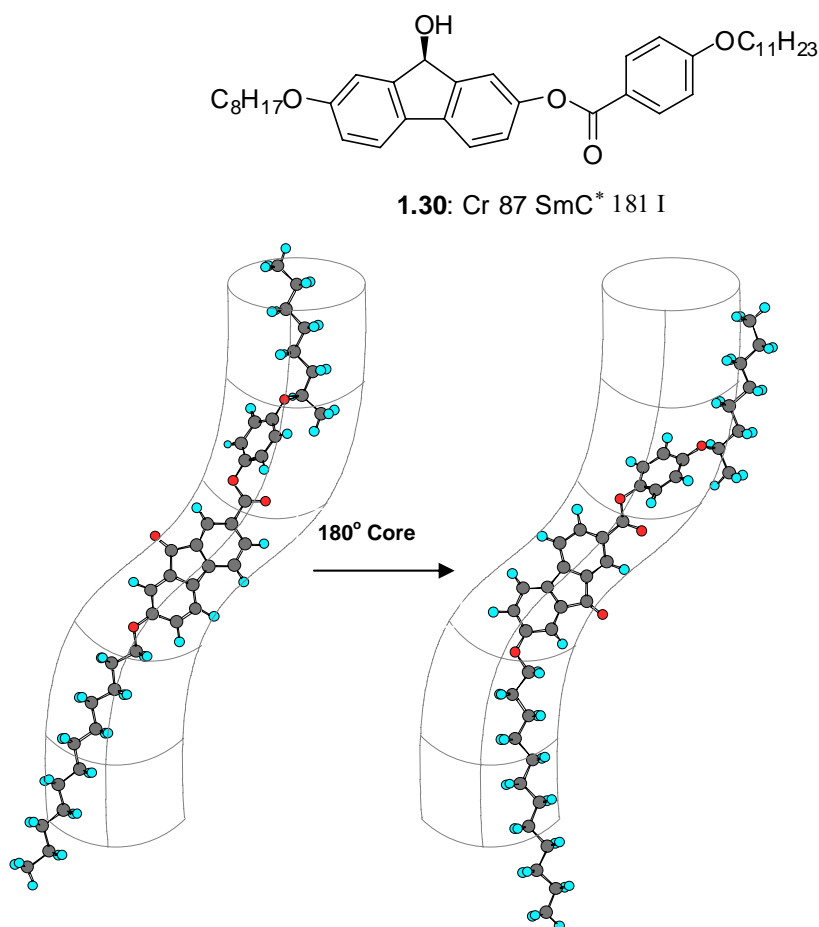
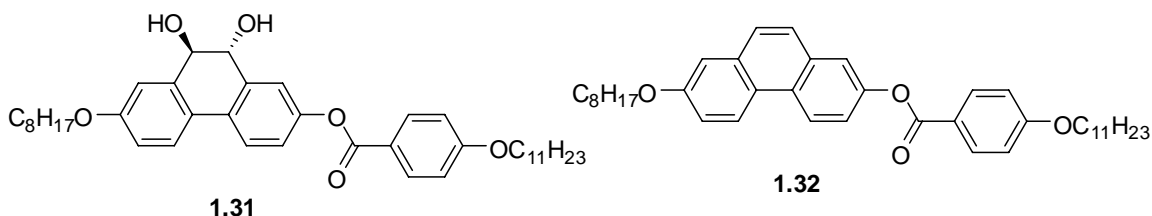


Figure 1.26 Molecular models (MM2) of **1.30** in relation to the mean-field potential according to the Boulder model. From left to right the fluorene core is rotated 180° with respect to the two side chains.

However a conformational analysis of **1.30** based on AM1 calculations suggest that there are only very subtle energy differences between conformations with different polar orientation. Thus, it is not clear whether the observed Ps is due to the conformational bias arising from the bent shape of the fluorenol core, or to intermolecular hydrogen bonding interactions *via* a cooperative effect.⁴³

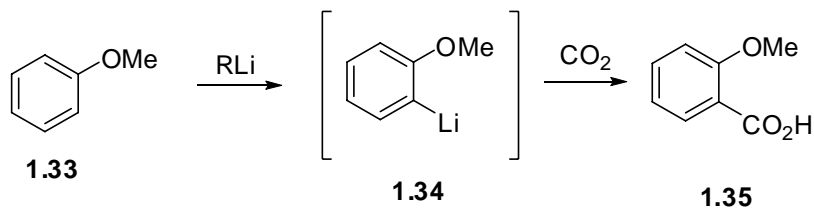
As a continuation of previous work and to answer the above question, a dihydrophenanthrenediol **1.31** was designed. One feature of this compound is that it has a linear core structure which should minimize any rotational bias in the SmC* phase that would contribute to polar ordering. If a Ps is observable in such a system, it may be attributed entirely to intermolecular hydrogen bonding. Furthermore, more intermolecular hydrogen bonds are expected because of the presence of the additional hydroxyl group in the core. As in compound **1.30**, the stereo-polar unit is located in the more ordered core region instead of the side chains to maximize the propagation and/or amplification of chirality transfer. It was envisaged that the chirality of compound **1.31** might be amplified by cooperative hydrogen bonding interactions, thus resulting in an increased polar order and increased Ps. Prior to undertaking the synthesis of **1.31**, compound **1.32** is to serve as model to determine the mesogenic properties of such a system, including whether it forms a SmC phase.



1.2 Synthetic Methodology

1.2.1 The Directed *ortho* Metalation (DoM) Reaction

The traditional method for the preparation of polysubstituted aromatic compounds involves the use of electrophilic aromatic substitution (EAS),⁴⁴ a methodology which is handicapped by poor and/or unpredictable regioselectivity. Over 60 years ago, Gilman⁴⁵ and Wittig⁴⁶ independently discovered the first example of the reaction which is currently known as the directed *ortho* metalation (DoM) reaction: the treatment of anisole with alkyllithium, followed by quench with CO₂ resulted in the formation of *ortho*-anisic acid **1.35** (Scheme 1.1). Their work initiated the development of the DoM reaction which changed profoundly the face of aromatic chemistry. The DoM strategy has evolved as a reliable method for the synthesis of contiguously substituted aromatic molecules in both industrial⁴⁷ and academic fields.^{48, 49, 50}



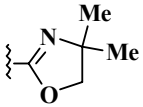
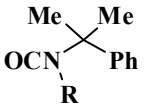
Scheme 1.1

The DoM reaction, simplistically described in Scheme 1.1, involves deprotonation *ortho* to a directed metalation group (DMG), e.g. OMe, by an alkyllithium or lithium amide base to give anionic intermediate **1.34**. Subsequent quench with an electrophile, e.g. CO₂, affords a 1,2-disubstituted aromatic **1.35**.

Due to the strongly basic environment of DoM reactions, DMGs must not be electrophilic. Steric hindrance and charge deactivation factors should be taken into the consideration for designing a good DMG. Over 60 years since the discovery of the DoM

reaction,^{45,46} variety of DMGs have been developed, which are classified as carbon- and heteroatom-based DMGs referring to the atom directly connected to the aromatic ring.⁵¹ In the selected DMGs listed in Table 1.1, carbon-based *N,N*-diethyl carboxamide, discovered by Beak in 1977,⁵² is one of the most popular DMGs in DoM chemistry by virtue of its strong directing effect and tolerance to nucleophilic attack at low temperatures. The oxazoline group, another carbon based DMG, invented by Meyers,⁵³ stands as a good DMG because it may be hydrolyzed to a carboxylic acid derivative after serving its purpose. The vigorous conditions for the hydrolysis (reflux in 4.5 M HCl) handicap the application of this methodology though. Among the heteroatom based DMGs, *N,N*-diethyl-*O*-carbamate, discovered and developed in the Snieckus laboratories in 1983,⁵⁴ occurs with a stronger directing effect compared to the corresponding *N,N*-diethyl carboxamide. Furthermore, it participates in several other anion-mediated transformations by connection with anionic *ortho*-Fries rearrangement and the directed remote metalation (DreM) (*vide infra*).^{52a} Some other heteroatom DMGs such as the *O*-sulfamate and *O*-phosphoramidate not only act as DMGs, but also exhibit facile Kumada-like cross coupling characteristics.⁵⁵ The relative efficiencies of DMGs in DoM reactions have been determined by intramolecular and intermolecular competition studies (Figure 1.26).⁵⁶

Table 1.1 Typical DMGs.

Carbon Based		Year	Heteroatom Based		Year
CONR	Hauser ⁵⁷	1964	OMe Wittig, ^{46b} Gilman ⁴⁵		1938,1939
	Meyers ⁵³	1975	SO ₂ NR ₂	Hauser ⁵⁸	1969
CONR ₂	Beak ⁵²	1977	NHBoc	Gschwend ⁵⁹	1979
CONR ₂	Beak ⁵²	1977	OCONEt ₂	Snieckus ⁵⁴	1983
CF ₃	Gschwend ⁶⁰	1979	NHCO ₂ <i>t</i> Bu	Muchowski ⁶¹	1989
CO ₂	Mortier ⁶²	1994	P(O) <i>t</i> Bu ₂	Snieckus ⁶³	1998
	Snieckus ⁶⁴	1999	OSO ₂ NR ₂	Snieckus ⁵²	2003
			OP(O)NEt ₂	Snieckus ⁶⁵	2003

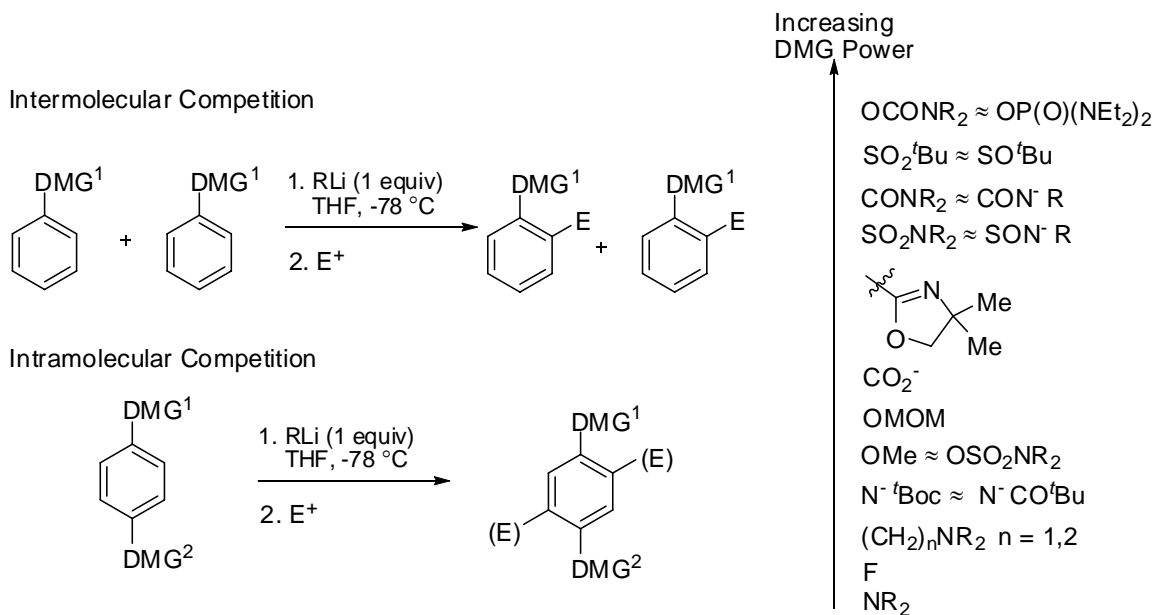
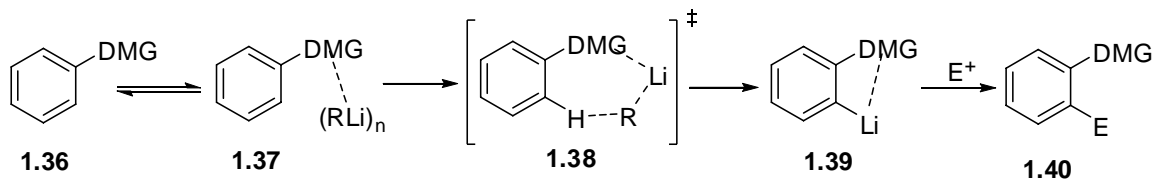


Figure 1.26 Hierarchy of DMGs.

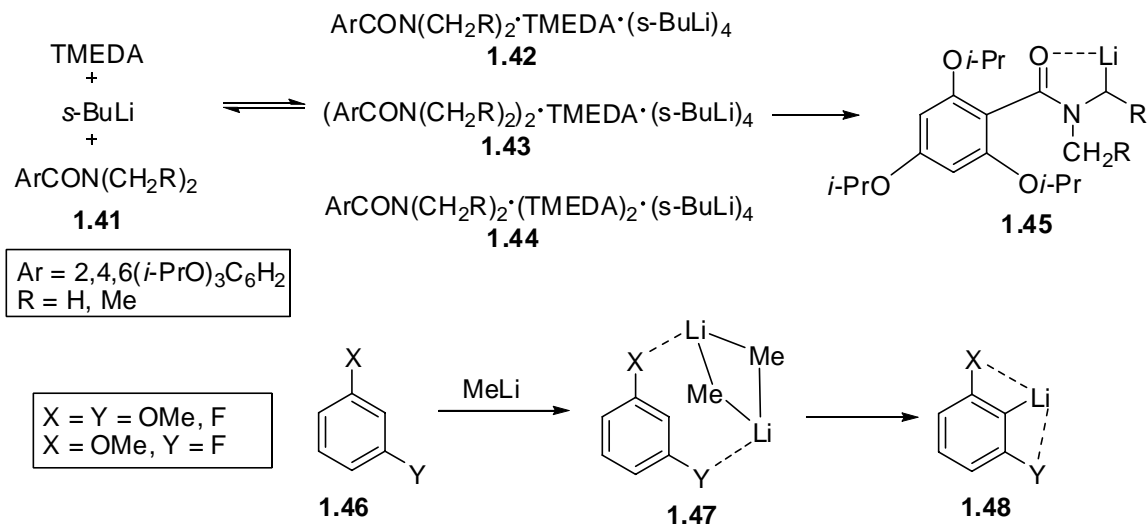
1.2.2 The Mechanism of the DoM Reaction

Although the DoM reaction has enjoyed broad utility for the synthesis of polysubstituted aromatic and heteroaromatic molecules, its mechanism remains a controversial subject.⁶⁶ In 1946, Roberts and Curtin,⁶⁷ suggested that the DoM reaction might involve an initial coordination of the BuLi with the lone pair of DMGs on the basis of the fact that the activation effect of CF₃ for benzene towards metalation is less than that of MeO. Based on this hypothesis, Beak and Meyers⁶⁸ proposed a two-step mechanism for the DoM reaction, involving an initial process referred to as the complex induced proximity effect (CIPE), a concept suggesting that the coordination of a DMG with the base brings reactive groups into the proximity of a reaction center. The mechanism is presented in Scheme 1.2. It proceeds by precoordination of the DMG with a lithium base to afford complex **1.37**. Subsequent lithiation via **1.38** gives **1.39**, which, upon electrophile quench, affords product **1.40**.



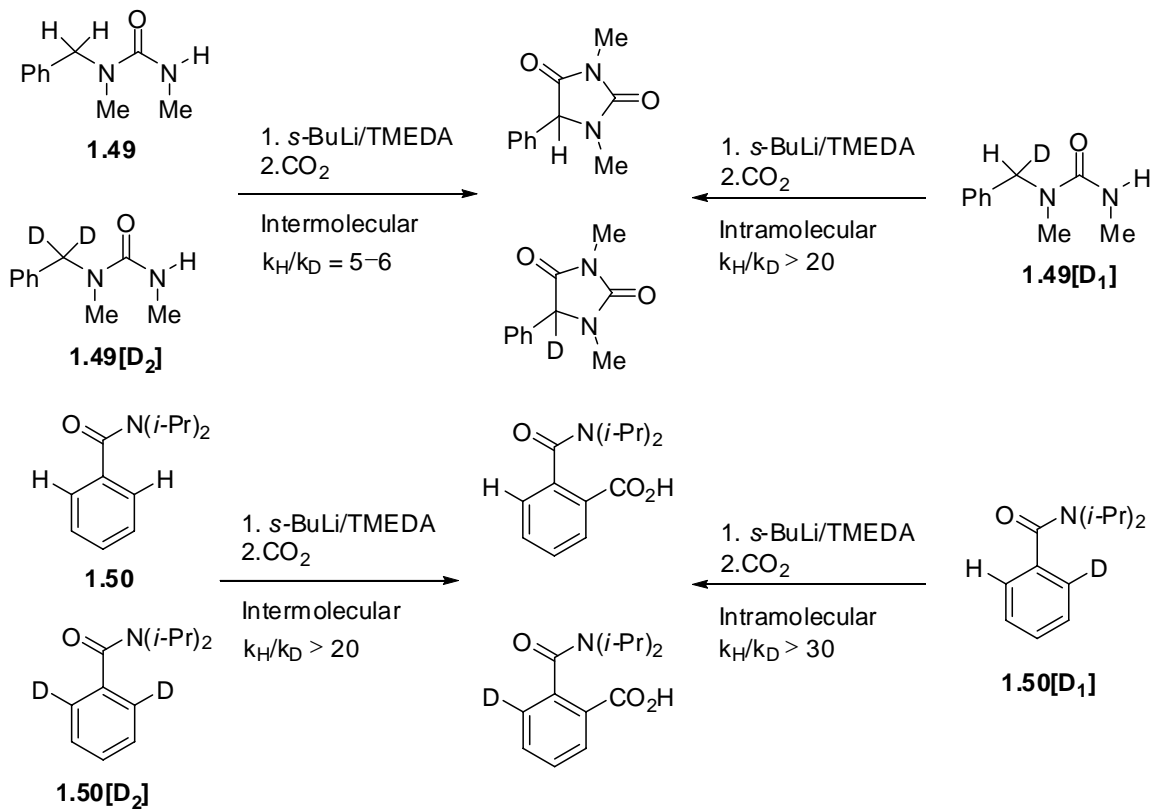
Scheme 1.2

Indirect evidence for this mechanism came from a stopped-flow IR spectroscopic study on the α' -metalation of *N,N*-dialkylbenzamides **1.41** with *s*-BuLi/TMEDA, which suggested the presence of amide-Li complex intermediates **1.42**, **1.43**, **1.44** before the formation of the lithiated product **1.45**.⁶⁹ Saa and coworkers found theoretical (MNDO) evidence for the formation of weak, chelated complexes **1.47** in the lithiation of 1,3-disubstituted aromatics **1.46**,⁷⁰ which suggests that a coordination event leads to a deprotonation process.



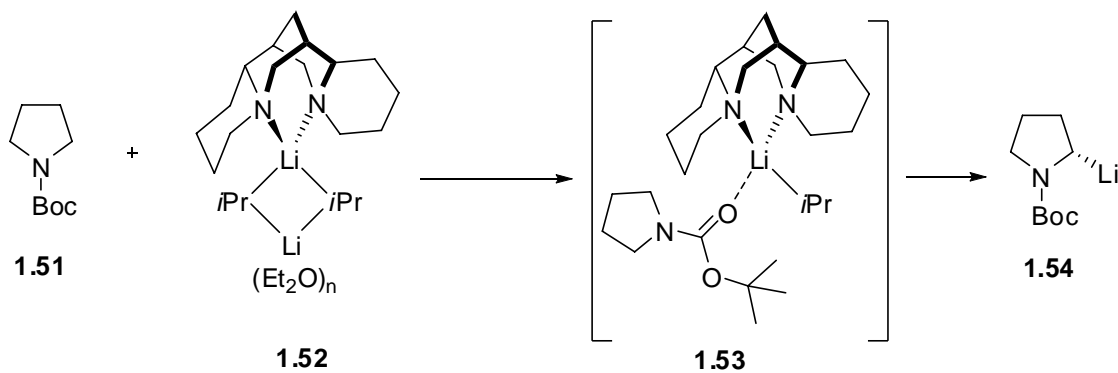
Scheme 1.2

The strongest, although indirect, evidence to support the CIPE mechanism comes from inter- and intramolecular kinetic isotope effect (KIEs) studies (Scheme 1.3).⁷¹ For the metalation of urea **1.49** (Scheme 1.3), if it proceeds by a one-step mechanism without prior complexation, approximately the same value of k_H/k_D is expected in both intermolecular and intramolecular cases, because the base has no choice of selection between protium and deuterium. Since this is not consistent with the experiment data which established $k_H/k_{D(\text{inter})} = 5\text{--}6$ and $k_H/k_{D(\text{intra})} > 20$, a one-step mechanism is safely excluded.^b However, the application of this approach to DoM on compound **1.50** resulted in comparable inter- and intramolecular KIEs: $k_H/k_{D(\text{inter})} > 20$ and $k_H/k_{D(\text{intra})} > 30$.^a Although this does not allow to differentiate definitely one- or two-step mechanism for DoM, the high intermolecular KIE excludes a pathway of a slow irreversible complexation following by a quick protium/deuterium transfer and indicates that deprotonation is the rating-determining step. If the lithiation of **1.49** and **1.50** is assumed to follow a similar pathway, the mechanism for DoM should be a quick reversible precoordination followed by a slow deprotonation.



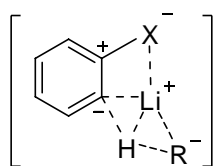
Scheme 1.3

The CIPE mechanism is further supported by the kinetic studies of the α -lithiation of *N*-Boc-pyrrolidine **1.51**.⁷² It was observed that the reaction is independent of the concentration of the sparteine-*i*-PrLi base complex **1.52**. The observed pseudo-first-order reaction kinetics is in agreement with the fast formation of complex **1.53**.



Scheme 1.4

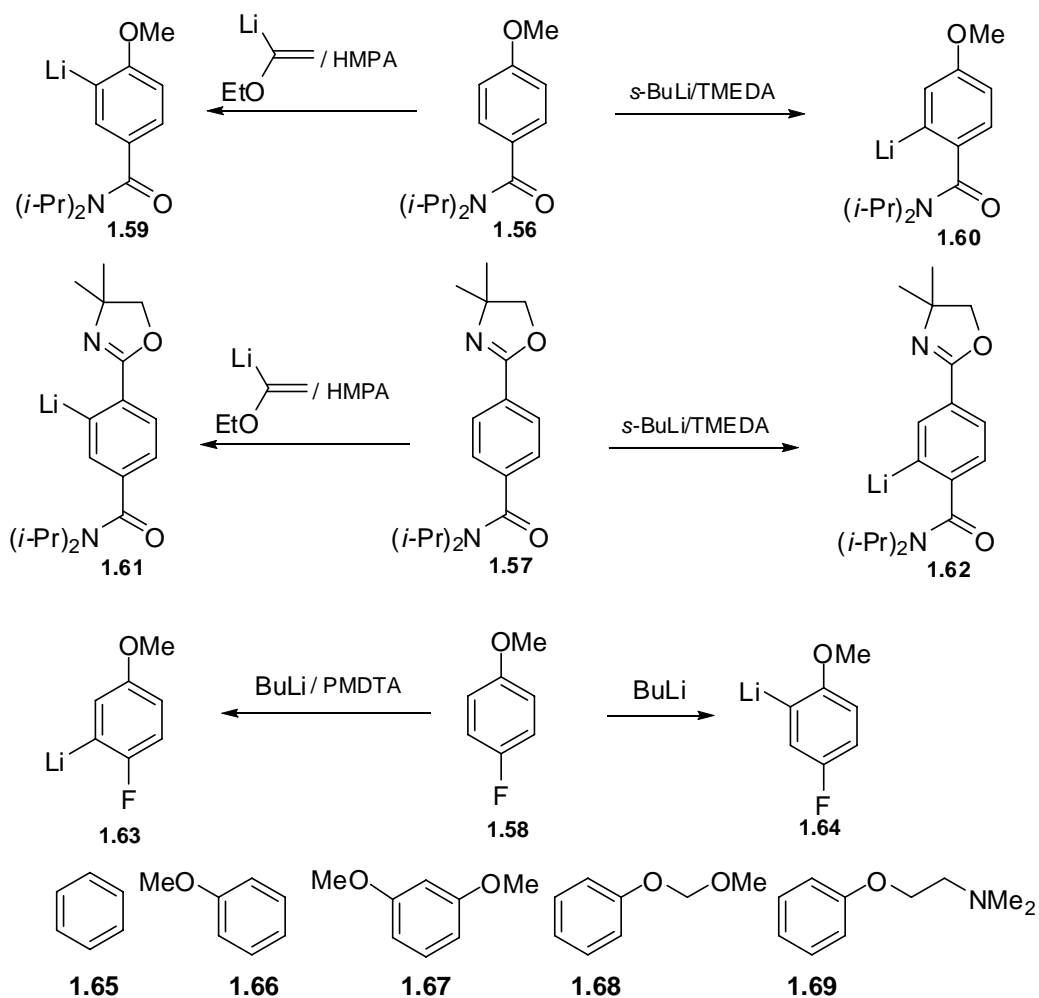
The existence of prelithiation complexes is supported by considerable evidence.⁷³ However, it was questioned by Schleyer based on his studies on the lithiation of anisole.⁷⁴ Treatment of anisole with *n*-butyllithium in toluene-*d*₈ at -64 °C in a 1:1 ratio resulted in the formation of a coordination complex as identified by ¹H, ¹³C and HOESY NMR spectroscopy which, however did not undergo lithiation even at rt. On the other hand, by the same spectroscopic tools, anisole was observed in a “free” state in a 1:1:1 ratio with *n*-butyllithium and TMEDA. In this form, anisole proved to be readily metalated at 0 °C despite its “free” character. This indicates that the precoordination may not be involved in the DoM process. Schleyer proposed a one-step mechanism, named kinetically enhanced metalation (KEM), based on *ab initio* calculations, in which complexation and deprotonation occur at the same time.⁷⁵ According to this mechanism, the directing and accelerating effect of the DMGs is not due to the prior complexation, but the stabilization of the transition state **1.55**. The KIE studies by Stratakis support the one-step mechanism by the fact that the KIEs of inter- and intramolecular lithiation of anisole by *n*-BuLi in Et₂O are identical ($k_H/k_D = 2.5 \pm 0.2$).⁷⁶



1.55

In 1994, Meyers discovered two different selectivities in the metalation of **1.56** and **1.57**.⁷⁷ With α -ethoxyvinyl lithium (EVL)/HMPA, metalation occurred at the position *ortho* to the weaker DMG group (MeO) instead of the amide (Scheme 1.5). However, treatment of **1.56** and **1.57** with *s*-BuLi/TMEDA resulted in metalation *ortho* to the amide. A similar result was observed by the treatment of **1.58** with BuLi and

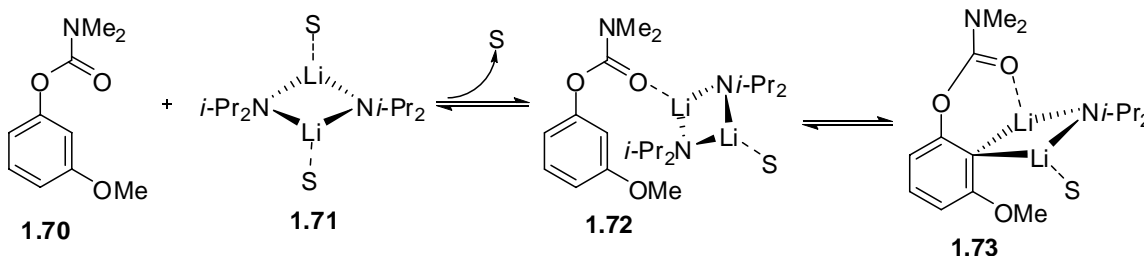
BuLi/pentamethyldiethylenetriamine (PMDTA).⁷⁸ This indicates the directing effect of DMGs may be operating as a result of coordination and acidity factors. Thus, if there is a strong DMG-base coordination, a CIPE mechanism is operative. On the other hand, if the coordination is undermined by a sterically bulky base such as EVL/HMPA, an inductive effect dominates. The importance of inductive effects in *DoM* chemistry is also supported by kinetic studies of Collum and coworkers.⁷⁹ By investigation of the *n*-BuLi/TMEDA mediated lithiation of arenes **1.65-1.69**, it was found that, while the lithiation rates for these five arenes are different, the rate laws are similar, which indicates strongly a common mechanism for all five cases. The different lithiation rates were ascribed to the different acidities based on inductive effects.



Scheme 1.5

In general, the DoM reaction is highly dependent on the nature of the DMGs, bases and solvents.⁸⁰ No single mechanism can be applied to all DMGs. The evidence up to date supports that strongly coordinating DMGs such as amides and *O*-carbamates tend to follow a CIPE mechanism, which was strongly supported by Collum's kinetic and structural studies on the anionic Snieckus-Fries rearrangement of aryl carbamate **1.70**.⁸¹ Through a careful choice of *meta*-substituents and solvents, Collum was able to spectroscopically (React-IR, and ⁶Li, ¹³C, ¹⁵N NMR) observe the precomplex **1.72** in *n*-

BuOMe before lithiated species **1.73**. On the other hand, as proposed by Beak,^{71b} weakly coordinating DMGs such as F and OMe may exert their directing effects by an inductive effect.

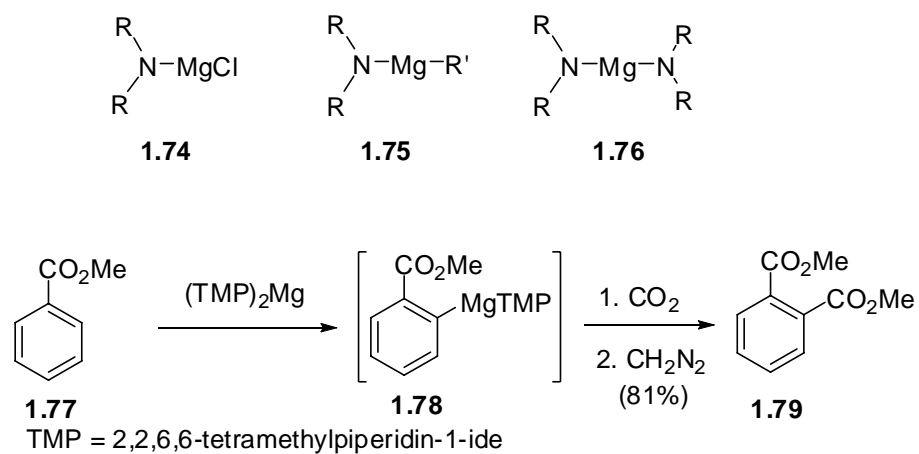


Scheme 1.6

1.2.3 Other Base Mediated DoMs

As mentioned above, alkyllithiums (RLi) and lithium amides (R₂NLi) are the traditional bases used in DoM chemistry. However, naturally, their strong nucleophilicity (Table 1.2) is not compatible with sensitive groups such as aldehydes, ketones, and esters. Furthermore, the extremely reactive and unstable features (Table 1.3) of these bases require *in situ* generation of the base (for lithium amides) or very low temp (< -78 °C for alkyllithiums), which sometimes negatively affect small-scale reactions and definitely complicates scale-up of these reactions. These drawbacks of using lithium bases have stimulated the development of alternative, less-nucleophilic metal bases for the DoM reaction. Eaton⁸² pioneered magnesium-based bases **1.74**, **1.75**, **1.76** as adjuncts or potential replacements of alkyl lithium and lithium amide bases in DoM. Existing as dimers in Et₂O at room temperature,⁸³ the lower nucleophilicity of these bases allows the use of esters as DMGs (Scheme 1.7). However, few applications have been found for the use of these bases due to their moderate solubility and low kinetic

basicity. Furthermore, the normal necessity of using a large excess of the bases (2-12 equiv) complicates the reactions with electrophiles (up to 10 equiv).



Scheme 1.7

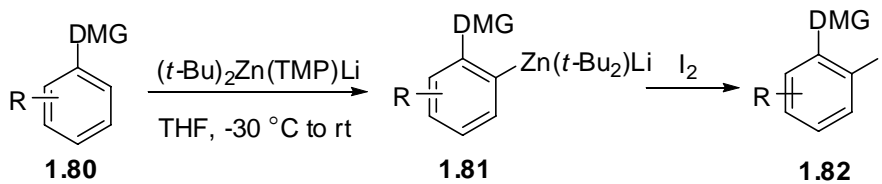
Table 1.2 The pKa values of selected conjugate acids of bases used in DoM.

	LDA ⁸⁴	LTMP ⁸²	<i>n</i> -BuLi	<i>s</i> -BuLi	<i>t</i> -BuLi
pKa	35.7(THF)	37.3(THF)	50	51	53

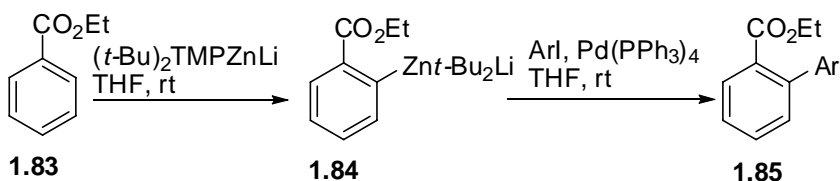
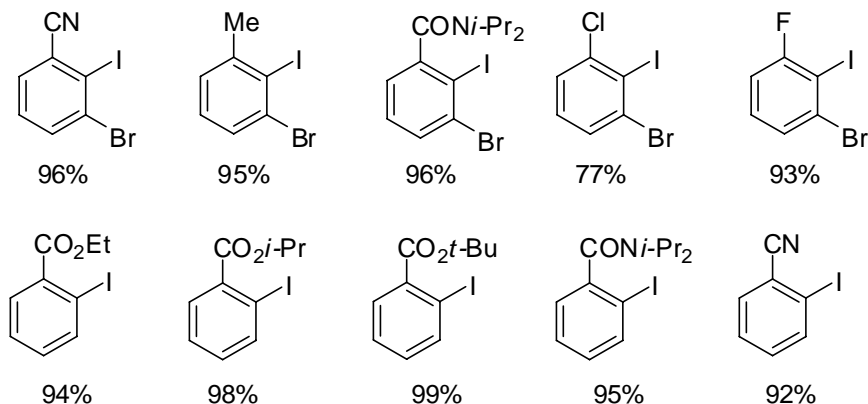
Table 1.3 The half-lives of butyllithium reagents in typical solvents.⁸⁵

Solvent/Temp (°C)	<i>n</i> -BuLi	<i>s</i> -BuLi	<i>t</i> -BuLi
THF/-20		80 min	40 min
THF/35	10 min		
THF/TMEDA/-20	3300 min		
THF/TMEDA/0	340 min		
THF/TMEDA/20	40 min		
Ether/-20		20 hr	480 min
Ether/0			61 min
Ether/20	153 hr		<30 min
Ether/TMEDA/ 20	600 min		
DME/-70		120 min	11 min
DME/-20	110 min	2 min	<2 min
DME/0	6 min		

In 1999, Kondo and coworkers invented lithium di-*t*-butyl(2,2,6,6-tetramethylpiperidino)zincate (*t*-Bu₂Zn(TMP)Li) and used it in the DoM reaction.⁸⁶ Arenes **1.80** bearing esters, nitriles and amides were regioselectively deprotonated at room temperature and the resulting zincates **1.81** were quenched with iodine to give products **1.82** in excellent yields (Scheme 1.8). Furthermore, the zincate **1.84** was used for Pd-catalyzed Negishi-like cross-coupling reactions to give biaryls **1.85**.^{86a}



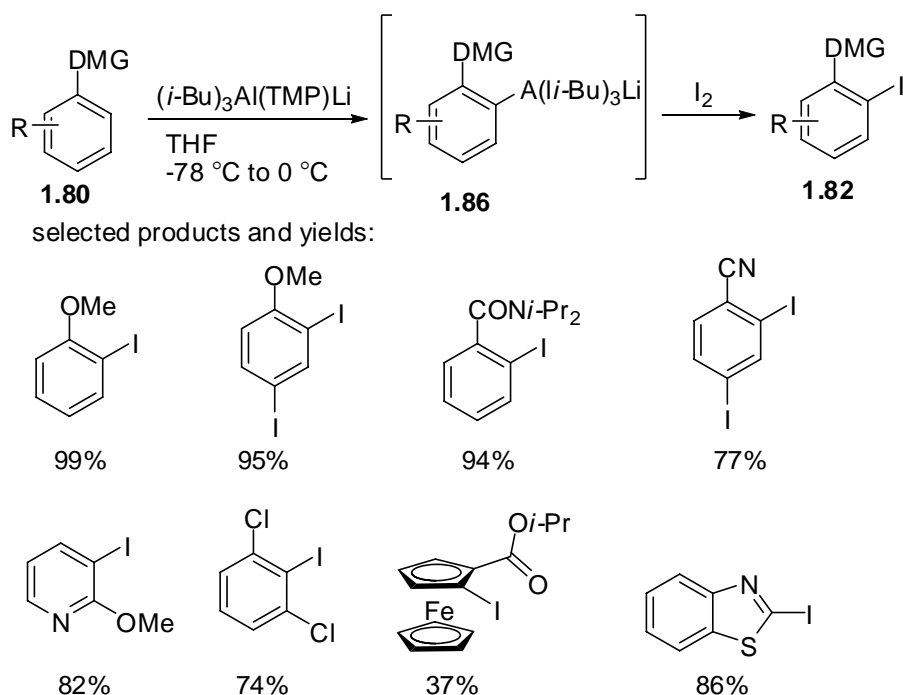
selected products and yields:



1.85a Ar = Ph 58%
1.85b Ar = 3-pyridyl 43%

Scheme 1.8

In 2004, Uchiyama and coworkers reported lithium triisobutyl(2,2,6,6-tetramethylpiperidino)aluminate-based DoM reaction.⁸⁷ Unlike dimerized magnesium-based bases, *i*-Bu₃Al(TMP)Li exists as a monomer in THF.⁸⁸ The *ortho* directed deprotonative alumination of **1.80** to give **1.86** was found to be applicable to a variety of functional groups such as OMe, CN and Cl as DMGs. In the process of alumination of 1-iodo-4-methoxybenzene and 4-iodobenzonitrile, benzyne formation was not observed (Scheme 1.9).



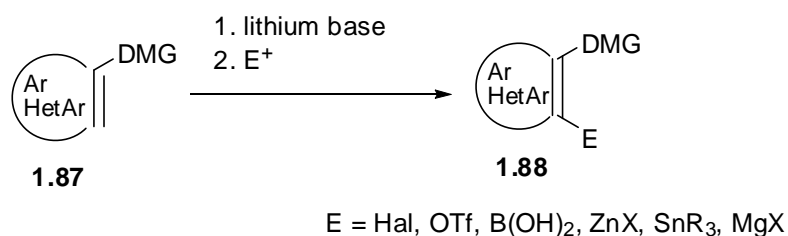
Scheme 1.9

Recently, Knochel developed mixed metal bases such as (TMP)MgCl·LiCl and (TMP)₂Zn·2MgCl₂·LiCl for use in DoM chemistry. The reactions using these bases are compatible not only with esters, nitriles and aryl ketones (for Mg/Li bases),⁸⁹ but also with extremely sensitive groups such as aldehydes and nitro groups (for Zn/Mg/Li bases).⁹⁰

Compared with the traditional lithium-based DoM reaction, the newly developed, softer metal base mediated metalation allows a broader range of functional groups to tolerate the reaction conditions. However, in comparison to lithium mediated metalation, the scope of these reactions has not yet been established.

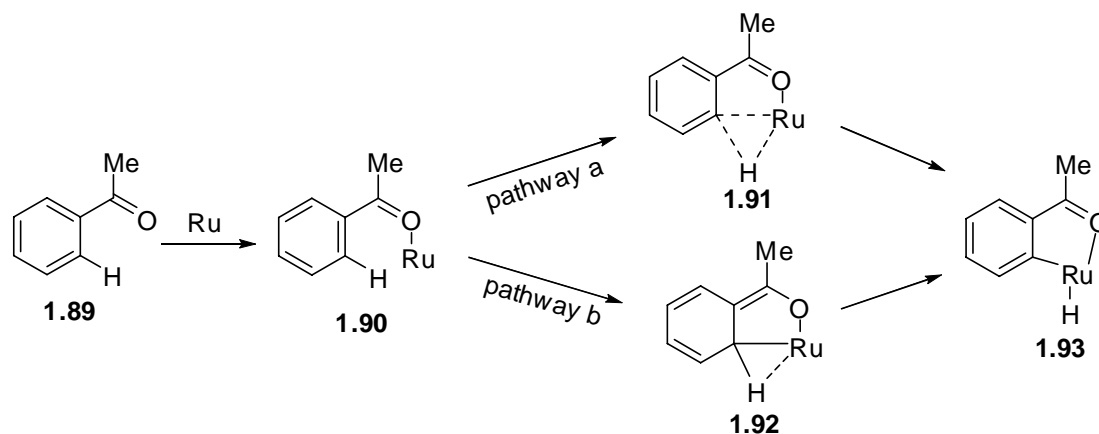
1.2.4 Directed C-H Activation

One of most the common applications of DoM chemistry is in the selective construction of activated species **1.88** for further cross-coupling. However, the obligation to stoichiometrically install and then subsequently dispose of the activating group E may be wasteful. Furthermore, preparation of such preactivated agents **1.88** often requires several steps. Therefore, the selective activation of a C-H bond assisted by a directing group to form a new C-C bond appears as an attractive alternative in the past decade, and may, in the near future, become a complementary/competitive methodology to DoM chemistry.⁹¹



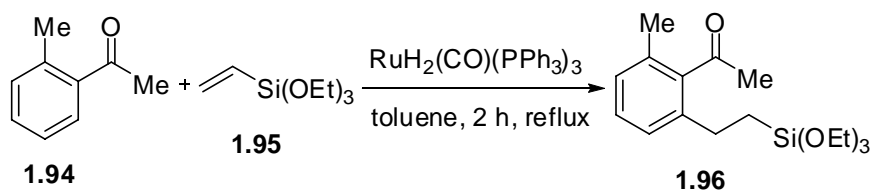
Scheme 1.10

Typically, directing group-assisted C-H activation involves nitrogen and oxygen coordinating functional groups to direct the activation of select C-H bond. The process is demonstrated in Scheme 1.11.⁹² An *ab initio* calculation study supported the pathway b mechanism.⁹³



Scheme 1.11

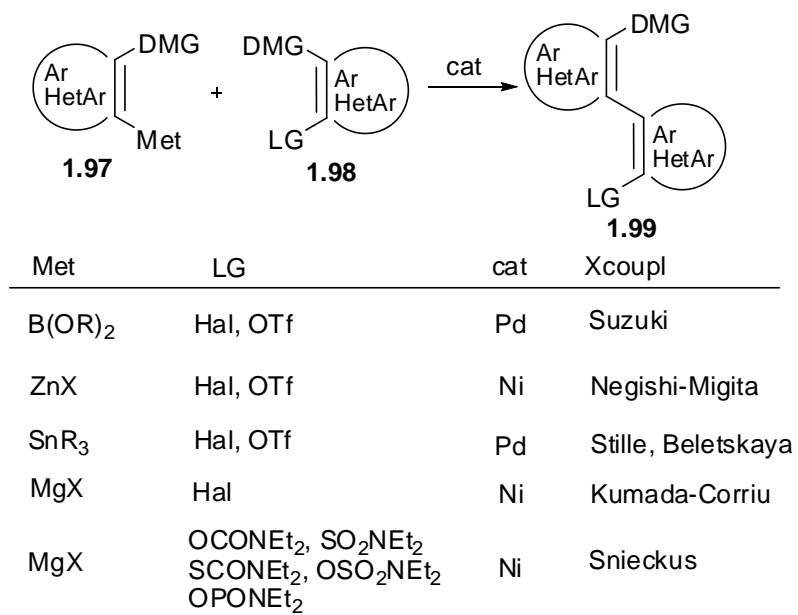
In 1993, Murai and Chatani first reported a ketone directed aromatic C-H activation/olefin coupling reaction in the presence of $\text{RuH}_2(\text{CO})(\text{PPh}_3)_3$ (Scheme 1.12).⁹⁴ Since then, a number of directing groups⁹⁵ such as hydroxyl,⁹⁶ esters,⁹⁷ aldehydes,⁹⁸ aldimines,⁹⁹ keteimines,¹⁰⁰ amidinates,¹⁰¹ hydrazones,¹⁰² nitriles¹⁰³ and carbonic acid¹⁰⁴ have been developed for various types of transformation such as C-H/olefin, C-H/acetylene, C-H/CO/olefin, C-H/aryl and C-H/ R_3Si couplings in the presence of Ru, Rh, Ir, Pd and Pt.¹⁰⁵ However, the methodology of the directed C-H activation has not been well established yet.



Scheme 1.12

1.2.5 The Combined DoM-Cross Coupling Reaction

Considering the presence of biaryl and heterobiaryl moieties in diverse classes of molecules, including natural products,¹⁰⁶ pharmaceuticals,¹⁰⁷ polymers,¹⁰⁸ and especially liquid crystals,¹⁰⁹ it is not surprising that the exploration of new methodologies¹¹⁰ to construct the key building blocks with typical substituent patterns has become a hot topic in the synthetic community since the time of the original reports of the first aryl-aryl bond forming reaction in 1941 by Kharasch.¹¹¹ The combination of DoM, which ensures regioselective construction of *ortho*-DMG boron, magnesium, zinc, and tin substrates allows efficient access to strategically functionalized biaryls and heterobiaryls (Scheme 1.13).¹¹²



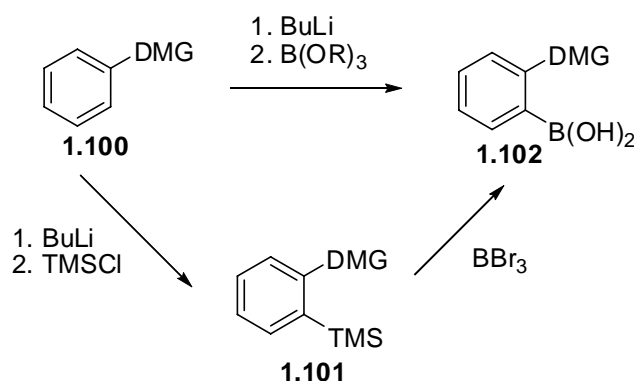
Scheme 1.13

The first transition metal-catalyzed cross-coupling reaction for biaryl formation, involving the reaction of ArMgX with ArHalide, was discovered independently by Kumada¹¹³ and Corriu¹¹⁴ in 1972. Four years later, an analogous nickel-catalyzed

coupling of ArZnX with ArHalide was discovered by Negishi.¹¹⁵ Negishi cross coupling reactions are compatible with a variety of substrate functional groups due to the lower nucleophilicity of organozincs compared with organomagnesiums. However, the applications of Kumada and Negishi cross coupling reactions are sometimes plagued by the unstable character of organozincs and organomagnesiums. The Stille¹¹⁶ cross coupling offers comparatively air- and water-stable organostannanes as the coupling partner; however, the toxicity of organostannanes, to some degree, limits the application of this method. The most widely used cross coupling method was discovered by Suzuki in 1979 using boronic acids as the organometallic species.¹¹⁷ Because of several advantages to this method, such as mild reaction conditions, commercial availability of a number of boronic acids, and environmental friendliness, the Suzuki cross coupling reaction has been developed into a general process for a wide range of selective carbon-carbon bond forming reactions.

The combination of DoM with the Suzuki cross-coupling protocol has been extensively studied in the Snieckus laboratories as a method which provides a variety of biphenyl-2-carboxamides with 2,2'-disubstituted and 2,2',6'-trisubstituted systems.^c The *ortho*-DMG arylboronic acids are readily available by metalation-boronation and metalation-silylation-*ipso*-borodesilylation sequences (Scheme 1.14).¹¹⁸ Due to their stability (and therefore commercial availability), low toxicity¹¹⁹ and structural diversity, boronic acids remarkably promote application of the combined DoM-cross-coupling strategy, e.g, in the fine chemical industry for the synthesis of comprehensive and diverse libraries of biaryls and heterobiaryls.¹²⁰ Although boronic acids normally undergo direct coupling as crude materials with aryl halides, they can be converted to stable derivatives

such as pinacolates and diethanol amine adducts,¹²¹ which are chromatographable and crystalline. Pd(PPh₃)₄ is widely used as the catalyst. For sterically hindered substrates, Pd₂(dba)₃ is often used. Base variation and solvent effects play a significant role in yield and efficacy of the process.¹¹²

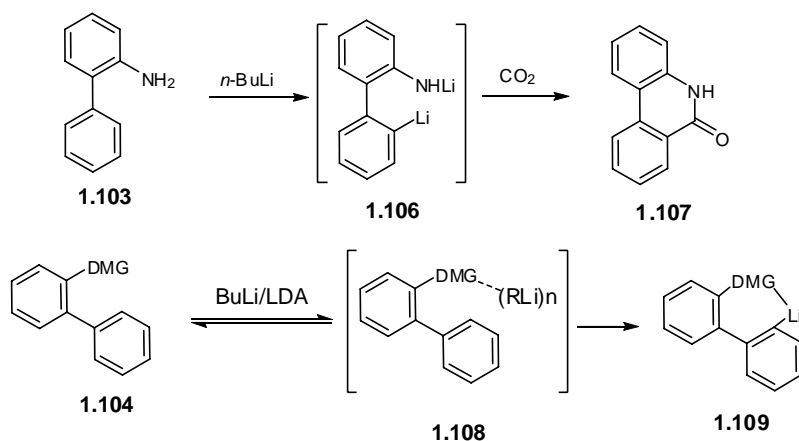


Scheme 1.14

1.2.6 The Directed Remote Metalation (DreM) Reaction

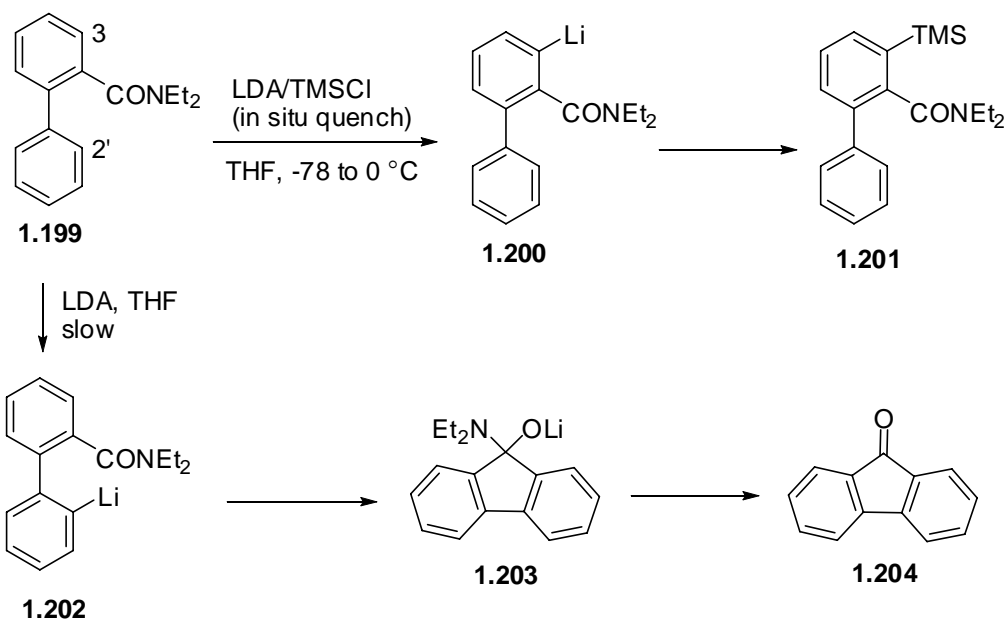
In 1969, Narasimhan reported a synthetic route from biaryl **1.103** to phenanthridin-6(5*H*)-one **1.107** (Scheme 1.15).¹²² This report may constitute the first case of a DreM reaction in the context of biaryls, although Narasimhan did not call it this way himself. Inspired by CIPE model of Beak and Meyers,⁶⁸ Snieckus¹²³ discovered and systematically developed a methodology of a DMG directed metalation of a C-H bond several bonds removed from the DMG, but with through-space proximity to it, which is referred to as the directed remote metalation (DreM). Today, DreM has been evolved as a general method to synthesize tricyclic systems such as fluorenones and phenanthrols (the aim of this thesis work, *vide infra*) by intramolecular cyclization of 2-DMG-bearing biaryls **1.104**. The mechanism of DreM may involve CIPE at a remote position to lead to

the deprotonation of a non-thermodynamically acidic hydrogen of **1.104** to give **1.109** (Scheme 1.15).



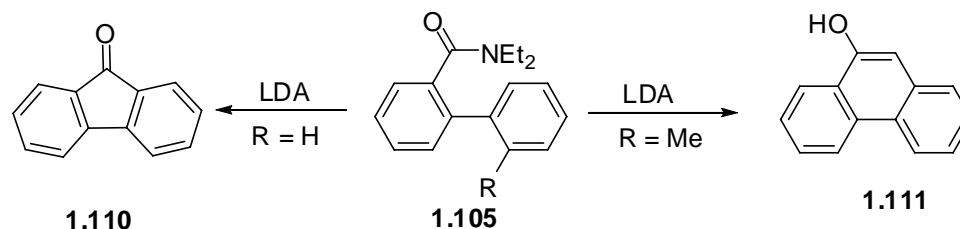
Scheme 1.15

A study by Snieckus and Mortier explored the mechanism of DreM (Scheme 1.16).¹²⁴ An *in situ* quench experiment using an excess of LDA/TMSCl premixed in THF ($-78\text{ }^\circ\text{C} \rightarrow 0\text{ }^\circ\text{C}$) prior to the addition of DMG-bearing biaryl **1.199** led to biarylsilane **1.201** exclusively. In contrast, LDA metalation in the absence of TMSCl led to the formation of fluorenone **1.204**. This suggests that the LDA-mediated DreM of **1.199** may involve initial complexation of **1.199** with LDA (CIPE), followed by formation of lithiated biaryl **1.200** in equilibrium. In the absence of electrophiles, the complex may lead to rate-determining deprotonation to **1.202**, which succumbs to faster cyclization to the tetrahedral carbinolamine alkoxide **1.203** by thermodynamic driving force.



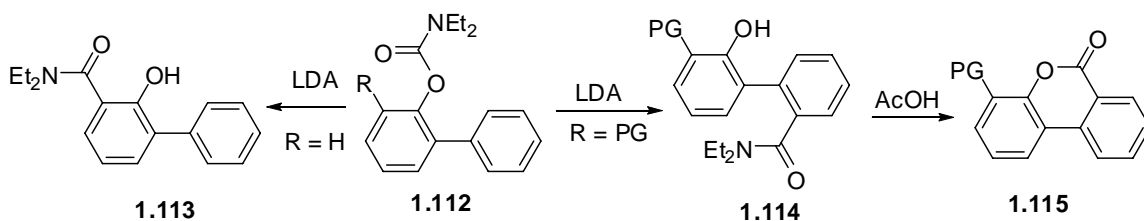
Scheme 1.16

The utility of DreM is illustrated by the efficient synthesis of fluorenone **1.110**¹²⁵ and phenanthrene **1.111**¹²⁶ (Scheme 1.17). The starting material **1.105** is readily available by a combined DoM plus cross coupling protocol. Under thermodynamic conditions (e.g. LDA, 0 °C), C2' or tolyl positions of **1.105** will be metalated. Thus, the intramolecular nucleophilic attacks on the amide group leads to the formation of the fluorenone and phenanthrol products. This synthetic sequence has been used to generate several natural products^{127,128} and liquid crystals (*vide infra*).¹²⁹



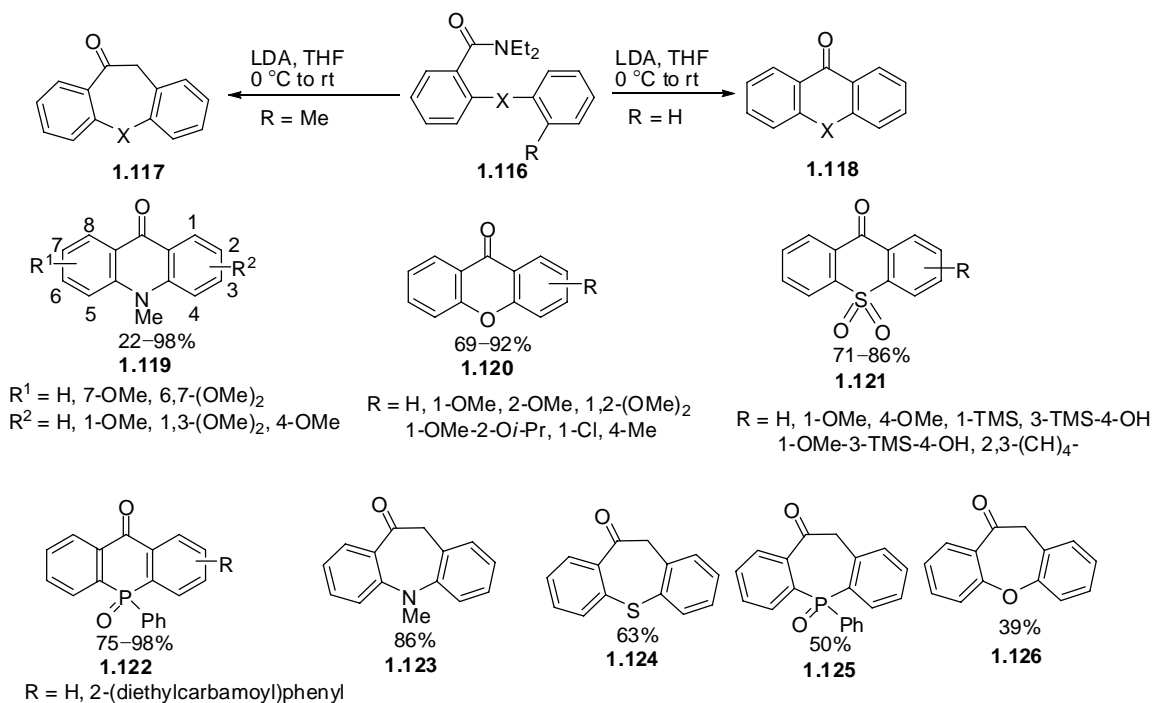
Scheme 1.17

As for the biaryl *O*-carbamate **1.112**, initial kinetic deprotonation by *s*-BuLi/TMEDA results in *ortho*-deprotonation, but with an additional complication: a rapid anionic *ortho*-Fries rearrangement to give **1.113** (Scheme 1.18).⁵⁴ Similar results were observed when LDA was used as the base.¹³⁰ However, if the *ortho* position is blocked by a protecting group, remote metalation and migration occurs under LDA conditions, to generate biaryl **1.114**, which, upon acidic treatment leads to the construction of dibenzopyranone **1.115**.¹³⁰ Several natural products have been synthesized by this method.¹³¹



Scheme 1.18

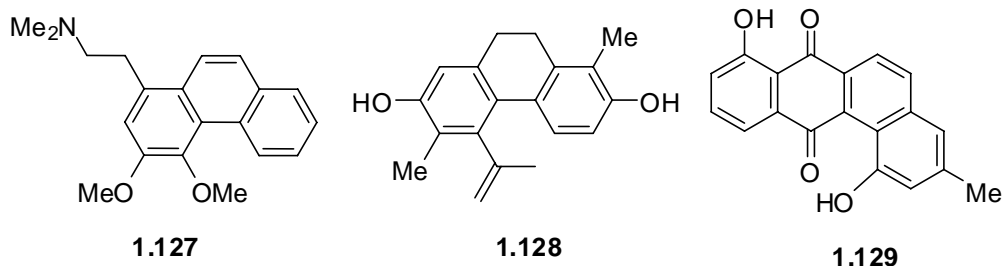
Extension of the DreM strategy to heteroarom linked biaryl Ar-X-Ar systems resulted in the development of a method for the synthesis of N, O, S and P containing tricyclics **1.117** and **1.118** (Scheme 1.19). Thus, treatment of **1.116** with LDA afforded acridones **1.119**,¹³² xanthenes **1.120**,¹³³ thioxanthenones **1.121**¹³⁴ and dibenzo-*[b, e]*phosphininones **1.122**.¹³⁵ Even the seven membered rings **1.117** were constructed in a similar way to give dibenzazepinones **1.123**,¹³⁶ dibenzothiepinones **1.124**,¹³⁷ dibenzophosphepinones **1.125**¹³⁵ and dibenzoxepinones **1.126**.¹³³



Scheme 1.19

1.3 The Synthesis of Phenanthrenes

The phenanthrenes are ubiquitous organic pollutants which cause great environmental concern because of their persistence, toxicity, mutagenicity and carcinogenicity.¹³⁸ Phenanthrenes and their oxidized/reduced derivatives also constitute a class of natural products, e.g. atherosperminine **1.127**,¹³⁹ juncusol **1.128**¹⁴⁰ and tetrangulol **1.129**¹⁴¹ (Scheme 1.20), and exhibit various biological activities such as antimicrobial,¹⁴² antimalarial,¹⁴³ anticancer¹⁴⁴ and emetic activities.¹⁴⁵ Since the discovery of phenanthrene and elucidation of its structure in 1872,¹⁴⁶ a number of methods¹⁴⁷ have been developed for the synthesis of phenanthrenes which are generally divided as intramolecular and intermolecular routes.

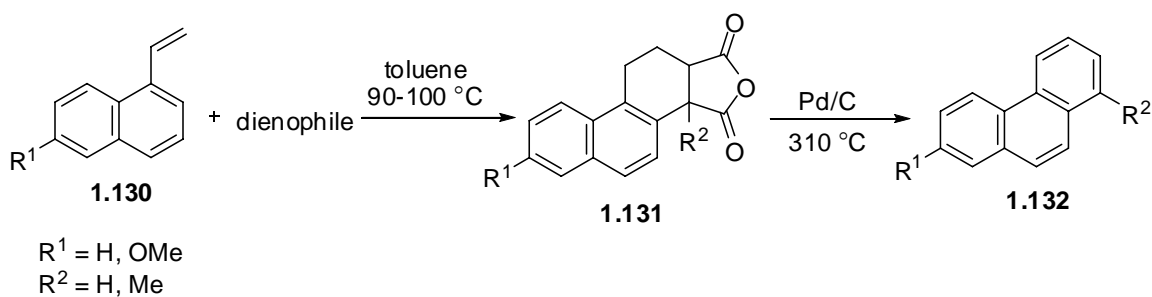


Scheme 1.20

1.3.1 Intermolecular Routes to Phenanthrenes

1.3.1.1 Diels-Alder Approach

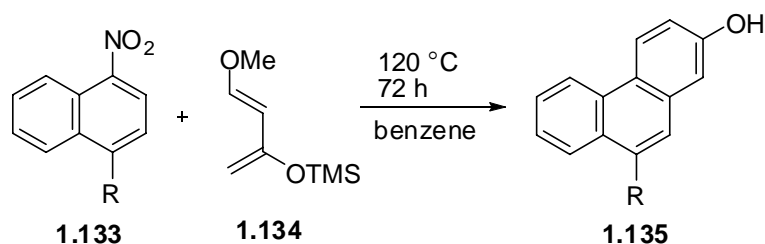
The Diels-Alder reaction is one of the most useful synthetic reactions for the construction of phenanthrenes. By varying the structural nature of dienes and dienophiles, many phenanthrenes with different substitution patterns may be constructed.^{147a} Classically, 1-vinylnaphthalenes **1.130** are used as dienes for Diels-Alder reactions¹⁴⁸ because of their electron rich constitution. The products **1.131** are readily dehydrogenated to the fully aromatic phenanthrenes **1.132**.



R^1	R^2	dienophile	yields % for 1.132
H	H	maleic anhydride	57
OMe	H	maleic anhydride	30
H	H	diethyl maleate	89
OMe	H	fumaric acid	72
OMe	Me	citraconic anhydride	60

Scheme 1.21

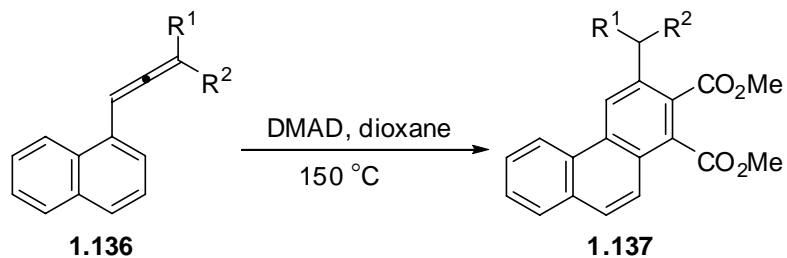
Recently Mancini and coworkers successfully used activated naphthalenes **1.133** as dienophiles in reaction with Danishefsky's diene **1.134** to afford 2,9-disubstituted phenanthrenes **1.135**.¹⁴⁹ The yield was improved with more electron poor naphthalenes. Other readily available dienes such as isoprene, *trans*-1-(*N*-acetyl-*N*-propylamino)-1,3-butadiene only gave *N*-(naphthyl)-pyrroles as products.



R	yield %
NO ₂	75
CN	53
COMe	50

Scheme 1.22

Another recent example of the Diels-Alder approach to phenanthrenes involved reaction of allenes **1.136** with dimethyl acetylenedicarboxylate (DMAD) to give products **1.137** (Scheme 1.23). In this reaction, the aromatic ring and the adjacent carbon-carbon double bond of the allene unit acted as the 1,3-diene.¹⁵⁰

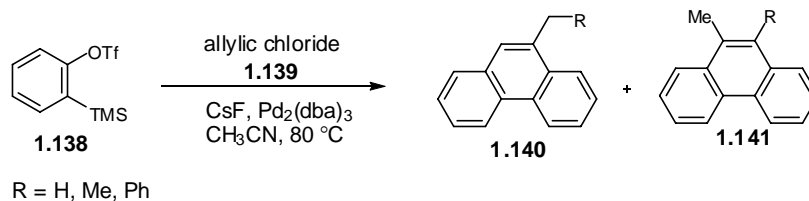


R ¹	R ²	time/h	yield %
Me	CO ₂ Et	10	72
<i>n</i> -Pr	CO ₂ Et	24	64
<i>n</i> -Bu	CO ₂ Et	24	58
<i>i</i> -Bu	CO ₂ Et	24	40
Allyl	CO ₂ Et	19	40
<i>n</i> -Pr	P(O)Ph ₂	72	76
<i>n</i> -Bu	P(O)Ph ₂	72	80
<i>n</i> -C ₅ H ₁₁	P(O)Ph ₂	72	70
<i>n</i> -C ₆ H ₁₃	P(O)Ph ₂	72	73
PhCH ₂ CH ₂	P(O)Ph ₂	72	65

Scheme 1.23

1.3.1.2 Pd-Catalyzed Cyclization Approach

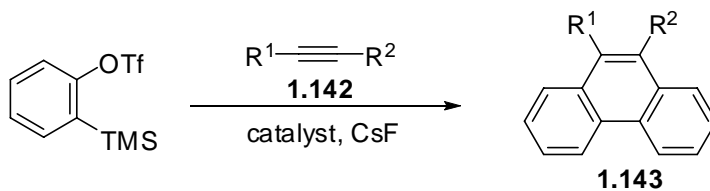
In this approach, benzyne are frequently used as fleeting intermediate species because of their high reactivity and precursor availability. Either alkenes¹⁵¹ and alkynes¹⁵² may be used as the cyclization partners (Scheme 1.24). In the case of cyclization of *in situ* generated benzyne with allylic chlorides **1.138**,¹⁵¹ a mixture of constitutional isomeric products **1.140** and **1.141** were produced.



allylic chloride	product	yield % (1.140 : 1.141)
	1.140a (R = H)	70
	1.140b + 1.141b (R = Me)	70 (7:3)
	1.140b + 1.141b (R = Me)	70 (6.5:3.5)
	1.140c + 1.141c (R = Ph)	71(7.3:2.7)

Scheme 1.24

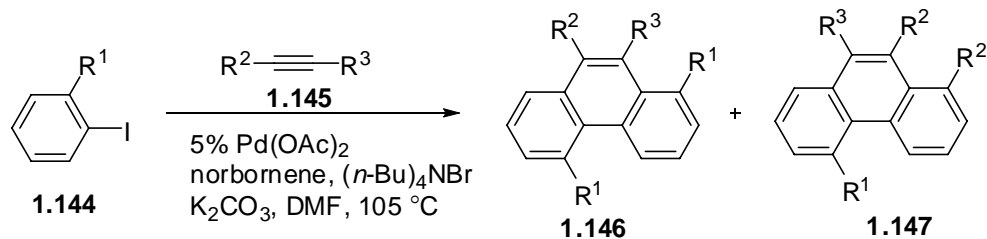
Yamamoto reported a synthesis of phenanthrenes from the reaction of alkynes **1.142**^{152b} with benzyne using $\text{Pd}(\text{OAc})_2/(\text{o-tol})_3\text{P}$ as a catalyst (Scheme 1.25). Phenanthrenes **1.143** were obtained exclusively in modest yields regardless of the electronic nature of the alkynes (entry 1-6). In a competitive work, Perez and coworkers^{152a} reported the reaction of benzyne with electron poor alkynes under $\text{Pd}(\text{PPh}_3)_4$ or $\text{Pd}_2(\text{dba})_3$ catalysis (entry 7 and 8) to afford phenanthrenes in comparable yields. On the other hand, when electron rich alkynes were involved (entry 9 and 10), the yields of phenanthrene products were low.



entry	R ¹	R ²	catalyst	yield %
1	<i>n</i> -Pr	<i>n</i> -Pr	Pd(OAc) ₂ /(<i>o</i> -tol) ₃ P	63
2	<i>n</i> -pentyl	<i>n</i> -pentyl	Pd(OAc) ₂ /(<i>o</i> -tol) ₃ P	67
3	CH ₂ OMe	CH ₂ OMe	Pd(OAc) ₂ /(<i>o</i> -tol) ₃ P	59
4	Ph	Me	Pd(OAc) ₂ /(<i>o</i> -tol) ₃ P	67
5	Ph	Et	Pd(OAc) ₂ /(<i>o</i> -tol) ₃ P	63
6	Ph	COMe	Pd(OAc) ₂ /(<i>o</i> -tol) ₃ P	76
7	CF ₃	CF ₃	Pd(PPh ₃) ₄	65
8	CO ₂ Et	Me	Pd(PPh ₃) ₄	63
9	Et	Et	Pd ₂ (dba) ₃	28
10	Ph	Ph	Pd ₂ (dba) ₃	34

Scheme 1.25

In a mechanistically different, yet also Pd-catalyzed approach (Catellani reaction) to phenanthrenes, iodobenzenes **1.144** are subjected to reaction with diphenyl or alkylphenylacetylenes **1.145** using norbornene as a co-catalyst (Scheme 1.26).^{152c} The products **1.146** and/or **1.147** would be made by ring closure. In the case involving diisopropylacetylene as reaction partner, no desired product was obtained.



R ¹	R ²	R ³	1.146%	1.147%
Me	Ph	Ph	82	
Et	Ph	Ph	85	
<i>n</i> -Pr	Ph	Ph	83	
<i>i</i> -Pr	Ph	Ph	93	
<i>n</i> -Bu	Ph	Ph	84	
OMe	Ph	Ph	64	
CH ₂ OMe	Ph	Ph	51	
CO ₂ Me	Ph	Ph	33	
<i>i</i> -Pr	4-MeOC ₆ H ₄	4-MeOC ₆ H ₄	80	
<i>i</i> -Pr	Ph	4-F ₃ CC ₆ H ₄	19	55
<i>i</i> -Pr	Ph	Me	32	11

Scheme 1.26

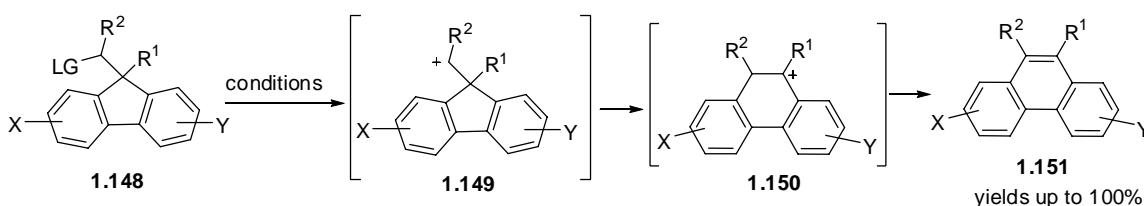
1.3.2 Intramolecular Cyclization Approaches to Phenanthrenes

The intramolecular route is the most popular general approach for the synthesis of phenanthrenes. This approach may be classified into six main categories: ring expansion, electrophilic cyclization, radical cyclization, photocyclization, ring-closing olefin metathesis, and the directed remote metalation (DreM) processes.

1.3.2.1 Ring Expansion Reactions

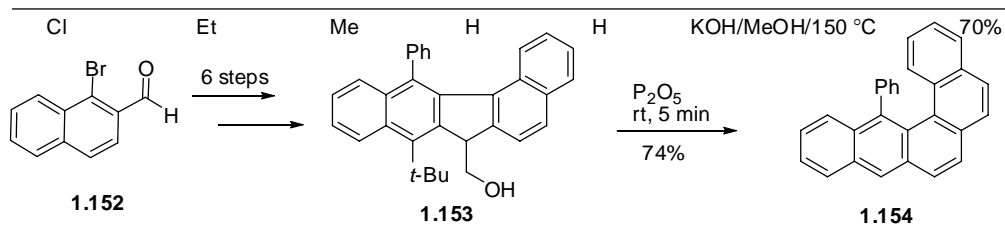
The construction of substituted phenanthrenes by the Wagner-Meerwein rearrangement of fluorenyl carbinol derivatives, first reported by Werner and Grob in 1904,¹⁵³ has been developed as one of the classical ways to access substituted phenanthrenes. Many of the starting materials **1.148** may be prepared from fluorenyl-9-carbocyclic acids by alkylation and reduction, so this method is useful for phenanthrene

synthesis. Carbocation-generating reactions include treatment of fluorenones with diazoalkanes,¹⁵⁴ treatment of carbinols with P₂O₅¹⁵⁵ and PPA,¹⁵⁶ diazotization of 9-aminomethylfluorenes,¹⁵⁷ and treatment of 9-LG-methylfluorenes **1.148** (LG = Cl,¹⁵⁸ Br,¹⁵⁹ OTs,¹⁶⁰ OCOCF₃¹⁶¹) with acids or bases (Scheme 1.27). A recent example is for the construction of polycyclic aromatic hydrocarbon **1.154**.¹⁶²



Selected examples of the synthesis:

LG	R ¹	R ²	X	Y	conditions	Yields
OTs	Me	H	H	H	HCO ₂ H	99%
OCOCF ₃	CO ₂ Me	CO ₂ Me	H	H	HCO ₂ H	62%
OH	H	H	2-Me	7-Me	P ₂ O ₅	77%
OAc	H	H	2-NO ₂	H	PPA	89%
Br	Br	<i>p</i> -MeOC ₆ H ₄	H	H	KOAc/AcOH	90%

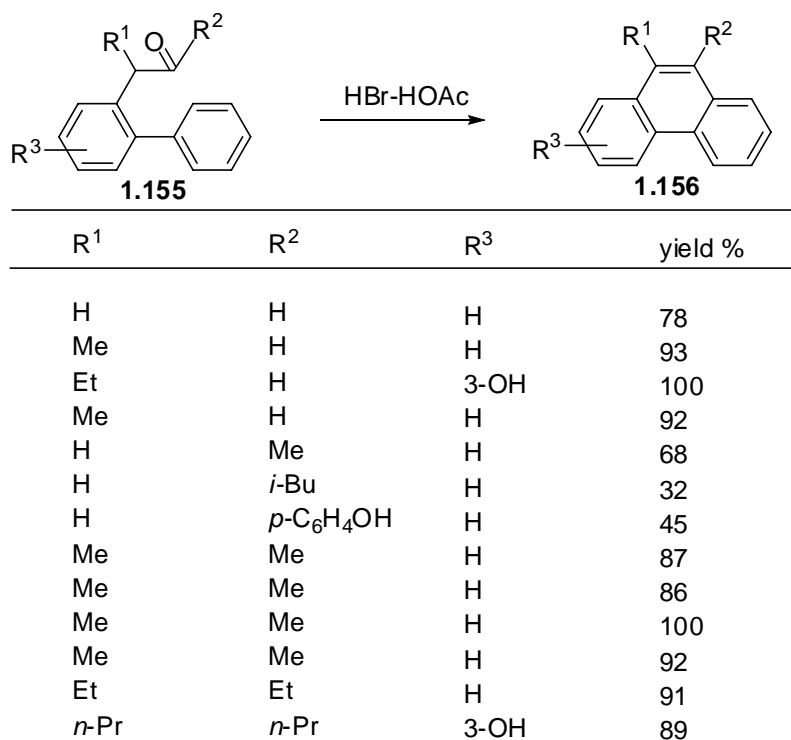


Scheme 1.27

1.3.2.2 Intramolecular Electrophilic Cyclization

Synthesis of phenanthrenes by acid catalyzed intramolecular electrophilic cyclization normally uses α -(2-biphenyl)acetones and α -(2-biphenyl)aldehydes **1.155**

(R = alkyl, H) as starting materials (Scheme 1.28).¹⁶³ Other functional groups such as ketoesters may lead to decarboxylation. This type of reaction, also called “aromatic cyclodehydration”,¹⁶⁴ can be catalyzed by many acids such as PPA, 85% sulfuric acid and hydrobromic acid and acetic acid mixture, and give rise to phenanthrenes under conditions much milder than those used for dehydrogenation. The starting materials **1.155** may be readily prepared from α -(2-biphenyl)-acetonitriles.



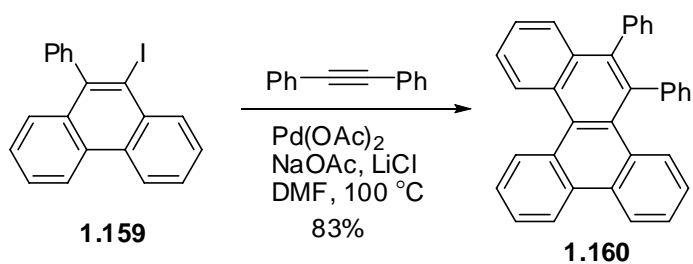
Scheme 1.28

Recently, Larock and coworkers reported an intramolecular cyclization of alkynyl biphenyl **1.157** to phenanthrenes **1.158** induced by various electrophiles (Scheme 1.29).¹⁶⁵ Functional groups as diverse as MeO, CHO, and NO₂, at various positions are tolerated in this reaction. The starting materials **1.157** are readily prepared by a Sonogashira reaction.¹⁶⁶ The reaction is carried out under mild conditions and gives rise

to various phenanthrenes in moderate to excellent yields. The resulting iodine-containing product **1.159** was elaborated to more complex product **1.160**.

Reaction scheme: A substituted alkyne (1.157) with substituents R¹, R², and R³ reacts with an electrophile E⁺ to form a phenanthrene derivative (1.158) with substituents R¹, R², R³, and E.

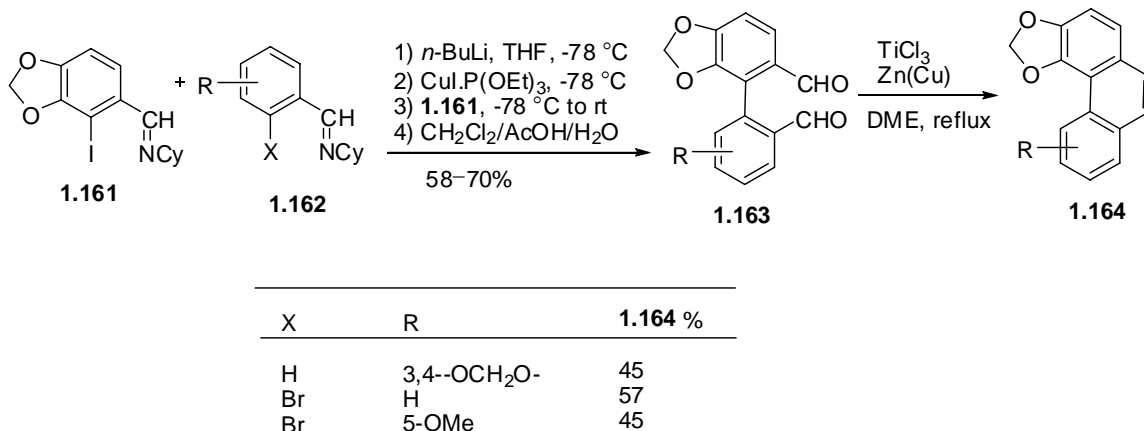
R ¹	R ²	R ³	E ⁺	yield %
Ph	H	H	ICI	99
Ph	H	H	I ₂ /NaHCO ₃	80
Ph	H	H	NBS	86
Ph	H	H	<i>p</i> -O ₂ NC ₆ H ₄ SCI	92
Ph	H	H	PhSeCl	0
4-MeC ₆ H ₄	H	H	ICI	98
4-MeOC ₆ H ₄	H	H	ICI	99
4-EtO ₂ CC ₆ H ₄	H	H	ICI	99
4-O ₂ NC ₆ H ₄ ,	H	H	ICI	57
Ph	4'-CHO	H	ICI	71
Ph	4'-NO ₂	H	ICI	17
Ph	3'-OMe	H	ICI	86
Ph	3',4'-(C ₄ H ₄)-	H	ICI	90
Ph	H	3-NO ₂	ICI	88
Ph	H	3',4'-(C ₄ H ₄)-	ICI	48
CH ₂ TMS,	H	H	ICI	50
			ICI	70
			ICI	96



Scheme 1.29

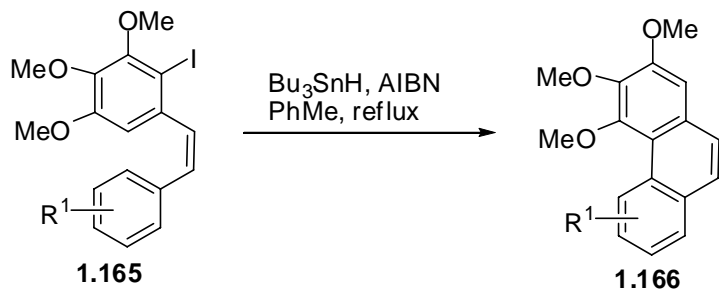
1.3.2.3 Intramolecular Radical Cyclization

Pfeffer and coworkers reported a combined Ullmann and McMurry route to various phenanthrenes **1.164** (Scheme 1.30),¹⁶⁷ Thus, Ullmann coupling of commercially or readily available imine **1.162** with iodo imine **1.161** afforded, after hydrolysis, biphenyls **1.163**. McMurry coupling of **1.163** led to phenanthrenes **1.164**.

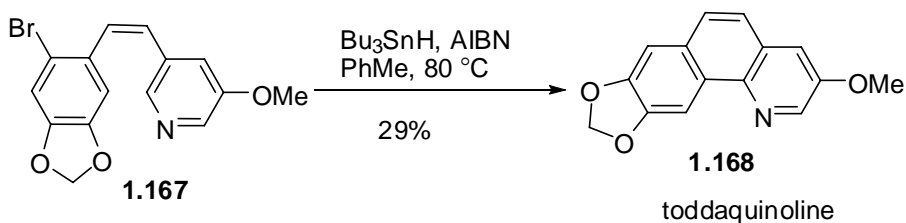


Scheme 1.30

Another report by Harrowven and coworkers¹⁶⁸ provided a 6-*exo/endo*-trig radical cyclization route to phenanthrenes (Scheme 1.31). Thus, using *cis*-stilbenes **1.165** as the radical acceptor led to phenanthrenes **1.166** in useful yields. However, unsymmetrical substrates e.g. R = 3-CN led to a mixture of regioisomers in a ratio of 1:1. This method was applied to the total synthesis of toddaquinoline **1.168**, an alkaloid from the root bark of Formosan *Toddalia asiatica*.

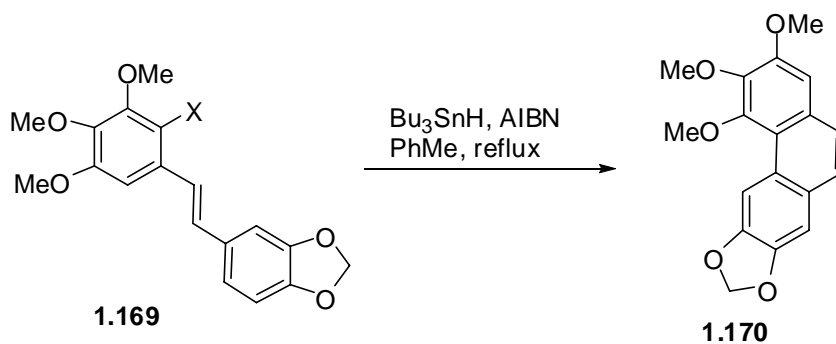


R ¹	yield %	regioselectivity
H	89	
2-CN	90	
3-CN	78	1:1(2-CN:4-CN)
4-CN	85	
3-OMe	82	1:1(2-OMe:4-OMe)
3,4-OCH ₂ O-	86	5:1(2,3-:3,4-)



Scheme 1.31

Interestingly, *trans*-stilbenes **1.169**, halogen-bearing stilbenes **1.169a** and **1.169b** are not good substrates for the synthesis of phenanthrenes **1.170**. This may be ascribed to the fact that the homolysis of halogen-carbon bond outpaces addition of the tributyltin radical to the alkene.¹⁶⁹

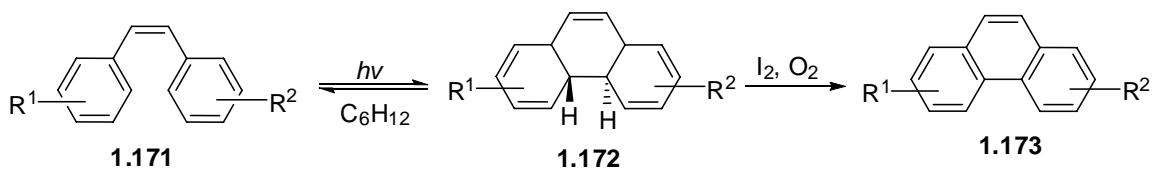


substrates	X	yield %
1.169a	I	< 5
1.169b	Br	32
1.169c	H	68

Scheme 1.32

1.3.2.4 Intramolecular Photocyclization (Mallory Reaction)

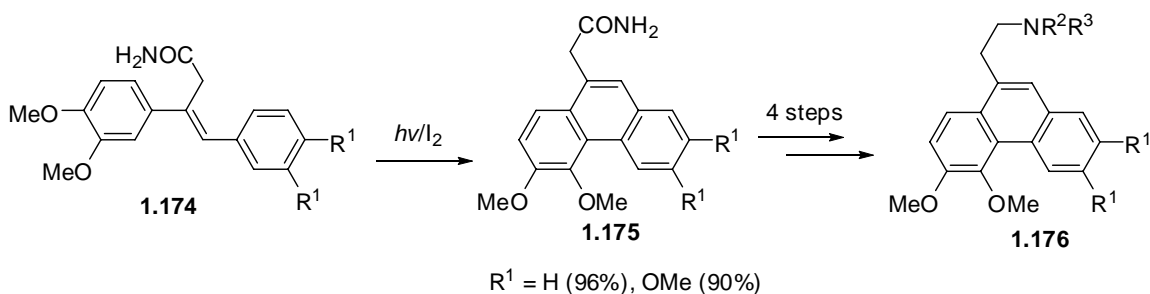
The photochemical synthesis of phenanthrenes was discovered in the early 1950s¹⁷⁰ and provides one of most widely used synthetic routes to substituted phenanthrenes. This reaction, now known as the Mallory reaction, uses stilbene precursors which are usually readily available by Wittig chemistry. *Trans*-stilbenes may be used since, during the photoreaction, they are photoisomerized to *cis*-stilbenes which undergo cyclization. The reaction proceeds, under the conditions of ultraviolet irradiation, by reversible molecular orbital controlled 6π -electrocyclization of *cis*-stilbene **1.171** to give *trans*-4a,4b-dihydrophenanthrene **1.172** which, upon the treatment with hydrogen acceptors such as iodine and oxygen, affords phenanthrene **1.173** in high yield. Some examples are shown in Scheme 1.33.¹⁷¹



R ¹	R ²	Phenanthrene (yield %)
2-Me	H	1-Me (57)
3-Me	H	2-Me (31), 4-Me (29)
3-OMe	H	2-OMe (58), 4-OMe (15)
3-Me	3'-Me	2,5-(Me) ₂ (54), 2,7-(Me) ₂ (28), 4,5-(Me) ₂ (18)
4-OMe	4'-OMe	3,6-(OMe) ₂ (79)
2-Br	H	1-Br (50)
3-CN	H	2-CN (71), 4-CN (19)
4-F	H	3-F (76)
4-Cl	H	3-Cl (76)
4-Br	H	3-Br (76)

Scheme 1.33

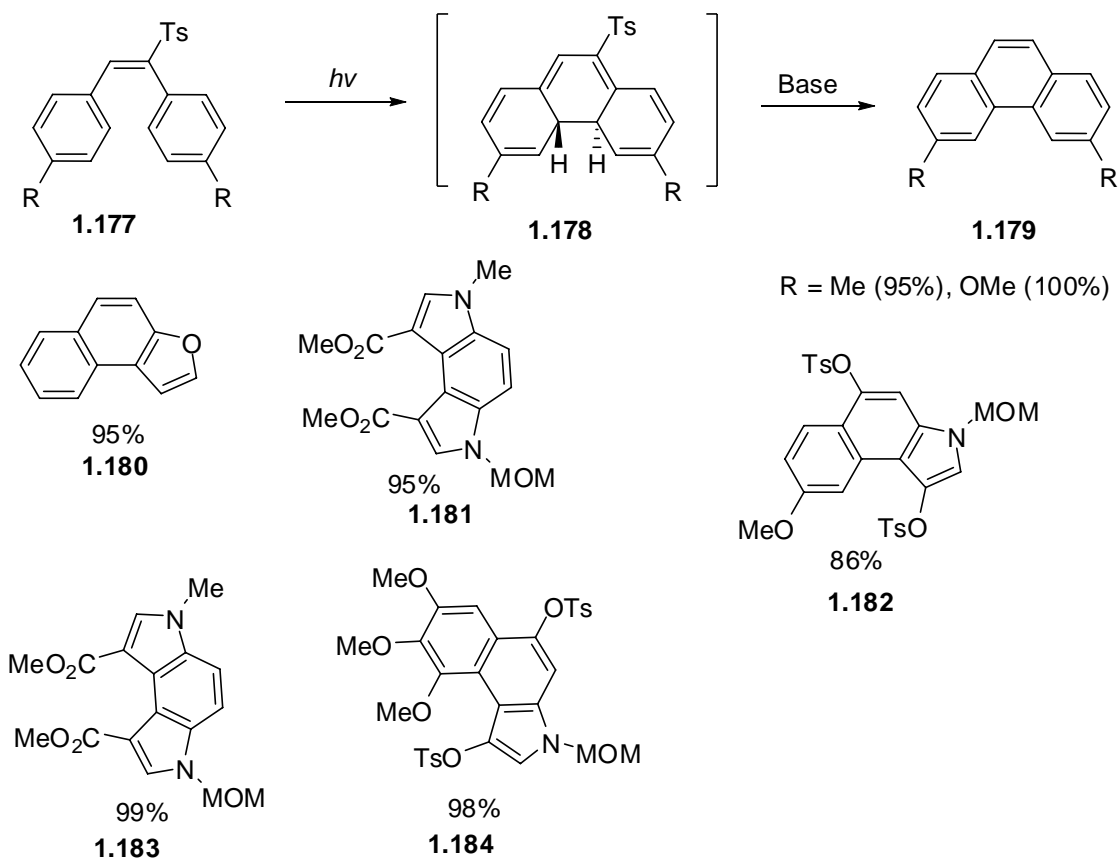
Although the Mallory reaction has drawbacks such as a limited success on multigram scale and lack of selectivity, it offers a general method for the construction of phenanthrenes. An exemplary application of the Mallory method is in the synthesis of phenanthrene alkaloids **1.176** (Scheme 1.34).¹⁷²



R¹ = OMe, R² = H, R³ = Me; Secoglucine (39% from **1.175**)
 R¹ = OMe, R² = R³ = Me; N-methyl Secoglucine (34% from **1.175**)

Scheme 1.34

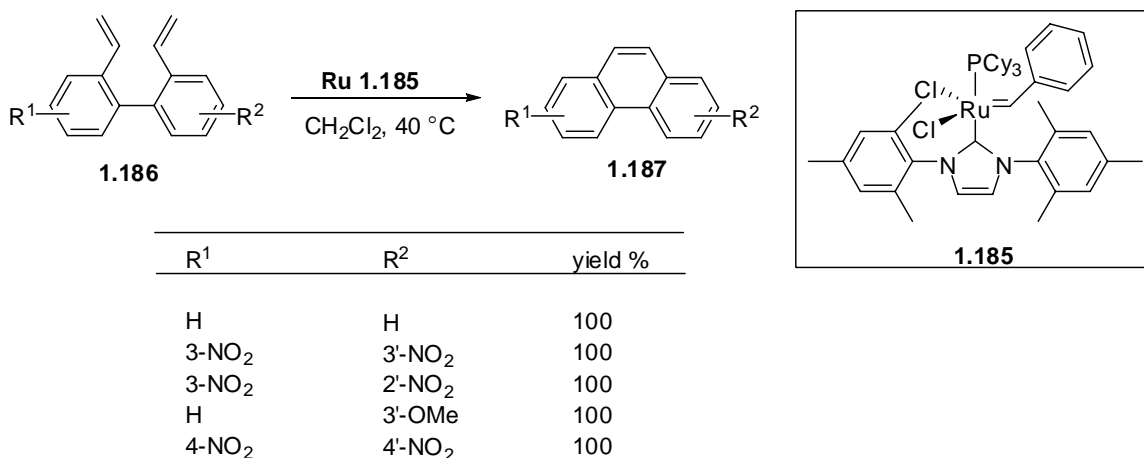
A recent Mallory photocyclization synthesis of phenanthrenes was reported by Tojo and coworkers.¹⁷³ Starting with tosyl-stilbenes **1.177**, easily obtained from condensation of arylmethyl sulfones with aromatic aldehydes, irradiation under basic conditions afforded phenanthrenes **1.179** in high yields (Scheme 1.35). Thus the dihydro intermediate **1.178** from the 6π -electrocyclic process undergoes, after isomerization, expected elimination of sulfinate to afford the final products. The method can be applied for synthesis of other polyhetero-aromatic compounds **1.180-1.184** as well.



Scheme 1.35

1.3.2.5 Ring-Closing Olefin Metathesis (RCM)

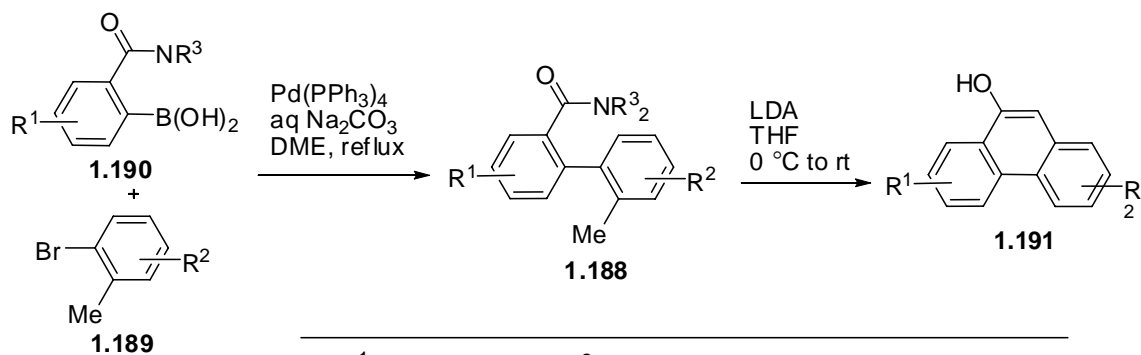
In 2004, Luliano and coworkers reported a general RCM method for the construction of substituted phenanthrenes **1.187** (Scheme 1.36).¹⁷⁴ Under the catalysis of second generation ruthenium-carbene complex **1.185**, divinyl biaryls **1.186** afforded five phenanthrenes **1.187** in quantitative yields. The reaction seems to proceed in high yields no matter the nature and position of the substituents in the starting material **1.186**.



Scheme 1.36

1.3.2.6 Directed Remote Metalation (DreM) Approach

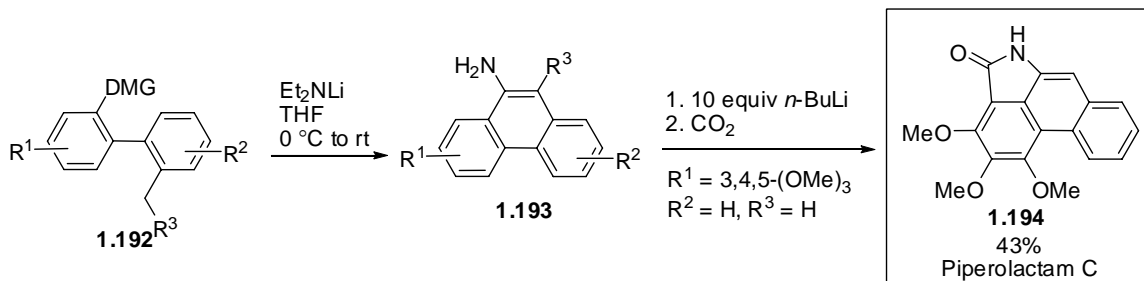
In 1988, Snieckus and coworkers reported a synthesis of phenanthrenes by application of the DreM concept (Scheme 1.37).¹²³ Treatment of biaryl amides **1.188**, readily available by Suzuki cross coupling of **1.189** with **1.190**, with LDA at 0°C to rt gave 9-phenanthrols **1.191** in excellent yields. Both EWGs (e.g. Cl) and EDGs (e.g. OMe) are tolerated in this reaction. The method is an example of the general DreM methodology which was modeled on the basis of the CIPE concept⁶⁸ and has become one of the general methods for the synthesis of phenanthrenes.



R ¹	R ²	R ³	yield %
H	H	<i>i</i> -Pr	98
H	H	Et	92
2-OMe	H	Et	92
H	4'-CONEt ₂	Et	78
4-OMe	4'-Cl	Et	93
H	4'-Cl	Et	96
6-OMe	H	Et	92
H	3',4'-(CH) ₄ '	Et	90

Scheme 1.37

Extension of this DreM strategy for the synthesis of phenanthrenes was later reported by the same group, by changing the cyclising functional groups from amides to nitrile and imines which led to a variety of 9-aminophenanthrenes **1.193** in yields ranging from 12% to 89%.¹⁷⁵ Furthermore, the application of this methodology was demonstrated by the first synthesis of the alkaloid piperolactam C (Scheme 1.38).



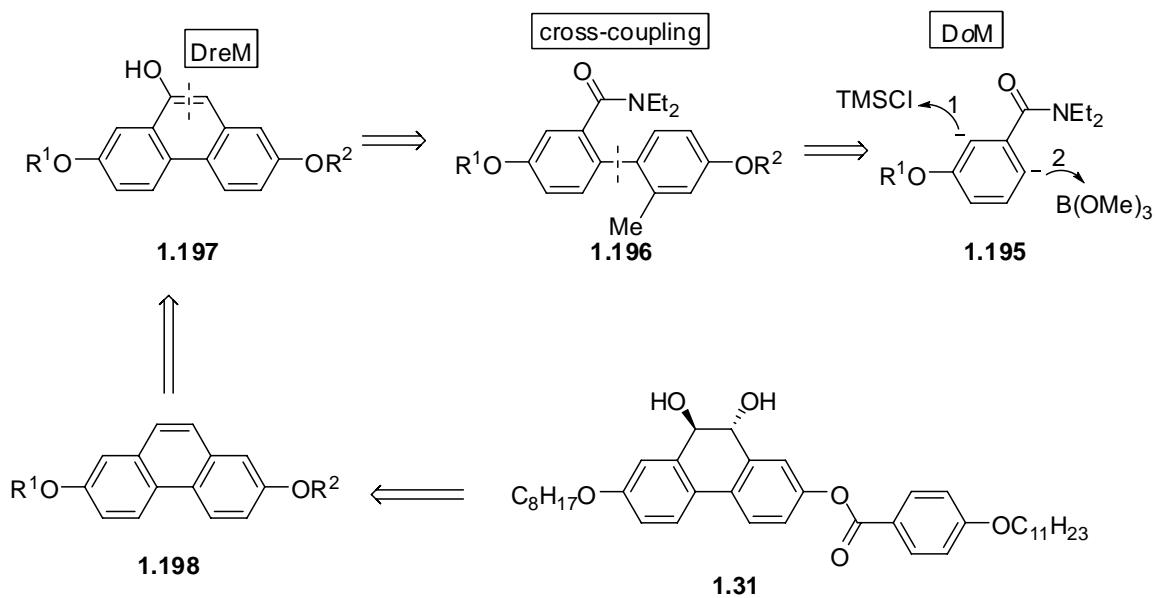
R ¹	R ²	R ³	DMG	yield %
			CN	88
			CH=NNMe ₂	50
			CH=NOMe	58
	4'-Me		CN	42
	4'-Me		CH=NNMe ₂	67
	4'-Me		CH=NOMe	58
	6'-Me		CN	81
	6'-Me		CH=NNMe ₂	72
	6'-Me		CH=NOMe	64
		OMe	CN	66
		OMe	CH=NNMe ₂	12
		OMe	CH=NOMe	73
2,3,4-(OMe) ₃			CN	40
2,3,4-(OMe) ₃			CH=NNMe ₂	61
	5',6'-(CH) ₄ -		CN	89
	5',6'-(CH) ₄ -		CH=NNMe ₂	43
	5',6'-(CH) ₄ -		CH=NOMe	63
	3',4'-(CH) ₄ -		CN	52
	3',4'-(CH) ₄ -		CH=NNMe ₂	41
	3',4'-(CH) ₄ -		CH=NOMe	74
2,3-(CH) ₄ -			CH=NNMe ₂	46
2,3-(CH) ₄ -			CH=NOMe	45

Scheme 1.38

1.4 Outline of Synthesis

The purpose of the research described in this thesis is to synthesize new SmC* LC substances with a phenanthrene core. For this aim, DoM and DreM methodologies have been applied for the construction of the target compounds (**1.31**) for which the retrosynthesis is outlined in Scheme 1.39. The key steps of this synthesis are: 1) the synthesis of the organometallic coupling partner **1.195** using DoM; 2) the synthesis of the biaryl **1.196** by Suzuki cross coupling reaction; 3) the cyclization of **1.197** under DreM

conditions to afford phenanthren-9-ol **1.197**; and 4) Pd-catalyzed reductive detriflation to the phenanthrene **1.198**, which, by dihydroxylation gives the final 9,10-dihydroxy-9,10-dihydrophenanthrene (**1.31**) for LC properties study.

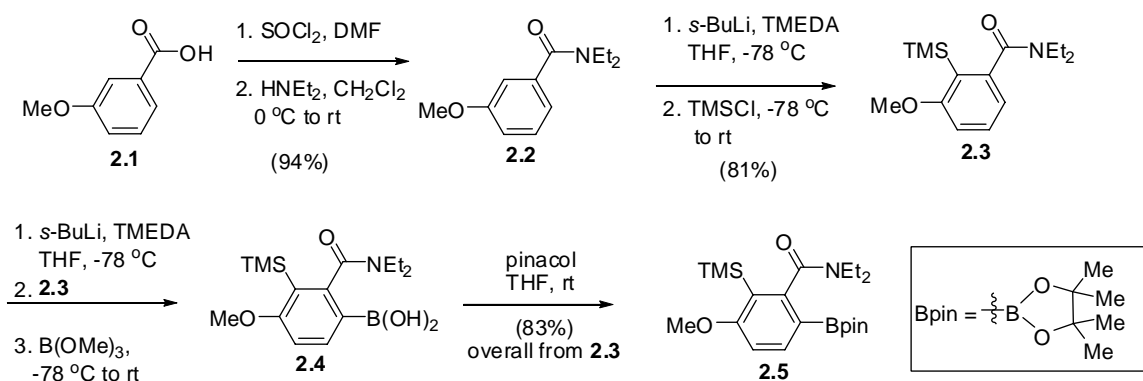


Scheme 1.39

CHAPTER 2–PHENANTHRENE AND 9,10-DIHYDROPHENANTERENE-9,10-
DIOL LIQUID CRYSTALS

2.1 Synthesis of 7-(octyloxy)phenanthren-2-yl 4-(undecyloxy)benzoate (1.32).

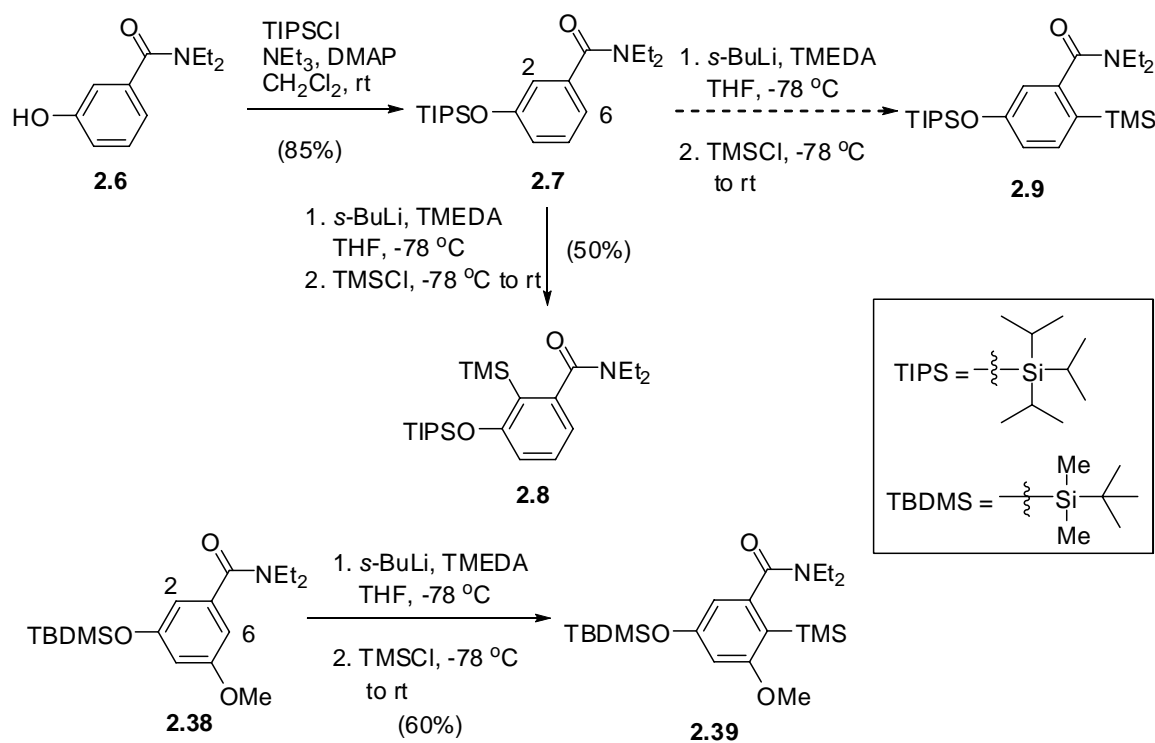
The development of an efficient synthetic route to compound **1.32** started with the preparation of the benzamide coupling partner **2.5** from the commercially available *m*-methoxybenzoic acid **2.1** by the pathway established by McCubbin (Scheme 2.1).¹²⁹



Scheme 2.1

Benzoic acid **2.1** was transformed into the benzamide **2.2** in 94% yield. The more reactive C2 metalation site was protected by the latent silylation technique¹⁷⁶ to afford **2.3** which, upon metalation and boronation, furnished the boronic acid **2.4**. For this reaction, a modified procedure to that used by McCubbin was used in which compound **2.3** was added into a solution of *s*-BuLi/TMEDA at -78 °C in THF, followed by quench and workup. Without purification, the crude **2.4** was converted into the boropinacolate **2.5** in an overall yield of 83% from the silyl derivative **2.3**. When the original procedure of McCubbin,¹²⁹ addition of *s*-BuLi to a solution of **2.3** at higher temperature (0 °C) in Et_2O , was used, a reduced overall yield of 73% from **2.3** to **2.5** was observed.

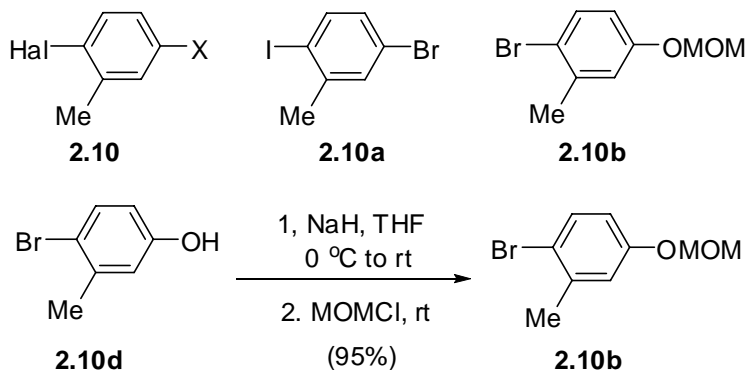
An attempt to shorten the synthesis of **1.32** by the pathway shown in Scheme 2.2 was undertaken. It was thought that the steric effect of the TIPS group might hinder the C2 position of **2.7** from metalation and force the metalation to occur at C6. However and interestingly, the model **2.7**, prepared from phenol **2.6**, upon metalation and silylation afforded product **2.8** rather than **2.9**. A possible rationalization of this result is the involvement of an O-inductive effect to promote deprotonation at C2. When C2 and C6 O-inductive effects are present, as in the case of **2.38**, but there is an additional steric effect at C2, metalation-silylation is observed to give the C6 substituted **2.39** as a single product.¹⁷⁷



Scheme 2.2

The choice of an appropriate Suzuki cross coupling partner **2.10** for reaction with **2.5** should take two factors into consideration: 1) it should be able to survive DreM

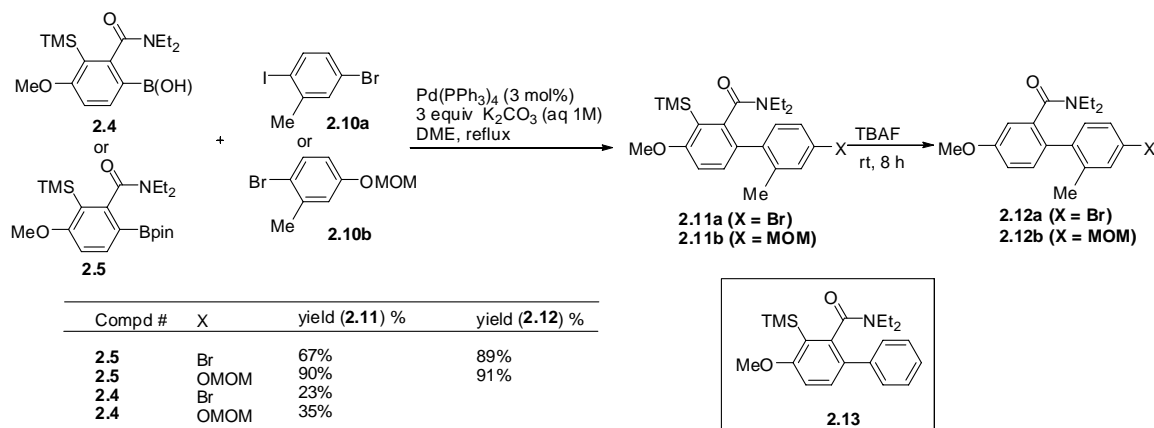
conditions and 2) the functional group X in **2.10** should be easily transformed into a phenolic group. Compound **2.10a** was chosen since it is inexpensive, commercially available, and easily transformed by metal halogen exchange followed by an “OH⁺” quench into a phenol.¹⁷⁸ As an alternative coupling partner, **2.10b** was chosen because it is readily available and stable to DreM conditions (Scheme 2.3).



Scheme 2.3

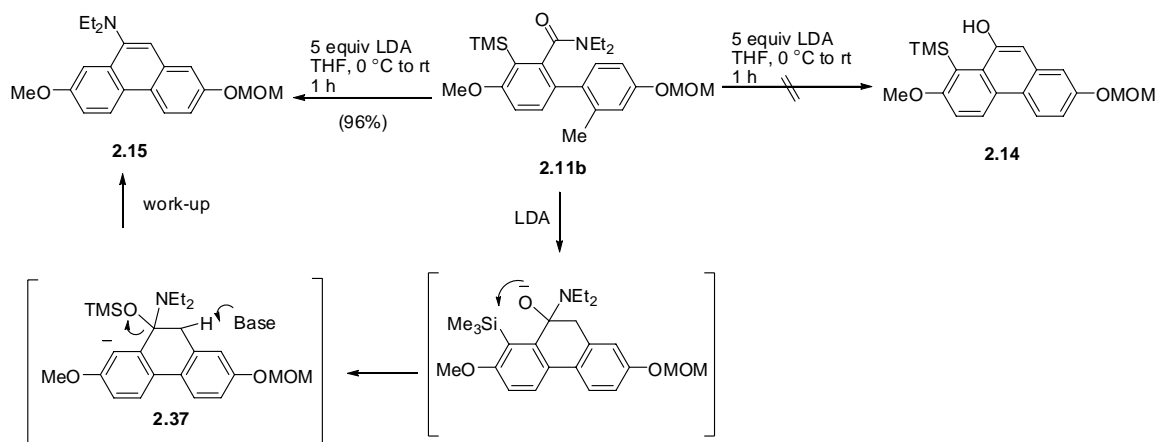
The crude **2.4** was at first used directly as a cross coupling partner without further purification but gave product **2.11** in low yield (<35%). Conversion into the boropinacolate **2.5** and purification gave better results in the Suzuki cross coupling reaction (Scheme 2.4).

Cross coupling of **2.5** with **2.10a** and **2.10b** under standard Suzuki conditions gave the biaryls **2.11a** and **2.11b** respectively. As expected, regioselective iodo cross coupling of **2.10a** was observed to afford **2.11a**. For a two-gram scale synthesis of **2.11b**, up to 2% of byproduct **2.13** was isolated resulting from phenyl group transferred from the PPh₃ ligand. The treatment of the biaryls **2.11a,b** with TBAF gave **2.12a,b** respectively in excellent yields.



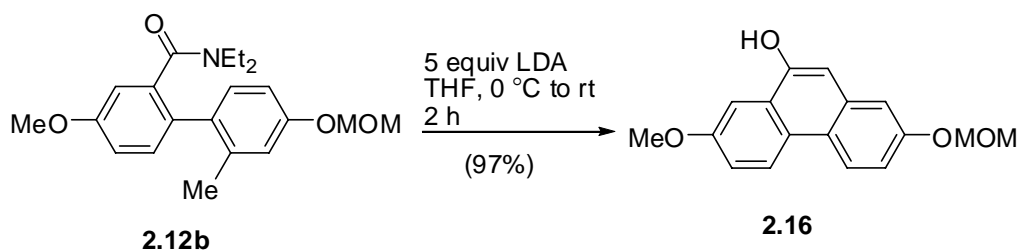
Scheme 2.4

Interestingly, the initial DreM cyclization attempts of **2.11b** under standard LDA conditions did not give the desired phenanthrene-9-ol **2.14** but the 9-aminophenanthrene **2.15** in excellent yield. This reaction was postulated to occur via an aromatic Brook rearrangement,¹⁷⁹ to afford intermediate **2.37**, which, upon elimination of trimethylsilyloxy and rearomatization, gave the 9-aminophenanthrene **2.15**. Further work on the generalization of this reaction is in progress.¹⁸⁰



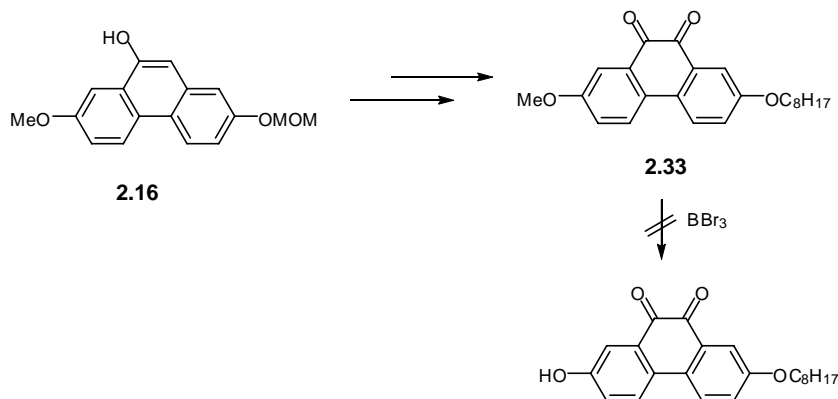
Scheme 2.5

On the other hand, the DreM reaction of the desilylated biaryl **2.12b** afforded phenanthrene-9-ol **2.16** in excellent yield. However, when the bromo biaryl **2.12a** was treated with LDA at low temperature (-30 °C), a dark black solution resulted and, upon quenching with saturated aqueous NH₄Cl, led to a mixture of starting material and intractable products. Changing the base from LDA to LTMP gave a similar result. It is possible that the formation of a benzyne intermediate is the reason for this result.¹⁸¹ However, two attempts to trap the benzyne as a cycloaddition product with furan were unsuccessful.



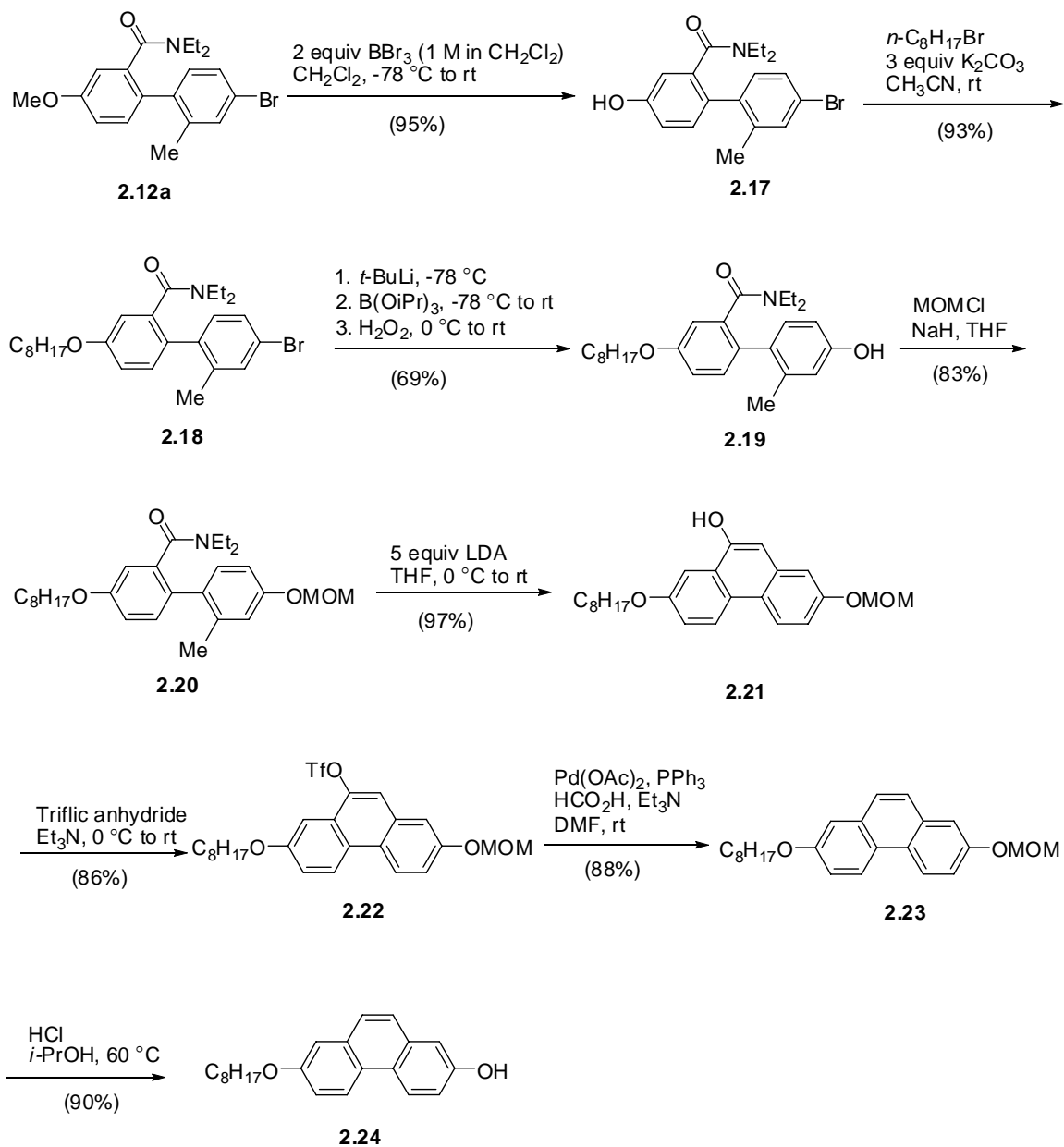
Scheme 2.6

Although compound **2.16** was obtained efficiently, it could not serve the purpose to obtain the final compound **1.32** because of the inability to achieve selective demethylation (Scheme 2.7).



Scheme 2.7

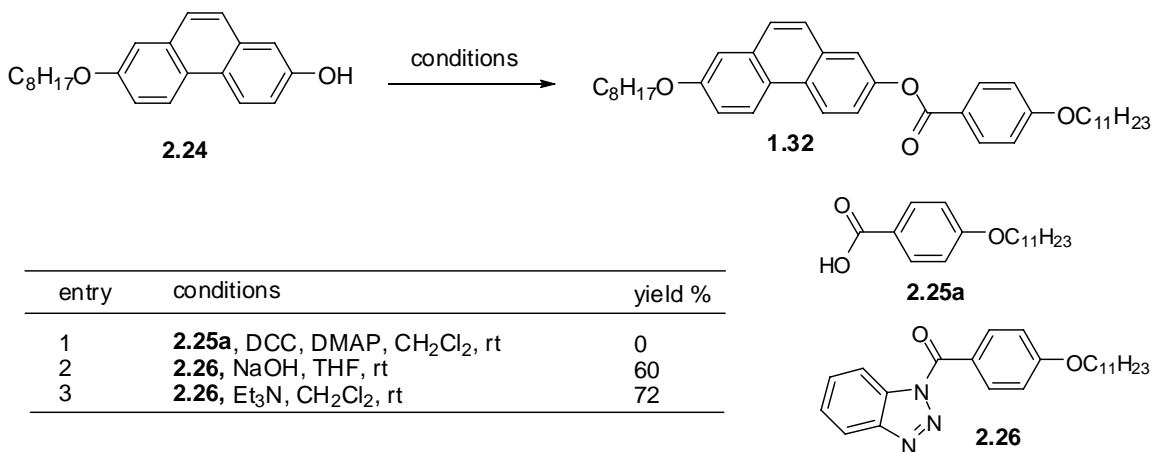
Therefore, an alternative strategy was adopted (Scheme 2.8). Initial demethylation of **2.12a** with BBr_3 afforded the phenol **2.17**,¹⁸² which upon alkylation with n-octyl bromide under K_2CO_3 conditions gave the octyl ether **2.18** in excellent yield. Metal halogen exchange of **2.18**, followed by $\text{B}(\text{O}i\text{-Pr})_3$ quench and peroxide oxidation,¹⁷⁸ afforded **2.19** in moderate yield. Protection of the phenol **2.19** as the MOM ether gave the DreM precursor **2.20**,¹⁸³ which under standard DreM conditions was converted into the phenanthrene-9-ol **2.21** in excellent yield. Triflation of **2.21** to **2.22**, followed by Pd-catalyzed hydrogenolytic cleavage¹⁸⁴ gave the phenanthrene **2.23** which, under acidic conditions afforded the phenanthren-2-ol **2.24**.¹⁸⁵



Scheme 2.8

Attempted esterification of **2.24** using the DCC/DMAP protocol¹⁸⁶ resulted in recovery of starting material. The electron-rich character of the phenanthrene **2.24** may be responsible for this failure. On the other hand, using 1-(4-undecyloxybenzoyl)triazole (**2.26**) under basic conditions¹⁸⁷ led to the formation of **1.32** in reasonable yields (Scheme

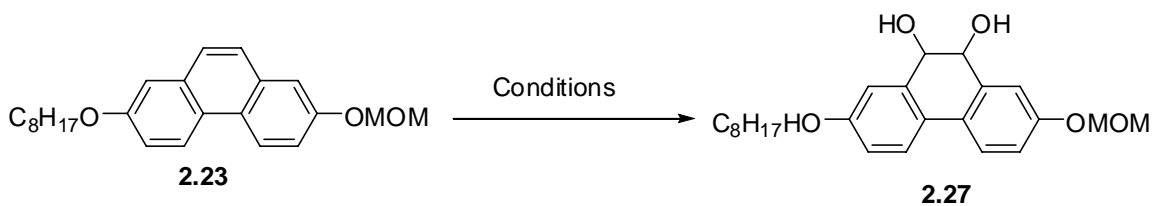
2.9). Thus, the synthesis of the target molecule **1.32** was achieved in 15 steps with an overall yield of 9% from commercially available starting material **2.1**.



Scheme 2.9

2.2. Synthesis of 9,10-Dihydroxy-7-(octyloxy)-9,10-dihydrophenanthren-2-yl 4-(undecyloxy)benzoate **1.31**

In order to achieve the synthesis of the 9,10-dihydrophenanthren-9,10-diol **1.31**, a standard dihydroxylation of **1.32** was envisaged.¹⁸⁸ In view of the small amounts of available **1.32**, compound **2.23** was selected as a test substrate for the dihydroxylation attempts. However, using a number of conditions which have been successful for this reaction on phenanthrene itself did not lead to the desired product **2.27** (Scheme 2.10) but led only to starting materials (entry 1), or cleavage of the MOM ether from **2.23** (entry 2), or a mixture of starting material and deprotected product (entry 3). The electron rich substituents, octyloxy and MOM, may make the bridge of the phenanthrene more aromatic-like rather than double bond like and not reactive towards oxidants.



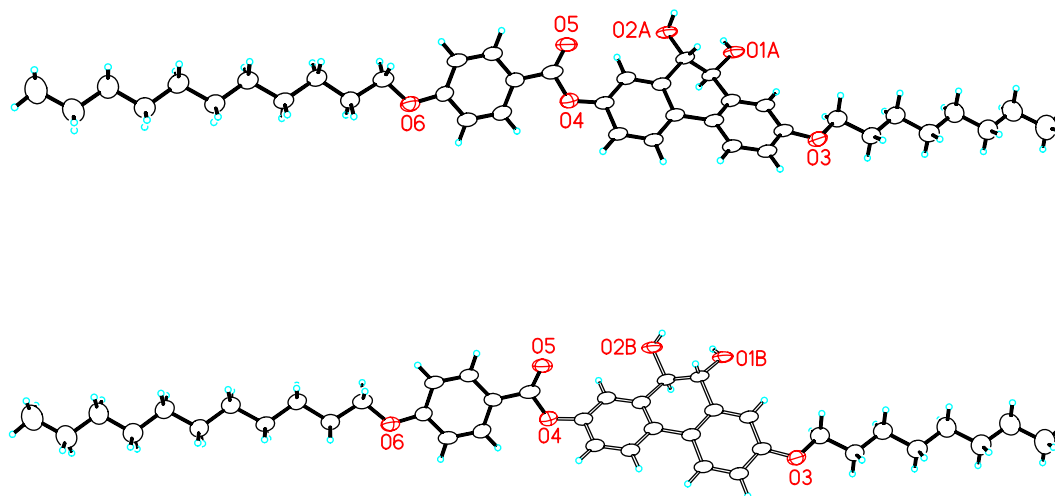
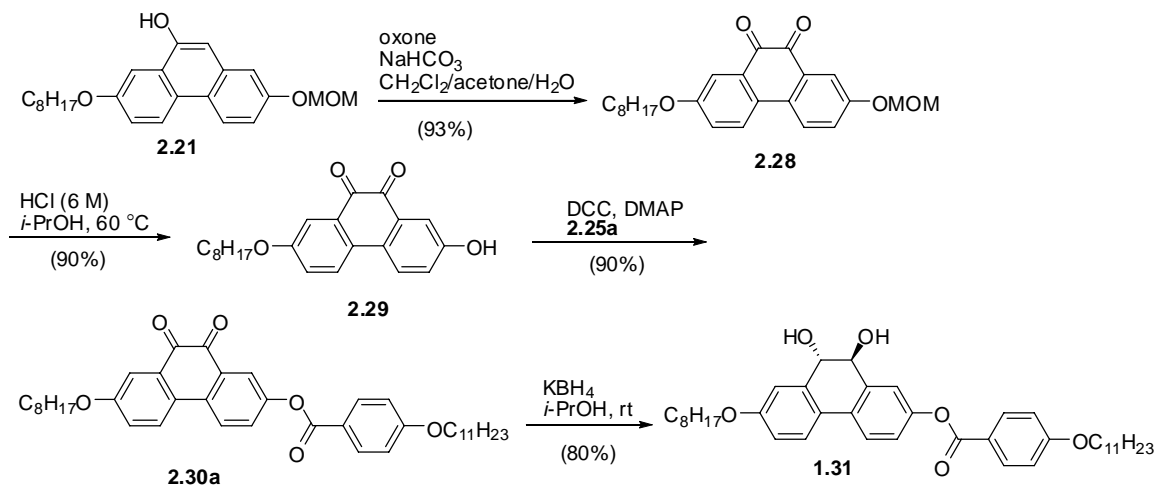
Entry	Conditions	Ref.	Result
1	OsO ₄ , pyridine, C ₆ H ₆ , rt-60 °C	188a	100% recovery of SM
2	NaIO ₄ , H ₂ SO ₄ , EtOAc/MeCN/H ₂ O	188b	100% deMOM product
3	AgOAc, I ₂ , HOAc	188c	60% SM 30% deMOM product

Scheme 2.10

The difficulty to affect the dihydroxylation of phenanthrene **2.23** prompted a change in strategy. A known classical synthesis of phenanthrene-9,10-diols involves the reduction of phenanthrene-9,10-diones,¹⁸⁹ which are readily available by oxidation of phenanthrene-9-ols.¹⁹⁰ In fact, the latter reaction is commonly observed by the gradual change of color of 9-phenanthrols, e.g. **2.21** from colorless to red, even upon standing in the air, indicative of the 9,10-quinone structure.

By adopting this tactic, the phenanthrene-9-ol **2.21** was oxidized to the red phenanthrene-9,10-dione **2.28** by the *in situ* generated dimethyldioxirane procedure.¹⁹⁰ MOM deprotection gave the purple dione **2.29**, which, upon DCC/DMAP mediated esterification, afforded the orange **2.30a** in excellent yield. Finally, reduction with KBH₄ gave the target *trans*-9,10-dihydrodiol **1.31** as a single diastereomer.¹⁸⁹ The relative

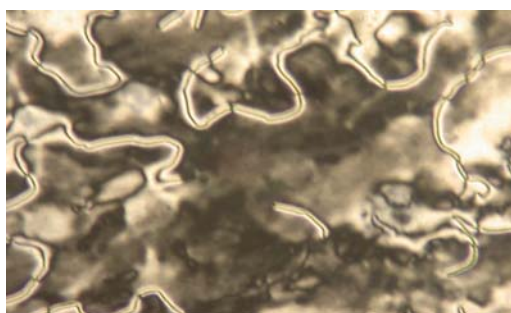
stereochemistry has been established by single crystal X-ray crystallographic analysis (Scheme 2.11).¹⁹¹



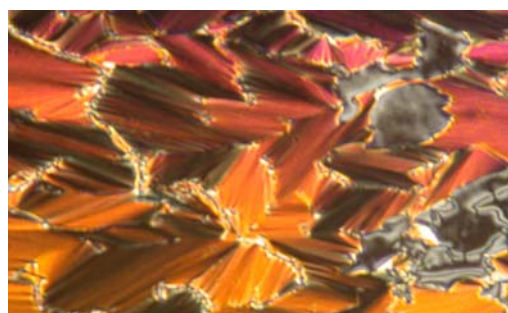
Scheme 2.11

2.3. Mesophase Characterization of Phenanthrene Liquid Crystal (1.32)

The mesophases formed by compound **1.32** were characterized by polarized microscopy and differential scanning calorimetry. The phenanthrene **1.32** forms nematic and SmC phases on heating and cooling. On cooling from its isotropic phase, **1.32** shows a schlieren texture (Figure 2.1(a)) at 208 °C by polarized microscopy, which is a typical texture of the nematic phase.¹⁹² At 184 °C, the schlieren texture turns into a fan texture (Figure 2.1(b)) with few schlieren domains coexisting with the broken fan texture, which is characteristic of a SmC phase. Crystallization occurs at 94 °C.



(a)



(b)



(c)

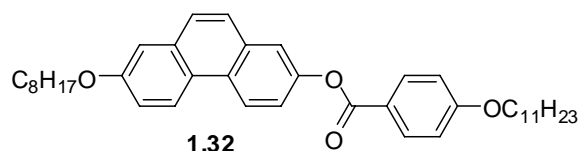


Figure 2.1 Photomicrographs of **1.32** (a) in the nematic phase at 208 °C; (b) in the SmC phase at 183 °C; (c) in the crystalline phase at 94 °C.

Table 2.1. The phase transition temperatures of **1.32** on cooling by polarized microscopy.

sample	SmC to Cr	N to SmC	I to N
1.32	94 °C	184 °C	208 °C

These observations are consistent with differential scanning calorimetry measurements. On cooling from isotropic to crystalline phases, three peaks are observed. The first small exotherm at 197 °C corresponds to the transition from isotropic to N phases; the second small exotherm at 176 °C corresponds to the transition from N to SmC phases; and the large exotherm at 94 °C corresponds to the transition from SmC to crystalline phases. On heating from crystalline to isotropic, the two endotherms at 110 °C and 112 °C are consistent with a crystal-crystal transition, and a crystal-SmC transition, respectively. The two endotherms at higher temperatures correspond to the phase transitions SmC-N and N-I, respectively. The broad SmC range is consistent with our expectation that a planar, polarizable phenanthrene core should result in strong van der Waal interactions between aromatic cores, thereby enhancing the amphiphilic character of the mesogens and the corresponding nanosegregation that is thought to promote lamellar smectic phases.

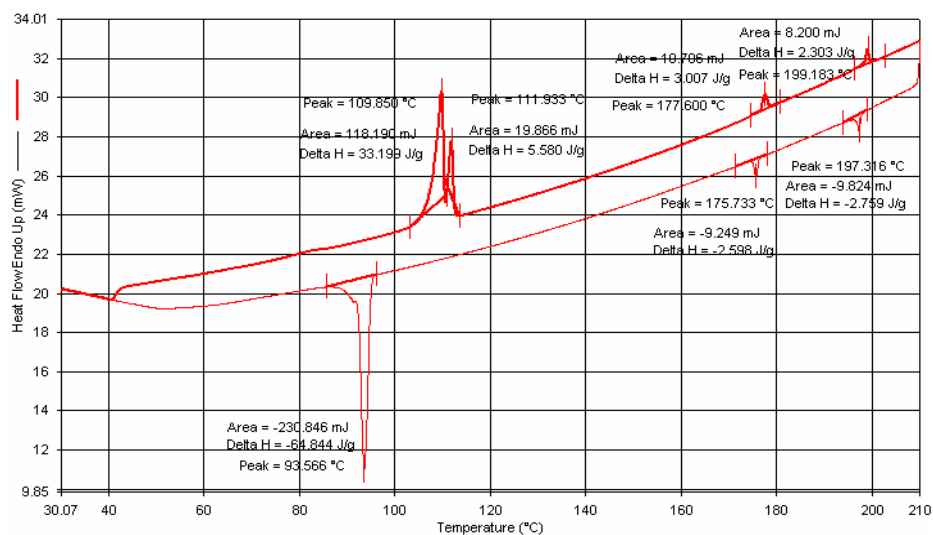


Figure 2.2 DSC measurement of **1.32**.

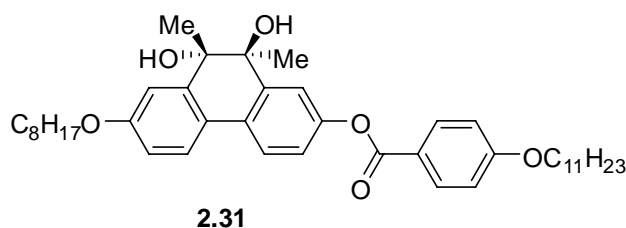
Table 2.2. The enthalpy changes of **1.32** at the transition temperature.

Heating							
Cr1 to Cr2		Cr2 to SmC		SmC to N		N to I	
T °C	ΔH kJ/mol	T °C	ΔH kJ/mol	T °C	ΔH kJ/mol	T °C	ΔH kJ/mol
109.9	19.8	111.9	3.3	177.6	1.8	199.2	1.4
Cooling							
SmC to Cr			N to SmC		I to N		
T °C	ΔH kJ/mol	T °C	ΔH kJ/mol	T °C	ΔH kJ/mol	T °C	ΔH kJ/mol
93.6	-55.8	175.7	-1.6	197.3	-1.7		

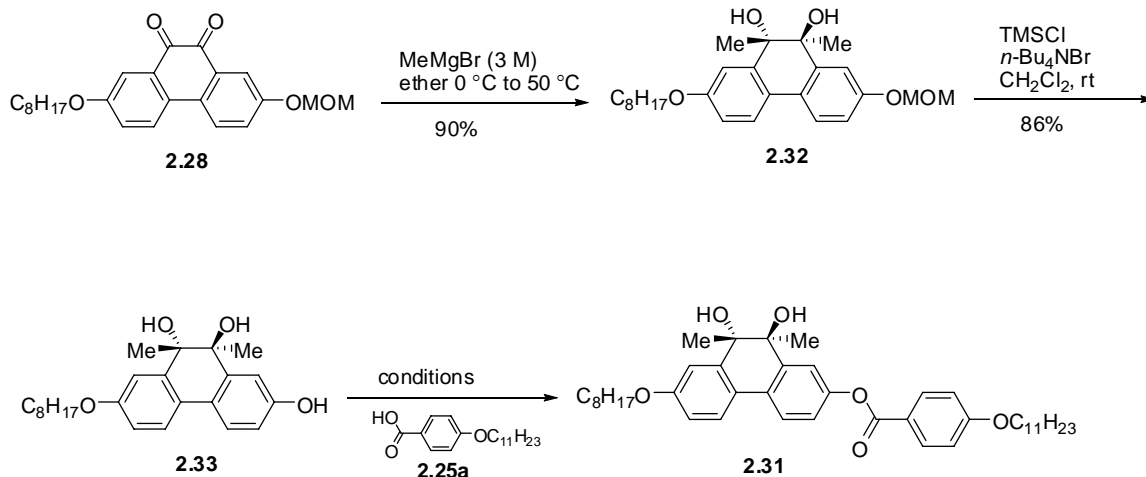
Performing the same measurements on the dihydrodiol **1.31** as carried out on **1.32** failed because the dihydrodiol is not stable. Thus, **1.31** was gradually reoxidized to 9,10-dihydrophenanthren-9,10-dione **2.30a** upon standing in air at room temperature. A quantitative experiment was carried out by measuring how much **1.31** was oxidized upon DSC measurement on a 3.75 mg sample after heating from 30 °C to 220 °C. Preparative TLC separation afforded 1.2 mg of **1.31** and 2.3 mg of **2.30a**.

2.4 Synthesis of the Stable 9,10-Dihydroxy-9,10-dimethyl-7-(octyloxy)-9,10-dihydrophenanthren-2-yl 4-(undecyloxy)benzoate **2.31**

The instability of the dihydrodiol **1.31** forced a modification of the target compound from **1.31** to **2.31**. Compound **2.31** is expected to retain all of the structural characteristics of **1.31** except that the C9 and C10 hydrogens are replaced by two methyl groups. It was hoped that the steric bulk of the methyls would not destroy the LC properties.



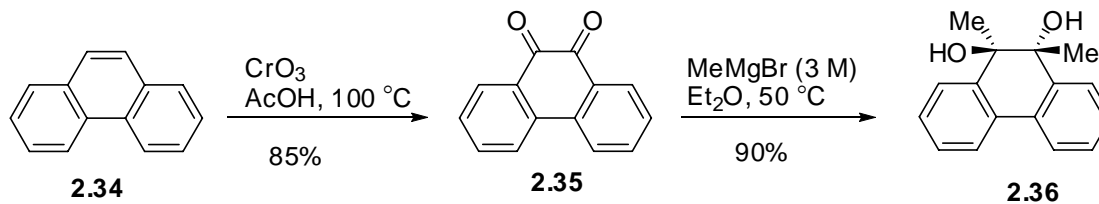
The synthesis of 9,10-dimethyl-9,10-dihydroxyphenanthrenediol **2.31** was initiated from the available 9,10-dione **2.28** (Scheme 2.12). Treatment with MeMgBr in a sealed tube at 50 °C¹⁹³ gave the *trans*-diol **2.32** as a single diastereomer¹⁹⁴ in high yield. In order to avoid any pinacol rearrangement,¹⁹⁵ the diol **2.32** was deprotected by *in situ*-produced TMSBr instead of HCl to give **2.33**.¹⁹⁶ Esterification of **2.33** under two conditions gave **2.31** in moderate to high yields.



Conditions	2.31 Yield %
2.25a DCC, DMAP, CH ₂ Cl ₂ , rt,	88
2.25a NaOH (0.5 M), THF, rt	61

Scheme 2.12

In order to predict the thermal stability of **2.31**, a model compound **2.36**¹⁹⁷ was synthesized as shown in Scheme 2.13. A DSC cell was prepared with 5.78 mg of **2.36** and was subjected to a DSC measurement in the same temperature range as used for **1.31** (30 °C to 220 °C). ¹H and ¹³C NMR data of the material in the DSC cell suggests no decomposition of **2.36** occurred under these conditions.



Scheme 2.13

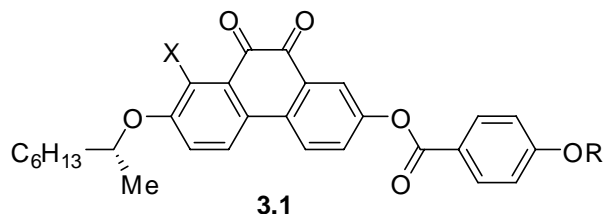
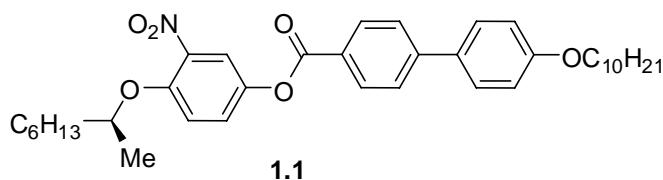
Unfortunately, analysis of **2.31** by polarized microscopy and differential scanning calorimetry revealed that it is not liquid crystalline, showing a single Cr-I melting point at 63–64 °C. This may be ascribed to the added lateral bulk of the methyl groups, which apparently weaken van der Waal's forces between aromatic cores, thereby reducing the amphiphilicity of the molecules that is thought to be at the origin of the formation of smectic phases.⁷

2.5. Summary

The synthesis of 9,10-dihydrophenanthrene-9,10-diol **1.31**, 9,10-dimethylphenanthrene-9,10-diols **2.31** and phenanthrene LC compound **1.32** were achieved by a combined directed *ortho* and remote metalation and cross coupling strategy. The LC characterization reveals that the model compound **1.32** is mesogenic with a narrow N phase and a broad SmC phase. Compound **1.31** was found to be too unstable due to oxidation to the phenanthrene dione to determine if it is mesogenic. Modification of **1.31** to compound **2.31** solved the oxidative degradation problem, but the new compound proved to be non-mesogenic because of the added lateral bulk of its core.

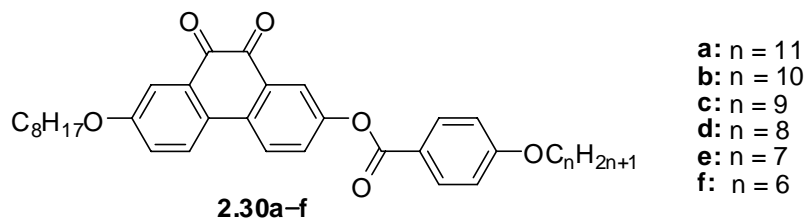
CHAPTER 3–PHENANTHRENE DIONE AND CHIRAL PHENANTHRENE DIONE LIQUID CRYSTALS

As discussed in the Introduction (Chapter 1), a chiral LC compound with a substituent *ortho* to a chiral side chain, e.g. compound **1.1**, may exhibit a relatively high spontaneous polarization P_S because of stereo-polar coupling.¹² A chiral 9,10-dihydrophenanthren-9,10-dione **3.1** was designed to explore the nature of this effect. In this case, the intention is to couple the same chiral 2-octyloxy side-chain to a highly polar core, which should impart an asymmetric conformational bias to the resulting stereo-polar unit, and therefore result in a high spontaneous polarization, provided that the transverse dipole of the core has a component along the polar axis of the SmC* phase. The effect of the coupling may be varied by changing the size of X.



Before undertaking the synthesis of **3.1**, the structurally similar achiral compounds **2.30a-f** were selected as model compounds for synthesis and LC characterization. As discussed in the Introduction (Chapter 1), the mesogenic properties of a LC should vary

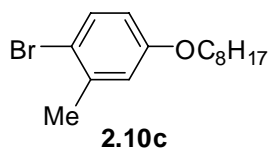
by changing the length of its side-chain(s), and we sought to select a side-chain length that provides the desired LC properties, which in this case is a SmC phase with the broadest possible temperature range, and a higher temperature nematic phase that would facilitate the alignment of a SmC* phase in a surface-stabilized configuration in a rubbed polyimide-coated glass cell.⁷



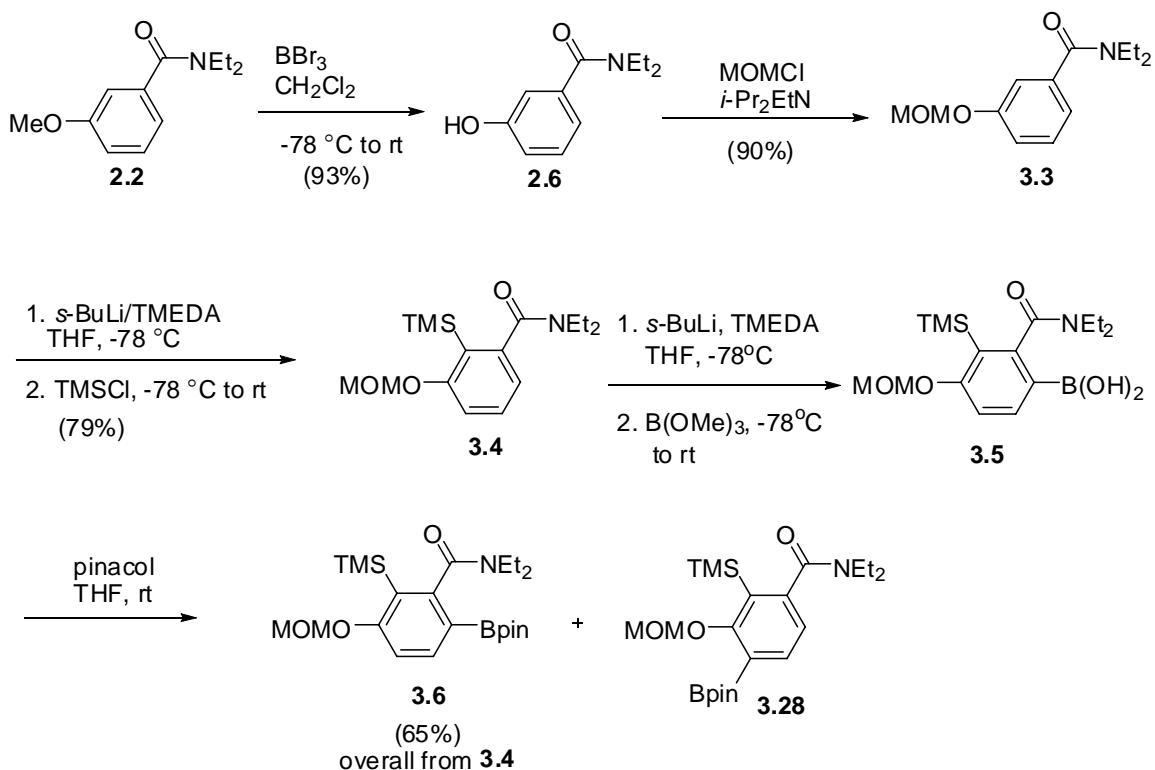
3.1 Synthesis of Phenanthredione Liquid Crystals **2.30a-f** by a Modified Route

The synthesis of the phenanthredione **2.30a** was described in Chapter 2. Compounds **2.30b-f** as well as compound **2.30a** were considered to be available by the same route (Scheme 2.9). Considering the lengthy, 15-step synthesis of **2.30a** from starting material **2.1**, two modified synthetic routes were explored to improve the efficiency for the synthesis of all phenanthrediones **2.30a-f**.

The original synthetic route for **2.30a** (Scheme 2.6) required the transformation of the bromo derivative **2.18** into the phenol **2.19** and then a protection-deprotection sequence to obtain the final product **2.30a**. Through the use of the cross coupling partner **2.10c**, which has one side chain already installed, the synthesis may be abbreviated by three steps.

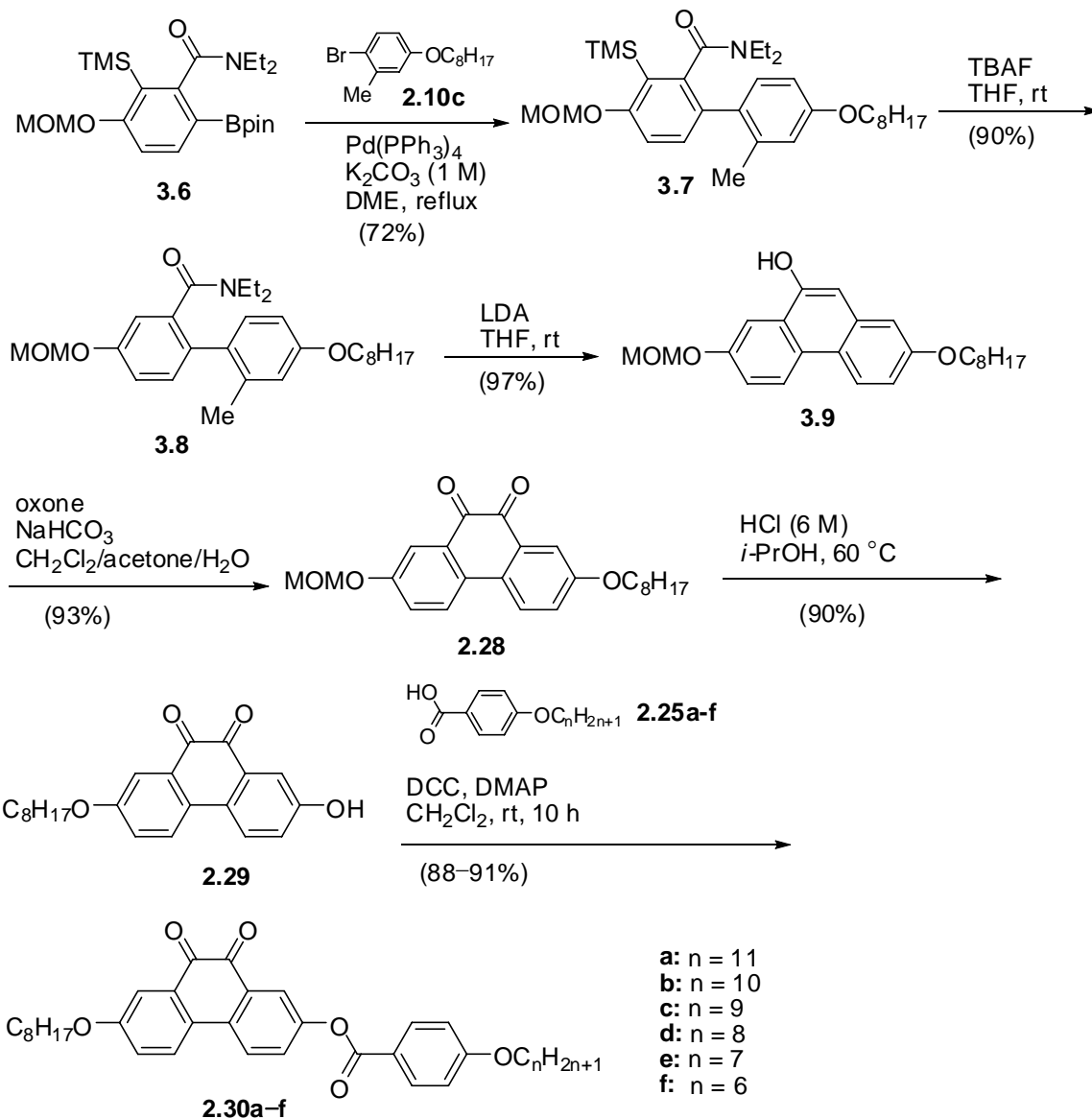


The proposed modified synthetic route began from the benzamide **2.2** by changing the protective group of the phenol **2.6** from Me (**2.2**) to MOM (**3.3**) which was achieved in high yields. DoM-silylation of compound **3.3** proceeded uneventfully to give compound **3.4**. The second DoM, boronation and pinacolation resulted in the formation of two regioisomers, the C6-Bpin (**3.6**) and the C4-Bpin derivative (**3.28**) in a ratio of 8:1 (by GC-MS). Two recrystallizations of the crude product from hexanes gave pure C6-Bpin isomer **3.6** in 65% yield. The overall yield from 3-methoxybenzoic acid **2.1** to cross coupling partner **3.6** is 40%.



Scheme 3.1

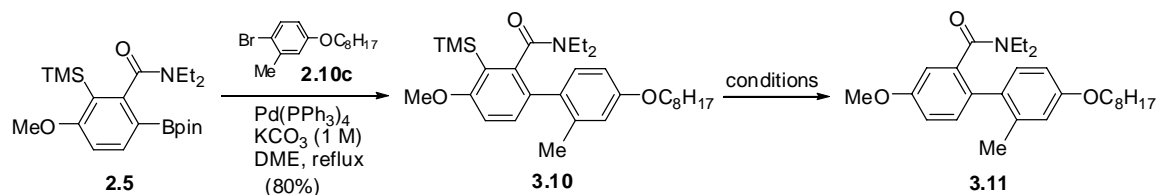
Under the standard Suzuki coupling conditions, **3.6** underwent cross coupling with **2.10c** to give biaryl **3.7** in moderate yield. Desilylation of **3.7** with TBAF afforded DreM precursor **3.8** in excellent yield. LDA treatment of **3.8** under standard conditions afforded 9-phenanthrol **3.9**, which upon oxidation gave 9,10-dione **2.28**. MOM deprotection and esterification according to the method described in Chapter 2 (Scheme 2.11) afforded the target molecules **2.30b-f** in 12 steps from 3-anisic acid and in 19% overall yield.



Scheme 3.2

In a second modified synthetic route to LC candidates **2.30a-f**, the modification of the protective group from Me to MOM after the Suzuki cross coupling was envisaged. In view of the poorer DMG quality of OMe compared to OMOM,⁵⁶ this route was proved to avoid the DoM regioselectivity problem of *ortho*-amide and *ortho*-MOM observed above (Scheme 3.1). The Suzuki cross coupling of **2.5** with bromobenzene **2.10c** proceeded well to afford biaryl **3.10**. The following desilylation step was unexpectedly difficult

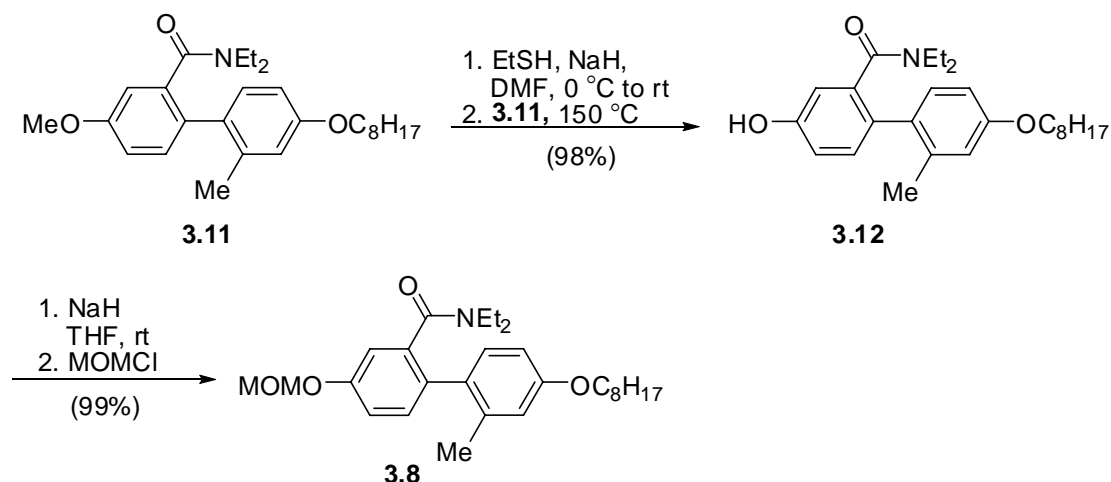
using the normal desilylation reagent TBAF. Thus, the reaction under TBAF conditions at rt for 12 hours resulted in a mixture of starting material and product **3.11** in a ratio of 3:1. However, modification of the reaction conditions to CsF in DMF at 100 °C¹⁹⁸ gave **3.11** in excellent yield. The hindered position of TMS and the electron-rich character of the aryl methoxybenzene may explain the failure of TBAF desilylation.



SM	conditions	yield%
3.10	TBAF, THF, rt	23% with 69% of SM recovered
3.10	CsF, DMF, 100 °C	98%

Scheme 3.3

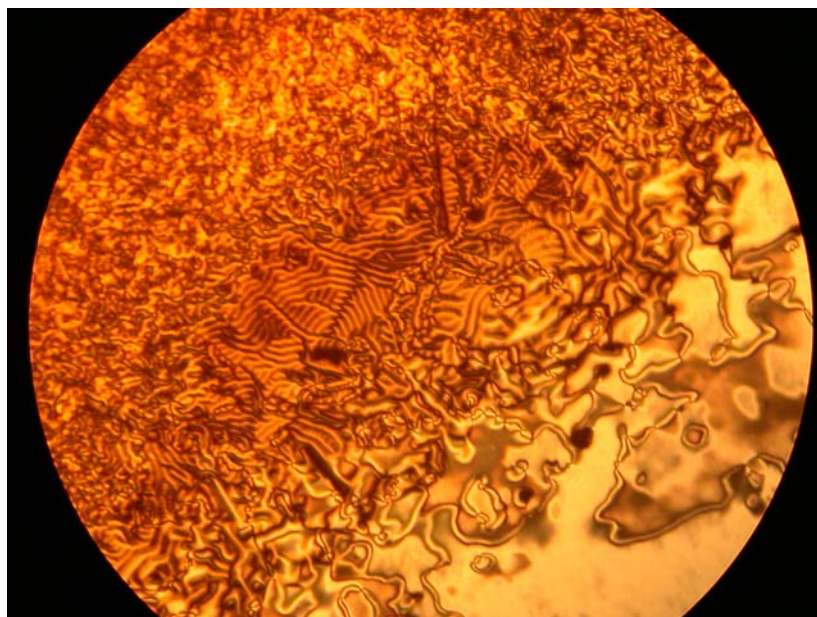
In view of the potential cleavage of the *n*-octyl side chain under strong Lewis acid **BBr₃** conditions, an anionic nucleophilic procedure using EtSNa in DMF at 150 °C¹⁹⁹ was adopted and led selectively to the phenol **3.12** in excellent yield (Scheme 3.4). MOM protection of phenol **3.12** gave compound **3.8**. Then following the synthetic route shown in Scheme 3.2 gave **2.30a-f** in 12 steps with an overall yield of 34–36%.



Scheme 3.4

3.2 Mesophase Characterization

The mesophases formed by compounds **2.30a-f** were characterized by polarized microscopy and differential scanning calorimetry. The data from polarized microscopy measurements, listed in Table 3.1, suggest that the phenanthrenediones **2.30a-c** form only SmC phases and that the phenanthrenediones **2.30d-f** form SmC and nematic phases. This is consistent with well established empirical structure-property relationships showing that longer aliphatic side-chains favor the formation of smectic phases at the expense of the nematic phase, which tends to be predominant in mesogens with relatively short side-chains.⁷ The typical textures of the N phase and SmC phases of **2.30f** as seen in the microscope are shown in Figure 3.1.²⁰⁰



(a)



(b)

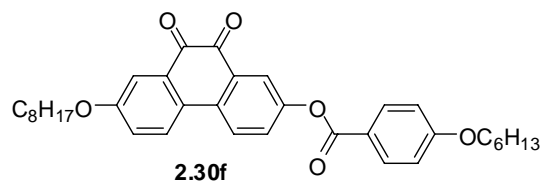
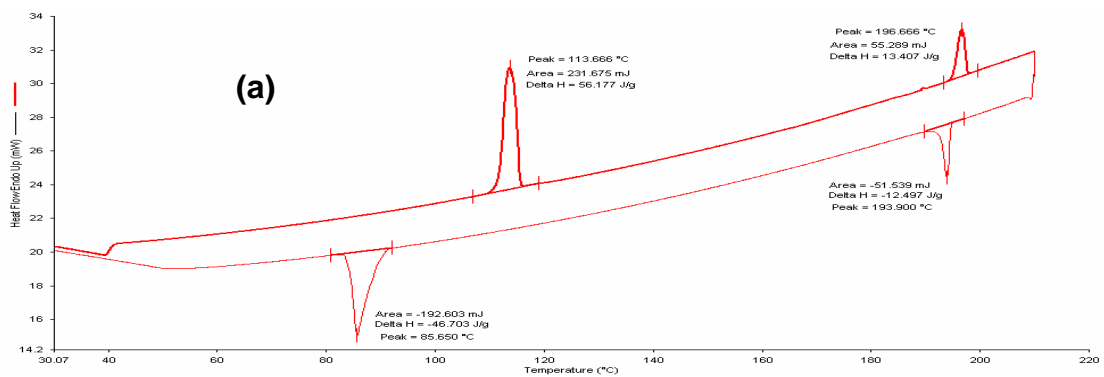


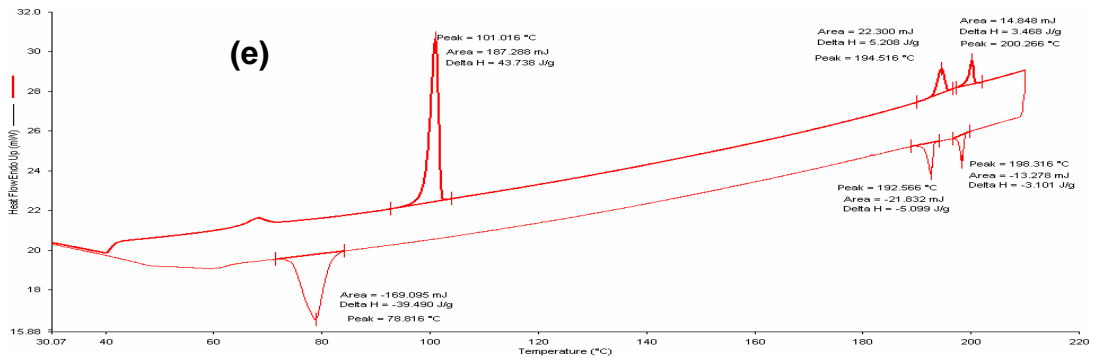
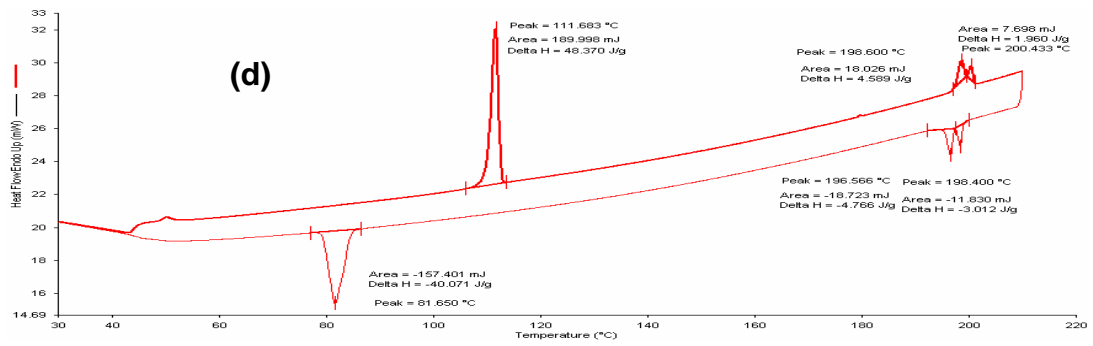
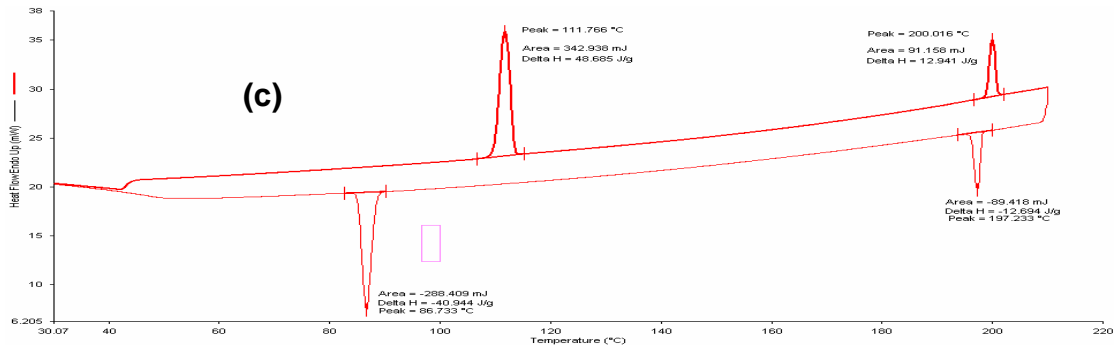
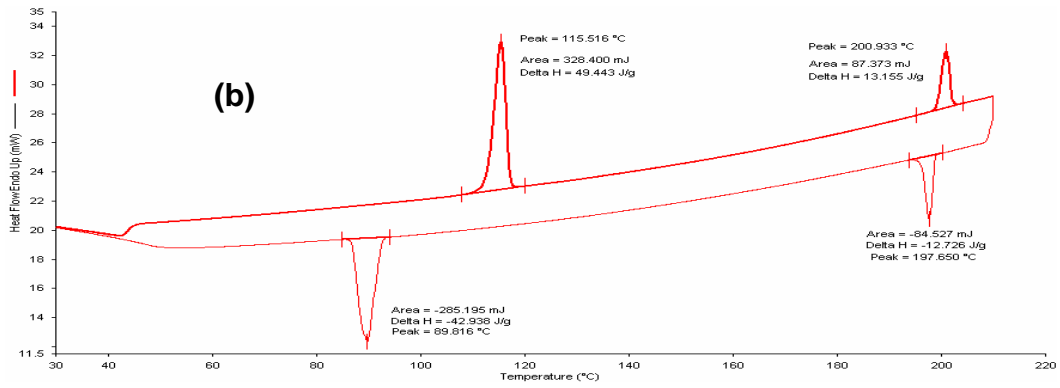
Figure 3.1 Photomicrographs of **2.30f** (a) in the N phase at 197 °C; (b) in the SmC phase at 185 °C.

Table 3.1 The phase transition temperatures of **2.30a-f** during cooling in polarized microscopy

mesogen	SmC to Cr	N to SmC	I to N	I to SmC
2.30a	87 °C			200 °C
2.30b	83 °C			195 °C
2.30c	79 °C			199 °C
2.30d	82 °C	199 °C	202 °C	
2.30e	78 °C	196 °C	201 °C	
2.30f	82 °C	186 °C	199 °C	

The DSC measurements are consistent with the polarized microscopy data. As shown in Figure 3.2a-c, there are only two peaks in both the heating and cooling profiles, which indicate one LC phase. In Figure 3.2d-f, there are three peaks in the heating and cooling profiles, which indicate that there are two LC phases.





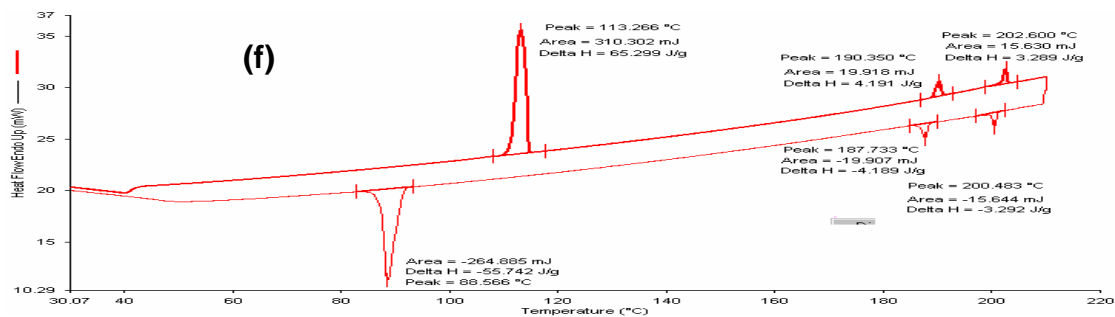


Figure 3.2 DSC measurement of **2.30**: (a) for **2.30a**; (b) for **2.30b**; (c) for **2.30c**; (d) for **2.30d**; (e) for **2.30e**; (f) for **2.30f**.

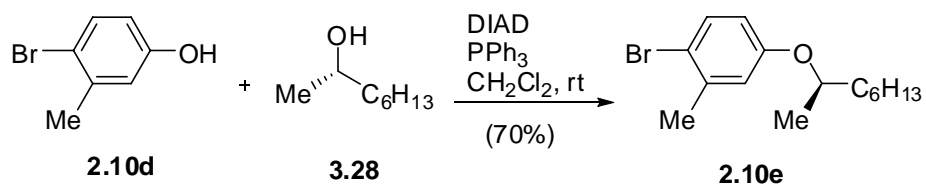
Table 3.2 The phase transition temperatures and enthalpy changes of **2.30a-f** by DSC.

mesogen	Heating							
	Cr to SmC		SmC to N		N To I		SmC to I	
	T °C	ΔH kJ/mol	T °C	ΔH kJ/mol	T °C	ΔH kJ/mol	T °C	ΔH kJ/mol
2.30a	113.7	35.2					196.7	8.4
2.30b	115.5	30.3					200.9	8.1
2.30c	111.8	29.2					200.0	7.7
2.30d	111.7	28.3	198.6	2.7	200.4	1.1		
2.30e	101.0	25.0	194.5	3.0	200.3	2.0		
2.30f	113.3	36.4	190.4	2.3	202.6	1.8		
mesogen	Cooling							
	SmC to Cr		N to SmC		I to N		I to SmC	
	T °C	ΔG kJ/mol	T °C	ΔG kJ/mol	T °C	ΔG kJ/mol	T °C	ΔG kJ/mol
2.30a	85.7	-29.3					193.9	-7.8
2.30b	89.8	-26.3					197.7	-7.8
2.30c	88.7	-24.5					197.2	-7.6
2.30d	81.7	-23.4	196.6	-2.8	198.4	-1.8		
2.30e	78.8	-22.5	192.6	-2.9	198.3	-1.8		
2.30f	88.7	-31.0	187.7	-2.3	200.5	-1.8		

Based on these data, the most promising derivative is **2.30f**, which forms a broad SmC phase and a nematic phase with the broadest temperature range. This compound was therefore chosen for the introduction of a chiral center.

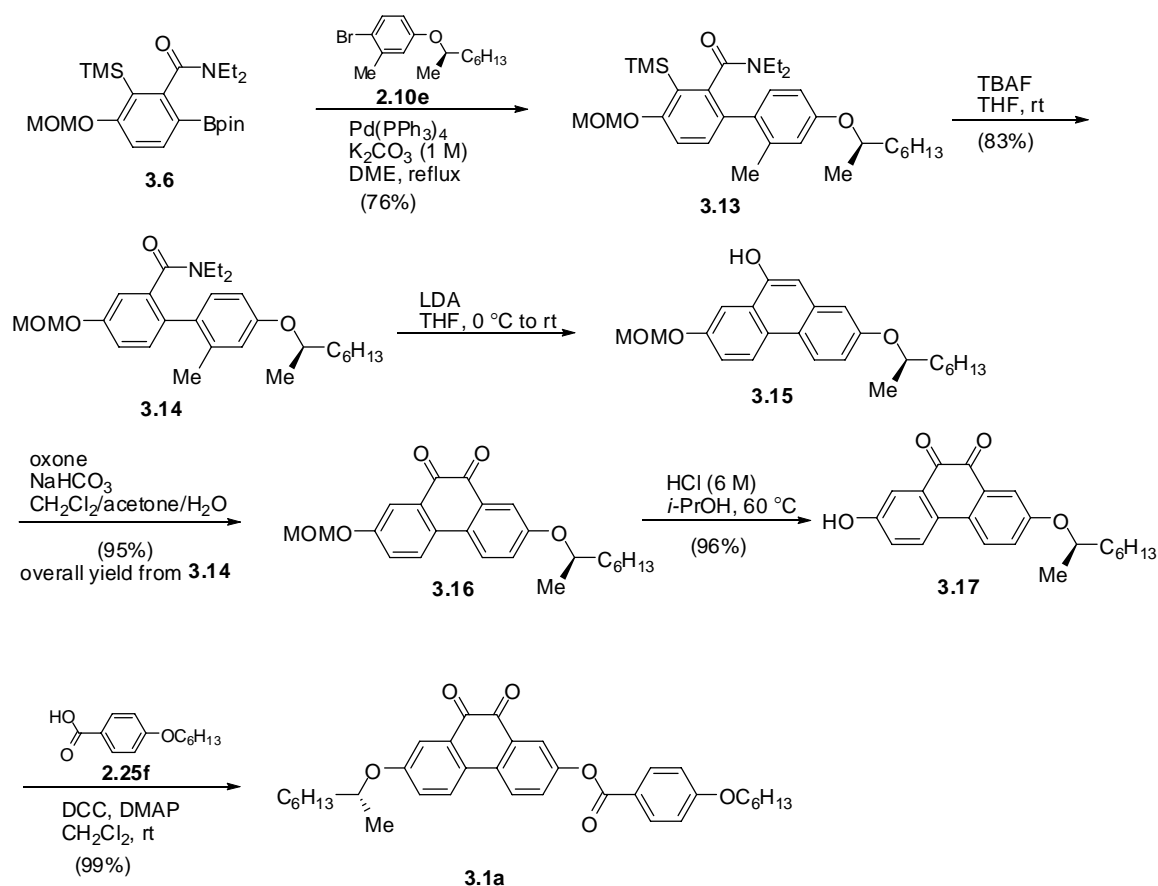
3.3 Synthesis of Chiral Phenanthrene-9,10-diones 3.1a-b

The synthesis of **3.1a** followed the same route as that carried out for **2.30** (Scheme 3.2) except for a change in the Suzuki cross coupling partner from **2.10c** to **2.10e**, which was prepared by a Mitsunobu reaction.



Scheme 3.5

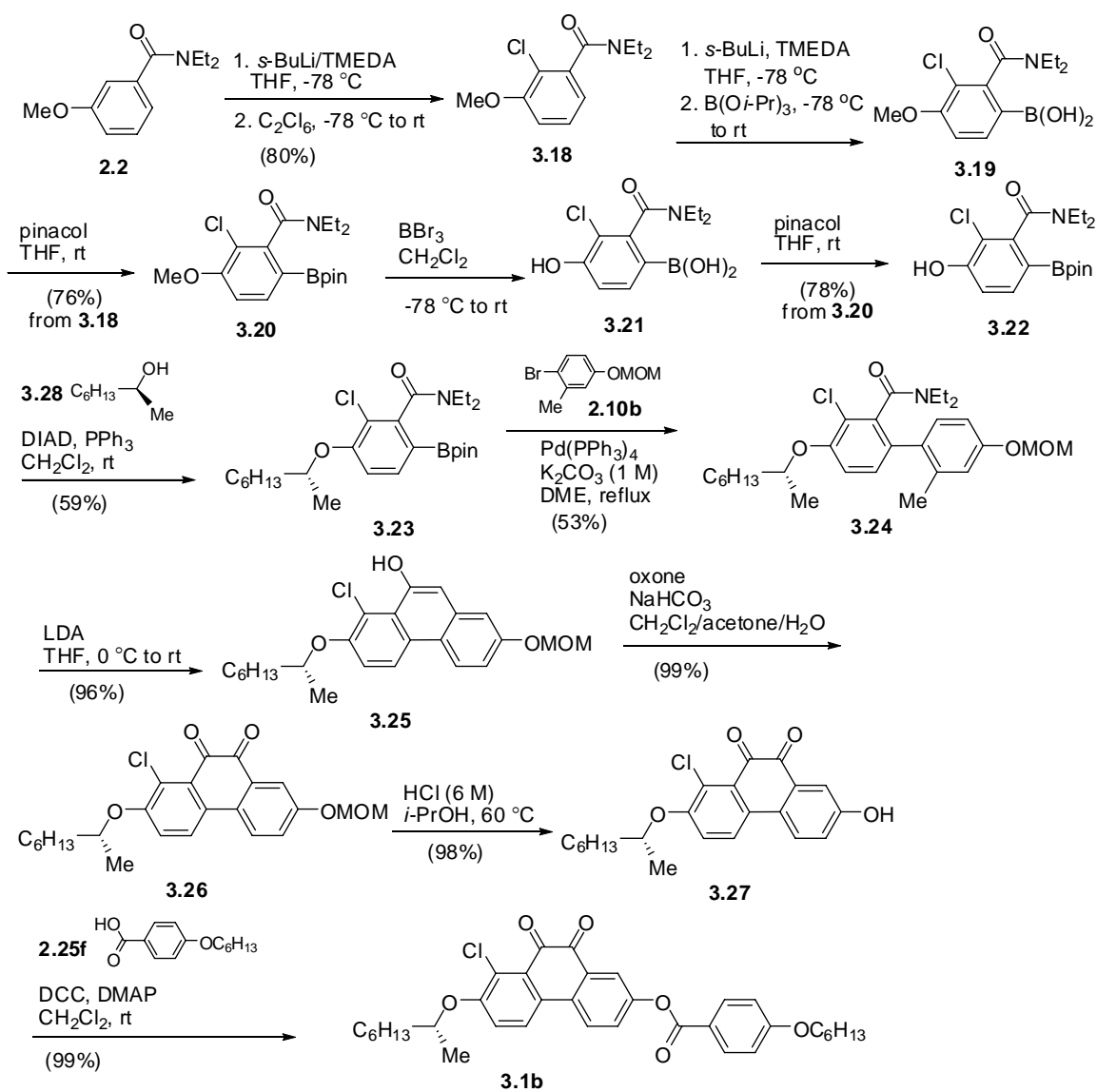
As shown in Scheme 3.6, the total synthesis of **3.1a** was fulfilled in 12 steps from 3-methoxybenzoic acid **2.1** with an overall yield of 23%.



Scheme 3.6

The synthesis of the chlorophenanthrene-9,10-dione **3.1b** presented an opportunity to showcase the value of DoM for the construction of polysubstituted aromatics. Thus (Scheme 3.7) the chloro group was installed at the beginning by standard DoM conditions on benzamide **2.2** followed by quench with C_2Cl_6 , to give compound **3.18**. DoM of **3.18** followed by B(Oi-Pr)_3 quench and pinacolation gave the Bpin derivative **3.20**. As perhaps not unexpectedly, under BBr_3 conditions both demethylation and depinacolation occurred to give phenol boronic acid **3.21**. Interestingly, borodesilylation of DMG-bearing arylsilanes has been observed in our laboratories under BBr_3 or BCl_3 conditions.²⁰¹ In view of the poor solubility of compound **3.21** in organic solvents, the

crude product was reconverted into the Bpin phenol **3.22** for purification. Mitsunobu reaction of **3.22** with **3.13** gave the ether **3.23** in a moderate yield which, under standard cross coupling conditions with **2.10b** gave the biaryl **3.24**. LDA treatment of **3.24** proceeded uneventfully to give phenanthrol **3.25** which, upon oxidation, afforded the red phenanthrene-9,10-dione **3.26**. Deprotection under acidic conditions gave the phenol **3.27** which, upon esterification, furnished the final product **3.1b**. The synthesis was achieved in 12 steps in an overall 13% yield from 3-methoxybenzoic acid **2.1**.



Scheme 3.7

Unfortunately, the mesophase characterization of chiral phenanthrene-9,10-diones **3.1a** and **3.1b** show that these compounds are not mesogenic, with single Cr-I melting points of 125–127 °C for **3.1a** and 199-200 °C for **3.1b**. It is likely that the lateral bulk of the chiral centers in these compounds are not compatible with the planar phenanthrene-9,10-dione core and destroy the mesogenic properties.

3.4 Summary

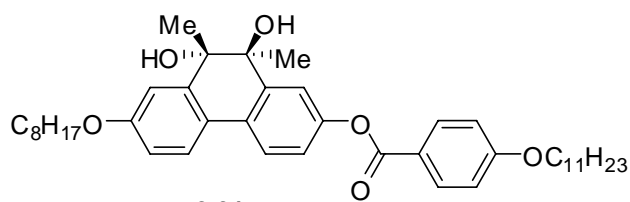
The synthesis of achiral phenanthrene-9,10-diones **2.30a-f** and chiral phenanthrene-9,10-dione **3.1a,b** was achieved in a modified synthetic route by changing the cross coupling partner **2.10** from bromo (**2.10a**) to *n*-octyloxy (**2.10c**) or methoxymethoxy (**2.10b**) groups (see Scheme 3.2 and Scheme 3.7). The new route was found to increase the Suzuki cross coupling efficiency and to save synthetic steps. Initial LC characterization reveals that compounds **2.30d-f** are mesogenic with a large range of SmC phases and an N phase. With the increase of chain length, the nematic phase become narrower and eventually disappears after $n = 9$ (**2.30a-c**), which is consistent with theory that aspect ratio favours the SmC phase. Unfortunately, the steric bulk of the chiral side chains in **3.1a** and **3.1b** destroy their LC characteristics.

CHAPTER 4–CHIRAL PHENANTHRENE-9,10-DIONE 3.1a,b AND CHIRAL PHENANTHRENE-9,10-DIOL (-)-4.1 AS DOPANTS

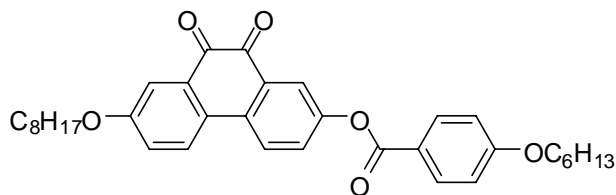
As discussed in Chapter 1, a non-mesogenic chiral dopant may induce a Ps in an achiral SmC host. The propensity of a dopant to induce a polarization is expressed by the polarization power according to the following equation:

$$\delta = \left(\frac{dP_0(x_d)}{dx_d} \right)_{x_d \rightarrow 0} \quad P_0 = P_s/\sin\theta$$

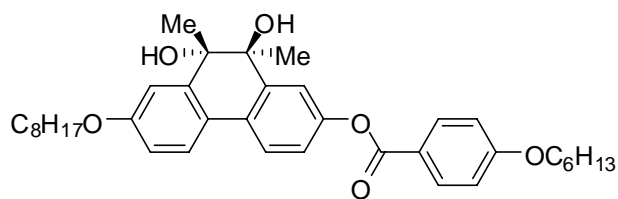
In studies described in Chapter 2, it was found that compound **2.31** is not a liquid crystalline material. However, it may induce a Ps as a single enantiomer in an achiral liquid crystal host, which may be enhanced by intermolecular hydrogen bonding between the dopant and the host. Considering that the phenanthrene-9,10-dione **2.30f** may be used as a host, we selected compound (-)-**4.1** instead of **2.31** as the dopant because the undecyloxy side chain of **2.31** does not match the hexyloxy side chain of **2.30f**. Thus, compound (-)-**4.1** was synthesized as the dopant to maximize its compatibility with the host **2.30f**.



2.31

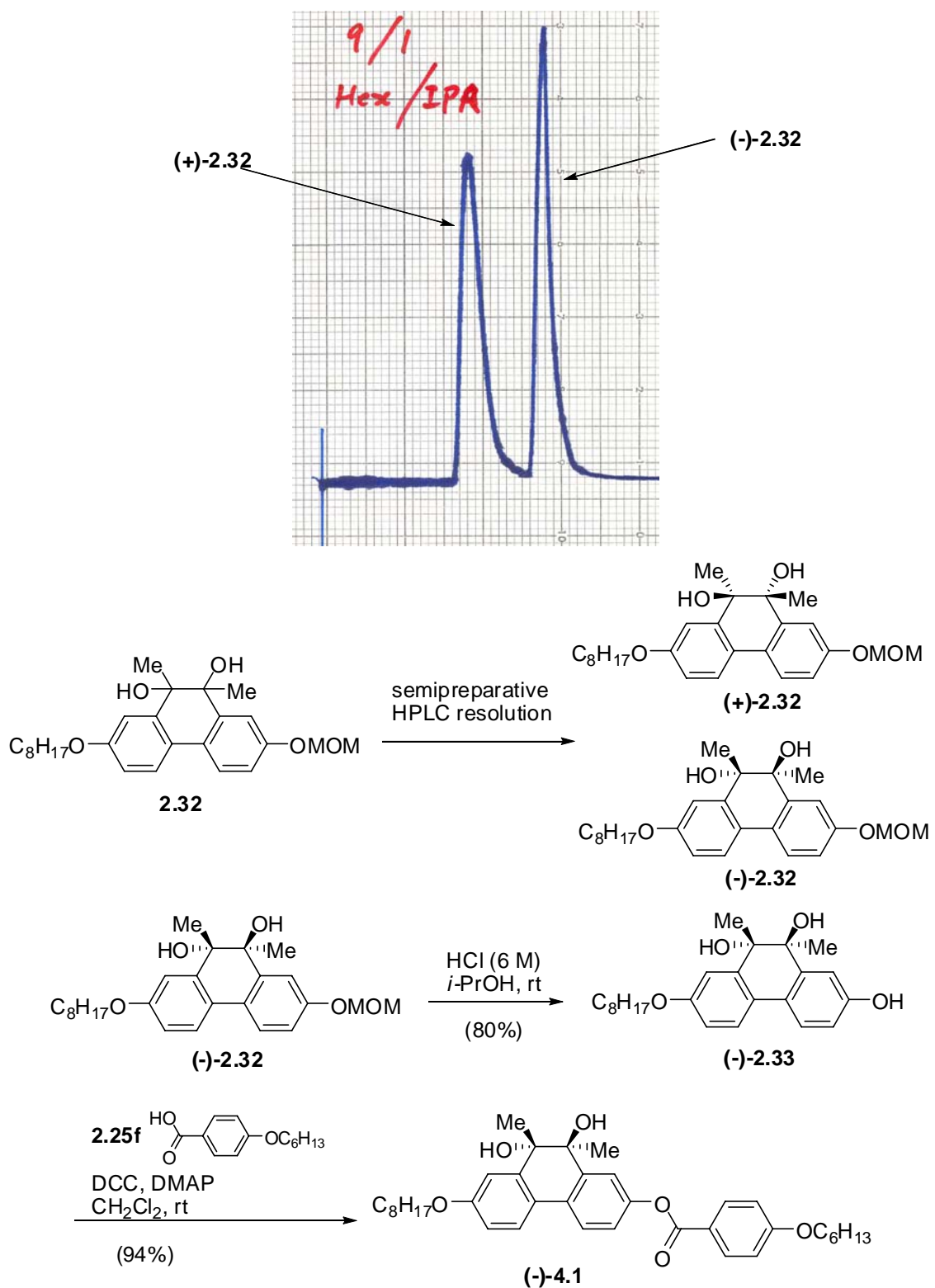


2.30f



(-)-4.1

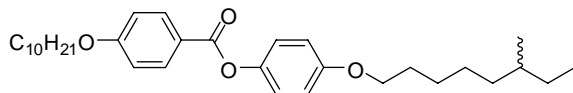
As shown in Scheme 4.1, the precursor **2.32** was resolved by semipreparative chiral stationary phase HPLC using a Daicel Chiralpak-AS column (10% *i*-PrOH in hexanes, 50 mL/min) to give pure enantiomers (+)-**2.32a** and (-)-**2.32**.²⁰² Enantiomer (-)-**2.32** was deprotected under acidic conditions to afford the phenol (-)-**2.33** which, upon esterification gave the benzoate (-)-**4.1**.



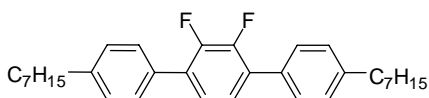
Scheme 4.1

4.1 Polarization Measurements

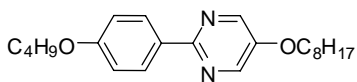
The resolved compound (-)-**4.1** was used as a chiral dopant in the liquid crystal hosts of **PhB**, **DFT**, **PhP1** and **2.30f**. The compound **PhB**, **DFT** and **PhP1** were chosen as hosts because they have low viscosity and a broad range of SmC phase. The host **2.30f** was chosen because it has the best LC properties in the **2.30a-f** series.



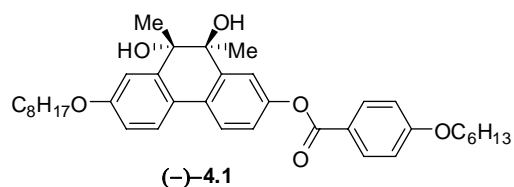
PhB: Cr 35 SmC 70.5 SmA 72 N 75 I



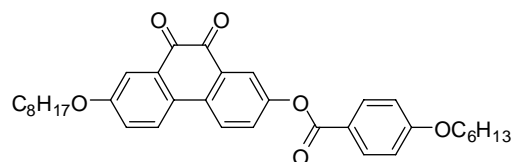
DFT: Cr 49 SmC 77 SmA 93 N 108 I



PhP1: Cr 58 SmC 85 SmA 95 N 97 I



(-)-**4.1**



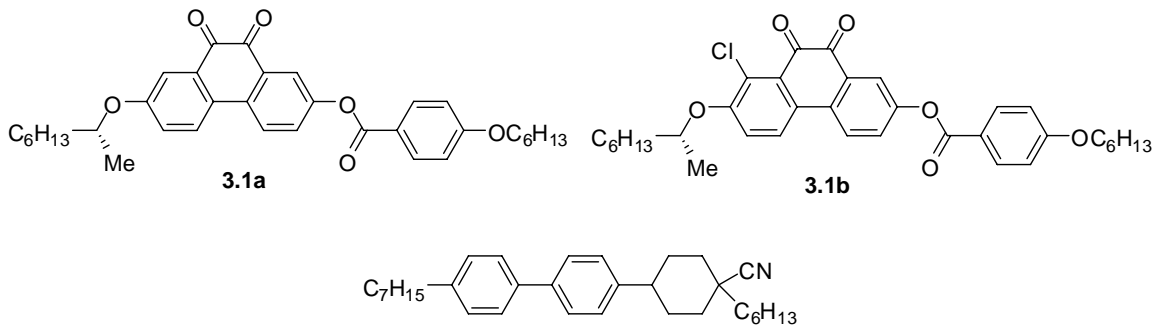
2.30f

The dopant (-)-**4.1** was purified by recrystallization (three times) from HPLC grade hexanes. Three homogeneous mixtures of optically pure dopant (-)-**4.1** (5 mol%) in **PhB**, **DFT** and **PhP1** were aligned as surface-stabilized ferroelectric liquid crystal (SSFLC) films using commercial ITO glass cells with rubbed polyimide surfaces and a cell gap of 4 μm . A homogeneous mixture of (-)-**4.1** in **2.30f** could not be formed even by reducing the molar fraction of (-)-**4.1** to 2.6 mol% as evidenced by observation of coexisting liquid and LC domains over a broad range of temperatures by polarized microscopy. This suggests that the 9,10-dimethylphenanthrene-9,10-diol core of (-)-**4.1** is not compatible with the phenanthrene-9,10-dione core of **2.30f**. Attempts were made to measure the

spontaneous polarizations of these samples (Ps) in the SmC phase at $T-T_c = -5$ K and -10 K by the triangular wave method.²⁰³

Although ferroelectric induction was achieved in each sample ((-)-**4.1/PhB**, ((-)-**4.1/DFT**, ((-)-**4.1/PhP1**, ((-)-**4.1/2.30f**) as evidenced by observation of electro-optical switching upon applying an electric field, the value of Ps was below the detection limit of the instrument, i.e., ca. 0.5 nC/cm^2 . This means that the polarization power cannot be any higher than ca. 35 nC/cm^2 assuming a tilt angle on the order of 20 degrees. This result may be rationalized by the fact that the chiral core is likely to have relatively little conformational asymmetry in the binding site of the SmC host due to a lack of steric coupling with the two side-chains and the rotational axis of the phenanthrene core. In other words, in the absence of other effects favoring polar ordering, such as chirality transfer feedback,²⁰⁴ the chiral polar core in (-)-**4.1** should be able to freely rotate with respect to the side-chains within the confines of the binding site of the host, thus resulting in negligible spontaneous polarization. Furthermore, this result suggests that any hydrogen bonding between the dopant and surrounding host molecules does not enhance the polar order of the dopant to any significant extent.

Compounds **3.1a** and **3.1b** were also used as dopants in hosts **PhB**, **DFT**, **PhP1**, **NCB76** and **2.30f**. Because the chlorine is larger than hydrogen, the chiral side-chain should be more strongly coupled to the polar core in **3.1b**, and result in a higher polarization power than with **3.1a**. **NCB76** was chosen because it has an axial CN group on a cyclohexane ring which may promote a perpendicular orientation of the flat-polar-dopants, e.g. **3.1a** and **3.1b**, with respect to the host core via strong dipole-dipole interactions.²⁰⁵



The dopants **3.1a** and **3.1b** were purified by recrystallization (three times) from HPLC grade ethyl acetate/hexanes (30/70). Homogeneous mixtures of optically pure dopant **3.1a** or **3.1b** (5 mol%) in **PhB**, **DFT**, **PhP1** and **NCB76** were aligned as surface-stabilized ferroelectric liquid crystal (SSFLC) films using commercial ITO glass cells with rubbed polyimide surfaces and a cell gap of 4 μm . Homogeneous mixtures of **3.1a** or **3.1b** (5 mol%) in **2.30f** were achieved but could not be aligned properly because the viscosity of the host is high and the cell resistivity proved to be too low at temperatures below the clearing point.

All the mixtures showed ferroelectric induction but no measurable polarization. This may be explained by the literature precedent²⁰⁶ suggesting that, in the case of biaxial smectic phases like the SmC phase, the plane of strongly biaxial (i.e., flat) mesogenic cores is normally oriented in the tilt plane, which would result in negligible polarizations from dopants with biaxial cores like **3.1a** and **3.1b** in which the transverse dipole is oriented along the plane of the core.

4.2 Summary

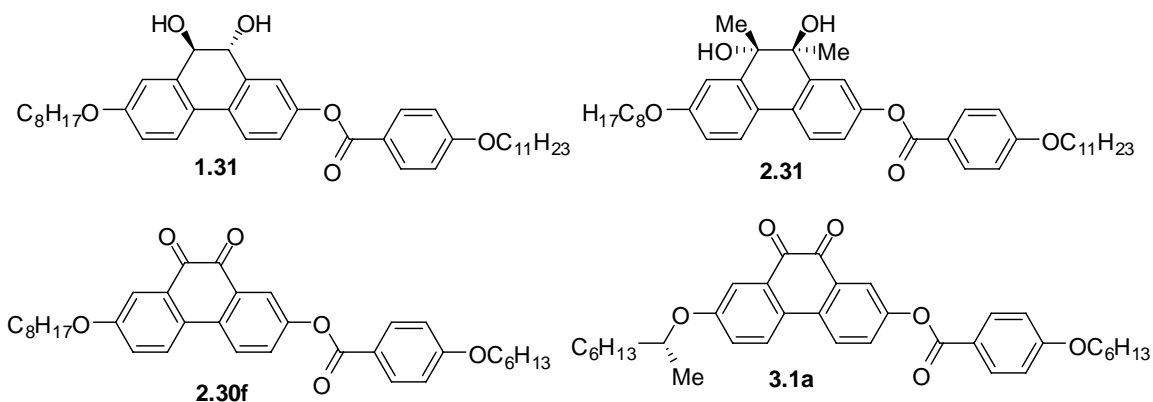
Spontaneous polarization measurements were carried out for samples consisting of about 5 mol% of dopants ((-)**4.1** or **3.1a** or **3.1b**) and 95 mol% of hosts (**PhB**, **DFT**,

PhP1, **NBC76** and **2.30f**). All the samples have an observable polarization that is too small to be measured by the triangular wave method.

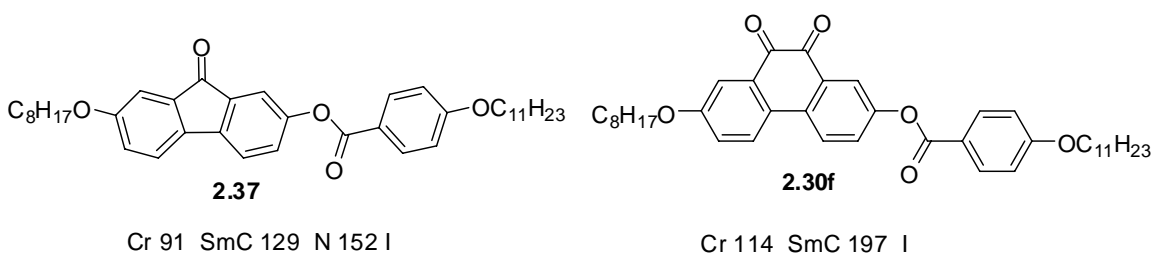
For Type II dopant **(-)-4.1**, intermolecular hydrogen bonding does not enhance the polar order to any significant extent. For Type I dopants **3.1a** and **3.1b**, considering that the polarization induced by a chiral 2-octyloxy side-chain unit on its own is normally on the order of 100 nC/cm^2 ,¹⁵ the alkoxy dipole in **3.1a** and **3.1b** should lie in the plane of the phenanthredione core. These results suggest that the core/alkoxy dipole of the dopant may lie near the tilt plane of the SmC* phase in each host, and therefore cannot contribute to the polarization. This is consistent with the assumption that biaxial cores tend to lie in the tilt plane in the SmC phase.

4.3 Conclusion

The question whether intermolecular hydrogen bonding promotes polar order in the SmC* phase is left unsolved because of the unstable character of compound **1.31**. Structural modification of **1.31** to **2.31** successfully stabilized the diol core, but destroyed its LC properties because of the increase of lateral bulk in the phenanthrene bridge, which indicates that the LC properties of phenanthrene derivatives are very sensitive to lateral bulk. This is demonstrated by the fact that **2.30f** has a SmC phase with a range of 77 K. However, compound **3.1a** has no LC properties at all despite the fact that the chirality is introduced in the alkoxy side chain, which is further evidence that lateral bulk (in this case, branching of the side-chain) strongly disfavours the formation of mesophases.



On the other hand, in comparison with the fluorenone **2.37**,⁴³ comma before ref which forms an enantiotropic SmC phase with a range of 38 K, as well as an enantiotropic N phase with a range of 23 K, the phenanthrenedione **2.30f** forms a much more stable SmC phase with a range of 83 K but does not form a N phase. This is consistent with the assumption that a more polar core with stronger van der Waals interactions favours the formation of a SmC phase. Therefore, the phenanthrenedione core may be useful in the design of materials forming SmC mesogens with broad, stable SmC phases.



Scheme 4.1

CHAPTER 5—EXPERIMENTAL

5.1. General Methods.

^1H NMR (300, 400, 500 and 600 MHz) and ^{13}C NMR (75, 100, 125 and 150 MHz) spectra were recorded on Bruker AC-300, AC-400, AC-500 and AV-600 instruments in CDCl_3 (unless otherwise indicated). The chemical shifts are reported in (ppm) relative to tetramethylsilane or CDCl_3 as internal standard. Low resolution mass spectra were recorded on a Micromass VG Quattro triple quadrupole mass spectrometer; peaks are reported as m/z (percent intensity relative to the base peak). High resolution mass spectra were recorded on a Micromass 70-250S double focusing mass spectrometer. Infrared spectra were recorded on a Bomem MB-100 FT-IR spectrometer as neat on NaCl plates. The X-ray crystallographic analysis was performed on a Bruker SMART CCD 1000 X-ray diffractometer with graphite-monochromated Mo K radiation ($\lambda = 0.71073 \text{ \AA}$) operating at 50 kV and 40 mA at 25 °C. Melting points were obtained using a Fisher Scientific hot stage apparatus and are uncorrected. Elemental analyses were performed by Canadian Microanalytical Service Ltd. (Delta, BC). Specific rotation was performed using a Rudolph Research Analytical AUTOPOL_V automatic polarimeter. Texture analyses were performed using a Nikon Eclipse E600 POL polarized microscope fitted with a Linkam LTS 350 hot stage and TMS 93 temperature controller. Spontaneous polarizations (P_S) were measured as a function of temperature by the triangular wave method (10-15 V/ μm , 80-100 Hz) using a Displaytech APT-III polarization testbed in conjunction with the Linkam hot stage. Polyimide-coated ITO glass cells with a 4 μm spacing (Displaytech Inc.) were used for all measurements.

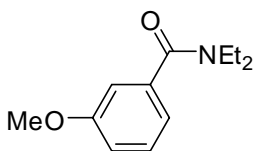
Alignment of the SmC* phase was achieved by slow cooling (0.1 K/min) from the isotropic phase while applying an AC field (4 Hz, 5 V/ μm) across the film. The sign of P_S along the polar axis was assigned from the relative configuration of the electric field and the switching position of the sample according to the established convention.

5.2 Materials.

All dry solvents used were purified under an argon atmosphere according to Perrin²⁰⁷ or purchased from commercial sources. THF and Et₂O were either freshly distilled from sodium benzophenone ketyl or from a solvent purification system made by Innovative Technology Inc. CH₂Cl₂ and DMF (reduced pressure) were freshly distilled from CaH₂ or purchased from commercial sources, and toluene and B(OMe)₃ were freshly distilled from sodium metal. Diisopropylamine (DIPA) and *N,N,N',N'*-tetramethylethylenediamine (TMEDA) were distilled from CaH₂. *n*-Butyllithium (hexane solution) and *s*-butyllithium (hexane solution) were purchased from Aldrich Chemical Company and periodically titrated against *s*-butanol with *N*-benzylbenzamide or 1,10-phenanthroline as an indicator.²⁰⁸ Pd(PPh₃)₄ was prepared according to a literature procedure.²⁰⁹ All commodity chemicals were purchased from commercial sources and used without further purification. 4-Alkoxybenzoic acids (hexyl, heptyl, octyl, nonyl, decyl and undecyl) were synthesized by literature procedures²¹⁰ and shown to have the expected physical and spectral properties. LDA was freshly prepared before use by stirring a 1:1 mixture of DIPA and *n*-BuLi in THF for 15 min at 0 °C.

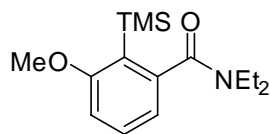
5.3 Specific Experimental Procedures

N,N-diethyl-3-methoxybenzamide (**2.2**)²¹¹



A solution of 3-methoxybenzoic acid **2.1** (20 g, 130 mmol), SOCl₂ (48 mL, 5.0 equiv) and DMF (5 mL, 0.05equiv) was stirred for 2 h at rt then concentrated under reduced pressure. The residue was dissolved in toluene (100 mL), and then concentrated under reduced pressure. This procedure was repeated two more times. The residue was dissolved in CH₂Cl₂ (600 mL) and cooled to 0 °C. HNEt₂ (41 mL, 3.0 equiv) was added dropwise and the solution allowed to warm to rt over 4 h. The mixture was diluted with H₂O and extracted with CH₂Cl₂ (30 mL × 3). The combined organic extracts were washed with brine, dried (MgSO₄) and concentrated to a yellow oil. Vacuum distillation (b.p. 140 °C, 4 mmHg) [lit. b.p. 177 °C, 14 mmHg] gave 26 g (94%) of **2.2** as a colourless oil: ¹H NMR (200 MHz, CDCl₃) δ 7.30 (m, 2H), 6.92 (m, 2H), 3.82 (s, 3H) 3.42 (m, 4H), 1.18 (m, 6H); ¹³C NMR (50 MHz, CDCl₃) δ 170.8, 159.4, 138.5, 129.4, 118.3, 114.9, 111.6, 55.2, 43.1, 39.0, 14.1, 12.8. The physical and spectroscopic data are consistent with those reported.⁴³

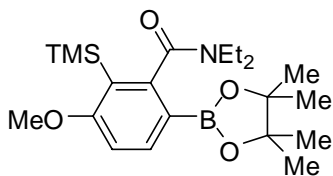
N,N-Diethyl-3-methoxy-2-(trimethylsilyl)benzamide (**2.3**)



To a solution of **2.2** (10 g, 48 mmol) and TMEDA (12 mL, 58 mmol, 1.2 equiv) in THF (120 mL) cooled to a range between -75 to -80 °C under Ar was added dropwise *s*-BuLi (1.4 M solution in hexanes, 41 mL, 58 mmol, 1.2 equiv). After the solution was stirred for 1 h, TMSCl (7.4 mL, 58 mmol, 1.2 equiv) was added dropwise at -75 to -80 °C. The resulting

solution was allowed to warm to rt over 4 h, neutralized with satd NH₄Cl (30 mL). After concentration under reduced pressure, the residue was extracted with CH₂Cl₂ (30 mL × 3). The combined organic extracts were washed with brine, dried (MgSO₄) and concentrated to a brown oil. Purification by flash column chromatography on silica gel (40% EtOAc/hexanes) and recrystallization from CH₂Cl₂/hexanes gave **2.3** (11 g, 81%) as a colorless solid: mp 54-55 °C [lit.¹²⁹ mp 54-55 °C]; ¹H NMR (400 MHz, CDCl₃) δ 7.31 (dd, *J* = 8.2, 7.6 Hz, 1H), 6.80 (d, *J* = 8.3 Hz, 1H), 6.74 (dd, *J* = 7.5, 0.9 Hz, 1H), 3.79 (s, 3H), 3.70-3.55 (m, 1H), 3.48-3.31 (m, 1H), 3.30-3.04 (m, 2H), 1.24 (t, *J* = 7.2 Hz, 3H), 1.05 (t, *J* = 7.1 Hz, 3H), 0.24 (s, 9H); ¹³C NMR (100 MHz, CDCl₃) δ 171.7, 164.8, 144.5, 130.4, 124.3, 118.8, 109.7, 55.1, 43.3, 38.9, 13.6, 12.8, 0.4. The physical and spectral data are consistent with those reported.^{176a}

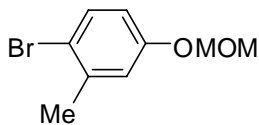
***N,N*-Diethyl-3-methoxy-6-(4,4,5,5-tetramethyl-1,3,2-dioxaborolan-2-yl)-2-(trimethylsilyl)benzamide (2.5)**



To a solution of TMEDA (0.65 mL, 4.3 mmol, 1.2 equiv) in THF (30 mL) at -75 to -80 °C under an Ar atmosphere was added dropwise *s*-BuLi (1.4 M solution in hexanes, 3.1 mL, 4.3 mmol, 1.2 equiv). After stirring for 10 min, to this mixture was added **2.3** (0.5 M solution in THF, 7.2 mL, 3.6 mmol) by dropwise addition. After 1 h, B(OMe)₃ (0.80 mL, 7.2 mmol, 2.0 equiv) was added dropwise. The mixture was allowed to warm to rt over 2 h, neutralized with satd NH₄Cl (10 mL) and the whole was extracted with CH₂Cl₂ (10 mL × 2). The combined organic layer was washed with brine, dried (NaSO₄), and concentrated under reduced pressure. The residue was dissolved in THF (10 mL) and the

resulting solution was treated with pinacol (0.85 g, 7.2 mmol, 2.0 equiv). The mixture was stirred for 2 h and was concentrated under reduced pressure to give a brown solid. Purification by flash column chromatography on silica gel (20% EtOAc/hexanes) and recrystallization (hexanes) gave 1.2 g (83%) of **2.5** as a colorless crystalline solid: mp 89-91 °C (hexanes); IR (thin film) 1639 cm⁻¹; ¹H NMR (400 MHz, CDCl₃) δ 7.85 (d, *J* = 8.4 Hz, 1H), 6.77 (d, *J* = 8.4 Hz, 1H), 3.81 (s, 3H), 3.77-3.66 (m, 1H), 3.32-3.22 (m, 1H), 3.15-3.06 (m, 2H), 1.35-1.19 (m, 15H), 1.00 (t, *J* = 7.2 Hz, 3H), 0.24 (s, 9H); ¹³C NMR (100 MHz, CDCl₃) δ 171.1, 167.0, 150.5, 139.5, 123.8, 108.6, 83.4, 54.9, 43.2, 39.2, 24.9, 24.6, 13.2, 12.5, 0.7; HRMS (EI) calcd for C₂₁H₃₆BNO₄Si: 404.2428, found 404.2442.

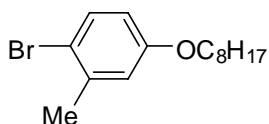
1-Bromo-4-(methoxymethoxy)-2-methylbenzene (**2.10b**).



A solution of 4-bromo-3-methylphenol (0.61 g, 3.3 mmol) in THF (2 mL) was added dropwise to a mixture of freshly washed (hexanes) NaH (60% in mineral oil, 0.10 g, 4.3 mmol, 1.3 equiv) by hexanes in THF (8 mL). After 10 min, MOMCl (0.42 g, 0.4 mL, 3.3 mmol, 1.0 equiv) was added dropwise. The mixture was stirred for 3 h, neutralized with satd NH₄Cl (10 mL) and the whole was extracted with CH₂Cl₂ (10 mL × 2). The combined organic layer was washed with brine, dried (Na₂SO₄) and concentrated under reduced pressure. Purification by flash column chromatography on silica gel (15-20% EtOAc/hexanes) gave 0.58 g of **2.10b** (76%) as a colorless oil: ¹H NMR (400 MHz, CD₃Cl) δ 7.41 (d, *J* = 8.7 Hz, 1H), 6.94 (d, *J* = 2.5 Hz, 1H), 6.76 (dd, *J* = 8.7, 2.5 Hz, 1H), 5.14 (s, 2H), 3.47 (s, 3H), 2.37 (s, 3H); ¹³C NMR (100 MHz, CDCl₃) δ 156.4, 138.9, 132.8, 118.7, 116.8,

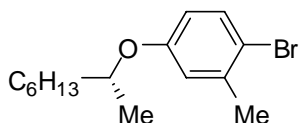
115.3, 94.4, 56.0, 23.1. The physical and spectral data are consistent with those reported.^{197b}

1-Bromo-2-methyl-4-(octyloxy)benzene (2.10c)



To a solution of 4-bromo-3-methylphenol (4.4 g, 24 mmol) and *i*-Pr₂EtN (8.4 mL, 47 mmol, 2.0 equiv) in CH₂Cl₂ (100 mL) was added 1-bromooctane (3.7 g, 3.4 mL, 28 mmol, 1.2 equiv). The mixture was stirred for 12 h, diluted with satd NH₄Cl (40 mL) and concentrated under reduced pressure. The resulting mixture was extracted with CH₂Cl₂ (25 mL × 3). The combined organic layer was washed with brine, dried (Na₂SO₄) and concentrated under reduced pressure to afford a yellow oil. Purification by flash column chromatography on silica gel (10 EtOAc/hexanes) gave 5.4 g **2.10c** (76%) as a colorless oil: IR (thin film) 1634 cm⁻¹; ¹H NMR (400 MHz, CDCl₃) δ 7.38 (d, *J* = 8.7 Hz, 1H), 6.79 (d, *J* = 2.9 Hz, 1H), 6.60 (dd, *J* = 8.7, 3.0 Hz, 1H), 3.91 (t, *J* = 6.6 Hz, 2H), 2.36 (s, 3H), 1.80-1.71 (m, 2H), 1.49-1.39 (m, 2H), 1.39-1.20 (m, 8H), 0.89 (t, *J* = 6.8 Hz, 3H); ¹³C NMR (100 MHz, CDCl₃) δ 158.4, 138.7, 132.7, 117.1, 115.1, 113.5, 68.2, 31.8, 29.3, 29.2, 26.0, 23.1, 22.7, 14.1; HRSM (EI) calcd for C₁₅H₂₃OBr: 298.0932, found 298.0930.

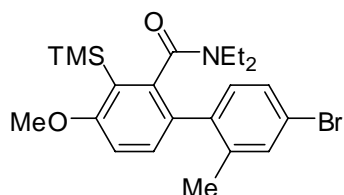
(*R*)-1-Bromo-2-methyl-4-(oct-2-yloxy)benzene (2.10e).



To a solution of 4-bromo-3-methylphenol (0.43 g, 2.5 mmol) in CH₂Cl₂ (10 mL) were added (*S*)-octan-2-ol (0.36 g, 0.45 mL, 2.8 mmol, 1.1 equiv), DIAD (0.77 g, 0.75 mL 3.8 mmol, 1.5 equiv) and Ph₃P (0.80 g, 3.1 mmol, 1.2 equiv). After stirring for 12 h, the reaction mixture was diluted with satd

NH₄Cl (20 mL), and the whole was extracted with CH₂Cl₂ (15 mL × 3). The combined organic layer was washed with brine and dried (Na₂SO₄), and concentrated under reduced pressure to afford a yellow oil. Purification by flash column chromatography on silica gel (20-30% EtOAc/hexanes) gave 0.53 g (70%) of **2.10e** as a colorless oil: IR (thin film) 1779 cm⁻¹; ¹H NMR (400 MHz, CD₃Cl) δ 7.38 (d, *J* = 8.7 Hz, 1H), 6.78 (d, *J* = 3.0 Hz, 1H), 6.60 (dd, *J* = 8.7, 3.0 Hz, 1H), 4.34-4.25 (m, 1H), 1.78-1.66 (m, 1H), 1.62-1.51 (m, 1H), 1.49-1.23 (m, 11H), 0.89 (t, *J* = 6.8 Hz, 3H); ¹³C NMR (100 MHz, CDCl₃) δ 157.4, 138.8, 132.8, 118.6, 115.0, 114.7, 74.2, 36.4, 31.8, 29.2, 25.5, 23.1, 22.6, 19.7, 14.1; HRMS (EI) calcd for C₁₅H₂₃OBr 298.0932, found 298.0941.

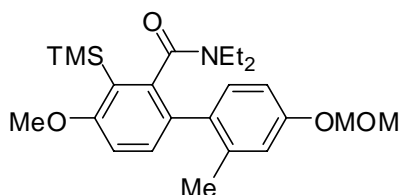
4'-Bromo-*N,N*-diethyl-4-methoxy-2'-methyl-3-(trimethylsilyl)biphenyl-2-carboxamide (2.11a).



To a solution of *N,N*-diethyl-3-methoxy-6-(4,4,5,5-tetramethyl-1,3,2-dioxaborolan-2-yl)-2-(trimethylsilyl)benzamide **2.5** (4.0 g, 9.9 mmol) in DME (90 mL, degassed) in a glove box were added sequentially 4-bromo-1-iodo-2-methylbenzene (3.2 g, 11 mmol, 1.5 mL, 1.1 equiv), (PPh₃)₄Pd (67 mg, 3.0 mmol%), and K₂CO₃ (1 M aq solution, 30 mL, 30 mmol, 3.0 equiv). The mixture was heated to reflux and stirred under Ar for 20 h. After cooling to rt, the reaction mixture was quenched with saturated NH₄Cl (30 mL) and concentrated under reduced pressure. The resulting residue was extracted with CH₂Cl₂ (20 mL × 3) and the combined organic layer was washed with brine, dried (Na₂SO₄), and concentrated under reduced pressure to afford a brown oil. Purification by flash column chromatography on silica gel (20% EtOAc/hexanes) and

recrystallization (CH₂Cl₂/hexanes) gave 3.0 g (67%) of **2.11a** as a mixture of colorless solid which was established to be a mixture of diastereomers.²¹² mp 147-149 °C, IR (thin film) 1635 cm⁻¹; ¹H NMR (600 MHz, CDCl₃) δ 7.53-7.25 (m, 3H), 7.13-7.01 (m, 2H), 3.83 (s, 3H), 3.62-3.51 (m, 1H), 3.11-2.53 (m, 3H), 2.20-1.97 (m, 3H), 0.97-0.74 (m, 3H), 0.53-0.32 (m, 3H), 0.21 (s, 9H); ¹³C NMR (150 MHz, CDCl₃) δ 168.1, 168.1, 163.8, 163.7, 143.0, 142.4, 140.5, 139.0, 138.1, 137.5, 132.8, 132.7, 132.3, 131.6, 131.4, 131.0, 129.3, 128.6, 127.5, 127.2, 123.5, 122.6, 120.3, 120.0, 110.0, 109.6, 55.3, 41.7, 41.8, 36.8, 36.2, 19.9, 19.6, 12.6, 12.5, 11.2, 10.6, 0.6, 0.5; HRMS (EI) calcd for C₂₂H₃₀NO₂BrSi: 447.1229, found 447.1239.

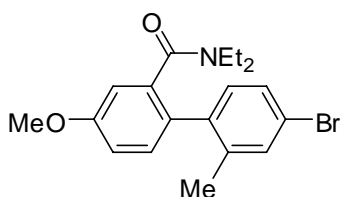
***N,N*-Diethyl-4-methoxy-4'-(methoxymethoxy)-2'-methyl-3-(trimethylsilyl)biphenyl-2-carboxamide (2.11b).**



To a solution of *N,N*-diethyl-3-methoxy-6-(4,4,5,5-tetramethyl-1,3,2-dioxaborolan-2-yl)-2-(trimethylsilyl)benzamide **2.5** (0.20 g, 0.49 mmol) in DME (2 mL, degassed) in a glove box were added sequentially 1-bromo-4-(methoxymethoxy)-2-methylbenzene **2.10b** (0.11 g, 0.49 mmol, 1.0 equiv), (PPh₃)₄Pd (26 mg, 4.0 mmol%) and K₂CO₃ (1.0 M aq solution, 1.5 mL, 1.5 mmol, 3.0 equiv). The mixture was heated to reflux and stirred under Ar for 20 h. After cooling to rt, the reaction mixture was quenched with saturated NH₄Cl (30 mL), concentrated under reduced pressure. the resulting residue was extracted with CH₂Cl₂ (10 mL × 3) and the combined organic layer was washed with brine, dried (Na₂SO₄), and concentrated under reduced pressure to afford a brown oil. Purification by flash column chromatography on

silica gel (20% EtOAc/hexanes) and recrystallization (CH₂Cl₂/hexanes) gave 0.19 g (90%) of **2.11b** as colorless solid diastereomers: mp 97–99 °C; ¹H NMR (400 MHz, CDCl₃) δ 7.30-6.68 (m, 5H), 5.14 (s, 2H), 3.84 (s, 3H), 3.78-3.66 (m, 1H), 3.43 (s, 3H), 3.25-2.45 (m, 3H), 2.24-1.99 (m, 3H), 1.05-0.77 (m, 3H), 0.62-0.38 (m, 3H), 0.25 (s, 9H); ¹³C NMR (100 MHz, CDCl₃) δ 169.0, 163.7, 163.6, 156.2, 155.9, 143.5, 143.1, 139.7, 136.5, 132.9, 132.2, 131.8, 129.7, 117.3, 116.8, 112.6, 111.8, 108.9, 108.7, 94.0, 55.3, 54.8, 54.7, 42.0, 41.9, 36.9, 36.37, 20.1, 20.0, 12.4, 11.0, 10.4, 0.0; HRMS (EI) calcd for C₂₄H₃₅NO₄Si: 429.2335, found 429.2331.

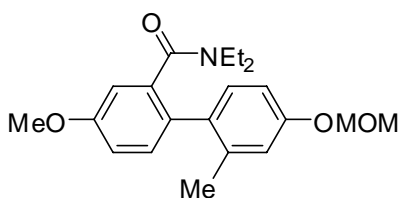
4'-Bromo-*N,N*-diethyl-4-methoxy-2'-methylbiphenyl-2-carboxamide (**2.12a**).



To a solution of **2.11a** (6.8 g, 15 mmol) in THF (150 mL) was added TBAF (1.0 M solution in THF, 45 mL, 45 mmol, 3.0 equiv) at rt. After stirring for 12 h, the reaction mixture was concentrated under reduced pressure. The resulting residue was diluted with satd NH₄Cl (30 mL), and the whole was extracted with CH₂Cl₂ (30 mL × 3). The combined organic layer was washed with brine, dried (Na₂SO₄), and concentrated under reduced pressure to afford a brown solid. Purification by flash column chromatography on silica gel (20-30% EtOAc/hexanes) and recrystallization (CH₂Cl₂/hexanes) gave 5.1 g (89%) of **2.11a** as a colorless solid: mp 216-218 °C; IR (thin film) 1631 cm⁻¹; NMR (600 MHz, CDCl₃) δ 7.37 (s, 1H), 7.26 (d, *J* = 4.9 Hz, 1H), 7.21-7.00 (m, 2H), 6.94 (dd, *J* = 8.4, 2.5 Hz, 1H), 6.88 (s, 1H), 3.84 (s, 3H), 3.79-2.62 (m, 4H), 2.18 (s, 3H), 0.93 (br, 3H), 0.77 (t, *J* = 6.9 Hz, 3H); ¹³C NMR (150 MHz, CDCl₃) δ 169.5, 159.0, 138.2, 132.8, 131.2, 128.2,

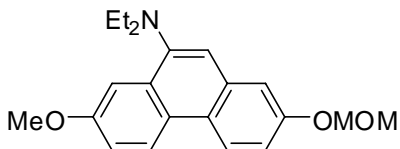
121.3, 114.3, 111.5, 55.4, 42.4, 38.0, 20.1, 13.8, 11.9; HRMS (EI) calcd for $C_{19}H_{21}NO_2Br$: 374.0576, found 374.0765.

***N,N*-Diethyl-4-methoxy-4'-(methoxymethoxy)-2'-methylbiphenyl-2-carboxamide
(2.12b).**



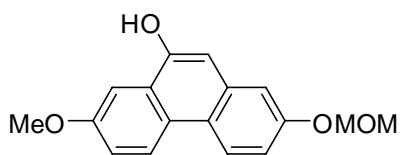
To a solution of **2.11b** (1.0 g, 2.3 mmol) in THF (10 mL) was added TBAF (1.0 M solution in THF, 7.0 mL, 7.0 mmol, 3.0 equiv) at rt. After stirring for 12 h the reaction mixture was concentrated under reduced pressure. The resulting residue was diluted with satd NH_4Cl (30 mL), and the whole was extracted with CH_2Cl_2 (10 mL \times 3). The combined organic layer was washed with brine, dried (Na_2SO_4), and concentrated under reduced pressure to afford a brown solid. Purification by flash column chromatography on silica gel (20-30% EtOAc/hexanes) gave 0.76 g (91%) of **2.11b** as a yellow oil: IR (thin film) 1653 cm^{-1} ; 1H NMR (400 MHz, $CDCl_3$) δ 7.14 (d, $J = 8.4$ Hz, 1H), 7.10-7.00 (m, 1H), 6.94 (dd, $J = 8.5, 2.7$ Hz, 1H), 6.89 (d, $J = 2.3$ Hz, 1H), 6.84 (d, $J = 2.6$ Hz, 1H), 6.80 (dd, $J = 8.4, 2.5$ Hz, 1H), 5.15 (s, 2H), 3.84 (s, 3H), 3.77-3.52 (m, 1H), 3.44 (s, 3H), 3.33-2.56 (m, 3H), 2.15 (s, 3H), 0.91 (t, $J = 7.3$ Hz, 3H), 0.72 (t, $J = 7.1$ Hz, 3H); ^{13}C NMR (100 MHz, CD_2Cl_2) δ (no quaternary carbons) 132.1, 118.0, 114.3, 113.3, 111.6, 94.8, 56.1, 55.8, 42.7, 38.1, 20.7, 13.9, 12.0; HRMS (EI) calcd for $C_{21}H_{27}NO_4$: 357.1940, found 357.1936.

***N,N*-Diethyl-7-methoxy-2-(methoxymethoxy) phenanthren-9-amine (2.15)**



To a solution of **2.11b** (0.20 g, 0.47 mmol) in THF (6 mL) under Ar at -5 to 0 °C was added freshly prepared LDA (1.0 M solution in THF, 2.3 mL, 2.3 mmol, 5.0 equiv) dropwise. The mixture was allowed to warm up to rt over 30 min and neutralized with satd NH₄Cl (10 mL). The whole was concentrated under reduced pressure and extracted with CH₂Cl₂ (15 mL × 2). The combined organic layer was washed with brine, dried (Na₂SO₄), and concentrated under reduced pressure to afford a yellow oil. Purification by flash column chromatography on silica gel (20% EtOAc/hexanes) gave 0.15 g of **2.15** (95%) as a yellow oil: ¹H NMR (300 MHz, CD₂Cl₂) δ 8.48 (d, *J* = 9.1 Hz, 1H), 8.42 (d, *J* = 9.1 Hz, 1H), 7.79 (d, *J* = 2.8 Hz, 1H), 7.37 (d, *J* = 2.5 Hz, 1H), 7.29 (s, 1H), 7.27-7.19 (m, 2H), 5.30 (s, 2H), 3.96 (s, 3H), 3.52 (s, 3H), 3.23 (q, *J* = 7.1 Hz, 4H), 1.11 (t, *J* = 7.0 Hz, 6H); ¹³C NMR (75 MHz, CD₂Cl₂) δ 158.4, 155.9, 146.6, 133.2, 132.1, 126.4, 124.6, 123.9, 123.7, 118.1, 117.2, 116.9, 112.0, 105.9, 95.2, 56.5, 55.9, 47.7, 12.7; HRMS (EI) calcd for C₂₁H₂₅NO₃ 339.1834, found 339.1846.

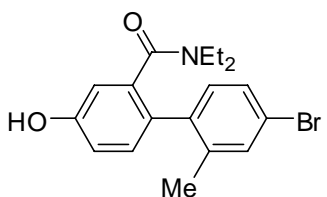
7-Methoxy-2-(methoxymethoxy)phenanthrene-9-ol (2.16).



To a solution of **2.12b** (0.85 g, 2.4 mmol) in THF (30 mL) was added under Ar freshly prepared LDA (1.0 M solution in THF, 12 mL, 12 mmol, 5.0 equiv) by dropwise addition at -5–0 °C. The mixture was allowed to warm up to rt over 30 min and neutralized with satd NH₄Cl (20 mL). The whole was concentrated under reduced pressure and extracted with CH₂Cl₂ (30 mL × 2). The combined organic layer was

washed with brine, dried (Na₂SO₄), and concentrated under reduced pressure to give a yellow solid. Purification by flash column chromatography on silica gel (20-30% EtOAc/hexanes) and recrystallization (EtOAc/hexanes) gave 0.66 g (97%) of **2.16** as a colorless solid: mp 112-113 °C; ¹H NMR (400 MHz, CD₂Cl₂) δ 8.46 (d, *J* = 9.1 Hz, 1H), 8.40 (d, *J* = 9.0 Hz, 1H), 7.32-7.26 (m, 2H), 7.19 (dd, *J* = 9.0, 2.6 Hz, 1H), 6.94 (s, 1H), 5.82 (s, 1H), 5.30 (s, 2H), 3.96 (s, 3H), 3.53 (s, 3H); ¹³C NMR (100 MHz, CD₂Cl₂) δ 158.4, 156.1, 150.3, 133.4, 126.4, 126.4, 124.5, 124.1, 122.4, 118.3, 116.0, 111.2, 106.8, 103.3, 95.2, 56.5, 56.0; HRMS (EI) calcd for C₁₇H₁₆O₄:284.1049, found 284.1048.

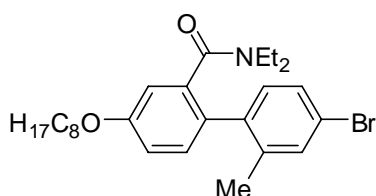
4'-Bromo-*N,N*-diethyl-4-hydroxy-2'-methylbiphenyl-2-carboxamide (2.17).



To a solution of **2.12a** (4.5 g, 12 mmol) in CH₂Cl₂ (anhydrous, 120 mL) at -65 to -78 °C under an Ar atmosphere was added dropwise freshly prepared BBr₃ (1.0 M solution in CH₂Cl₂, 24 mL, 24 mmol, 2.0 equiv). The mixture was allowed to warm up to rt and stirred over 30 min, quenched with satd NH₄Cl (30 mL) and the whole was extracted with CH₂Cl₂ (20 mL × 3). The combined organic layer was washed with brine, dried (Na₂SO₄), and concentrated under reduced pressure to give a brown solid. Purification by flash column chromatography on silica gel (45-50% EtOAc/hexanes) and recrystallization (CH₂Cl₂/hexanes) gave 4.10 g (95%) of **2.17** as a colorless crystalline solid: mp 217-218 °C; IR (thin film) 3208, 1601 cm⁻¹; ¹H NMR (600 MHz, CD₃Cl) δ 8.82 (br, 1H), 7.36 (s, 1H), 7.25 (d, *J* = 8.3 Hz, 1H), 7.11 (br, 1H), 6.98 (d, *J* = 8.2 Hz, 1H), 6.85 (s, 1H), 6.77 (d, *J* = 6.0 Hz, 1H), 3.93-3.53 (m, 1H), 3.33-2.52 (m, 3H), 2.18 (s, 3H), 0.86 (br, 3H), 0.78 (t, *J* = 6.7 Hz, 3H); ¹³C NMR (150 MHz, CDCl₃) δ 171.0, 156.4,

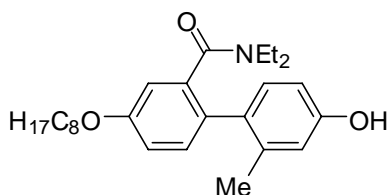
136.5, 132.9, 131.4, 128.4, 121.2, 116.7, 100.0, 42.7, 38.5, 20.1, 13.5, 11.8; HRMS (EI) calcd for C₁₈H₁₉NO₂Br: 360.0599, found 360.0604.

4'-Bromo-*N,N*-diethyl-2'-methyl-4-(octyloxy)biphenyl-2-carboxamide (2.18).



A solution of **2.17** (4.0 g, 11 mmol), *n*-C₈H₁₆Br (2.3 g, 2.1 mL, 12 mmol, 1.1 equiv) and K₂CO₃ (4.5 g, 33 mmol, 3.0 equiv) in CH₃CN (110 mL) was stirred under Ar at rt for 12 h. The reaction mixture was diluted with satd NH₄Cl (20 mL), and the whole was extracted with CH₂Cl₂ (15 mL × 3). The combined organic layer was washed with brine and dried (Na₂SO₄), and concentrated under reduced pressure to afford a yellow oil. Purification by flash column chromatography on silica gel (20-30% EtOAc/hexanes) gave 4.9 g (93%) of **2.18** as a yellow oil: (thin film) 1635 cm⁻¹; ¹H NMR (400 MHz, CD₃Cl) δ 7.37 (d, *J* = 1.6 Hz, 1H), 7.26 (dd, *J* = 7.8, 1.8 Hz, 1H), 7.19-6.99 (m, 2H), 6.92 (dd, *J* = 8.5, 2.7 Hz, 1H), 6.87 (d, *J* = 2.4 Hz, 1H), 3.98 (t, *J* = 6.5 Hz, 2H), 3.89-2.58 (m, 4H), 2.18 (s, 3H), 1.83-1.75 (m, 2H), 1.51-1.41 (m, 2H), 1.40-1.23 (m, 8H), 0.98-0.84 (m, 6H), 0.76 (t, *J* = 7.10 Hz, 3H); ¹³C NMR (100 MHz, CDCl₃) δ 169.6, 158.5, 138.0, 132.7, 131.2, 128.1, 121.2, 114.8, 112.0, 68.2, 42.3, 38.0, 31.8, 29.3, 29.2, 26.0, 22.6, 20.1, 14.1, 13.8, 11.8; HRMS (EI) calcd for C₂₆H₃₅NO₂Br: 472.1851, found 472.1845.

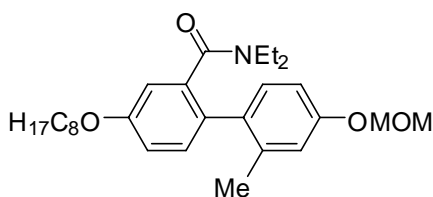
***N,N*-Diethyl-4'-(hydroxy)-2'-methyl-4-(octyloxy)biphenyl-2-carboxamide (2.19).**



To a solution of **2.18** (0.50 g, 1.1 mmol) in THF (10 mL) cooled to -78 °C was added under Ar *t*-BuLi (2.1 M solution in hexanes, 1.3 mL, 2.1 mmol, 2.0 equiv)

dropwise. After the solution was stirred for 10 min, B(*i*-PrO)₃ (0.40 mg, 0.49 mL, 2.1 mmol, 2.0 equiv) was added dropwise and the mixture was allowed to warm up to rt over 30 min. The mixture was cooled to 0 °C and H₂O₂ (35% aq solution, 0.50 mL, 5.3 mmol, 5.0 equiv) was added dropwise. After the solution was warmed to rt over 15 min, it was diluted with NH₄Cl (20 mL) and the whole was extracted with CH₂Cl₂ (10 mL × 3). The combined organic layer was washed with brine, dried (Na₂SO₄), and concentrated under reduced pressure to give a brown solid. Purification by flash column chromatography on silica gel (40% EtOAc/hexane) and recrystallization (CH₂Cl₂/hexanes) gave 0.30 g (69%) of **2.19** as a colorless solid: mp 100-101 °C; IR (thin film) 3252, 1616 cm⁻¹; ¹H NMR (400 MHz, CD₃Cl) δ 9.23 (s, 1H), 7.09 (d, *J* = 8.1 Hz, 1H), 6.94 (d, *J* = 8.4 Hz, 1H), 6.87 (d, *J* = 7.0 Hz, 1H), 6.77 (s, 1H), 6.61 (s, 1H), 6.51 (d, *J* = 8.2 Hz, 1H), 3.99 (t, *J* = 5.8 Hz, 2H), 3.60-3.43 (m, 1H), 3.08-2.65 (m, 3H), 2.03 (s, 3H), 1.76-1.66 (m, 2H), 1.47-1.20 (m, 10H), 0.91-0.79 (m, 6H), 0.66 (t, *J* = 6.7 Hz, 3H); ¹³C NMR (100 MHz, CDCl₃) δ 170.5, 157.9, 156.1, 137.7, 132.0, 130.2, 116.9, 114.8, 112.5, 111.7, 68.2, 42.6, 38.2, 31.8, 29.3, 29.2, 29.2, 26.0, 22.6, 20.3, 14.1, 13.7, 12.0; HRMS (EI) calcd for C₂₆H₃₇NO₃: 411.2773, found 411.2766.

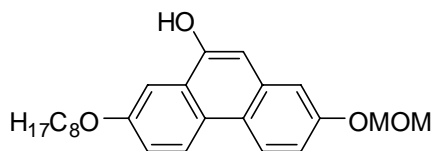
***N,N*-Diethyl-4'-(methoxymethoxy)-2'-methyl-4-(octyloxy)biphenyl-2-carboxamide (2.20).**



A solution of **2.19** (1.8 g, 4.3 mmol) in THF (10 mL) was added to freshly washed (hexanes) NaH (60% in mineral oil, 0.21 g, 8.6 mmol, 2.0 equiv) under Ar. After stirring for 10 min, MOMCl (0.69 g, 8.6 mmol,

2.0 equiv) was added dropwise. The reaction mixture was allowed to warm to rt and stirred for 3 h, and neutralized with satd NH₄Cl (15 mL) and the whole was extracted with CH₂Cl₂ (20 mL × 2). The combined organic layer was washed with brine, dried (Na₂SO₄) and concentrated under reduced pressure. Purification by flash column chromatography on silica gel (20-30% EtOAc/hexanes) gave 1.8 g of **2.20** (83%) as a yellow oil: IR (thin film) 1635 cm⁻¹; ¹H NMR (400 MHz, CD₃Cl) δ 7.24-7.00 (m, 2H), 6.91 (dd, *J* = 8.5, 2.7 Hz, 1H), 6.89 (d, *J* = 2.5 Hz, 1H), 6.87 (d, *J* = 2.2 Hz, 1H), 6.81 (dd, *J* = 8.3, 2.1 Hz, 1H), 5.16 (s, 2H), 3.99 (br, 2H), 3.84-3.64 (m, 1H), 3.46 (s, 3H), 3.28-2.59 (m, 3H), 2.19 (s, 3H), 1.83-1.75 (m, 2H), 1.52-1.41 (m, 2H), 1.41-1.23 (m, 8H), 0.89 (t, *J* = 6.9 Hz, 3H); ¹³C NMR (100 MHz, CDCl₃) δ 169.9, 158.2, 156.4, 138.3, 131.5, 129.6, 117.5, 114.7, 112.9, 111.8, 94.3, 68.2, 55.8, 42.2, 37.8, 31.8, 29.3, 29.2, 29.2, 26.0, 22.6, 20.5, 14.1, 13.7, 11.8.; HRMS (EI) calcd for C₂₈H₄₁NO₄: 455.3036, found 455.3026.

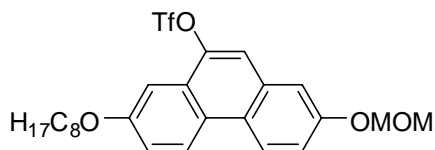
2-(Methoxymethoxy)-7-(octyloxy)phenanthren-9-ol (**2.21**).



A solution of **2.20** (1.5 g, 3.3 mmol) in THF (30 mL) was added under Ar freshly prepared LDA (1.0 M solution in THF, 16 mL, 16 mmol, 5.0 equiv) by dropwise addition at -5—0 °C. The mixture was allowed to warm up to rt over 30 min, neutralized with satd NH₄Cl (20 mL). The whole was concentrated under reduced pressure and extracted with CH₂Cl₂ (30 mL × 2). The combined organic layer was washed with brine, dried (Na₂SO₄), and concentrated under reduced pressure to give a yellow solid. Purification by flash column chromatography on silica gel (20-30%

EtOAc/hexanes) and recrystallization (EtOAc/hexanes) gave 1.2 g (97%) of **2.21** as a colorless solid: mp 123-124 °C; IR (thin film) 3513 cm⁻¹; ¹H NMR (400 MHz, DMSO) δ 10.28 (s, 1H), 8.54 (d, $J = 9.2$ Hz, 1H), 8.46 (d, $J = 9.1$ Hz, 1H), 7.58 (d, $J = 2.5$ Hz, 1H), 7.29-7.22 (m, 2H), 7.10 (dd, $J = 9.0, 2.5$ Hz, 1H), 6.98 (s, 1H), 5.29 (s, 2H), 4.09 (t, $J = 6.5$ Hz, 2H), 3.42 (s, 3H), 1.82-1.72 (m, 2H), 1.50-1.40 (m, 2H), 1.38-1.21 (m, 8H), 0.86 (t, $J = 5.7$ Hz, 3H); ¹³C NMR (100 MHz, DMSO) δ 157.2, 155.6, 151.8, 133.8, 126.9, 125.8, 124.7, 124.2, 121.2, 118.1, 115.0, 110.9, 105.8, 104.1, 94.3, 68.2, 56.2, 31.8, 29.3, 29.2, 29.1, 25.6, 15.5; HRMS (EI) calcd for C₂₄H₃₀O₄: 382.2144, found 382.2152.

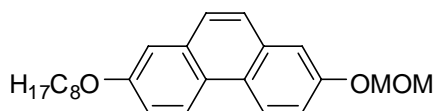
2-(Methoxymethoxy)-7-(octyloxy)phenanthren-9-yl trifluoromethanesulfonate (2.22).



To a solution of **2.21** (1.0 g, 2.6 mmol) in Et₃N (25 mL) cooled to 0 °C was added under Ar Tf₂O (4.4 g, 2.6 mL, 16 mmol, 6.0 equiv) dropwise. The mixture was allowed to warm up to rt over 2 h and the whole was diluted with satd NH₄Cl (10 mL), extracted with CH₂Cl₂ (10 mL \times 2). The combined organic layer was washed with brine, dried (Na₂SO₄), and concentrated under reduced pressure to give a brown residue. Purification by flash column chromatography on silica gel (20-30% EtOAc/hexanes) and recrystallization (CH₂Cl₂/hexanes) gave 1.2 g of **2.22** (86%) as a colorless solid: mp 51-52 °C; IR (thin film) 1216 cm⁻¹; ¹H NMR (600 MHz, CDCl₃) δ 8.50-8.44 (m, 2H), 7.65 (s, 1H), 7.47 (s, 1H), 7.43 (s, 1H), 7.38 (d, $J = 9.1$ Hz, 1H), 7.34 (d, $J = 9.1$ Hz, 1H), 5.31 (s, 2H), 4.12 (t, $J = 6.4$ Hz, 2H), 3.53 (s, 3H), 1.90-1.83 (m, 2H), 1.54-1.48 (m, 2H),

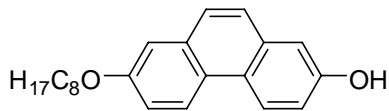
1.42-1.24 (m, 8H), 0.89 (t, $J = 6.7$ Hz, 3H); ^{13}C NMR (150 MHz, CDCl_3) δ 158.2, 155.7, 144.5, 130.6, 126.1, 125.8, 124.9, 118.8 (q, $J_{\text{C-F}} = 320$ Hz), 124.3, 123.8, 119.6, 119.4, 118.1, 112.5, 102.4, 94.6, 68.3, 56.2, 31.8, 29.4, 29.2, 29.1, 26.1, 22.7, 14.1; HRMS (EI) calcd for $\text{C}_{25}\text{H}_{29}\text{O}_6\text{F}_3\text{S}$ 514.1637, found 514.1641.

2-(Methoxymethoxy)-7-(octyloxy)phenanthrene (2.23).



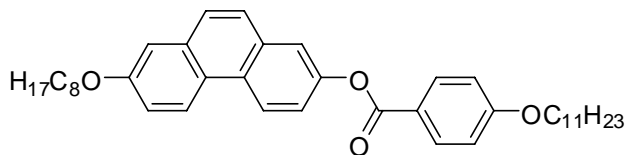
To a solution of **2.22** (0.25 g, 4.8 mmol) in DMF (5 mL) were added sequentially $\text{Pd}(\text{OAc})_2$ (54 mg, 0.21 mmol, 5 mol%), PPh_3 (13 mg, 0.48 mmol, 10 mol%), HCO_2H (0.73 mL, 1.9 mmol, 4.0 equiv) and Et_3N (0.51 mL, 3.9 mmol, 8.0 equiv) under Ar at rt. The mixture was stirred for 12 h and the whole was diluted with NH_4Cl (10 mL), extracted with Et_2O (10 mL \times 2). The combined organic layer was washed with brine, dried (Na_2SO_4), and concentrated under reduced pressure to afford a yellow solid. Purification by flash column chromatography on silica gel (20-30% EtOAc /hexanes) and recrystallization (EtOAc /hexanes) gave 0.15 g of **2.23** (88%) as a colorless solid: mp 72-73 $^\circ\text{C}$; IR (thin film) 1616 cm^{-1} ; ^1H NMR (400 MHz, CDCl_3) δ 8.53-8.45 (m, 2H), 7.64 (s, 2H), 7.47 (d, $J = 2.5$ Hz, 1H), 7.35 (dd, $J = 9.0, 2.6$ Hz, 1H), 7.27 (dd, $J = 8.9, 2.7$ Hz, 1H), 7.23 (d, $J = 2.5$ Hz, 1H), 5.32 (s, 2H), 4.11 (t, $J = 6.6$ Hz, 2H), 3.55 (s, 3H), 1.92-1.80 (m, 2H), 1.58-1.45 (m, 2H), 1.45-1.23 (m, 8H), 0.91 (t, $J = 6.8$ Hz, 3H); ^{13}C NMR (100 MHz, CDCl_3) δ 157.3, 155.0, 132.5, 132.2, 127.1, 127.0, 125.7, 124.6, 123.7, 123.7, 117.9, 117.6, 112.4, 109.4, 94.7, 68.2, 56.1, 31.8, 29.4, 29.3, 29.3, 26.1, 22.7, 14.1; HRMS (EI) calcd for $\text{C}_{24}\text{H}_{30}\text{O}_3$ 366.2195, found 366.2188.

7-(Octyloxy)phenanthren-2-ol (**2.24**).



A solution of **2.23** (0.30 g, 0.82 mmol) in *i*-PrOH (10 mL) was added HCl (6.0 M, 1.6 mL, 9.6 mmol, 6.0 equiv). The whole was heated to 60 °C for 10 h and concentrated under reduced pressure. The resulting residue was diluted with satd NH₄Cl (5 mL) and extracted with CH₂Cl₂ (5 mL × 2). The combined organic layer was washed with brine, dried (Na₂SO₄), and concentrated under reduced pressure to afford a yellow solid. Purification by flash column chromatography on silica gel (30-40% EtOAc/hexanes) and recrystallization (EtOA/hexanes) gave 0.24 g of **2.24** (90%) as a colorless solid: mp 146-147 °C; IR (thin film) 3309 cm⁻¹; ¹H NMR (400 MHz, CDCl₃) δ 8.51-8.40 (m, 2H), 7.62 (d, *J* = 8.9 Hz, 1H), 7.57 (d, *J* = 8.9 Hz, 1H) 7.30-7.15 (m, 4H), 5.00 (br, 1H), 4.11 (t, *J* = 6.6 Hz, 2H), 1.91-1.81 (m, 2H), 1.58-1.45 (m, 2H), 1.45-1.20 (m, 8H), 0.90 (t, *J* = 5.8 Hz, 3H); ¹³C NMR (100 MHz, CDCl₃) δ 157.2, 153.3, 132.4, 132.3, 127.3, 126.5, 125.0, 124.7, 124.0, 123.6, 117.6, 116.7, 111.7, 109.5, 68.2, 31.8, 29.4, 29.3, 29.3, 26.1, 22.7, 14.1; HRMS (EI) calcd for C₂₂H₂₆O₂ 322.1933, found 322.1923.

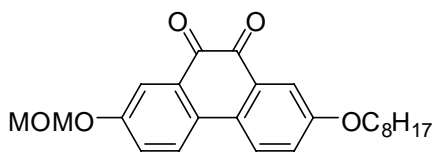
7-(Octyloxy)phenanthren-2-yl 4-(undecyloxy)benzoate (**1.32**)



To a solution of **2.24** (45 mg, 0.15 mmol) and (1*H*-benzo[d][1,2,3]triazol-1-yl)(4-(undecyloxy)phenyl)methanone **2.26** (30 mg, 0.75 mmol, 5.0 equiv) in THF (1.5 mL) was added NaOH (0.50 M aq solution, 0.38 mL, 0.75 mmol, 5.0 equiv) at rt. The mixture was stirred for 10 h and diluted with satd NH₄Cl (5 mL). The whole was concentrated

under reduced pressure. The residue was extracted with CH_2Cl_2 (3 mL \times 2) and the combined organic layer was washed with brine, dried (Na_2SO_4), and concentrated under reduced pressure. Purification by flash column chromatography on silica gel (10% EtOAc/hexane) and recrystallization (EtOAc), 54 mg of **1.32** (60%) was given as a colorless solid: mp 100-111 °C, IR (thin film) 1725 cm^{-1} ; ^1H NMR (400 MHz, CD_2Cl_2) δ 8.57 (d, J = 10.0 Hz, 1H), 8.19 (d, J = 8.9 Hz, 2H), 7.72 (s, 2H), 7.70 (d, J = 2.4 Hz, 1H), 7.48 (dd, J = 9.0, 2.4 Hz, 1H), 7.33-7.29 (m, 2H), 7.02 (d, J = 8.92 Hz, 2H), 4.13 (t, J = 6.60 Hz, 2H), 4.07 (t, J = 6.6 Hz, 2H), 1.92-1.78 (m, 4H), 1.59-1.44 (m, 4H), 1.44-1.25 (m, 22H), 0.93-0.86 (m, 6H); ^{13}C NMR (100 MHz, CD_2Cl_2) δ 165.6, 164.3, 158.6, 149.4, 133.9, 132.7, 132.3, 128.8, 128.0, 127.5, 124.8, 124.7, 124.1, 122.1, 121.9, 120.4, 118.3, 114.9, 110.0, 69.0, 68.8, 32.5, 32.4, 30.2, 30.2, 30.1, 30.0, 29.9 (4C), 29.7 (2C), 26.5, 23.3, 23.3, 14.5; HRMS (EI) calcd for $\text{C}_{40}\text{H}_{52}\text{O}_4$ 596.3866, found 596.3843.

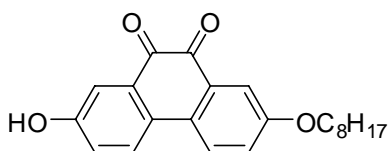
2-(Methoxymethoxy)-7-(octyloxy)phenanthrene-9,10-dione (2.28).



To a solution of **2.21** (0.53 g, 1.4 mmol), NaHCO_3 (7.9 g) in acetone (33 mL), CH_2Cl_2 (33 mL), H_2O (66 mL) was added slowly oxone (6.3 g) at rt. The mixture was stirred for 1 h and concentrated under reduced pressure. The resulting mixture was extracted with CH_2Cl_2 (15 mL \times 2). The combined organic layer was washed with brine, dried (Na_2SO_4), and concentrated under reduced pressure to afford a red solid. Purification by flash column chromatography on silica gel (40% EtOAc/hexanes) and recrystallization (EtOAc/hexanes) gave 0.51 g (93%) of **2.28** as a red solid: mp 72-73 °C; IR (thin film) 1676 cm^{-1} ; ^1H NMR (400 MHz, CDCl_3) δ 7.75 (d,

$J = 8.8$ Hz, 1H), 7.74 (d, $J = 8.8$ Hz, 1H), 7.70 (d, $J = 2.7$ Hz, 1H), 7.54 (d, $J = 2.7$ Hz, 1H), 7.29 (dd, $J = 8.7, 2.7$ Hz, 1H), 7.17 (dd, $J = 8.8, 2.8$ Hz, 1H), 5.23 (s, 2H), 4.03 (t, $J = 6.5$ Hz, 2H), 3.49 (s, 3H), 1.85-1.75 (m, 2H), 1.51-1.41 (m, 2H), 1.41-1.26 (m, 8H), 0.89 (t, $J = 6.6$ Hz, 3H); ^{13}C NMR (100 MHz, CDCl_3) δ 180.2, 180.2, 159.4, 157.2, 131.2, 131.1, 130.3, 129.1, 125.1, 125.0, 124.6, 124.2, 116.3, 113.2, 94.2, 68.6, 56.3, 31.8, 29.3, 29.2, 29.1, 25.9, 22.6, 14.1; HRMS (EI) calcd for $\text{C}_{24}\text{H}_{28}\text{O}_5$: 396.1937, found 396.1949.

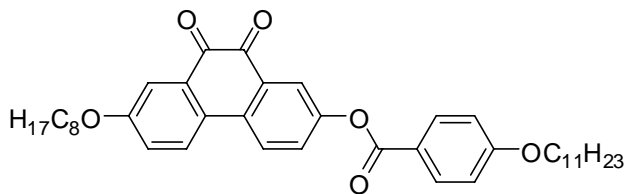
2-Hydroxy-7-(octyloxy)phenanthrene-9,10-dione (2.29).



A solution of **2.28** (0.27 g, 0.68 mmol) in 2-propanol (1.3 mL) was added HCl (6.0 M, 0.68 mL, 4.1 mmol, 6.0 equiv). The mixture was stirred at 60 °C for 6 h, and diluted with NH_4Cl (10 mL). The whole was extracted CH_2Cl_2 (10 mL \times 2). The combined organic layer was washed with brine, dried (Na_2SO_4), concentrated under reduced pressure to afford a red solid. Purification by flash column chromatography on silica gel (40-50% EtOAc/hexanes) and recrystallization (CH_2Cl_2) gave 0.22 g (90%) of **2.29** as a red solid: mp 116-117 °C; IR (thin film) 1670, 1653 cm^{-1} ; ^1H NMR (600 MHz, CDCl_3 , 37 °C) δ 7.72 (d, $J = 8.6$ Hz, 2H), 7.55 (d, $J = 2.5$ Hz, 2H), 7.19-7.14 (m, 2H), 5.29 (s, 1H), 4.04 (t, $J = 6.5$ Hz, 2H), 1.84-1.78 (m, 2H), 1.50-1.44 (m, 2H), 1.41-1.24 (m, 8H), 0.90 (t, $J = 6.8$ Hz, 3H); ^{13}C NMR (150 MHz, CDCl_3 , 37 °C) δ 180.4, 180.4, 159.5, 156.2, 131.3, 131.2, 129.7, 129.3, 125.4, 125.0, 124.3, 123.8, 116.0, 113.5, 68.6, 31.8, 29.3, 29.2, 29.1, 26.0, 22.6, 14.0; HRMS (EI) calcd for $\text{C}_{22}\text{H}_{24}\text{O}_4$: 352.1675, found 352.1688.

7-(Octyloxy)-9,10-dioxo-9,10-dihydrophenanthren-2-yl 4-(undecyloxy)benzoate

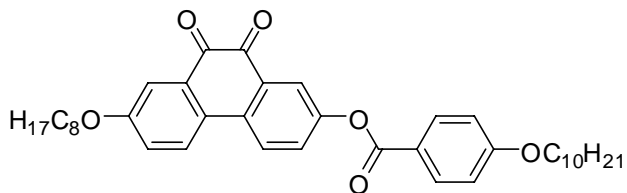
(2.30a).



A solution of **2.29** (30 mg, 0.085 mmol), 4-(undecyloxy)benzoic acid (30 mg, 0.10 mmol, 1.2 equiv), DCC (21 mg, 0.10 mmol, 1.2 equiv), DMAP (2 mg) in CH₂Cl₂ (1.5 mL) was stirred for 10 h at rt under Ar. After concentration by reduced pressure, the residue was purified by flash column chromatography on silica gel (10% EtOAc/hexanes) and recrystallization (EtOAc) to give 48 mg (90%) of **2.30a** as a red solid: mp 112-113 °C, IR (thin film) 1722, 1673 cm⁻¹; ¹H NMR (400 MHz, CDCl₃) δ 8.13 (d, *J* = 8.8 Hz, 2H), 7.94(d, *J* = 2.5 Hz, 1H), 7.91 (d, *J* = 8.9 Hz, 1H), 7.85 (d, *J* = 8.9 Hz, 1H), 7.61 (d, *J* = 2.7 Hz, 1H), 7.54 (dd, *J* = 8.7, 2.5 Hz, 1H), 7.23 (dd, *J* = 8.8, 2.7 Hz, 1H), 6.98 (d, *J* = 8.8 Hz, 2H), 4.09-4.02 (m, 4H), 1.87-1.77 (m, 4H), 1.52-1.42 (m, 4H), 1.42-1.21 (m, 22H), 0.94-0.84 (m, 6H); ¹³C NMR (100 MHz, CDCl₃) δ 179.9, 179.7, 164.4, 163.9, 160.1, 151.2, 133.9, 132.4, 131.8, 131.1, 129.8, 128.4, 125.7, 124.8, 124.2, 123.2, 120.7, 114.4, 113.5, 68.7, 68.4, 31.9, 31.7, 29.6 (2C), 29.4, 29.3 (2C), 29.2, 29.1(2C), 26.0 (2C), 22.7 (2C), 14.1 (2C); HRMS (EI) calcd for C₄₀H₅₀O₆K: 665.3244, found 665.3270.

7-(Octyloxy)-9,10-dioxo-9,10-dihydrophenanthren-2-yl 4-(decyloxy)benzoate

(2.30b).

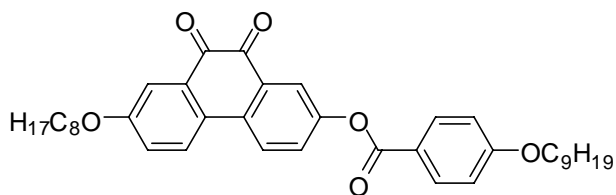


The solution of **2.29** (50 mg, 0.14 mmol), 4-(decyloxy)benzoic acid (47 mg, 0.17 mmol, 1.2 equiv), DCC (35

mg, 0.17 mmol, 1.2 equiv), DMAP (5 mg) in CH₂Cl₂ (2 mL) was stirred for 10 h at rt under Ar. After concentration by reduced pressure, the residue was purified by flash column chromatography on silica gel (10% EtOAc/hexanes) and recrystallization (EtOAc) to give 76 mg (88%) of **2.30b** as a red solid: mp 115-116 °C, IR (thin film) 1722, 1673 cm⁻¹; ¹H NMR (400 MHz, CDCl₃) δ 8.13 (d, *J* = 8.9 Hz, 2H), 7.94 (d, *J* = 2.6 Hz, 1H), 7.92 (d, *J* = 8.9 Hz, 1H), 7.86 (d, *J* = 9.0 Hz, 1H), 7.62 (d, *J* = 2.9 Hz, 1H), 7.54 (dd, *J* = 8.7, 2.6 Hz, 1H), 7.24 (dd, *J* = 8.8, 2.9 Hz, 1H), 6.98 (d, *J* = 9.0 Hz, 2H), 4.11-4.02 (m, 4H), 1.87-1.78 (m, 4H), 1.52-1.43 (m, 4H), 1.42-1.22 (m, 20H), 0.93-0.85 (m, 6H); ¹³C NMR (100 MHz, CDCl₃) δ 179.9, 179.7, 164.4, 163.9, 160.1, 151.2, 133.9, 132.4, 131.8, 131.1, 129.8, 128.4, 125.7, 124.8, 124.2, 123.2, 120.7, 114.4, 113.5, 68.7, 68.4, 31.9, 31.8, 29.5, 29.4, 29.3, 29.2, 29.1, 26.0, 22.7, 14.1; HRMS (EI) calcd for C₃₉H₄₈O₆: 612.3451, found 612.3453.

7-(Octyloxy)-9,10-dioxo-9,10-dihydrophenanthren-2-yl 4-(nonyloxy)benzoate

(**2.30c**).



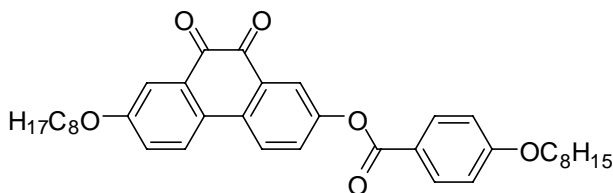
The solution of **2.29** (50 mg, 0.14 mmol), 4-(nonyloxy)benzoic acid (45 mg, 0.17 mmol, 1.2 equiv), DCC (35 mg, 0.17 mmol, 1.2 equiv), and DMAP

(5 mg) in CH₂Cl₂ (2 mL) was stirred for 10 h at rt under Ar. After concentration under reduced pressure, the residue was purified by flash column chromatography on silica gel (10% EtOAc/hexanes) and recrystallization (EtOAc) to give 74 mg (88%) of **2.30c** as a red solid: mp 111-112 °C, IR (thin film) 1722, 1673 cm⁻¹; ¹H NMR (600 MHz, CDCl₃) δ

8.13 (d, $J = 8.9$ Hz, 2H), 7.94 (d, $J = 2.6$ Hz, 1H), 7.91 (d, $J = 8.8$ Hz, 1H), 7.85 (d, $J = 9.0$ Hz, 1H), 7.61 (d, $J = 2.8$ Hz, 1H), 7.54 (dd, $J = 8.7, 2.6$ Hz, 1H), 7.23 (dd, $J = 8.8, 2.8$ Hz, 1H), 6.98 (d, $J = 8.9$ Hz, 2H), 4.08-4.03 (m, 4H), 1.86-1.79 (m, 4H), 1.51-1.44 (m, 4H), 1.41-1.24 (m, 18H), 0.92-0.86 (m, 6H); ^{13}C NMR (150 MHz, CDCl_3) δ 179.9, 179.7, 164.4, 163.9, 160.1, 151.2, 133.9, 132.4, 131.8, 131.1, 129.8, 128.4, 125.7, 124.8, 124.2, 123.2, 120.7, 114.4, 113.5, 68.7, 68.4, 31.9, 31.8, 29.5, 29.4, 29.3, 29.2 (2C), 29.1 (2C), 26.0 (2C), 22.7, 22.6, 14.1; HRMS (EI) calcd for $\text{C}_{38}\text{H}_{46}\text{O}_6$: 598.3294, found 598.3273.

7-(Octyloxy)-9,10-dioxo-9,10-dihydrophenanthren-2-yl 4-(octyloxy)benzoate

(2.30d).

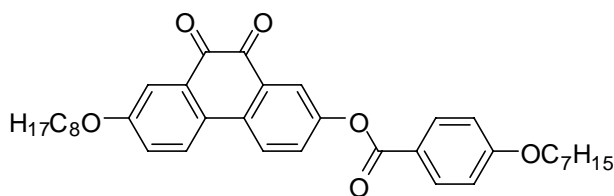


The solution of **2.29** (40 mg, 0.11 mmol), 4-(octyloxy)benzoic acid (34 mg, 0.14 mmol, 1.2 equiv), DCC (28 mg, 0.14 mmol, 1.2 equiv) and DMAP (4 mg) in CH_2Cl_2 (2 mL) was stirred for 10 h at rt under Ar. After concentration by reduced pressure, the residue was purified by flash column chromatography on silica gel (10% EtOAc/hexanes) and recrystallization (EtOAc) to give 56 mg (88%) of **2.30d** as a red solid: mp 111-112 °C, IR (thin film) 1722, 1673 cm^{-1} ; ^1H NMR (600 MHz, CDCl_3) δ 8.13 (d, $J = 8.8$ Hz, 2H), 7.94 (d, $J = 2.5$ Hz, 1H), 7.91 (d, $J = 8.8$ Hz, 1H), 7.85 (d, $J = 9.0$ Hz, 1H), 7.60 (d, $J = 2.7$ Hz, 1H), 7.54 (dd, $J = 8.6, 2.5$ Hz, 1H), 7.23 (dd, $J = 8.8, 2.8$ Hz, 1H), 6.98 (d, $J = 8.9$ Hz, 2H), 4.09-4.00 (m, 4H), 1.88-1.76 (m, 4H), 1.51-1.43 (m, 4H), 1.41-1.22 (m, 16H), 0.89 (t, $J = 6.7$ Hz, 6H); ^{13}C NMR (150 MHz, CDCl_3) δ 179.9, 179.7, 164.4, 163.9, 160.1, 151.2,

133.9, 132.4, 131.8, 131.1, 129.8, 128.4, 125.7, 124.8, 124.2, 123.1, 120.7, 114.4, 113.5, 68.7, 68.4, 31.8, 29.3, 29.2, 29.1 (2C), 26.0, 25.9, 22.6, 14.1; HRMS (EI) calcd for C₃₇H₄₄O₆: 584.3138, found 584.3165.

7-(Octyloxy)-9,10-dioxo-9,10-dihydrophenanthren-2-yl 4-(heptyloxy)benzoate

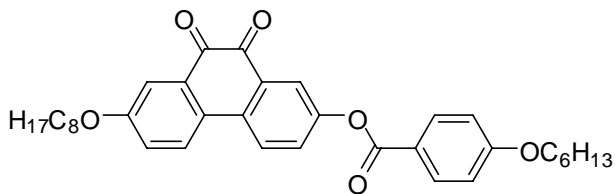
(2.30e).



The solution of **2.29** (60 mg, 0.17 mmol), 4-(heptyloxy)benzoic acid (48 mg, 0.20 mmol, 1.2 equiv), DCC (42 mg, 0.20 mmol, 1.2 equiv), DMAP (6 mg) in CH₂Cl₂ (2 mL) was stirred for 10 h at rt under Ar. After concentration by reduced pressure, the residue was purified by flash column chromatography on silica gel (10% EtOAc/hexanes) and recrystallization (EtOAc) to give 88 mg (91%) of **2.30e** as a red solid: mp 101-102 °C, IR (thin film) 1723, 1673 cm⁻¹; ¹H NMR (600 MHz, CDCl₃) δ 8.13 (d, *J* = 8.8 Hz, 2H), 7.93 (d, *J* = 2.5 Hz, 1H), 7.91 (d, *J* = 8.8 Hz, 1H), 7.84 (d, *J* = 8.9 Hz, 1H), 7.60 (d, *J* = 2.7 Hz, 1H), 7.53 (dd, *J* = 8.6, 2.5 Hz, 1H), 7.23 (dd, *J* = 8.7, 2.7 Hz, 1H), 6.98 (d, *J* = 8.8 Hz, 2H), 4.10-4.02 (m, 4H), 1.88-1.77 (m, 4H), 1.52-1.44 (m, 4H), 1.42-1.23 (m, 14H), 0.94-0.86 (m, 6H); ¹³C NMR (150 MHz, CDCl₃) δ 180.0, 179.8, 164.4, 163.9, 160.1, 151.2, 133.9, 132.4, 131.9, 131.1, 129.8, 128.4, 125.7, 124.8, 124.2, 123.2, 120.7, 114.5, 113.5, 68.7, 68.4, 31.8 (2C), 29.3, 29.2, 29.1 (2C), 29.0, 26.0, 25.9, 22.7, 22.6, 14.0 (2C); HRMS (EI) calcd for C₃₆H₄₂O₆: 570.2981, found 570.2971.

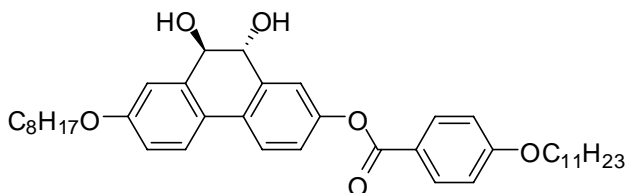
7-(Octyloxy)-9,10-dioxo-9,10-dihydrophenanthren-2-yl 4-(hexyloxy)benzoate

(2.30f).



The solution of **2.29** (60 mg, 0.17 mmol), 4-(hexyloxy)benzoic acid (45 mg, 0.20 mmol, 1.2 equiv), DCC (42 mg, 0.20 mmol, 1.2 equiv) and DMAP (6 mg) in CH₂Cl₂ (2 mL) was stirred for 10 h at rt under Ar. After concentration by reduced pressure, the residue was purified by flash column chromatography on silica gel (10% EtOAc/hexanes) and recrystallization (EtOAc) to give 85 mg (90%) of **2.30f** as a red solid: mp 113-114 °C, IR (thin film) 1723, 1674 cm⁻¹; ¹H NMR (600 MHz, CDCl₃) δ 8.13 (d, *J* = 8.8 Hz, 2H), 7.94 (d, *J* = 2.4 Hz, 1H), 7.91 (d, *J* = 8.8 Hz, 1H), 7.85 (d, *J* = 9.0 Hz, 1H), 7.61 (d, *J* = 2.6 Hz, 1H), 7.54 (dd, *J* = 8.6, 2.4 Hz, 1H), 7.23 (dd, *J* = 8.7, 2.6 Hz, 1H), 6.98 (d, *J* = 8.8 Hz, 2H), 4.08-4.03 (m, 4H), 1.86-1.79 (m, 4H), 1.52-1.44 (m, 4H), 1.41-1.25 (m, 12H), 0.95-0.87 (m, 6H); ¹³C NMR (150 MHz, CDCl₃) δ 179.9, 179.7, 164.4, 163.9, 160.1, 151.2, 133.9, 132.4, 131.8, 131.1, 129.8, 128.4, 125.7, 124.8, 124.2, 123.2, 120.7, 114.4, 113.5, 68.7, 68.4, 31.8, 31.5, 29.3, 29.2, 29.1, 29.0, 26.0, 25.6, 22.6, 22.6, 14.1, 14.0; HRMS (EI) calcd for C₃₅H₄₀O₆: 556.2825, found 556.2849.

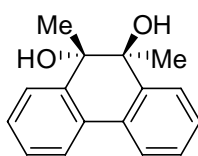
trans-9,10-Dihydroxy-7-(octyloxy)-9,10-dihydrophenanthren-2-yl 4-(undecyloxy)benzoate (1.31)



To a solution of **2.30a** (0.20 g, 0.32 mmol) in 2-propanol (10 mL) was added KBH₄ (0.17 g, 3.2 mmol, 10

equiv) slowly. After stirring for 12 h under Ar at rt, the mixture was neutralized dropwise with satd NH₄Cl (8 mL) and the resulting solution was extracted with CH₂Cl₂ (8 mL × 3). The combined organic layer was washed with brine, dried (Na₂SO₄), and concentrated under reduced pressure to give a yellow solid. Purification by flash column chromatography on silica gel (10-20% EtOAc/hexanes) and Recrystallization (CH₂Cl₂/hexane) gave 0.16 g (80%) of **1.31** as a colorless solid: mp 97-98 °C; IR (thin film) 3417, 1729 cm⁻¹; ¹H NMR (600 MHz, MHz, DMSO) δ 8.08 (d, *J* = 8.6 Hz, 2H), 7.76 (d, *J* = 8.4 Hz, 1H), 7.71 (d, *J* = 8.5 Hz, 1H), 7.40 (s, 1H), 7.21-7.15 (m, 2H), 7.11 (d, *J* = 8.5 Hz, 2H), 6.90 (d, *J* = 8.2 Hz, 1H), 5.69 (s, 1H), 5.64 (s, 1H), 4.45 (s, 2H), 4.08 (t, *J* = 6.2 Hz, 2H), 4.01 (t, *J* = 6.3 Hz, 2H), 1.80-1.69 (m, 4H), 1.47-1.39 (m, 4H), 1.37-1.19 (m, 22H), 0.89-0.83 (m, 6H); ¹³C NMR (150 MHz, MHz, DMSO) δ 164.2, 163.1, 158.6, 149.6, 139.8, 139.1, 131.8, 129.9, 124.6, 124.1, 123.6, 120.8, 120.8, 119.0, 114.6, 113.5, 111.7, 72.2, 72.1, 67.9, 67.4, 31.2, 31.1, 28.8 (3C), 28.6 (3C), 28.5, 28.4, 25.4, 25.3, 21.9, 13.8; HRMS (EI) calcd for C₄₀H₅₄O₆: 630.3920, found 630.3902.

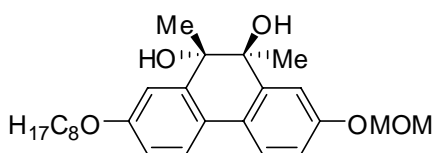
9,10-Dimethyl-9,10-dihydrophenanthrene-9,10-diol (2.36)



A solution of phenanthrene-9,10-dione (0.10 g, 0.48 mmol) in Et₂O (1.5 mL) in a sealed tube cooled to 0 °C was added MeMgBr (3.0 M in Et₂O, 0.64 mL, 4.0 equiv) dropwise under Ar. The tube was sealed, and the mixture was stirred for 10 h at 50 °C. Satd NH₄Cl (10 mL) was added to the mixture dropwise and the whole was extracted with Et₂O (10 mL × 3). The combined organic layer was washed with brine, dried (Na₂SO₄), and concentrated under reduced pressure to afford a yellow solid. Purification by flash column chromatography on silica

gel (30% hexanes/toluene) and recrystallization from CH₂Cl₂/hexanes gave 0.10 g (90%) of **2.36** as a colorless solid: mp 134-135 °C (lit^b 134-136 °C (CH₂Cl₂/hexanes)); IR (thin film) 3442 cm⁻¹; ¹H NMR (400 MHz, CDCl₃) δ 7.76-7.67 (m, 4H), 7.41-7.33 (m, 4H), 2.25 (s, 2H), 1.34 (s, 6H); ¹³C NMR (100 MHz, CDCl₃) δ 142.3, 131.7, 128.4, 127.7, 123.6 (2C), 77.5, 24.4. The physical and spectral data are consistent with those reported.^{197b}

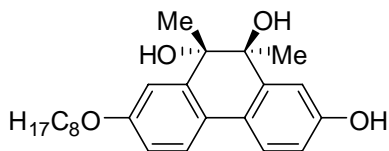
2-(Methoxymethoxy)-9,10-dimethyl-7-(octyloxy)-9,10-dihydrophenanthrene-9,10-diol (2.32).



A solution of **2.28** (0.10 g, 0.25 mmol) in Et₂O (1.5 mL) in a sealed tube cooled to 0 °C was added MeMgBr (3.0 M in Et₂O, 0.36 mL, 4.0 equiv) dropwise under Ar. The tube was sealed, and the mixture was stirred for 10 h at 50 °C. Satd NH₄Cl (10 mL) was added to the mixture dropwise and the whole was extracted with Et₂O (10 mL × 3). The combined organic layer was washed with brine, dried (Na₂SO₄), and concentrated under reduced pressure to afford a yellow solid. Purification by flash column chromatography on silica gel (30% hexanes/toluene) and recrystallization (CH₂Cl₂/hexanes) gave 0.097 g (90%) of **2.32** as a colorless solid: mp 69-70 °C; IR (thin film) 3442 cm⁻¹; ¹H NMR (400 MHz, CDCl₃) δ 7.54 (d, *J* = 8.4 Hz, 2H), 7.33 (d, *J* = 2.6 Hz, 1H), 7.22 (d, *J* = 2.7 Hz, 1H), 6.98 (dd, *J* = 8.5, 2.7 Hz, 1H), 6.84 (dd, *J* = 8.5, 2.7 Hz, 1H), 5.23 (q, *J* = 6.7 Hz, 2H), 4.05-3.98 (m, 2H), 3.52 (s, 3H), 2.21 (d, *J* = 5.4 Hz, 2H), 1.84-1.75 (m, 2H), 1.53-1.41 (m, 2H), 1.40-1.20 (m, 14H), 0.89 (t, *J* = 6.7 Hz, 3H); ¹³C NMR (100 MHz, CDCl₃) δ 159.1, 156.9, 143.3 (2C), 125.8,

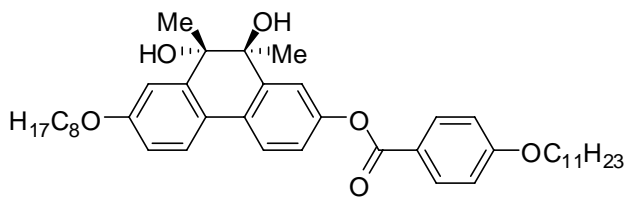
124.5, 124.3, 124.2, 115.0, 113.5, 111.6, 109.7, 94.5, 77.6, 77.5, 68.1, 56.1, 31.8, 29.4 (2C), 29.2, 26.1, 24.3, 24.3, 22.7, 14.1; HRMS (EI) calcd for C₂₆H₃₆O₅ 428.2563, found 428.2543.

9,10-Dimethyl-7-(octyloxy)-9,10-dihydrophenanthrene-2,9,10-triol (2.33).



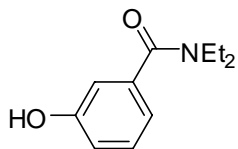
To a solution of **2.32** (30 mg, 0.076 mmol) and *n*-Bu₄NBr (0.12 mg, 0.38 mmol, 5.0 equiv) in CH₂Cl₂ (1 mL) was added TMSCl (41 mg, 48 uL, 5.0 equiv) at rt under Ar. The mixture was stirred for 1 h, diluted with satd NH₄Cl (5 mL) and the whole was extracted with CH₂Cl₂ (10 mL × 3). The combined organic layer was washed with brine, dried (Na₂SO₄), and concentrated under reduced pressure to afford a yellow oil. Purification by flash column chromatography on silica gel (40-50% hexanes/toluene) and recrystallization (EtOAc/hexanes) gave 25 mg (86%) of **2.33** as a colorless solid: mp 127-128 °C; IR (thin film) 3431 cm⁻¹; ¹H NMR (400 MHz, CD₃OD) δ 7.51 (d, *J* = 8.6 Hz, 1H), 7.47 (d, *J* = 8.5 Hz, 1H), 7.21 (d, *J* = 2.6 Hz, 1H), 7.12 (d, *J* = 2.6 Hz, 1H), 6.79 (dd, *J* = 8.5, 2.7 Hz, 1H), 6.70 (dd, *J* = 8.4, 2.6 Hz, 1H), 4.04-3.97 (m, 2H), 1.83-1.73 (m, 2H), 1.54-1.44 (m, 2H), 1.42-1.25 (m, 8H), 1.22 (s, 3H), 1.21 (s, 3H), 0.91 (t, *J* = 6.7 Hz, 3H); ¹³C NMR (100 MHz, CD₃OD) δ 160.1, 158.1, 146.0, 145.6, 126.4, 125.3, 125.2, 125.0, 115.1, 114.4, 112.2, 111.3, 78.6, 78.4, 69.1, 33.2, 30.7, 30.6, 27.4, 24.8, 23.9, 14.6; HRMS (EI) calcd for C₂₄H₃₂O₄ 384.2301, found 384.2298.

9,10-Dihydroxy-9,10-dimethyl-7-(octyloxy)-9,10-dihydrophenanthren-2-yl 4-undecyloxybenzoate (2.31).



To a solution of **2.33** (35 mg, 0.091 mmol) in CH_2Cl_2 (4 mL) were added 4-(undecyloxy)benzoic acid (27 mg, 0.091 mmol, 1 equiv), DCC (11 mg, 0.053 mmol, 1.2 equiv), DMAP (2 mg). The mixture was stirred for 10 h under Ar at rt, neutralized with satd NH_4Cl (5 mL) and extracted with CH_2Cl_2 (10 mL \times 2). The combined organic layer was washed with brine, dried (Na_2SO_4), and concentrated under reduced pressure to afford a brown solid. Purification by flash column chromatography on silica gel (10% EtOAc/hexanes) and recrystallization (EtOAc/hexanes) gave 47 mg (88%) of **2.31** as a colorless solid: mp 63-64 °C (hexane); IR (thin film) 3459, 1729 cm^{-1} ; ^1H NMR (400 MHz, CD_2Cl_2) δ 8.13 (d, J = 8.8 Hz, 2H), 7.68 (d, J = 8.6 Hz, 1H), 7.63 (d, J = 8.7 Hz, 1H), 7.49 (d, J = 2.4 Hz, 1H), 7.23 (d, J = 2.6 Hz, 1H), 7.16 (dd, J = 8.4, 2.4 Hz, 1H), 7.00 (d, J = 8.9 Hz, 2H), 6.87 (dd, J = 8.5, 2.6 Hz, 1H), 4.09-4.00 (m, 4H), 2.50-2.12 (br, 2H), 1.87-1.75 (m, 4H), 1.53-1.43 (m, 4H), 1.43-1.22 (m, 28H), 0.93-0.84 (m, 6H); ^{13}C NMR (100 MHz, CD_3Cl_2) δ 165.3, 164.1, 160.1, 150.9, 144.5, 143.7, 132.5, 129.9, 125.5, 124.4, 124.1, 122.0, 121.2, 117.7, 114.7, 113.7, 110.3, 77.7, 77.6, 68.8, 68.5, 32.3 (2C), 30.0 (2C), 29.8 (2C), 29.7, 29.5, 26.5, 26.4, 24.7, 24.5, 23.1, 14.3; HRMS (EI) calcd for $\text{C}_{42}\text{H}_{58}\text{O}_6$ 658.4233, found 658.4218.

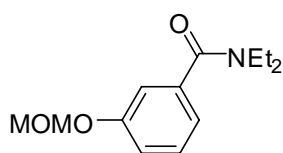
***N,N*-Diethyl-3-hydroxybenzamide (2.6).**



To a solution of *N,N*-diethyl-3-methoxybenzamide **2.2** (4.0 g, 19 mmol) in CH_2Cl_2 (anhydrous, 20 mL) at -65 to -78 °C under an Ar atmosphere was added dropwise freshly prepared BBr_3 (1.0 M

solution in CH₂Cl₂, 39 mL, 39 mmol, 2.0 equiv). The mixture was allowed to warm up to rt and stirred over 30 min, quenched with satd NH₄Cl (30 mL) dropwise and the whole was extracted with CH₂Cl₂ (20 mL × 3). The combined organic layer was washed with brine, dried (Na₂SO₄), and concentrated under reduced pressure to give a brown solid. Purification by flash column chromatography on silica gel (45-50% EtOAc/hexanes) and recrystallization (CH₂Cl₂/hexanes) gave 3.5 g (93%) of **2.6** as a colorless crystalline solid: mp 99-100 °C [lit²¹³ mp 82 °C (EtOAc)]; ¹H NMR (500 MHz, MHz, CDCl₃) δ 8.12 (br, 1H), 7.15 (t, *J* = 7.8 Hz, 1H), 6.89-6.88 (m, 1H), 6.78 (dd, *J* = 8.2, 2.2 Hz, 2H), 3.60-3.51 (m, 2H), 3.31-3.22 (m, 2H), 1.25 (t, *J* = 6.7 Hz, 3H), 1.10 (t, *J* = 6.6 Hz, 3H); ¹³C NMR (125 MHz, MHz, CDCl₃) δ 172.0, 156.9, 137.2, 129.4, 117.1, 117.0, 114.2, 43.5, 39.5, 14.1, 12.8. Spectral data are consistent with those reported.²¹⁴

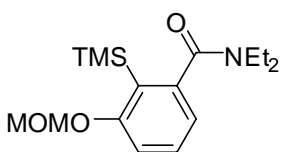
***N,N*-Diethyl-3-(methoxymethoxy)benzamide (3.3).**



A solution of **2.6** (2.7 g, 14 mmol) and MOMCl (2.0 g, 2.1 mL, 15 mmol, 1.1 equiv) in *i*-Pr₂EtN (10 mL) was stirred at rt under Ar for 10 h. The solution was diluted with satd NH₄Cl (10 mL) and the whole was extracted with CH₂Cl₂ (20 mL × 2). The combined organic layer was washed with brine, dried (Na₂SO₄) and concentrated under reduced pressure. Purification by flash column chromatography on silica gel (20-30% EtOAc/hexanes) gave 3.0 g (90%) of **3.3** as a colorless oil: ¹H NMR (500 MHz, CDCl₃) δ 7.29-7.23 (m, 1H), 7.04-6.99 (m, 2H), 6.95 (d, *J* = 6.6 Hz, 1H), 5.14 (s, 2H), 3.49 (br, 2H), 3.43 (s, 3H), 3.21 (br, 2H), 1.20 (br, 3H) 1.07 (br, 3H); ¹³C NMR (125 MHz, CDCl₃) δ 170.7, 157.1, 138.5,

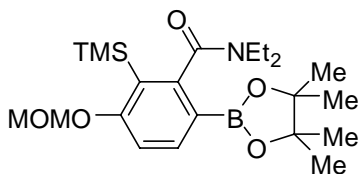
129.5, 119.5, 116.8, 114.1, 94.3, 55.9, 43.1, 39.1, 14.0, 12.8. The physical and spectral data are consistent with those reported.¹²⁹

***N,N*-Diethyl-3-(methoxymethoxy)-2-(trimethylsilyl)benzamide (3.4).**



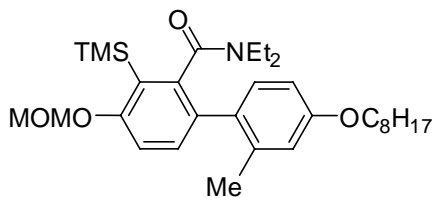
To a solution of TMEDA (1.6 g, 2.1 mL, 14 mmol, 1.2 equiv) in THF (100 mL) at -78 to -80 °C under Ar was added dropwise *s*-BuLi (1.0 M solution in hexanes, 13 mL, 14 mmol, 1.2 equiv). After 10 min, **3.3** (0.50 M in THF, 23 mL, 11 mmol) was added by dropwise addition. After stirring for 1 h, to the mixture was added TMSCl (1.7 mL, 14 mmol, 1.2 equiv) dropwise. The resulting solution was allowed to warm up to rt over 4 h, and neutralized with satd NH₄Cl (30 mL). Concentrated under reduced pressure, the whole was extracted with CH₂Cl₂ (20 mL × 3). The combined organic layer was washed with brine, dried (Na₂SO₄), and concentrated under reduced pressure. Purification by flash chromatography on silica gel (20-30% EtOAc/hexane) and recrystallization (hexane) gave 2.8 g (79%) of **3.4** as a colorless solid: mp 63-64 °C [lit mp = 62-65 °C (hexanes)]; ¹H NMR (400 MHz, CDCl₃) δ 7.29 (dd, *J* = 8.2, 7.6 Hz, 1H), 7.06 (dd, *J* = 8.3, 0.6 Hz, 1H), 6.78 (dd, *J* = 7.5, 0.7 Hz, 1H), 5.18 (s, 2H), 3.73-3.58 (m, 1H), 3.48 (s, 3H), 3.46-3.33 (m, 1H), 3.31-3.06 (m, 2H), 1.25 (t, *J* = 7.2 Hz, 3H), 1.07 (t, *J* = 7.1 Hz, 3H), 0.03 (s, 9H); ¹³C NMR (100 MHz, CDCl₃) δ 171.7, 162.7, 144.6, 130.5, 124.6, 119.7, 112.6, 94.1, 56.1, 43.3, 39.0, 13.7, 12.8, 0.6. Physical and spectral data are consistent with those reported.¹²⁹

***N,N*-Diethyl-3-(methoxymethoxy)-6-(4,4,5,5-tetramethyl-1,3,2-dioxaborolan-2-yl)-2-(trimethylsilyl)benzamide (3.6).**



To a solution of **3.4** (1.0 g, 3.2 mmol) in Et₂O (30 mL) at -5 °C under Ar was added *s*-BuLi (1.4 M in hexane, 4.6 mL, 6.5 mmol, 2.0 equiv) dropwise. After the mixture was stirred for 2 h, B(O*i*-Pr)₃ (1.5 mL, 6.5 mmol, 2.0 equiv) was added dropwise. The mixture was neutralized with NH₄Cl (20 mL) and extracted with EtOAc (20 mL × 3). The combined organic layer was washed with brine and dried (Na₂SO₄). Without further purification, the mixture was treated with pinacol (0.76 g, 6.5 mmol, 2.0 equiv) and the whole was stirred for 1 h and concentrated under reduced pressure. Purification by flash chromatography on silica gel (10% EtOAc/hexane) and recrystallization (hexanes) gave 0.85 g (65%) of **3.6** as a colorless solid: mp 89-91 °C [lit²¹⁵ mp 89-90 °C (hexanes)]; IR (thin film) 1639 cm⁻¹; ¹H NMR (400 MHz, CDCl₃) δ 7.83 (d, *J* = 8.4 Hz, 1H), 7.02 (d, *J* = 8.4 Hz, 1H), 5.19 (s, 2H), 3.78-3.67 (m, 1H), 3.47 (s, 3H), 3.34-3.23 (m, 1H), 3.15-3.08 (m, 2H), 1.30 (t, *J* = 7.2 Hz, 3H), 1.28-1.24 (m, 12H), 1.02 (t, *J* = 7.2 Hz, 3H), 0.27 (s, 9H); ¹³C NMR (100 MHz, CDCl₃) δ 171.2, 164.9, 150.2, 139.5, 124.0, 111.4, 94.0, 83.5, 56.2, 43.3, 39.4, 24.9, 24.6, 13.1, 12.5, 0.8. Physical and spectral data are consistent with those reported.²¹⁵

***N,N*-Diethyl-4-(methoxymethoxy)-2'-methyl-4'-(octyloxy)-3-(trimethylsilyl)biphenyl-2-carboxamide (3.7)**

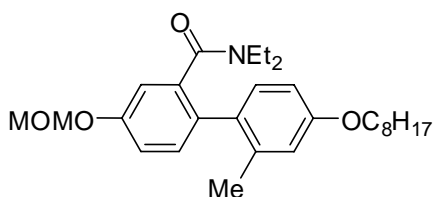


To a solution of **3.7** (1.0 g, 2.3 mmol) in DME (23 mL, degassed) in a glove box was sequentially added,

1-bromo-2-methyl-4-(octyloxy)benzene **2.10c** (0.69, 2.3 mmol, 1.0 equiv), (PPh₃)₄Pd (0.13 g, 0.069 mmol, 3 mol%) and K₂CO₃ (1.0 M aq solution, 6.9 mL, 6.9 mmol, 3.0 equiv). The mixture was heated to reflux and stirred under Ar for 20 h. After cooling to rt, the reaction mixture was quenched with satd NH₄Cl (15 mL) and concentrated under reduced pressure, and the resulting residue was extracted with CH₂Cl₂ (10 mL × 2). The combined organic layer was washed with brine, dried (Na₂SO₄), concentrated under reduced pressure to afford a brown oil. Purification by flash column chromatography on silica gel (20% EtOAc/hexanes) gave 0.76 g (72%) of **3.7** as a colorless oil which was shown to be a mixture of diastereomers²¹²: IR (thin film) 1635 cm⁻¹; ¹H NMR (600 MHz, CDCl₃) δ 7.33-6.58 (m, 5H), 5.27-5.15 (m, 2H), 3.97-3.88 (m, 2H), 3.79-3.69 (m, 1H), 3.55-3.46 (m, 3H), 3.24-2.49 (m, 3H), 2.21-2.06 (m, 3H), 1.80-1.71 (m, 2H), 1.48-1.22 (m, 10H), 1.02-0.80 (m, 6H), 0.66-0.43 (m, 3H), 0.33-0.24 (m, 9H); ¹³C NMR (150 MHz, CDCl₃) δ 169.6, 169.3, 161.8, 161.7, 158.5, 158.2, 143.6, 143.4, 140.0, 136.5, 133.4, 132.7, 132.4, 132.2, 131.0, 130.4, 129.9, 125.1, 124.2, 116.4, 115.4, 112.0, 111.9, 110.8, 110.6, 94.3, 68.0, 56.2, 56.2, 42.4, 42.3, 37.6, 37.1, 31.8, 29.3, 29.2, 26.0, 22.6, 20.8, 20.5, 14.1, 12.9, 11.6, 11.1, 0.9, 0.8; NMR HRMS (EI) calcd for C₃₁H₄₉NO₄Si: 527.3431, found 527.3438.

***N,N*-Diethyl-4-(methoxymethoxy)-2'-methyl-4'-(octyloxy)biphenyl-2-carboxamide**

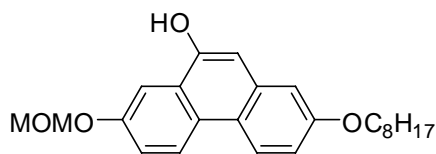
(3.8).



To a solution of **3.7** (0.60 g, 1.14 mmol) in THF (8 mL) was added TBAF (1 M solution in THF, 3.4 mL, 3.4 mmol 3 equiv) at rt. After stirring for 12 h the

reaction mixture was concentrated under reduced pressure. The resulting residue was diluted with satd NH₄Cl (10 mL), and the whole was extracted with Et₂O (15 mL × 3). The combined organic layer was washed with brine, dried (Na₂SO₄), and concentrated under reduced pressure to afford a brown oil. Purification by flash column chromatography on silica gel (20% EtOAc/hexanes) gave 0.47 g (90%) of **3.8** as a colorless oil: IR (thin film) 1634 cm⁻¹; ¹H NMR (600 MHz, CDCl₃) δ 7.22-6.92 (m, 4H), 6.75 (s, 1H), 6.66 (d, *J* = 7.5 Hz, 1H), 5.29-5.09 (m, 2H), 3.92 (t, *J* = 6.6 Hz, 2H), 3.81-3.59 (m, 1H), 3.49 (s, 3H), 3.31-2.56 (m, 3H), 2.18 (s, 3H), 1.81-1.67 (m, 2H), 1.49-1.20 (m, 10H), 0.88 (t, *J* = 6.6 Hz, 6H), 0.74 (t, *J* = 7.0 Hz, 3H); ¹³C NMR (100 MHz, CDCl₃) δ 169.7, 158.4, 156.2, 138.4, 131.7, 115.9, 114.1, 111.0, 94.5, 67.9, 56.0, 42.3, 37.9, 31.8, 29.3, 29.2 (2C), 26.0, 22.6, 20.5, 14.0, 13.6, 11.9; HRMS (EI) calcd for C₂₈H₄₁NO₄: 455.3036, found 455.3020.

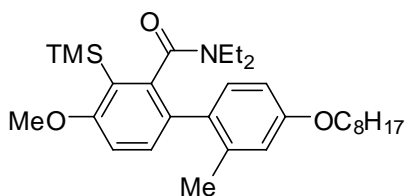
7-(Methoxymethoxy)-2-(octyloxy)phenanthren-9-ol (**3.9**).



A solution of **3.8** (0.65 g, 1.4 mmol) in THF (15 mL) was added under Ar freshly prepared LDA (1 M solution in THF, 7.2 mL, 7.2 mmol, 5.0 equiv) by dropwise addition at -5–0 °C. The mixture was allowed to warm up to rt over 30 min, neutralized with satd NH₄Cl (10 mL) and the whole was concentrated under reduced pressure. The residue was extracted with CH₂Cl₂ (10 mL ×2) and the combined organic layer was washed with brine, dried (Na₂SO₄), and concentrated under reduced pressure to give a yellow solid. Purification by flash column chromatography on silica gel (20-30% EtOAc/hexanes) and recrystallization (CH₂Cl₂/hexanes) gave 0.53 g (97%) of **3.9** as a

colorless solid: mp 124-126 °C; IR (thin film) 3513 cm⁻¹; ¹H NMR (400 MHz, CDCl₃) δ 8.46 (d, *J* = 9.1 Hz, 1H), 8.37 (d, *J* = 9.1 Hz, 1H), 7.88 (d, *J* = 2.6 Hz, 1H), 7.37 (dd, *J* = 9.0, 2.6 Hz, 1H), 7.11 (dd, *J* = 9.0, 2.5 Hz, 1H), 7.03 (d, *J* = 2.5 Hz, 1H), 6.90 (s, 1H), 5.74 (br, 1H), 5.38 (s, 2H), 4.06 (t, *J* = 6.6 Hz, 2H), 3.59 (s, 3H), 1.89-1.79 (m, 2H), 1.56-1.44 (m, 2H), 1.43-1.27 (m, 8H), 0.90 (t, *J* = 6.7, Hz, 3H); ¹³C NMR (100 MHz, CDCl₃) δ 157.6, 154.9, 149.7, 133.2, 126.9, 125.6, 123.9, 123.6, 120.9, 118.5, 114.9, 107.9, 106.4, 106.4, 94.5, 68.1, 56.2, 31.8, 29.4, 29.3, 29.3, 26.1, 22.7, 14.1; HRMS (EI) calcd for C₂₄H₃₀O₄: 382.2144, found 382.2152.

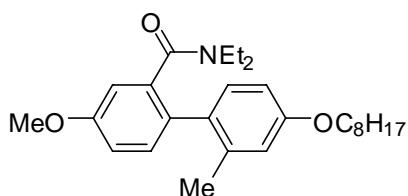
***N,N*-Diethyl-4-methoxy-2'-methyl-4'-(octyloxy)-3-(trimethylsilyl)biphenyl-2-carboxamide (3.10).**



To a solution of *N,N*-diethyl-3-methoxy-6-(4,4,5,5-tetramethyl-1,3,2-dioxaborolan-2-yl)-2-(trimethylsilyl)benzamide **2.5** (2.0 g, 4.9 mmol) in DME (50 mL, degassed) in a glove box were added sequentially 1-bromo-2-methyl-4-(octyloxy)benzene **2.10c** (1.5 g, 4.9 mmol, 1.0 equiv), (PPh₃)₄Pd (0.16 mg, 3 mmol%) and K₂CO₃ (1.0 M aq solution, 15 mL, 15 mmol, 3 equiv). The mixture was heated to reflux and stirred under Ar for 20 h. After cooling to rt, the reaction mixture was diluted with saturated NH₄Cl (15 mL) and concentrated under reduced pressure, and the resulting residue was extracted with CH₂Cl₂ (10 mL × 2). The combined organic layer was washed with brine, dried (Na₂SO₄), and concentrated under reduced pressure. Purification by flash column chromatography on silica gel (20% EtOAc/hexanes) and recrystallization (CH₂Cl₂/hexanes) gave 2.0 g (80%) of **3.10** as a colorless solid which

was shown to be a mixture of diastereomers: mp 66-68 °C; IR (thin film) 1633 cm⁻¹; ¹H NMR (400 MHz, CH₂Cl₂) δ 7.23-6.90 (m, 2H), 6.87 (d, *J* = 8.5 Hz, 1H), 6.77-6.67 (m, 1H), 6.67-6.58 (m, 1H), 3.93 (t, *J* = 6.6 Hz, 2H), 3.84 (s, 3H), 3.76-3.64 (m, 1H), 3.22-2.48 (m, 3H), 2.22-2.02 (m, 3H), 1.80-1.70 (m, 2H), 1.49-1.23 (m, 10H), 1.03-0.79 (m, 6H), 0.64-0.41 (m, 3H), 0.25 (s, 9H); ¹³C NMR (100 MHz, CH₂Cl₂) δ 169.9, 169.8, 164.6, 164.4, 159.1, 158.8, 144.4, 144.1, 140.3, 137.3, 133.9, 133.1, 133.0, 132.9, 131.7, 130.6, 129.9, 125.0, 124.1, 116.8, 115.7, 111.4, 111.1, 109.8, 109.6, 68.5, 55.7, 55.7, 42.9, 42.8, 38.0, 37.3, 32.4, 29.9, 29.8, 26.6, 23.2, 21.1, 20.9, 14.4, 13.3, 12.0, 11.5, 0.9; HRMS (EI) calcd for C₃₀H₄₇NO₃Si: 497.3325, found 497.3337.

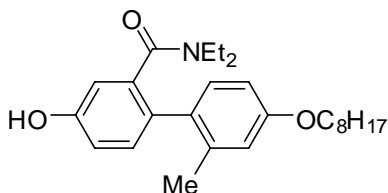
***N,N*-Diethyl-4-methoxy-2'-methyl-4'-(octyloxy)biphenyl-2-carboxamide (3.11).**



To a solution of **3.10** (1.9 g, 3.8 mmol) in DMF (15 mL) was added CsF (2.9 g, 19 mmol, 5.0 equiv). The whole was heated to 100 °C and stirred for 2 h. After cooling to rt, the reaction mixture was diluted with satd NH₄Cl (10 mL), and the whole was extracted with Et₂O (15 mL × 3). The combined organic layer was washed with brine and dried (Na₂SO₄), and concentrated under reduced pressure to afford a yellow oil. Purification by flash column chromatography on silica gel (20% EtOAc/hexanes) gave 1.6 g (98%) of product **3.11** as a colorless oil: IR (thin film) 1634 cm⁻¹; ¹H NMR (600 MHz, CDCl₃, 37 °C) δ 7.22-6.99 (m, 2H), 6.91 (dd, *J* = 8.5, 2.0 Hz, 1H), 6.87 (s, 1H), 6.75 (s, 1H), 6.66 (d, *J* = 7.8 Hz, 1H), 3.93 (t, *J* = 6.6 Hz, 2H), 3.83 (s, 3H), 3.79-3.59 (m, 1H), 3.39-2.55 (m, 3H), 2.17 (s, 3H), 1.79-1.73 (m, 2H), 1.47-1.41 (m, 2H), 1.38-1.24 (m, 8H), 0.94-0.82 (m, 6H), 0.76 (t, *J* = 7.0 Hz, 3H); ¹³C NMR (150 MHz, CDCl₃,

37 °C) δ 169.9, 158.6, 158.5, 138.5, 131.7, 116.2, 114.2, 111.5, 111.1, 68.0, 55.3, 42.2, 37.9, 31.8, 29.3 (2C), 29.2, 26.0, 22.6, 20.4, 14.0, 13.7, 11.9; HRMS (EI) calcd for $C_{27}H_{39}NO_3$: 425.2930, found 425.2914.

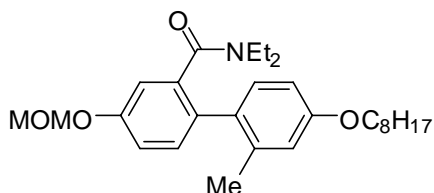
***N,N*-Diethyl-4-hydroxy-2'-methyl-4'-(octyloxy)biphenyl-2-carboxamide (3.12).**



A solution of EtSH (2.6 mL, 35 mmol, 10 equiv) in DMF (25 mL) was added to freshly washed (hexanes) NaH (60% in mineral oil, 1.4 g, 35 mmol, 10 equiv) by hexanes dropwise. The whole was stirred for 10 min and **3.11** (1.5 g, 3.5 mmol) was added. The mixture was heated to 150 °C and stirred for 1 h. After cooling to rt, the reaction mixture was neutralized dropwise with satd NH_4Cl (20 mL) and extracted with Et_2O (15 mL \times 3). The combined organic layer was washed with brine, dried (Na_2SO_4), and concentrated under reduced pressure to afford a yellow solid. Purification by flash column chromatography on silica gel (60% EtOAc/hexanes) and recrystallization (CH_2Cl_2 /hexanes) gave 1.6 g (98%) of **3.12** as a colorless crystalline solid: mp 107-109 °C; IR (thin film) 3224, 1603 cm^{-1} ; 1H NMR (150 MHz, $CDCl_3$, 37 °C) δ 8.62 (br, 1H), 7.25-7.05 (m, 1H), 7.01 (d, $J = 8.3$ Hz, 1H), 6.90 (s, 1H), 6.79 (d, $J = 7.9$ Hz, 1H), 6.76 (s, 1H), 6.69 (d, $J = 8.0$ Hz, 1H), 3.94 (t, $J = 6.6$ Hz, 2H), 3.83-3.66 (m, 1H), 3.26-2.59 (m, 3H), 2.19 (s, 3H), 1.80-1.74 (m, 2H), 1.49-1.42 (m, 2H), 1.39-1.24 (m, 8H), 0.90 (t, $J = 6.7$ Hz, 3H), 0.88-0.82 (m, 3H), 0.79 (t, $J = 7.0$ Hz, 3H); ^{13}C NMR (150 MHz, $CDCl_3$, 37 °C) δ 171.4, 158.4, 156.0, 136.9, 131.8, 116.5, 116.3, 111.3, 68.1, 42.6, 38.4, 31.8, 29.4, 29.3, 29.2, 26.1, 22.6, 20.4, 14.0, 13.5, 11.9; HRMS (EI) calcd for $C_{27}H_{36}NO_3$: 411.2773, found 411.2776.

***N,N*-Diethyl-4-(methoxymethoxy)-2'-methyl-4'-(octyloxy)biphenyl-2-carboxamide**

(3.8)

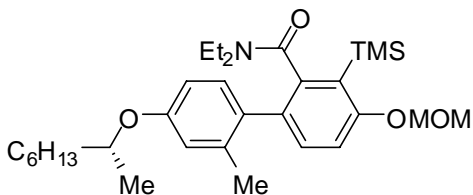


A solution of **3.12** (1.4 g, 3.3 mmol) in THF (10 mL) was added to freshly washed (hexanes) NaH (60% in mineral oil, 0.40 g, 9.9 mmol, 3.0 equiv) by hexanes.

After 10 min, MOMCl (0.32 g, 3.9 mmol, 1.2 equiv) was added. The mixture was stirred for 1.5 h, neutralized dropwise with satd NH₄Cl (10 mL) and extracted with CH₂Cl₂ (20 mL × 2). The combined organic layer was washed with brine, dried (Na₂SO₄) and concentrated under reduced pressure. Purification by flash column chromatography on silica gel (20% EtOAc/hexanes) gave 1.5 g of **3.8** (99%) as a colorless oil: IR (thin film) 1634 cm⁻¹; ¹H NMR (400 MHz, CD₃Cl) δ 7.20-6.96 (m, 4H), 6.75 (d, *J* = 2.2 Hz, 1H), 6.72-6.61 (m, 1H), 5.30-5.09 (m, 2H), 3.93 (t, *J* = 6.6 Hz, 2H), 3.84-3.59 (m, 1H), 3.50 (s, 3H), 3.37-2.55 (m, 3H), 2.18 (s, 3H), 1.81-1.72 (m, 2H), 1.51-1.39 (m, 2H), 1.38-1.22 (m, 8H), 0.97-0.84 (m, 6H), 0.75 (t, *J* = 7.1 Hz, 3H); ¹³C NMR (100 MHz, CD₃Cl) δ 169.8, 158.4, 156.2, 138.5, 131.8, 116.2, 115.9, 114.0, 111.1, 94.5, 67.9, 56.0, 42.3, 37.9, 31.8, 29.3, 29.3, 29.2, 26.0, 22.6, 20.5, 14.1, 13.6, 11.9; HRMS (EI) calcd for C₂₈H₄₁NO₄: 455.3036, found 455.3020.

(*R*)-*N,N*-Diethyl-4-(methoxymethoxy)-2'-methyl-4'-(oct-2-yloxy)-3-

(trimethylsilyl)biphenyl-2-carboxamide (3.13).

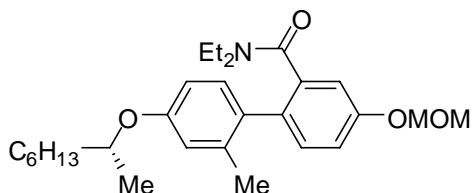


To solution of *N,N*-Diethyl-3-(methoxymethoxy)-6-(4,4,5,5-tetramethyl-1,3,2-dioxaborolan-2-yl)-2-

(trimethylsilyl)benzamide **3.6** (0.56 g, 1.3 mmol) in DME (10 mL, degassed) in a glove box were added sequentially (*R*)-1-bromo-2-methyl-4-(oct-2-yloxy)benzene **2.10e** (0.46 g, 1.5 mmol, 1.2 equiv), Pd(PPh₃)₄ (59 mg, 4 mmol%) and K₂CO₃ (1.0 M aq solution, 3.8 mL, 3.8 mmol, 3.0 equiv). The mixture was heated to reflux and stirred under Ar for 14 h. After cooling to rt, the reaction mixture was quenched with saturated NH₄Cl (15 mL) and concentrated under reduced pressure. The resulting residue was extracted with CH₂Cl₂ (10 mL × 3). The combined organic layer was washed with brine, dried (Na₂SO₄), and concentrated under reduced pressure to afford a brown oil. Purification by flash column chromatography on silica gel (20% EtOAc/hexanes) and recrystallization (CH₂Cl₂/hexanes) gave 0.51 g (76%) of **3.13** as a colorless solid which was shown to be a mixture of diastereomers: mp 82-83 °C; IR (thin film) 1636 cm⁻¹; ¹H NMR (400 MHz, CDCl₃) δ 7.33-6.88 (m, 3H), 6.78-6.69 (m, 1H), 6.68-6.59 (m, 1H), 5.26-5.17 (m, 2H), 4.36-4.28 (m, 1H), 3.83-3.71 (m, 1H), 3.55-3.48 (m, 3H), 3.24-2.47 (m, 3H), 2.22-2.06 (m, 3H), 1.77-1.64 (m, 1H), 1.59-1.49 (m, 1H), 1.48-1.22 (m, 11H), 1.02-0.83 (m, 6H), 0.65-0.43 (m, 3H), 0.32-0.28 (m, 9H); ¹³C NMR (100 MHz, CDCl₃) 169.5, 169.3, 161.8, 161.7, 157.6, 157.3, 157.2, 143.6, 143.4, 140.1, 136.6, 136.6, 133.4, 132.7, 132.3, 132.2, 130.9, 130.4, 130.0, 125.0, 124.2, 117.9, 117.8, 116.8, 116.7, 112.0, 111.9, 111.8, 94.3, 73.8, 73.7, 73.7, 56.3, 56.2, 42.4, 42.3, 37.5, 37.0, 36.6, 36.5, 36.3, 31.8, 29.3, 25.5, 22.6, 20.8, 20.5, 19.9, 19.8, 19.7, 19.6, 14.1, 12.9, 11.6, 11.0, 0.8; ¹H NMR (400 MHz, DMSO, 67 °C) δ 7.20-6.60 (m, 5H), 5.27-5.21 (m, 2H), 4.42-4.33 (m, 1H), 3.63-3.52 (m, 1H), 3.47 (s, 3H), 3.13-3.00 (m, 1H), 2.89-2.56 (m, 2H), 2.08 (s, 3H), 1.72-1.59 (m, 1H), 1.59-1.48 (m, 1H), 1.47-1.17 (m, 11H), 0.87 (t, *J* = 6.8 Hz, 6H), 0.52 (s, 3H), 0.26 (s, 9H); ¹³C NMR (100 MHz, DMSO, 67 °C) δ 168.2, 160.8, 156.7, 143.1, 116.7, 111.6, 111.5, 93.9,

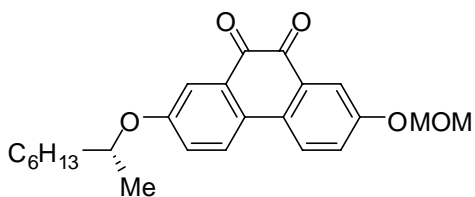
72.9, 55.5, 41.4, 36.3, 35.5, 35.4, 30.7, 28.0, 24.3, 21.4, 19.7, 19.2, 19.1, 13.2, 12.1, 10.7, 0.4; HRMS (EI) calcd for C₃₂H₄₉NO₄Si 527.3431, found 527.3442.

(R)-N,N-Diethyl-4-(methoxymethoxy)-2'-methyl-4'-(oct-2-yloxy)biphenyl-2-carboxamide (3.14).



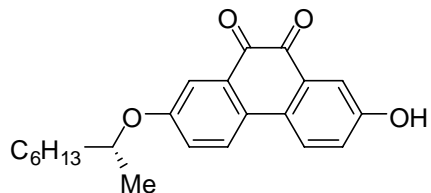
To solution of **3.13** (0.46 g, 0.87 mmol) in THF (7 mL) was added TBAF (1.0 M solution in THF, 2.6 mL, 2.6 mmol 3.0 equiv) at rt. After stirring for 12 h, the reaction mixture was concentrated under reduced pressure. The resulting mixture was diluted with satd NH₄Cl (30 mL) and extracted with CH₂Cl₂ (10 mL × 3). The combined organic layer was washed with brine, dried (Na₂SO₄), and concentrated under reduced pressure to afford a brown solid. Purification by flash column chromatography on silica gel (20-30% EtOAc/hexanes) and recrystallization (CH₂Cl₂/hexanes) gave 0.31 g (83%) of **3.14** as a colorless solid: mp 190-191 °C; IR (thin film) 1635 cm⁻¹; ¹H NMR (400 MHz, CDCl₃) δ 7.23-6.96 (m, 4H), 6.74 (d, *J* = 2.3 Hz, 1H), 6.65 (d, *J* = 8.2 Hz, 1H), 5.31-5.08 (m, 2H), 4.37-4.27 (m, 1H), 3.87-3.66 (m, 1H), 3.49 (s, 3H), 3.35-2.58 (m, 3H), 2.17 (s, 3H), 1.77-1.65 (m, 1H), 1.58-1.48 (m, 1H), 1.46-1.20 (m, 11H), 0.98-0.80 (m, 6H), 0.72 (t, *J* = 7.0 Hz, 3H); ¹³C NMR (100 MHz, CDCl₃) δ 169.8, 157.5, 156.2, 138.5, 131.7, 117.6, 115.9, 114.0, 112.2, 94.5, 73.7, 56.0, 42.2, 37.8, 36.4, 31.8, 29.2, 25.5, 22.5, 20.5, 19.7, 14.0, 13.6, 11.8; HRMS (EI) calcd for C₂₈H₄₁NO₄ 455.3036, found 455.3014.

(R)-2-(Methoxymethoxy)-7-(oct-2-yloxy)phenanthrene-9,10-dione (3.16).



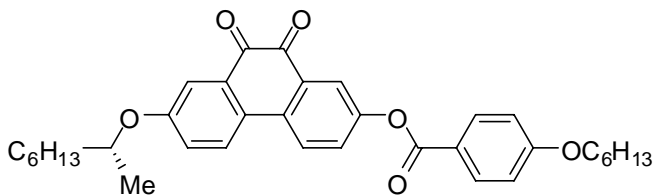
To a solution of **3.14** (0.25 g, 0.55 mmol) in THF (6 mL) under Ar at -5 to 0 °C was added freshly prepared LDA (1.0 M solution in THF, 2.7 mL, 2.7 mmol, 5.0 equiv) dropwise. The mixture was allowed to warm up to rt over 30 min and neutralized with satd NH₄Cl (10 mL). The whole was concentrated under reduced pressure and extracted with CH₂Cl₂ (15 mL × 2). The combined organic layer was washed with brine, dried (Na₂SO₄), and concentrated under reduced pressure to afford a yellow solid. Without further purification, the resulting mixture was dissolved in acetone (30 mL), CH₂Cl₂ (30 mL), and H₂O (60 mL). To the solution were added sequentially NaHCO₃ (6.2 g) and Oxone (4.8 g), and the whole was stirred for 1 h. The resulting mixture was diluted with satd NH₄Cl (30 mL) and extracted with CH₂Cl₂ (10 mL × 3). The combined organic layer was washed with brine, dried (Na₂SO₄), and concentrated under reduced pressure. Purification by flash column chromatography on silica gel (20-30% EtOAc/hexanes) and recrystallization (CH₂Cl₂/hexanes) gave 0.21 g (95%) of **3.16** as a red solid: mp 62-63 °C (EtOAc/hexanes); IR (thin film) 1676 cm⁻¹; ¹H NMR (400 MHz, CDCl₃) δ 7.79-7.74 (m, 2H), 7.72 (d, *J* = 2.8 Hz, 1H), 7.56 (d, *J* = 2.8 Hz, 1H), 7.30 (dd, *J* = 8.8, 2.8 Hz, 1H), 7.17 (dd, *J* = 8.8, 2.9 Hz, 1H), 5.24 (s, 2H), 4.54-4.43 (m, 1H), 3.49 (s, 3H), 1.81-1.68 (m, 1H), 1.65-1.54 (m, 1H), 1.51-1.20 (m, 11H), 0.88 (t, *J* = 6.8 Hz, 3H); ¹³C NMR (100 MHz, CDCl₃) δ 180.4, 180.3, 158.6, 157.2, 131.3, 131.1, 130.5, 128.9, 125.3, 125.2, 125.0, 124.6, 116.3, 114.5, 94.3, 74.4, 56.3, 36.3, 31.8, 29.2, 25.4, 22.6, 19.6, 14.1; HRMS (EI) calcd for C₂₄H₂₈O₅ 396.1937, found 396.1931.

(R)-2-Hydroxy-7-(oct-2-yloxy)phenanthrene-9,10-dione (3.17).



To a solution of **3.16** (0.16 g, 0.40 mmol) in 2-propanol (3 mL) was added HCl (6.0 M, 0.40 mL, 2.4 mmol, 6.0 equiv). The mixture was heated to 60 °C for 4 h, diluted with satd NH₄Cl (5 mL) and concentrated under reduced pressure. The residue was extracted with CH₂Cl₂ (5 mL × 2). The combined organic layer was washed with brine, dried (Na₂SO₄), and concentrated under reduced pressure to give a red solid. Purification by flash column chromatography on silica gel (30-40% EtOAc/hexanes) and recrystallization (EtOAc/hexanes) gave 0.14 g (96%) of **3.17** as a red solid: mp 124-125 °C; IR (thin film) 3374, 1667 cm⁻¹; ¹H NMR (600 MHz, CD₂Cl₂) δ 7.79 (d, *J* = 8.7 Hz, 2H), 7.53 (d, *J* = 2.6 Hz, 1H), 7.50 (d, *J* = 2.5 Hz, 1H), 7.21-7.15 (m, 2H), 5.69 (br, 1H), 4.53-4.47 (m, 1H), 1.80-1.70 (m, 1H), 1.65-1.59 (m, 1H), 1.51-1.22 (m, 11H), 0.88 (t, *J* = 6.7 Hz, 3H); ¹³C NMR (150 MHz, CD₂Cl₂) δ 181.1 (2C), 159.4, 156.9, 132.1, 132.0, 130.4, 129.7, 126.3, 126.0, 125.6, 124.4, 116.2, 115.3, 75.2, 37.1, 32.5, 30.0, 26.1, 23.4, 20.1, 14.6; HRMS (EI) calcd for C₂₂H₂₄O₄ 352.1675, found 352.1675.

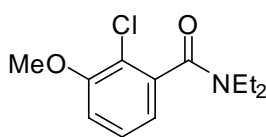
(R)-7-(Oct-2-yloxy)-9,10-dioxo-9,10-dihydrophenanthren-2-yl 4-hexyloxybenzoate (3.1a).



To a solution of **3.17** (0.11 g, 0.34 mmol) in CH₂Cl₂ (4 mL) were added 4-hexyloxybenzoic acid (91 mg, 0.40 mmol, 1.2 equiv), DCC (84 mg, 0.40 mmol, 1.2 equiv) and DMAP (6 mg). The

mixture was stirred for 10 h under Ar at rt, neutralized with satd NH₄Cl (5 mL) and extracted with CH₂Cl₂ (10 mL × 2). The combined organic layer was washed with brine, dried (Na₂SO₄), and concentrated under reduced pressure to afford a red solid. Purification by flash column chromatography on silica gel (10% hexanes/toluene) and recrystallization (hexanes/toluene) gave 0.10 g (99%) of **3.1a** as a red solid: mp 125–127 °C; IR (thin film) 1733 cm⁻¹; ¹H NMR (400 MHz, CDCl₃) δ 8.13 (d, *J* = 8.9 Hz, 2H), 7.94 (d, *J* = 2.6 Hz, 1H), 7.91 (d, *J* = 8.8 Hz, 1H), 7.85 (d, *J* = 8.9 Hz, 1H), 7.61 (d, *J* = 2.8 Hz, 1H), 7.54 (dd, *J* = 8.7, 2.6 Hz, 1H), 7.21 (dd, *J* = 8.8, 2.8 Hz, 1H), 6.98 (d, *J* = 8.9 Hz, 2H), 4.56-4.47 (m, 1H), 4.05 (t, *J* = 6.5 Hz, 2H), 1.91-1.69 (m, 3H), 1.68-1.59 (m, 1H), 1.54-1.22 (m, 17H), 0.97-0.84 (m, 6H); ¹³C NMR (100 MHz, CDCl₃) δ 180.0, 179.8, 164.4, 163.9, 159.2, 151.1, 134.0, 132.4, 131.9, 131.0, 129.8, 128.1, 125.8, 125.1, 124.8, 123.1, 120.7, 114.6, 114.4, 74.5, 68.4, 36.3, 31.8, 31.5, 29.2, 29.0, 25.6, 25.4, 22.6, 19.6, 14.1, 14.0; HRMS (EI) calcd for C₃₅H₄₀O₆ 556.2825, found 556.2802.

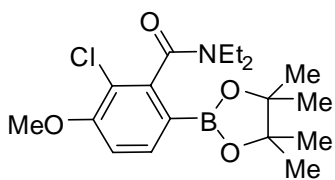
2-Chloro-*N,N*-diethyl-3-methoxybenzamide (**3.18**).



To a solution of *N,N*-diethyl-3-methoxybenzamide **2.2** (4.0 g, 19 mmol) and TMEDA (4.4 mL, 29 mmol, 1.5 equiv) in THF (190 mL) at -75 to -80 °C under Ar was added *s*-BuLi (1.0 M solution in hexanes, 29 mL, 29 mmol, 1.5 equiv) dropwise. After stirring for 1 h, Cl₃CCl₃ (1.0 M solution in THF, 29 mL, 29 mmol 1.5 equiv) was added by dropwise addition. The mixture was allowed to warm up to rt over for 4 h and neutralized with satd NH₄Cl (45 mL) and concentrated under reduced pressure. The residue was extracted with CH₂Cl₂ (20 mL × 3). The combined organic layer was washed with brine and dried (Na₂SO₄), and concentrated

under reduced pressure to give a brown oil. Purification by flash column chromatography on silica gel (20-30% EtOAc/hexane) gave 3.7 g (80%) of **3.18** as a light yellow oil: ^1H NMR (600 MHz, CDCl_3) δ 7.22 (t, $J = 7.9$ Hz, 1H), 6.88 (dd, $J = 8.3, 0.9$ Hz, 1H), 6.82 (dd, $J = 7.6, 1.2$ Hz, 1H), 3.86 (s, 3H), 3.76-3.68 (m, 1H), 3.38-3.31 (m, 1H), 3.16-3.05 (m, 2H), 1.22 (t, $J = 7.3$ Hz, 3H), 1.01 (t, $J = 7.1$ Hz, 3H); ^{13}C NMR (150 MHz, CDCl_3) δ 170.9, 167.4, 155.1, 138.1, 127.8, 118.9, 111.8, 56.2, 42.5, 38.8, 13.8, 12.5; HRMS (EI) calcd for $\text{C}_{12}\text{H}_{16}\text{NO}_2\text{Cl}$ 241.0870, found 241.0867.

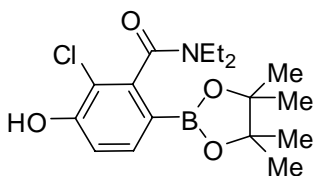
2-Chloro-*N,N*-diethyl-3-methoxy-6-(4,4,5,5-tetramethyl-1,3,2-dioxaborolan-2-yl)benzamide (3.20)



To a solution of **3.18** (0.20 g, 0.83 mmol), TMEDA (0.14 mg, 1.2 mmol, 1.5 equiv) in THF (10 mL) at -75 to -80 °C under an Ar atmosphere was added dropwise *s*-BuLi (0.90 M solution in hexanes, 1.4 mL, 1.2 mmol, 1.5 equiv). After stirring for 1 h, $\text{B}(\text{OMe})_3$ (0.13 g, 0.14 mL, 1.2 mmol, 1.5 equiv) was added dropwise. The mixture was allowed to warm to rt over 4 h, neutralized with a solution of satd NH_4Cl (10 mL) and the residue was extracted with CH_2Cl_2 (10 mL x 2). The combined organic layer was washed with brine, dried (NaSO_4), and concentrated under reduced pressure to afford a yellow oil. Without further purification THF (10 mL) was added and the resulting solution was treated with pinacol (0.20 g, 1.7 mmol, 2.0 equiv). The mixture was stirred for 2 h and was concentrated under reduced pressure to give a yellow oil. Purification by flash column chromatography on silica gel (40% EtOAc/hexanes) and recrystallization (hexanes) gave 0.23 g (76%) of **3.20** as a colorless crystalline solid: mp 89-91 °C; IR

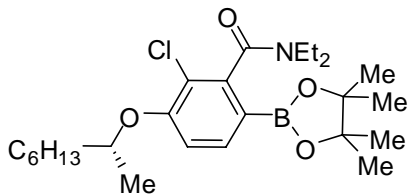
(thin film) 1645 cm^{-1} ; ^1H NMR (600 MHz, CDCl_3) δ 7.72 (d, $J = 8.3$ Hz, 1H), 6.87 (d, $J = 8.3$ Hz, 1H), 3.91 (s, 3H), 3.74-3.43 (m, 2H), 3.18-3.03 (m, 2H), 1.30 (t, $J = 7.2$ Hz, 3H), 1.27 (s, 12H), 1.05 (t, $J = 7.2$ Hz, 3H); ^{13}C NMR (150 MHz, CDCl_3) δ 167.4, 157.2, 143.9, 135.8, 119.0, 110.5, 83.8, 56.1, 42.8, 38.7, 24.7, 13.3, 12.4; HRMS (EI) calcd for $\text{C}_{18}\text{H}_{26}\text{NO}_4\text{ClB}$ 366.1643, found 366.1631.

2-Chloro-*N,N*-diethyl-3-hydroxy-6-(4,4,5,5-tetramethyl-1,3,2-dioxaborolan-2-yl)benzamide (3.22).



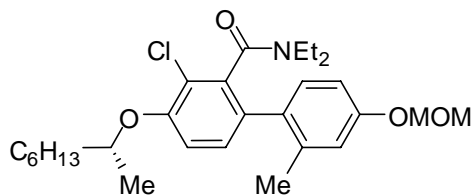
To a solution of **3.20** (0.55 g, 1.5 mmol) in CH_2Cl_2 (anhydrous, 10 mL) at -65 to -78 $^\circ\text{C}$ under an Ar atmosphere was added dropwise freshly prepared BBr_3 (1.0 M solution in CH_2Cl_2 , 4.5 mL, 4.5 mmol, 3 equiv). The mixture was allowed to warm up to rt and stirred over 30 min. Pinacol (0.80 mg, 6.8 mmol, 4.7 equiv) was added to the solution and the whole was stirred for 3 h, concentrated under reduced pressure to afford a brown solid. Purification by washing with 1:1 solution of EtOAc/hexanes and recrystallization (CH_2Cl_2) gave 0.41 g (78%) of **3.22** as a colorless solid: mp 234-237 $^\circ\text{C}$; IR (thin film) 3447, 1624 cm^{-1} ; ^1H NMR (400 MHz, CDCl_3) δ 7.64 (d, $J = 8.2$ Hz, 1H), 6.95 (d, $J = 8.2$ Hz, 1H), 6.39 (s, 1H), 3.80-3.34 (m, 2H), 3.22-3.04 (m, 2H), 1.31 (t, $J = 7.2$ Hz, 3H), 1.28 (s, 12H), 1.06 (t, $J = 7.2$ Hz, 3H); ^{13}C NMR (100 MHz, CDCl_3) δ 167.5, 154.1, 143.1, 136.1, 116.8, 115.4, 83.9, 43.0, 39.0, 24.8, 13.4, 12.5; HRMS (EI) calcd for $\text{C}_{17}\text{H}_{24}\text{BNO}_4\text{Cl}$ 352.1487, found 352.1500.

(R)-2-Chloro-N,N-diethyl-3-(oct-2-yloxy)-6-(4,4,5,5-tetramethyl-1,3,2-dioxaborolan-2-yl)benzamide (3.23).



To a solution of **3.22** (0.58 g, 1.6 mmol) in CH₂Cl₂ (16 mL) were added sequentially (*S*)-octan-2-ol (0.24 g, 1.9 mmol, 1.5 equiv), DIAD (0.49 g, 2.4 mmol, 1.5 equiv) and Ph₃P (0.53 g, 2.0 mmol, 1.3 equiv). After stirring for 12 h under Ar at rt, the reaction mixture was diluted with satd NH₄Cl (20 mL) and concentrated under reduced pressure. The residue was extracted with CH₂Cl₂ (15 mL × 3) and the combined organic layer was washed with brine, dried (Na₂SO₄), and concentrated under reduced pressure to afford a yellow oil. Purification by flash column chromatography on silica gel (20-30% EtOAc/hexanes) gave 0.45 g (59%) of **3.23** as a colorless oil: IR (thin film) 1717 cm⁻¹; ¹H NMR (500 MHz, CD₃Cl) δ 7.67 (d, *J* = 8.3 Hz, 1H), 6.85 (d, *J* = 8.4 Hz, 1H), 4.47-4.39 (m, 1H), 3.73-3.42 (m, 2H), 3.19-3.06 (m, 2H), 1.85-1.71 (m, 1H), 1.66-1.54 (m, 1H), 1.51-1.20 (m, 26H), 1.06 (t, *J* = 7.1 Hz, 3H), 0.87 (t, *J* = 6.5 Hz, 3H); ¹³C NMR (125 MHz, CDCl₃) δ 167.7, 156.3, 144.2, 135.5, 120.3, 113.3, 83.8, 75.7, 42.9, 38.8, 36.3, 31.7, 29.2, 25.3, 24.8, 22.6, 19.7, 14.0, 13.4, 12.5; HRMS (EI) calcd for C₂₅H₄₁NO₄BCl 465.2817, found 465.2803.

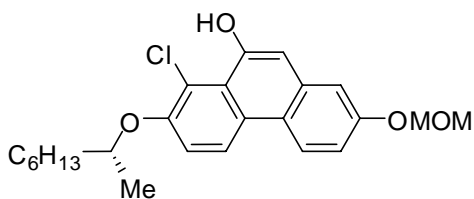
(R)-3-Chloro-N,N-diethyl-4'-(methoxymethoxy)-2'-methyl-4-(oct-2-yloxy)biphenyl-2-carboxamide (3.24).



To a solution of **3.23** (0.40 g, 0.86 mmol) in DME (10 mL, degassed) in a glove box were added sequentially 1-bromo-4-(methoxymethoxy)-2-

methylbenzene **2.10b** (0.24 g, 1.0 mmol, 1.2 equiv), (PPh₃)₄Pd (35 mg, 3.5 mol%), and K₂CO₃ (1.0 M aq solution, 2.6 mL, 2.6 mmol, 3.0 equiv). The mixture was heated to reflux and stirred under Ar for 14 h. After cooling to rt, the reaction mixture was quenched with saturated NH₄Cl (15 mL) and concentrated under reduced pressure. The resulting residue was extracted with CH₂Cl₂ (10 mL × 3) and the combined organic layer was washed with brine, dried (Na₂SO₄), and concentrated under reduced pressure to afford a brown oil. Purification by flash column chromatography on silica gel (20% EtOAc/hexanes) gave 0.23 g (53%) of **3.24** as a colorless oil which was shown to be a mixture of diastereomers: IR (thin film) 1635 cm⁻¹; ¹H NMR (600 MHz, CD₂Cl₂, °C) δ 7.28-6.73 (m, 5H), 5.18-5.11 (m, 2H), 4.49-4.40 (m, 1H), 3.68-3.53 (m, 1H), 3.42 (s, 3H), 3.28-2.66 (m, 3H), 2.21-2.03 (m, 3H), 1.85-1.75 (m, 1H), 1.68-1.58 (m, 1H), 1.53-1.20 (m, 11H), 1.11-0.81 (m, 6H), 0.72-0.55 (m, 3H); ¹³C NMR (150 MHz, CD₂Cl₂, 5 °C) δ 166.5, 156.9, 153.4, 132.6, 130.5, 130.1, 129.6, 117.8, 117.6, 114.5, 114.0, 113.4, 112.7, 94.6, 76.3, 56.1, 54.0, 42.6, 37.7, 36.8, 32.3, 29.7, 25.8, 23.1, 20.7, 20.0, 14.4, 13.8, 11.7; HRMS (EI) calcd for C₂₈H₄₀NO₄Cl 489.2646, found 489.2632.

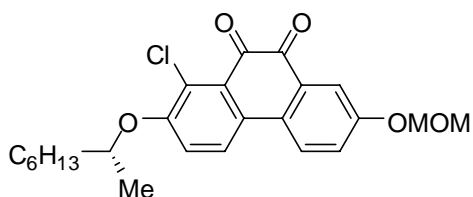
(R)-8-Chloro-2-(methoxymethoxy)-7-(oct-2-yloxy)phenanthren-9-ol (3.25)



To a solution of **3.24** (0.25 g, 0.50 mmol) in THF (3 mL) under Ar at -5 to 0 °C was added freshly prepared LDA (1.0 M solution in THF, 2.5 mL, 2.5 mmol, 5.0 equiv) dropwise. The mixture was allowed to warm up to rt over 30 min and neutralized with satd NH₄Cl (10 mL). The whole was concentrated under reduced pressure and extracted with CH₂Cl₂ (15 mL × 2).

The combined organic layer was washed with brine, dried (Na₂SO₄), and concentrated under reduced pressure to afford a brown solid. Purification by flash column chromatography on silica gel (40% EtOAc/hexanes) and recrystallization (CH₂Cl₂/hexanes) gave 0.21 g of **3.25** (96%) as a colorless solid: mp: 96-97 °C; IR (thin film) 3502, 1672 cm⁻¹; ¹H NMR (500 MHz, CDCl₃) δ 8.56 (d, *J* = 9.1 Hz, 1H), 8.53 (s, 1H), 8.41 (d, *J* = 9.1 Hz, 1H), 7.40-7.34 (m, 2H), 7.29-7.25 (m, 2H), 5.40 (s, 2H), 4.65-4.57 (m, 1H), 3.63 (s, 3H), 2.00-1.89 (m, 1H), 1.81-1.72 (m, 1H), 1.67-1.33 (m, 11H), 0.99 (t, *J* = 6.8 Hz, 3H); ¹³C NMR (125 MHz, CDCl₃) δ 155.9, 151.8, 150.5, 133.4, 127.8, 123.8, 123.2, 121.7, 121.1, 116.6, 115.8, 115.7, 110.8, 110.2, 94.5, 76.9, 56.1, 36.5, 31.7, 29.2, 25.4, 22.6, 19.9, 14.0; HRMS (EI) calcd for C₂₄H₂₉O₄Cl 416.1754, found 416.1744.

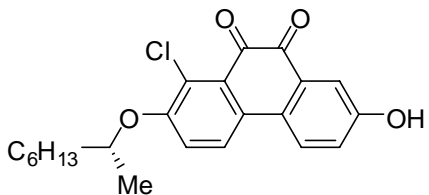
(R)-1-Chloro-7-(methoxymethoxy)-2-(oct-2-yloxy)phenanthrene-9,10-dione (3.26).



To a solution of **3.25** (0.16 mg, 0.39 mmol), NaHCO₃ (9.2 g), acetone (26 mL), CH₂Cl₂ (26 mL) and H₂O (52 mL) was slowly added Oxone (7.0 g). After stirring for 1 h, the whole was concentrated under reduced pressure. The residue was extracted with CH₂Cl₂ (15 mL × 2). The combined organic layer was washed with brine, dried (Na₂SO₄), and concentrated under reduced pressure to afford a red solid. Purification by flash column chromatography on silica gel (40% EtOAc/hexanes) and recrystallization (CH₂Cl₂) gave 168 mg (99%) of **3.26** as a red solid: mp 108-109 °C; IR (thin film) 1671 cm⁻¹; ¹H NMR (400 MHz, CD₂Cl₂) δ 7.89-7.75 (m, 2H), 7.62 (d, *J* = 2.8 Hz, 1H), 7.34 (dd, *J* = 8.8, 2.8

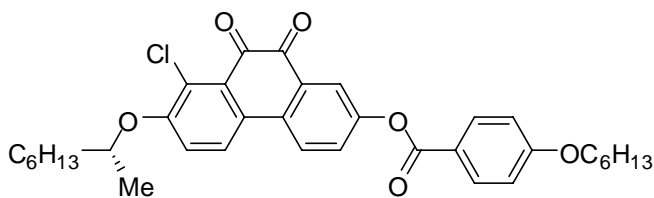
Hz, 1H), 7.23 (d, $J = 8.9$ Hz, 1H), 5.25 (s, 2H), 4.52-4.44 (m, 1H), 3.48 (s, 3H), 1.90-1.76 (m, 1H), 1.73-1.61 (m, 1H), 1.53-1.22 (m, 11H), 0.88 (t, $J = 6.8$ Hz, 3H); ^{13}C NMR (100 MHz, CD_2Cl_2) δ 180.4, 180.3, 158.6, 157.2, 131.3, 131.1, 130.5, 128.9, 125.3, 125.2, 125.0, 124.6, 116.3, 114.5, 94.3, 74.4, 56.3, 36.3, 31.8, 29.2, 25.4, 22.6, 19.6, 14.1; HRMS (EI) calcd for $\text{C}_{24}\text{H}_{27}\text{O}_5\text{Cl}$ 430.1547, found 430.1535.

(R)-1-Chloro-7-hydroxy-2-(oct-2-yloxy)phenanthrene-9,10-dione (3.27).



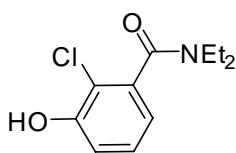
A solution of **3.26** (0.060 g, 0.15 mmol) in 2-propanol (2 mL) was added HCl (6.0 M, 0.15 mL, 0.91 mmol, 6.0 equiv). The mixture was heated to 60 °C and stirred for 4 h, diluted with satd NH_4Cl (5 mL) and the whole was extracted with CH_2Cl_2 (5 mL \times 2). The combined organic layer was washed with brine, dried (Na_2SO_4), concentrated under reduced pressure to give a red solid. Purification by flash column chromatography on silica gel (40-50% EtOAc/hexanes) and recrystallization (EtOAc/hexanes) gave 52 mg (98%) of **3.27** as a red solid: mp 121-122 °C; IR (thin film) 3350, 1674 cm^{-1} ; ^1H NMR (500 MHz, CD_2Cl_2) δ 7.81 (d, $J = 8.78$ Hz, 1H), 7.78 (d, $J = 8.95$ Hz, 1H), 7.46 (d, $J = 2.7$ Hz, 1H), 7.24-7.18 (m, 2H), 5.55 (br, 1H), 4.51-4.44 (m, 1H), 1.86-1.78 (m, 1H), 1.71-1.62 (m, 1H), 1.54-1.24 (m, 11H), 0.88 (t, $J = 6.9$ Hz, 3H); ^{13}C NMR (100 MHz, CDCl_3) δ 181.4, 181.3, 156.7, 154.9, 130.6, 130.4, 129.1, 128.0, 127.9, 125.9, 124.4, 123.1, 120.8, 115.3, 36.3, 31.7, 29.2, 25.3, 22.6, 19.7, 14.1; HRMS (EI) calcd for $\text{C}_{22}\text{H}_{23}\text{O}_4\text{Cl}$ 386.1285, found 386.1276.

(R)-8-Chloro-7-(oct-2-yloxy)-9,10-dioxo-9,10-dihydrophenanthren-2-yl 4-(hexyloxy)benzoate (3.1b).



To a solution of **3.27** (0.070 g, 0.18 mmol) in CH₂Cl₂ (2 mL) were added sequentially 4-hexyloxybenzoic acid (45 mg, 0.22 mmol, 1.2 equiv), DCC (45 mg, 0.22 mmol, 1.2 equiv) and DMAP (6 mg). The mixture was stirred for 10 h under Ar at rt and concentrated under reduced pressure to afford a red solid. Purification by flash column chromatography on silica gel (10% hexanes/toluene) and recrystallization (hexanes/toluene) gave 0.10 g (99%) of **3.1b** as a red solid: mp 199-200 °C; IR (thin film) 1727, 1674 cm⁻¹; ¹H NMR (400 MHz, CDCl₃) δ 8.13 (d, *J* = 8.9 Hz, 2H), 7.93 (d, *J* = 8.9 Hz, 1H), 7.90 (d, *J* = 2.6 Hz, 1H), 7.83 (d, *J* = 9.1 Hz, 1H), 7.57 (dd, *J*₁ = 8.7, 2.6 Hz, 1H), 7.22 (d, *J* = 9.0 Hz, 1H), 6.98 (d, *J* = 9.0 Hz, 2H), 4.55-4.42 (m, 1H), 4.06 (t, *J* = 6.6 Hz, 2H), 1.90-1.78 (m, 3H), 1.73-1.61 (m, 1H), 1.54-1.44 (m, 3H), 1.44-1.25 (m, 14H), 0.97-0.84 (m, 6H); ¹³C NMR (100 MHz, CDCl₃) δ 181.3, 180.9, 164.4, 163.9, 155.7, 151.4, 133.7, 132.4, 130.8, 129.9, 129.4, 129.0, 128.1, 125.3, 123.7, 122.399, 120.618, 120.132, 114.447, 68.399, 36.256, 31.730, 31.537, 29.191, 29.041, 25.7, 25.3, 22.6, 22.6, 19.7, 14.1, 14.0; HRMS (EI) calcd for C₃₅H₃₉O₆Cl 590.2435, found 590.2414.

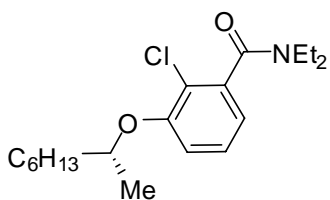
2-Chloro-*N,N*-diethyl-3-hydroxybenzamide (3.28).



To a solution of **3.18** (1.6 g, 6.6 mmol) in CH₂Cl₂ (anhydrous, 15 mL) at -65 to -78 °C under an Ar atmosphere was added dropwise freshly prepared BBr₃ (1.0 M solution in CH₂Cl₂, 20 mL, 20 mmol,

3.0 equiv). The mixture was allowed to warm up to rt and stirred over 30 min, quenched with satd NH₄Cl (30 mL) and extracted with CH₂Cl₂ (20 mL × 3). The combined organic layer was washed with brine, dried (Na₂SO₄), and concentrated under reduced pressure to give a brown solid. Purification by flash column chromatography on silica gel (50-60% EtOAc/hexanes) and recrystallization (EtOAc/hexanes) gave 1.2 g (83%) of **3.19** as a colorless crystals: mp 146-147 °C (EtOAc/hexanes); IR (thin film) 3229, 1717 cm⁻¹; ¹H NMR (600 MHz, CDCl₃) δ 7.14 (t, *J* = 7.9 Hz, 1H), 6.96 (dd, *J* = 8.2, 1.4 Hz, 1H), 6.79 (dd, *J* = 7.5, 1.4 Hz, 1H), 6.53 (br, 1H), 3.82-3.65 (m, 1H), 3.51-3.31 (m, 1H), 3.21-3.11 (m, 2H), 1.27 (t, *J* = 7.1 Hz, 3H), 1.06 (t, *J* = 7.1 Hz, 3H); ¹³C NMR (600 MHz, CDCl₃) δ 167.7, 152.2, 137.1, 128.2, 118.8, 116.6, 116.6, 42.8, 39.2, 13.9, 12.6; HRMS (EI) calcd for C₁₁H₁₄NO₂Cl 227.0713, found 227.0708.

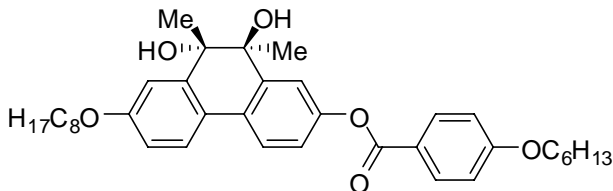
(*R*)-2-Chloro-*N,N*-diethyl-3-(octan-2-yloxy)benzamide (3.29).



A solution of **3.28** (0.85 g, 3.7 mmol) in CH₂Cl₂ (37 mL) were added (*S*)-octan-2-ol (0.54 g, 0.65 mL, 4.1 mmol, 1.1 equiv), DIAD (1.1 g, 1.0 mL 5.6 mmol, 1.5 equiv) and Ph₃P (1.2 g, 4.5 mmol). After stirring under Ar for 12 h, the reaction mixture was diluted with satd NH₄Cl (20 mL) and extracted with CH₂Cl₂ (15 mL × 3). The combined organic layer was washed with brine and dried (Na₂SO₄), and concentrated under reduced pressure to afford a yellow oil. Purification by flash column chromatography on silica gel (20-30% EtOAc/hexanes) gave 0.94 g (74%) of **3.29** as a colorless oil: IR (thin film) 1717 cm⁻¹; ¹H NMR (400 MHz, CD₃Cl) δ 7.20 (t, *J* = 7.9 Hz, 1H), 6.82 (dd, *J* = 7.5, 1.2 Hz, 1H), 6.90 (d, *J* = 8.2 Hz, 1H), 4.44-4.32 (m, 1H), 3.83-3.71 (m, 1H), 3.45-3.29 (m,

1H), 3.19-3.10 (m, 2H), 1.87-1.71 (m, 1H), 1.69-1.53 (m, 1H), 1.52-1.17 (m, 14H), 1.05 (t, $J = 7.1$ Hz, 3H), 0.91-0.84 (m, 3H); ^{13}C NMR (400 MHz, CDCl_3) δ 167.7, 154.1, 138.3, 127.6, 120.4, 120.2, 118.8, 115.2, 115.0, 76.2, 76.1, 42.6, 38.8, 36.4, 36.3, 31.8, 31.7, 29.2, 29.2, 25.4, 25.3, 22.6, 19.8, 19.6, 14.0, 13.9, 12.6; HRMS (EI) calcd for $\text{C}_{19}\text{H}_{30}\text{NO}_2\text{Cl}$ 339.1965, found 339.1953.

(-)-9,10-Dihydroxy-9,10-dimethyl-7-(octyloxy)-9,10-dihydrophenanthren-2-yl 4-(hexyloxy)benzoate ((-)-4.1).



To a solution of (-)-**2.33** (17 mg, 0.044 mmol) in CH_2Cl_2 (4 mL) were added 4-(hexyloxy)benzoic acid (11 mg, 0.044 mmol, 1 equiv), DCC (11 mg, 0.053 mmol, 1.2 equiv) and DMAP (2 mg). The mixture was stirred for 10 h under Ar at rt, neutralized with satd NH_4Cl (5 mL) and extracted with CH_2Cl_2 (10 mL \times 2). The combined organic layer was washed with brine, dried (Na_2SO_4), and concentrated under reduced pressure to afford a yellow solid. Purification by flash column chromatography on silica gel (10% EtOAc/hexanes) and recrystallization (hexanes) gave 25 mg (94%) of (-)-**4.1** as a colorless solid: mp 42-43 $^\circ\text{C}$; IR (thin film) 3477, 1735 cm^{-1} ; ^1H NMR (500 MHz, CDCl_3) δ 8.15 (d, $J = 8.8$ Hz, 2H), 7.65 (d, $J = 8.5$ Hz, 1H), 7.59 (d, $J = 8.6$ Hz, 1H), 7.52 (d, $J = 2.3$ Hz, 1H), 7.25 (d, $J = 2.4$ Hz, 1H), 7.17 (dd, $J = 8.4, 2.3$ Hz, 1H), 6.97 (d, $J = 8.8$ Hz, 2H), 6.86 (dd, $J = 8.5, 2.4$ Hz, 1H), 4.09-3.99 (m, 4H), 2.41 (d, $J = 4.9$ Hz, 1H), 2.32 (d, $J = 4.1$ Hz, 1H), 1.86-1.77 (m, 4H), 1.54-1.44 (m, 4H), 1.42-1.25 (m, 18H), 0.96-0.86 (m, 6H); ^{13}C NMR (500 MHz, CD_3OD) δ 165.0, 163.5, 159.6, 150.4, 143.8, 143.1, 132.3, 129.5, 125.0, 124.0, 123.7, 121.5,

120.8, 117.3, 114.3, 113.5, 109.7, 77.5, 77.5, 68.3, 68.1, 31.8, 31.5, 29.4, 29.3, 29.2, 29.1,
26.1, 25.7, 24.4, 24.1, 22.7, 22.6, 14.1, 14.0; HRMS (EI) calcd for C₃₇H₄₈O₆ 588.3451,
found 588.3450.

REFERENCES

- ¹ Reinitzer, F. *Monatsh. Chem.* **1888**, *9*, 421.
- ² Lehman, O. *Z. Phys. Chem.* **1889**, *4*, 462.
- ³ McMillan, W. L. *Phys. Rev. A.: Atomic, Molecular, Optical Physics* **1973**, *8*, 1921.
- ⁴ Wulff, A. *Phys. Rev. A.: Atomic, Molecular, Optical Physics* **1975**, *10*, 365.
- ⁵ Bartolino, R.; Douclet, J.; Durand, G. *Ann. Phys.* **1978**, *3*, 389.
- ⁶ Gray G. W.; Hartley, J. B.; Ibbotson, A.; Jones, B. *J. Chem. Soc.* **1955**, 3133.
- ⁷ For a review, see: de Gennes, P. G.; Prost, J. *The Physics of Liquid Crystals*, Oxford University Press, **1996**.
- ⁸ Clark, N. A.; Lagerwall, S. T. *Appl. Phys. Lett.* **1980**, *36*, 899.
- ⁹ Meyer, R. B.; Liebert, L.; Strzelecki, L.; Keller, P. *J. Phys. (Paris) Lett.* **1975**, *36*, L69.
- ¹⁰ Walba, D. M.; Slater, S. C.; Thurmes, W. N.; Clark, N. A.; Handschy, M. A.; Supon, F. *J. Am. Chem. Soc.* **1986**, *108*, 5210.
- ¹¹ Walba, D. M.; Mallouck, T. E., Ed. *Advances in the Synthesis and Reactivity of Solids* JAI Press: Greenwich, CT, **1991**; Vol. 1, pp 173-235.
- ¹² Walba, D. M.; Ros, M. B.; Clark, N. A.; Shao, R.; Johnson, K. M.; Robinson, M. G.; Liu, J. Y.; Doroski, D. *Mol. Cryst. Liq. Cryst.* **1991**, *198*, 51.
- ¹³ Stegemeyer, H.; Meister, R.; Hoffmann, U.; Sprick, A.; Becker, A. *J. Mater. Chem.* **1995**, *5*, 2183
- ¹⁴ Osipov, M. A.; Stegemeyer, H.; Sprick, A. *Phys. Rev. E*, **1996**, *54*, 6387.
- ¹⁵ Lemieux, R. P. *Acc. Chem. Res.* **2001**, *34*, 845.
- ¹⁶ Yang K.; Lemieux, R. P. *Mol. Cryst. Liq. Cryst.* **1995**, *260*, 247.
- ¹⁷ Yang K.; Campbell, B.; Birch, G.; Williams, V. E.; Lemieux, R. P. *J. Am. Chem. Soc.* **1996**, *118*, 9557.
- ¹⁸ Paleos, C. M. Tsiourvas, D. *Angew. Chem. Int. Ed.* **1995**, *34*, 1696.
- ¹⁹ Kato, T.; Frechet, J. M. *J. Am. Chem. Soc.* **1989**, *111*, 8533.
- ²⁰ Pajak, J.; Rospenk, M.; Galewski, Z.; Sobczyk, L. *J. Mol. Struct.* **2004**, *700*, 191.
- ²¹ Kato, T.; Fujishima, A.; Frechet, J. M. *Chem. Lett.* **1990**, 919.
- ²² Kato, T.; Wilson, P. G.; Fujishima, A.; Frechet, J. M. *Chem. Lett.* **1990**, 2002.

-
- ²³ Kato, T.; Adachi, H.; Fujishima, A.; Frechet, J. M. *Chem. Lett.* **1992**, 265.
- ²⁴ Schubert, H.; Hoffmann, S.; Hauschild, J. Z. *Chem.* **1997**, *17*, 414.
- ²⁵ Hildebrant, F.; Schroeter, J. A.; Tschierske, C.; Festag, R.; Kleppinger, R.; Wendorff, J. H. *Angew. Chem.Int. Ed.* **1995**, *34*, 1631.
- ²⁶ Yu, L. J. *Liq. Cryst.* **1993**, *14*, 1303.
- ²⁷ Kihara, H.; Kato, T.; Uryu, T.; Ujiie, S.; Kumar, U.; Frechet, J. M.; Bruce, D. W.; Price, D. J. *Liq. Cryst.* **1996**, *21*, 25.
- ²⁸ Imrie, C.; Loubser, C.; Engelbrecht, P.; McClelland, C. W.; Zheng, Y. *J. Organomet. Chem.* **2003**, *665*, 48.
- ²⁹ Fischer, E.; Helferich, B. *Justus Liebigs Ann. Chem.* **1911**, *383*, 68.
- ³⁰ Noller, C. R.; Rockwell, W. C. *J. Am. Chem. Soc.* **1938**, *60*, 2076.
- ³¹ Pfannemuller, B.; Welte, W.; Chin, E.; Goodby, J. W. *Liq. Cryst.* **1986**, *1*, 357.
- ³² Van Doren H. A.; Van der Geest, R.; De Ruijter, C. F.; Kellogg, R. M.; Wynberg, H.; *Liq. Cryst.* **1990**, *7*, 109.
- ³³ Jeffery, G. A. Wingert, L. M. *Liq. Cryst.* **1992**, *12*, 179.
- ³⁴ Praefcke, K.; Levelut, A. M.; Kohne, B.; Eckert, A. *Liq. Cryst.* **1989**, *6*, 263.
- ³⁵ Praefcke, K.; Kohne, B.; Diele, S.; Pelzl, D.; Kjacr, A. *Liq. Cryst.* **1992**, *11*, 1.
- ³⁶ Van der Meer, B. W.; Vertogen, G. *J. de Phys.* **1979**, *40*, C3-222.
- ³⁷ Takatoh, K.; Sunohara, K.; Sakamoto, M. *Mol. Cryst. Liq. Cryst.* **1988**, *164*, 167.
- ³⁸ Gray, G. W. *J. Chem. Soc.* **1958**, 552.
- ³⁹ Byron, D. J.; Harwood, D. J.; Wilson, R. C. *J. Chem. Soc., Perkin Trans. II* **1983**, 197.
- ⁴⁰ Sienkowska, M. J.; Farrar, J. M.; Zhang, F.; Kusuma, S.; Heiney, P. A.; Kaszynski, P. *J. Mater. Chem.* **2007**, *17*, 1399.
- ⁴¹ Scherowsky, G.; Chen X. H. *Liq. Cryst.* **1994**, *17*, 803.
- ⁴² Scherowsky, G.; Chen X. H. *J. Mater. Chem.* **1995**, *5*, 417.
- ⁴³ McCubbin, A. J. Ph.D thesis, Queen's University, ON, Canada, **2004**.
- ⁴⁴ Taylor, R. *Electrophilic Aromatic Substitution*; John Wiley & Sons, 1990.
- ⁴⁵ Gilman, H.; Bebb, R. L. *J. Am. Chem. Soc.* **1939**, *61*, 109.

-
- ⁴⁶ a) Wittig, G.; Fuhrnam, G. *Chem. Ber.* **1940**, *73*, 1197; b) Wittig, G.; Pockels, U.; Droge, H. *Chem. Ber.* **1938**, *71B*, 1903.
- ⁴⁷ Phillion, D. P.; Walker, D. M. *J. Org. Chem.* **1995**, *60*, 8417.
- ⁴⁸ Gschwend, H. W.; Rodriguez, H. R. *Org. React. (N. Y.)* **1979**, *26*, 1.
- ⁴⁹ For reviews, see: Macklin, T.; Snieckus, V. In Dyker, G. Ed. *Handbook of C-H Transformations*, Wiley-VCH: New York, **2005**; 106-118.
- ⁵⁰ Clayden, J. *The Chemistry of Organolithium Compounds*, Rappoport, Z.; Marek, I. Ed.; John Wiley & Sons, UK, **2004**.
- ⁵¹ For a complete list, see reviews: a) Hartung, C. G.; Snieckus, V. In Astruc, D. Ed. *Modern Arene Chemistry*, Wiley-VCH; New York, **2002**, 330-267; b) Snieckus, V. *Chem. Rev.* **1990**, *90*, 879; c) Anctil, E.; Snieckus, V. In Diederich, F.; de Meijere, A. Ed. *Metal-Catalyzed Cross-Coupling Reactions* Wiley-VCH, Germany, **2004**. 761-808.; d) ref 49.
- ⁵² a) Beak, P.; Brown, R. A. *J. Org. Chem.* **1977**, *42*, 1823. b) Snieckus, V. *Heterocycles* **1980**, *14*, 1649. c) Beak, P.; Snieckus, V. *Acc. Chem. Res.* **1982**, *15*, 306.
- ⁵³ a) Meyers, A. I.; Mihelich, E. D. *J. Org. Chem.* **1975**, *40*, 3158; b) Meyers, A. I.; Mihelich, E. D. *Angew. Chem. Int. Ed.* **1976**, *15*, 270. c) Reuman, M.; Meyers, A. I. *Tetrahedron* **1985**, *41*, 837.
- ⁵⁴ Sibi, M. P.; Snieckus, V. *J. Org. Chem.* **1983**, *48*, 1935.
- ⁵⁵ a) Macklin, T. K.; Snieckus, V. *Org. Lett.* **2005**, *7*, 2519. b) Blackburn, T.; Snieckus, V. Queen's University, unpublished results.
- ⁵⁶ a) Rohonnstad, P.; Wensbo, D. *Tetrahedron Lett.* **2002**, *43*, 3137; b) Bennetau, B.; Mortier, J.; Moyroud, J.; Guesnet, J.-I. *J. Chem. Soc., Perkin Trans.* **1995**, 1265; c) Castagnetti, E.; Schlosser, M. *Chem. Eur. J.* **2002**, *8*, 799. For a review, see: ref 51b.
- ⁵⁷ Puterbaugh, W. H.; Hauser, C. R. *J. Org. Chem.* **1964**, *29*, 853. For a review, see: Kaiser, E. M.; Slocum, D. W., In McManus, S. P. Ed. *Organic Reactive Intermediates* Academic Press, New York, **1973**, 337.
- ⁵⁸ Watanabe, H.; Schwarz, R. A.; Hauser, C. R.; Lewis, J.; Slocum, D. W. *Can. J. Chem.* **1969**, *47*, 1543.
- ⁵⁹ Fahrner, W.; Gschwend, H. W. *J. Org. Chem.* **1979**, *44*, 1133.

-
- ⁶⁰ Gschwend, H. W.; Rodriguez, H. R. *Org. React. (N.Y.)* **1979**, *26*, 1. For a review, see: Schlosser, M. *Angew. Chem. Int. Ed.* **2006**, *45*, 5432.
- ⁶¹ Tye, H.; Eldred, C.; Wills, M. *Synlett* **1995**, 770.
- ⁶² Mortier, J.; Moyroud, J. *J. Org. Chem.* **1994**, *59*, 4042.
- ⁶³ Gray, M.; Chapell, B. J.; Felding, J.; Taylor, N. J.; Snieckus, V. *Synlett* **1998**, 442.
- ⁶⁴ Metallinos, C.; Nerdinger, S.; Snieckus, V. *Org. Lett.* **1999**, *1*, 1183.
- ⁶⁵ Alessi, M. Ph. D. thesis, Queen's University, Canada, 2008.
- ⁶⁶ For a review, see: Clayden, J. In Rappoport, Z.; Marek I. Ed: *The Chemistry of Organolithium Compounds* John Wiley & Sons, UK, **2004**. pp495-646.
- ⁶⁷ Roberts, J. D.; Curtain, D. Y. *J. Am. Chem. Soc.* **1946**, *68*, 1658.
- ⁶⁸ Beak, P.; Meyers, A. I. *Acc. Chem. Res.* **1986**, *19*, 356.
- ⁶⁹ Hay, D. R.; Song, Z.; Smith, S. G.; Beak, P. *J. Am. Chem. Soc.* **1988**, *110*, 8145.
- ⁷⁰ a) Saa, J. M.; Morey, J.; Frontera, A.; Deya, P. M. *J. Am. Chem. Soc.* **1995**, *117*, 1105; b) Saa, J. M.; Deya, P. M.; Suner, G. A.; Frontera, A. *J. Am. Chem. Soc.* **1992**, *114*, 9093.
- ⁷¹ a) Anderson, D. R.; Faibish, N. C.; Beak, P. *J. Am. Chem. Soc.* **1999**, *121*, 7553; b) Resek, J. E.; Beak, P. *J. Am. Chem. Soc.* **1994**, *116*, 405.
- ⁷² Gallagher, D. J.; Beak, P. *J. Org. Chem.* **1995**, *60*, 7092.
- ⁷³ Whisler, M. C.; MacNeil, S.; Snieckus, V.; Beak, P. *Angew. Chem. Int. Ed.* **2004**, *43*, 2206.
- ⁷⁴ Bauer, W.; Schleyer, P. v. R. *J. Am. Chem. Soc.* **1989**, *111*, 7191.
- ⁷⁵ a) Hommes, N. J. R. v. E.; Schleyer, P. v. R. *Angew. Chem., Int. Ed.* **1992**, *31*, 755; b) Hommes, N. J. R. v. E.; Schleyer, P. v. R. *Tetrahedron* **1994**, *50*, 5903.
- ⁷⁶ Stratakis, M. *J. Org. Chem.* **1997**, *62*, 3024.
- ⁷⁷ Shimano, M.; Meyers, A. I. *J. Am. Chem. Soc.* **1994**, *116*, 10815.
- ⁷⁸ Wu, T. -S.; Huang, S. -C.; Wu, P. -L. *Heterocycles* **1997**, *45*, 969.
- ⁷⁹ Chadwick, S. T.; Rennels, R. A.; Rutherford, J. L.; Collum, D. B. *J. Am. Chem. Soc.* **2000**, *122*, 8640.

-
- ⁸⁰ Slocum, D. W.; Dietzel, P. *Tetrahedron Lett.* **1999**, *40*, 1823.
- ⁸¹ a) Riggs, J. C.; Singh, K. J.; Yun, M.; Collum, D. B. *J. Am. Chem. Soc.* **2008**, *130*, 13709; b) Singh, K. J.; Collum, D. B. *J. Am. Chem. Soc.* **2006**, *128*, 13753; Chadwick, S. T.; Ramirez, A.; Gupta, L.; Collum, D. B. *J. Am. Chem. Soc.* **2007**, *129*, 2259.
- ⁸² a) Zhang, M. -X.; Eaton, P. E. *Angew. Chem. Int. Ed.* **2002**, *41*, 2169; b) Eaton, P. E.; Lukin, K. A. *J. Am. Chem. Soc.* **1993**, *115*, 11370; c) Eaton, P. E.; Lee, C. -H.; Xiong Y. *J. Am. Chem. Soc.* **1989**, *111*, 8016.
- ⁸³ Chang, C.-C.; Ameerunisha, M. S. *Coordin. Chem. Rev.* **1999**, *189*, 199.
- ⁸⁴ Fraser, R. R.; Mansour, T. S. *J. Org. Chem.* **1984**, *49*, 3442.
- ⁸⁵ Stanetty, P.; Koller, H.; Mihovilovic, M. *J. Org. Chem.* **1992**, *57*, 6833.
- ⁸⁶ a) Kondo, Y.; Shilai, H.; Uchiyama, M.; Sakamoto, T. *J. Am. Chem. Soc.* **1999**, *121*, 3539; b) Imahori, T.; Uchiyama, M.; Sakamoto, T.; Kondo, Y. *Chem. Commun.* **2001**, 2450. c) For a review, see: Mulvey, R. E.; Mongin, F.; Uchiyama, M.; Kondo, Y. *Angew. Chem. Int. Ed.* **2007**, *46*, 3802.
- ⁸⁷ Uchiyama, M.; Naka, H.; Matsumoto, Y.; Ohwada, T. *J. Am. Chem. Soc.* **2004**, *126*, 10526.
- ⁸⁸ Naka, H.; Uchiyama, M.; Matsumoto, Y.; Wheatley, A. E. H.; MacPartlin, M.; Morey, J. V.; Kondo, Y. *J. Am. Chem. Soc.* **2007**, *129*, 1921.
- ⁸⁹ a) Krasovskiy, A.; Krasovskaya, V.; Knochel, P. *Angew. Chem. Int. Ed.* **2006**, *45*, 2958; b) Lin, W.; Baron, O.; Knochel, P. *Org. Lett.* **2006**, *8*, 5673.
- ⁹⁰ Wunderlich, S. H.; Knochel, P. *Angew. Chem. Int. Ed.* **2007**, *46*, 7685.
- ⁹¹ Alberico, D.; Scott, M. E.; Lautens, M. *Chem. Rev.* **2007**, *107*, 174.
- ⁹² Kakiuchi, F.; Sekine, S.; Tanaka, Y.; Kamatani, A.; Sonoda, M.; Chatani, N.; Murai, S. *Bull. Chem. Soc. Jpn.* **1995**, *68*, 62.
- ⁹³ Matsubara, T.; Koga, N.; Musaev, D. G.; Morokuma, K. *J. Am. Chem. Soc.* **1998**, *120*, 12692.
- ⁹⁴ Murai, S.; Kakiuchi, F.; Sekine, S.; Tanaka, Y.; Kamatani, A.; Sonoda, M.; Chatani, N. *Nature* **1993**, *366*, 529.
- ⁹⁵ For a review, see Kakiuchi, F.; Murai, S. *Acc. Chem. Res.* **2002**, *35*, 826.

-
- ⁹⁶ Dorta, R.; Togni, A. *Chem. Commun.* **2003**, 760,
- ⁹⁷ Sonoda, M.; Kakiuchi, F.; Kamatani, A.; Chatani, N.; Murai, S. *Chem. Lett.* **1996**, 109.
- ⁹⁸ Kakiuchi, F.; Sato, T.; Igi, K.; Chatani, N.; Murai, S. *Chem. Lett.* **2001**, 30, 386.
- ⁹⁹ Kakiuchi, F.; Yamauchi, M.; Chatani, N.; Murai, S. *Chem. Lett.* **1996**, 25, 111.
- ¹⁰⁰ Kakiuchi, F.; Sato, T.; Tsujimoto, T.; Yamauchi, M.; Chatani, N.; Murai, S. *Chem. Lett.* **1998**, 1055.
- ¹⁰¹ Kakiuchi, F.; Sato, T.; Yamauchi, M.; Chatani, N.; Murai, S. *Chem. Lett.* **1999**, 19.
- ¹⁰² Kakiuchi, F.; Tsujimoto, T.; Sonoda, M.; Chatani, N.; Murai, S. *Synlett* **2001**, 948.
- ¹⁰³ Kakiuchi, F.; Sonoda, M.; Tsujimoto, T.; Chatani, N.; Murai, S. *Chem. Lett.* **1999**, 1083.
- ¹⁰⁴ Mei, T.-S.; Giri, R.; Mangel, N.; Yu, J.-Q. *Angew. Chem.* **2008**, 120, 5293.
- ¹⁰⁵ For a review, see: Kakiuchi, F.; Chatani, N. *Adv. Syn. Cat.* **2003**, 345, 1077.
- ¹⁰⁶ Hitoshi, A.; Takashi, H. *Heterocycles* **2008**, 75, 1305.
- ¹⁰⁷ For a review, see: Horton, D. A.; Bourne, G. T.; Smythe, M. L. *Chem. Rev.* **2003**, 103, 893.
- ¹⁰⁸ For a review, see: Yamamoto, T. *Synlett*, **2003**, 115.
- ¹⁰⁹ For a review, see: Lemieux, R. P. *Acc. Chem. Res.* **2001**, 34, 845.
- ¹¹⁰ For a review, see: a) Hassan, J.; Svignon, M.; Gozzi, C.; Schulz, E.; Lemaire, M. *Chem. Rev.* **2002**, 102, 1359; b) Cepanec, I. *Synthesis of Biaryls* Elsevier, **2004**.
- ¹¹¹ Kharasch, M. S.; Fields, E. K. *J. Am. Chem. Soc.* **1941**, 63, 2316.
- ¹¹² For a review, see: a) Anctil, E. J. –G.; Snieckus, V. *J. Organomet. Chem.* **2002**, 653, 150; b) Ref. 51c.
- ¹¹³ Tamao, K.; Sumitani, K.; Kumada, M. *J. Am. Chem. Soc.* **1972**, 94, 4374.
- ¹¹⁴ Corriu, R. J. P.; Masse, J. P. *J. Chem. Soc., Chem. Commun.* **1972**, 144.
- ¹¹⁵ a) Baba, S.; Negishi, E. *J. Am. Chem. Soc.* **1976**, 98, 6729; b) Negishi, E.; Baba, S. *J. Am. Chem. Soc.* **1976**, 98, 596; c) Negishi, E. –i.; King, A. O.; Villani, M.; Silveirn, R. *J. Org. Chem.* **1978**, 43, 358.

-
- ¹¹⁶ a) Milstein, D.; Stille, J. K. *J. Am. Chem. Soc.* **1978**, *100*, 3636; b) Milstein, D.; Stille, J. K. *J. Am. Chem. Soc.* **1979**, *101*, 4992; c) Kashin, A. N.; Bumagina, I. G.; Bumagin, N. A.; Beletskaya, I. P.; *Zh. Org. Khim.* **1981**, *17*, 21.
- ¹¹⁷ a) Miyaura, N.; Yamada, K.; Suzuki, A. *Tetrahedron Lett.* **1979**, *36*, 3437; b) Miyaura, N.; Suzuki, A. *J. Chem. Soc., Chem. Commun.* **1979**, 866; c) Miyaura, N.; Yanaki, T.; Suzuki, A. *Synth. Commun.* **1981**, *11*, 513.
- ¹¹⁸ a) Zhao, Z.; Snieckus, V. *Org. Lett.* **2005**, *7*, 2523; b) Fu, J. -M.; Snieckus, V. *Can. J. Chem.* **2000**, *78*, 905.
- ¹¹⁹ Yang, W.; Gao, X.; Wang, B. in *Boronic Acids: Preparation and Applications in Organic Chemistry and Medicine*, Hall, D. G., Ed.; Wiley, New York. **2005**, p 481.
- ¹²⁰ a) Baxendale, I. R.; Griffiths-Jones, C. M.; Ley, S. V.; Tranmer, G. K. *Chem. Eur. J.* **2006**, *12*, 4407; b) Collins, I. *J. Chem. Soc., Perkin Trans. 1*, **2002**, 1921.
- ¹²¹ Alessi, M.; Larkin, A. L.; Ogilvie, K. A.; Green, L. A.; Lai, S.; Lopez, S.; Snieckus, V. *J. Org. Chem.* **2007**, *72*, 1588.
- ¹²² a) Narasimhan, N. S.; Alurkar, R. H. *Ind. J. Chem.* **1969**, *7*, 1280; b) Narasimhan, N. S.; Chandrachood, P. S.; Shete, N. R. *Tetrahedron* **1981**, *37*, 825.
- ¹²³ Fu, J. -M.; Sharp, M. J.; Snieckus, V. *Tetrahedron Lett.* **1988**, *29*, 5459.
- ¹²⁴ Tilly, D.; Fu, J.-M.; Zhao, B.-P.; Alessi, M.; Castanet, A.-S; Snieckus, V.; Mortier, J. *J. Org. Chem.* in press.
- ¹²⁵ a) Fu, J. -M.; Zhao, B. -P.; Sharp, M. J.; Snieckus, V. *J. Org. Chem.* **1991**, *56*, 1683; b) Fu, J. -M.; Zhao, B. -P.; Sharp, M. J.; Snieckus, V. *Can. J. Chem.* **1994**, *72*, 227.
- ¹²⁶ Fu, J. -M.; Snieckus, V. *Can. J. Chem.* **2000**, *78*, 905.
- ¹²⁷ Mohri, S. -I.; Stefinovic, M.; Snieckus, V. *J. Chem. Soc.* **1997**, *62*, 7072.
- ¹²⁸ a) Wang, X.; Snieckus, V. *Tetrahedron Lett.* **1998**, *39*, 961; b) Cai, X.; Snieckus, V. *Org. Lett.* **2004**, *6*, 2293.
- ¹²⁹ McCubbin, J. A.; Xia, T.; Ruiyao, W.; Yue, Z.; Snieckus, V.; Lemieux, R. P. *J. Am. Chem. Soc.* **2004**, *126*, 1161.
- ¹³⁰ Wang, W.; Snieckus, V. *J. Org. Chem.* **1992**, *57*, 424.
- ¹³¹ a) Chauder, B.; Green, L.; Snieckus, V. *Pure Appl. Chem.* **1999**, *33*, 900; b) James, C. A.; Snieckus, V. *Tetrahedron Lett.* **1997**, *38*, 8149; c) ref 117; d) 125 b.

-
- ¹³² MacNeil, S. L.; Gray, M.; Briggs, L. E.; Li, J. J.; Snieckus, V. *Synlett* **1998**, 419.
- ¹³³ Familoni, O. B.; Ionica, I.; Bower, J. F.; Snieckus, V. *Synlett* **1997**, 1081.
- ¹³⁴ Beaulieu, F.; Snieckus, V. *J. Org. Chem.* **1994**, *59*, 6508.
- ¹³⁵ Gray, M.; Chapell, B. J.; Taylor, N.; Snieckus, V. *Angew. Chem. Int. Ed.* **1996**, *35*, 1558.
- ¹³⁶ a) MacNeil, S. Ph. D. thesis; Queen's University, 2001. b) MacNeil, S, Snieckus, V. *J. Org. Chem.* in press.
- ¹³⁷ Moreau, P.; Snieckus, V. unpublished results.
- ¹³⁸ For a review, see: a) Cerniglia, C. E.; Heitkamp, M. A. In Varanasi, U. Ed. *Metabolism of Polycyclic Aromatic Hydrocarbons in the Aquatic Environment* CRC Press, Inc., Boca Raton, Fla. **1989**. p41-68. b) Golubev, S. N.; Schelud'ko, A. V.; Muratova, A. Y.; Makarov, O. E.; Turkovskaya, O. V. *Water Air Soil Pollut.* **2009**, *198*, 5.
- ¹³⁹ Seijas, J. A.; de Lera, A. R.; Villaverde, M. C.; Castedo, L. *J. Chem. Soc., Chem. Commun.* **1985**, 839.
- ¹⁴⁰ Jacobi, P. A.; Kravitz, J. I.; Zheng, W. *J. Org. Chem.* **1995**, *60*, 376.
- ¹⁴¹ Kunstmann, M. P.; Mitscher, L. A. *J. Org. Chem.* **1966**, *31*, 2920.
- ¹⁴² Chapatwala, K. D.; de La Cruz, A. A.; Miles, D. H. *Life Sci.* **1981**, *29*, 1997.
- ¹⁴³ Traxler, J. T.; Krbecek, L. O.; Riter, R. R.; Wagner, R. G.; Huffmann, C. W. *J. Med. Chem.* **1971**, *14*, 90.
- ¹⁴⁴ Wilson, S.; Ruenitz, P. C. *J. Pharm. Sci.* **1992**, *82*, 571.
- ¹⁴⁵ Cannon, J. G.; Khonji, R. R. *J. Med. Chem.* **1975**, *18*, 110.
- ¹⁴⁶ a) Ostermayer, E.; Fittig, R. *Chem. Ber.* **1872**, *5*, 933; b) Glaser, C. *Chem. Ber.* **1872**, *5*, 982.
- ¹⁴⁷ For a review, see: a) Floyd, A. J.; Dyke, S. F.; Ward, S. E. *Chem. Rev.* **1976**, *76*, 509. b) Bradsher, C. K. *Chem. Rev.* **1987**, *87*, 1277.
- ¹⁴⁸ Bachmann, W. E.; Scott, L. B. *J. Am. Chem. Soc.* **1948**, *70*, 1462.

-
- ¹⁴⁹ Paredes, E.; Biolatto, B.; Kneeteman, M.; Mancini, P. M. *Tetrahedron Lett.* **2002**, *43*, 4601.
- ¹⁵⁰ Jiang, X.-F.; Kong, W.-Q.; Chen, J.; Ma, S.-M. *Org. Biomol. Chem.* **2008**, *6*, 3606.
- ¹⁵¹ Yoshikawa, E.; Radhakrishnan, K. V.; Yamamoto, Y. *J. Am. Chem. Soc.* **2000**, *122*, 7280.
- ¹⁵² a) Pena, D.; Perez, D.; Guitian, E.; Castedo, L. *J. Am. Chem. Soc.* **1999**, *121*, 5827; b) Radhakrishnan, K. V.; Yoshikawa, E.; Yamamoto, Y. *Tetrahedron Lett.* **1999**, *40*, 7533. c) Catellani, M.; Motti, E.; Baratta, S. *Org. Lett.* **2001**, *3*, 3611
- ¹⁵³ Werner, A.; Grob, A. *Chem. Ber.* **1904**, *37*, 2887.
- ¹⁵⁴ Schultz, R. S.; Schultz, E. D.; Cochran, J. *J. Am. Chem. Soc.* **1940**, *62*, 2902.
- ¹⁵⁵ a) Brown, W. G.; Bluestein, B. *J. Am. Chem. Soc.* **1940**, *62*, 3256; b) Brown, W. G.; Bluestein, B. *J. Am. Chem. Soc.* **1943**, *65*, 1235; c) Benjamin, B. M.; Collins, C. J. *J. Am. Chem. Soc.* **1953**, *75*, 402; d) Collins, C. J.; Benjamin, B. M. *J. Am. Chem. Soc.* **1953**, *75*, 1644.
- ¹⁵⁶ a) Bavin, P. M. G. *Can. J. Chem.* **1960**, *38*, 911; b) Anet, F. A. L.; Bavin, P. M. G. *Can. J. Chem.* **1957**, *35*, 1084; c) Greenhow, E. J.; McNeil, D.; White, E. N. *J. Chem. Soc.* **1952**, 986.
- ¹⁵⁷ Quelet, R.; Hoch, J.; Borgel, C.; Mansourl, M.; Pineau, R.; Tchiroukine, E.; Vinot, N. *Bull. Soc. Chim. Fr.* **1956**, 26.
- ¹⁵⁸ Greenhow, E. J.; McNeil, D. *J. Chem. Soc.* **1956**, 3204.
- ¹⁵⁹ a) Rappoport, Z.; Gal, A. *J. Chem. Soc.* **1972**, *37*, 1174; b) Sisl, A. J. *J. Org. Chem.* **1970**, *35*, 2670.
- ¹⁶⁰ Anet, F. A. L.; Bavin, P. M. G. *Can. J. Chem.* **1956**, *34*, 991.
- ¹⁶¹ Bavin, P. M. G. *Can. J. Chem.* **1964**, *42*, 1409.
- ¹⁶² Yang, Y.-H.; Dai, W.-X.; Zhang, Y.-Z.; Petersen, J. L.; Wang, K. K. *Tetrahedron* **2006**, *62*, 4364.
- ¹⁶³ a) Bradsher, C. K.; Jackson, W. J. Jr. *J. Am. Chem. Soc.* **1955**, *76*, 734; b) Bradsher, C. K.; Jackson, W. J. Jr. *J. Am. Chem. Soc.* **1955**, *76*, 4140.
- ¹⁶⁴ Bradsher, C. K.; Wert, R. W. *J. Am. Chem. Soc.* **1940**, *62*, 2806.

-
- ¹⁶⁵ Yao, T.-L.; Campo, M. A.; Larock, R. C. *J. Org. Chem.* **2005**, *70*, 3511.
- ¹⁶⁶ For a review, see: Campbell, I. B. *The Sonogashira Cu-Pd-Catalyzed Alkyne Coupling Reaction. Organocopper Reagents*; Taylor, R. J. K., Ed.; IRL Press: Oxford, UK, 1994; pp 217-235.
- ¹⁶⁷ Gies, A.-E.; Pfeffer, M. *J. Org. Chem.* **1999**, *64*, 3650.
- ¹⁶⁸ Harrowven, D. C.; Nunn, M. I. T.; Fenwick, D. R. *Tetrahedron Lett.* **2002**, *43*, 3185.
- ¹⁶⁹ a) Harrowven, D. C.; Sutton, B. J.; Coulton, S. *Tetrahedron Lett.* **2001**, *42*, 9061; b) Harrowven, D. C.; Sutton, B. J.; Coulton, S. *Tetrahedron Lett.* **2001**, *42*, 2907.
- ¹⁷⁰ a) Buckles, R. E. *J. Am. Chem. Soc.* **1955**, *77*, 1040; b) Parker, C. O.; Spoerri, P. E. *Nature* **1950**, *166*, 603.
- ¹⁷¹ a) Wood, C. S.; Mallory, F. B. *J. Org. Chem.* **1964**, *29*, 3373; b) Mallory, F. B.; Mallory, C. W. *Org. React.* **1984**, *30*, 1; c) Mallory, F. B.; Rudolph, M. J.; Oh, S. M. *J. Org. Chem.* **1989**, *54*, 4619.
- ¹⁷² Estevez, J. C.; Villaverde, R. J.; Castedo, L. *Can. J. Chem.* **1990**, *68*, 964.
- ¹⁷³ Almeida, J. F.; Castedo, L.; Fernandez, D.; Neo, A. G.; Romero, V.; Tojo, G. *Org. Lett.* **2003**, *5*, 4939.
- ¹⁷⁴ Luliano, A.; Piccioli, P.; Fabbri, D. *Org. Lett.* **2004**, *6*, 3711.
- ¹⁷⁵ Benesch L.; Bury, P.; Guillaneux, D.; Houldsworth, S.; Wang, X.; Snieckus, V. *Tetrahedron. Lett.* **1998**, *39*, 961.
- ¹⁷⁶ a) Mills, R. J.; Taylor, N. J.; Snieckus, V. *J. Org. Chem.* **1989**, *54*, 4372; b) Sperry, J.; Gibson, J. S.; Sejberg, J. J. P.; Brimble, M. A. *Org. Biomol. Chem.* **2008**, *6*, 4261; c) Chau, N. T. T.; Nguyen, T. H.; Castanet, A.-S.; Nguyen, K. P. P. *Tetrahedron* **2008**, *64*, 10552.
- ¹⁷⁷ Patel, J.; Snieckus, V. unpublished results, Queen's University. The results indicates that steric effect plays important rule in the determent of regio-activity of DoM.
- ¹⁷⁸ a) Taddei, M.; Ricci, A. *Synthesis* **1986**, 633; b) Ruzaev, G. A.; Shoshunov, V. A.; Dodonov, V. A.; Brilkina, T. G. *Organic Peroxides*, Swern, D., Ed., Wiley Interscience, New York, 1972.
- ¹⁷⁹ a) Moser, W. H.; Eendsley, K. E.; Colyer, J. T. *Org. Lett.* **2000**, *2*, 717; b) Moser, W. H.; Zhang, J.; Lecher, C. S.; Frazier, T. L.; Pink, M. *Org. Lett.* **2002**, *4*, 1981.

-
- ¹⁸⁰ Gan, W.; Snieckus, V., in progress, Queen's University.
- ¹⁸¹ a) Townsend, C. A.; Davis, S. G.; Christensen, S. B.; Link, J. C. *J. Am. Chem. Soc.* **1981**, *103*, 6885; b) Chen, Y.-L.; Hau, C.-K.; Wang, H; He, H; Wong, M.-S.; Lee, A. W. M. *J. Org. Chem.* **2006**, *71*, 3512.
- ¹⁸² Williard, P. G.; Fryhle, C. B. *Tetrahedron Lett.* **1980**, *21*, 3731.
- ¹⁸³ Jeganathan, S.; Tsukamoto, M.; Schlosser, M. *Synthesis* **1990**, 109.
- ¹⁸⁴ a) Chen, Q.-Y.; He, Y.-B.; Yang, Z.-Y. . *J. Chem. Soc. Chem. Commun.* **1986**, 1453; b) Cai, X.; Brown, S.; Hodson, P.; Snieckus V. *Can. J. Chem.* **2004**, *82*, 195.
- ¹⁸⁵ Yardley, J. P.; Fletcher III, H. *Synthesis* **1976**, 244.
- ¹⁸⁶ Neises, B.; Steglisch, W. *Angew. Chem. Int. Ed.* **1978**, *17*, 522.
- ¹⁸⁷ Ines, T.; Zecchini, G.; Agrosi, F; Paradisi, M. *J. Heterocyclic Chem.* **1986**, *23*, 1459.
- ¹⁸⁸ a) Moriconi, E. J.; Wallenberger, F. T.; O'Connor, W. F. *J. Chem. Soc.* **1959**, *24*, 86; b) Ho, C.-M.; Yu, W.-Y.; Che, C.-M. *Angew. Chem. Int. Ed.* **2004**, *43*, 3303.
- ¹⁸⁹ a) Moriconi, E. J.; Wallenberger, F. T.; O'Connor, W. F. *J. Org. Chem.* **1959**, *24*, 86; b) Platt, K. L.; Oesch, F. *Synthesis* **1982**, 459.
- ¹⁹⁰ a) Crandall, J. K.; Zucco, M.; Kirch, R. S.; Coppert, D. M. *Tetrahedron Lett.* **1991**, *32*, 5441; b) Murray, R. W.; Jeyaraman, R. *J. Org. Chem.* **1985**, *50*, 2847
- ¹⁹¹ See appendix 1.
- ¹⁹² Dierking, I. *Textures of Liquid Crystals* Weinheim: Wiley-VCH, **2003**, p7.
- ¹⁹³ Gardner, P. D.; Sarrafizadeh, R. H. *J. Am. Chem. Soc.* **1960**, *82*, 4287.
- ¹⁹⁴ The stereochemistry was evidenced by model compound **2.37**.
- ¹⁹⁵ For a review, see: Molar, A. in *Fine Chemicals through Heterogeneous Catalysis* Ed: Sheldon, R. A.; van Bekkum, H, Wiley-VCH, New York, **2001**, p232.
- ¹⁹⁶ Hanessian, S.; Delorme, D.; Dufresne, Y. *Tetrahedron Lett.* **1984**, *25*, 2515.
- ¹⁹⁷ Relative stereochemistry was determined by comparing ¹H and ¹³C NMR data and mp with literature: a) Lin, S.-Z, Chen, Q.-A.; You, T.-P. *Synlett* **2007**, 2101; b) Sarobe, M.; van Heerbeek, R.; Jenneskens, L. W.; Zwikker, J. W. *Liebigs Ann./Recl.* **1997**, 2499. A resolution that was tried suggested it is *trans* diol (see Appendix 2)

-
- ¹⁹⁸ Sinhababu, A. K.; Kawase, M.; Borchardt, R. T. *Synthesis* **1988**, 710.
- ¹⁹⁹ Kende, A. S.; Rizzi, J. P. *Tetrahedron Lett.* **1981**, 1779.
- ²⁰⁰ The textures of **2.33a-e** in the microscopy are shown in Appendix 3.
- ²⁰¹ Zhao, Z.-D.; Snieckus V. *Org. Lett.* **2005**, 7, 2523.
- ²⁰² The sign of specific rotation was determined by the final compound (-)-**4.1**, whose specific rotation was measured using an AUTOPOL-V Automatic Polarimeter. $[\alpha]^{21} = -64.8 \text{ mL/dm}\cdot\text{g}$.
- ²⁰³ Miyasato, K.; Abe, S.; Takezoe, H.; Fukuda, A.; Kuze, E. *Jpn. J. Appl. Phys.* **1983**, 22, L661.
- ²⁰⁴ Vizitiu, D.; Lazar, C.; Halden, B. J.; Lemieux, R. P. *J. Am. Chem. Soc.* **1999**, 121, 8229.
- ²⁰⁵ Schulmeyer, H.; Meister, R.; Altenbach, H. J.; Szewczyk, D. *Liq. Cryst.* **1993**, 14, 1007.
- ²⁰⁶ Lelidis, I. *Liq. Cryst.* **1998**, 25, 531.
- ²⁰⁷ Perrin, D. D.; Armarego, W. L. F.; Perrin, D. R. *Purification of Laboratory Chemicals*; 2nd ed.; Pergamon Press: Oxford, 1980.
- ²⁰⁸ Watson, S. C.; Eastham, J. F. *J. Organomet. Chem.* **1967**, 9, 165.
- ²⁰⁹ Coulson, D. R. *Inorg. Synth.* **1972**, 13, 121.
- ²¹⁰ Gray, G. W.; Jones, B. *J. Chem. Soc.* **1953**, 4179.
- ²¹¹ Grammaticakis, P. *Bull. Soc. Chim. Fr.* **1964**, 924.
- ²¹² It was established by vary temperature ¹H NMR, which was shown in Appendix 4.
- ²¹³ Tilly, G. *Chimica Therapeutica* **1967**, 57.
- ²¹⁴ Chauder, B. A.; Kalinin, A. V.; Snieckus, V. *Synthesis* **2001**, 140.
- ²¹⁵ Lai P.-S. M.Sc. thesis, Queen's University, Kingston, ON, Canada, 2007.

APPENDICES

Appendix 1. Single Crystal X-ray Data for 1.31

A crystal of the compound (colorless, plate-shaped, size 0.35 x 0.20 x 0.04 mm) was mounted on a glass fiber with grease and cooled to -93 °C in a stream of nitrogen gas controlled with Cryostream Controller 700. Data collection was performed on a Bruker SMART APEX II X-ray diffractometer with graphite-monochromated Mo K radiation ($\lambda = 0.71073 \text{ \AA}$), operating at 50 kV and 30 mA over 2 θ ranges of 5.38 ~ 50.00°. No significant decay was observed during the data collection.

Data were processed on a PC using the Bruker AXS Crystal Structure Analysis Package:^[1] Data collection: APEX2 (Bruker, 2006); cell refinement: SAINT (Bruker, 2005); data reduction: SAINT (Bruker, 2005); structure solution: XPREP (Bruker, 2005) and SHELXTL (Bruker, 2000); structure refinement: SHELXTL; molecular graphics: SHELXTL; publication materials: SHELXTL. Neutral atom scattering factors were taken from Cromer and Waber.^[2] The crystal is monoclinic space group $P2_1/c$, based on the systematic absences, E statistics and successful refinement of the structure. The structure was solved by direct methods. Full-matrix least-square refinements minimizing the function $\sum w (F_o^2 - F_c^2)^2$ were applied to the compound. All non-hydrogen atoms were refined anisotropically except the oxygen atoms of the lattice water. All of the other H atoms were placed in geometrically calculated positions, with C-H = 0.95 (aromatic), 0.99 (CH₂) and 0.98 Å (CH₃), and refined as riding atoms, with Uiso(H) = 1.5 UeqC(methyl), or 1.2 Ueq(other C). The two isomers, S, S- and R, R- co-crystallized,

which results in the partially disorder of the molecule. The SHELX commands, EADP and EXYZ were used to resolve the disorder. Also, the presence of the two long chains in the molecule makes the single crystal growth a tough job. As a result, only thin and very soft plate-shaped crystals were obtainable, and the quality of the crystal is not great. Therefore, some “Alerts” from CheckCIF are expected.

Convergence to final $R_1 = 0.1174$ and $wR_2 = 0.2758$ for 2533 ($I > 2\sigma(I)$) independent reflections, and $R_1 = 0.2629$ and $wR_2 = 0.3713$ for all 6767 ($R(\text{int}) = 0.2468$) independent reflections, with 375 parameters and 0 restraints, were achieved.^[3] The largest residual peak and hole to be 0.371 and $-0.431 \text{ e}/\text{\AA}^3$, respectively. Crystallographic data, atomic coordinates and equivalent isotropic displacement parameters, bond lengths and angles, anisotropic displacement parameters, hydrogen coordinates and isotropic displacement parameters, and torsion angles are given in Table 1 to 6. The molecular structure and the cell packing are shown in Figures 1 and 2.

[1] Bruker AXS Crystal Structure Analysis Package:

Bruker (2000). SHELXTL. Version 6.14. Bruker AXS Inc., Madison, Wisconsin, USA.

Bruker (2005). XPREP. Version 2005/2. Bruker AXS Inc., Madison, Wisconsin, USA.

Bruker (2005). SAINT. Version 7.23A. Bruker AXS Inc., Madison, Wisconsin, USA.

Bruker (2006). APEX2. Version 2.0-2. Bruker AXS Inc., Madison, Wisconsin, USA.

[2] Cromer, D. T.; Waber, J. T. *International Tables for X-ray Crystallography*;

Kynoch Press: Birmingham, UK, 1974; Vol. 4, Table 2.2 A.

[3] $R_1 = \sum ||Fo| - |Fc|| / \sum |Fo|$

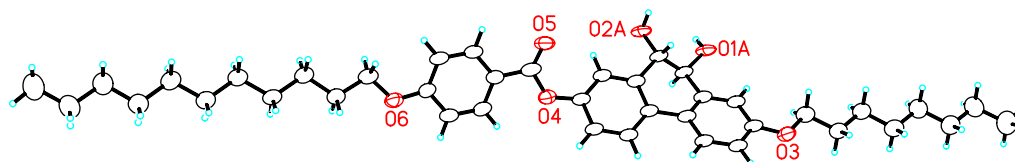
$$wR_2 = \{ \sum [w (Fo^2 - Fc^2)^2] / \sum [w(Fo^2)^2] \}^{1/2}$$

$$(w = 1 / [\sigma^2(Fo^2) + (0.1338P)^2 + 8.06P], \text{ where } P = [\text{Max}(Fo^2, 0) + 2Fc^2] / 3)$$

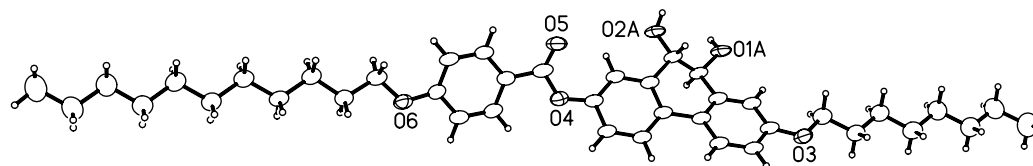
Figure 1. Molecular Structure (Displacement ellipsoids for non-H atoms are shown at the 50% probability level and H atoms are represented by circles of arbitrary size.)

a) Isomer A(50%):

i)

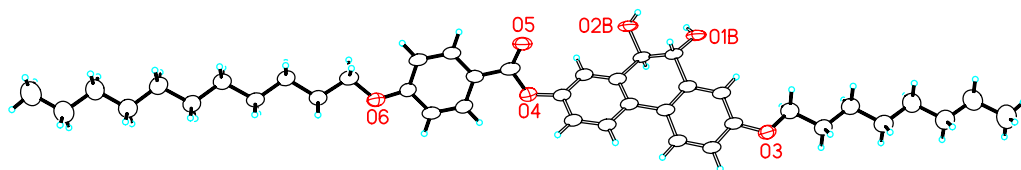


ii)



b) Isomer B(50%):

i)



ii)

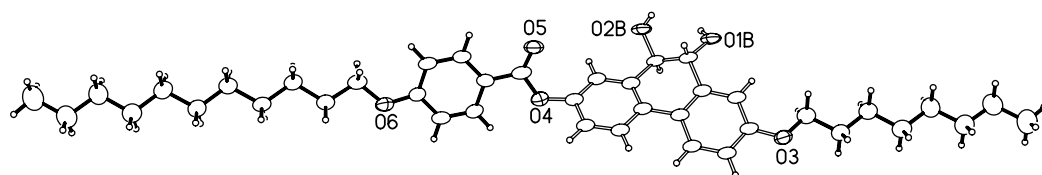
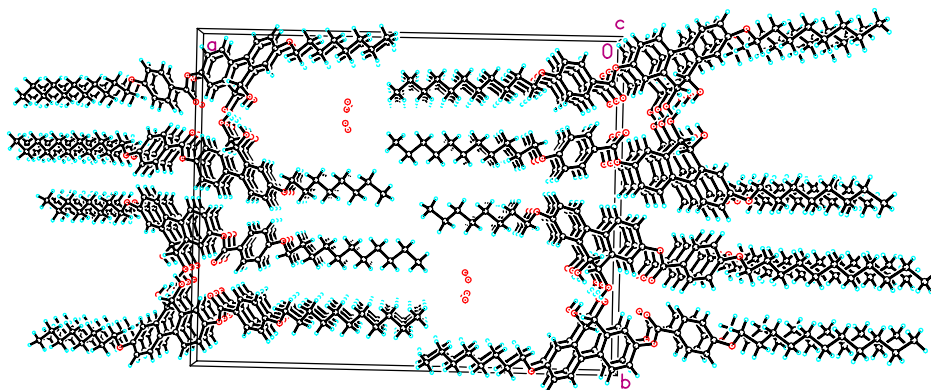


Figure 2. Unit cell packing

a)



b)

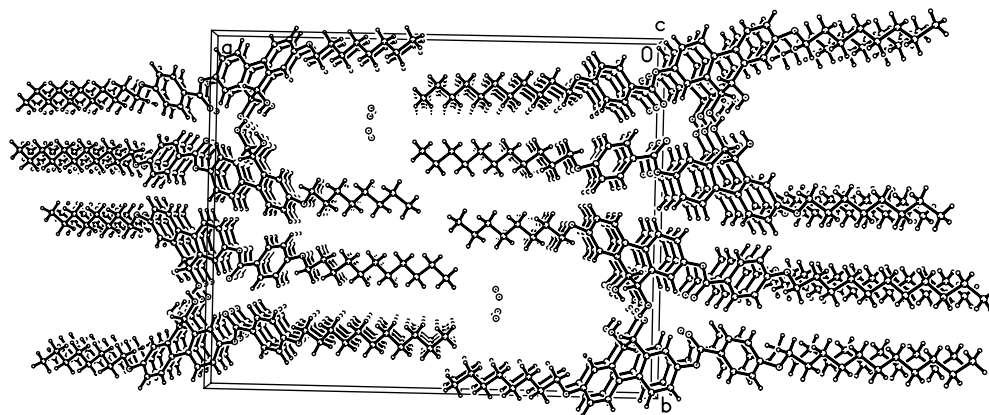


Table 1. Crystal data and structure refinement for vs21

Identification code	vs21
Empirical formula	C ₄₀ H _{57.69} O _{7.84}
Formula weight	664.03
Temperature	180(2) K
Wavelength	0.71073 Å
Crystal system	Monoclinic
Space group	P2(1)/c
Unit cell dimensions	a = 30.28(5) Å = 90°.

	$b = 24.01(4) \text{ \AA}$	$= 91.45(2)^\circ$.
	$c = 5.303(9) \text{ \AA}$	$= 90^\circ$.
Volume	$3854(11) \text{ \AA}^3$	
Z	4	
Density (calculated)	1.144 Mg/m^3	
Absorption coefficient	0.078 mm^{-1}	
F(000)	1442	
Crystal size	$0.35 \times 0.20 \times 0.04 \text{ mm}^3$	
Theta range for data collection	2.69 to 25.00° .	
Index ranges	$-35 \leq h \leq 35$, $-28 \leq k \leq 28$, $-6 \leq l \leq 6$	
Reflections collected	25811	
Independent reflections	6767 [R(int) = 0.2468]	
Completeness to theta = 25.00°	99.6 %	
Absorption correction	Multi-scan	
Max. and min. transmission	0.9969 and 0.9732	
Refinement method	Full-matrix least-squares on F^2	
Data / restraints / parameters	6767 / 0 / 375	
Goodness-of-fit on F^2	1.028	
Final R indices [$I > 2\sigma(I)$]	$R1 = 0.1174$, $wR2 = 0.2758$	
R indices (all data)	$R1 = 0.2629$, $wR2 = 0.3713$	
Extinction coefficient	$0.069(8)$	
Largest diff. peak and hole	0.371 and $-0.431 \text{ e.\AA}^{-3}$	

Table 2. Atomic coordinates ($\times 10^4$) and equivalent isotropic displacement parameters ($\text{\AA}^2 \times 10^3$)

for vs21. $U(\text{eq})$ is defined as one third of the trace of the orthogonalized U^{ij} tensor.

	x	y	z	$U(\text{eq})$
O(1A)	-1152(4)	1904(4)	10470(20)	49(1)
O(2A)	-513(2)	2280(2)	6985(9)	49(1)
O(1B)	-1272(5)	2014(5)	9710(30)	49(1)
O(2B)	-513(2)	2280(2)	6985(9)	49(1)
O(3)	-2091(2)	209(2)	10975(9)	49(1)
O(4)	504(2)	1193(2)	1401(9)	51(1)
O(5)	305(2)	2003(2)	-324(9)	54(2)
O(6)	2040(2)	1277(2)	-6063(9)	49(1)
C(1A)	-1248(5)	162(7)	6370(30)	41(1)
C(2A)	-1605(6)	35(8)	7820(30)	41(1)
C(3A)	-1736(5)	399(6)	9660(30)	41(1)
C(4A)	-1509(4)	889(5)	10060(20)	41(1)
C(5A)	-1152(4)	1016(4)	8610(20)	41(1)

C(6A)	-1021(5)	652(5)	6760(30)	41(1)
C(1B)	-1212(7)	163(9)	6400(40)	41(1)
C(2B)	-1559(7)	6(10)	7900(50)	41(1)
C(3B)	-1760(7)	396(8)	9420(40)	41(1)
C(4B)	-1613(5)	943(6)	9440(30)	41(1)
C(5B)	-1266(5)	1100(6)	7940(30)	41(1)
C(6B)	-1066(6)	710(7)	6420(30)	41(1)
C(7A)	-898(5)	1532(5)	9050(30)	44(2)
C(8A)	-747(7)	1764(7)	6630(30)	44(2)
C(7B)	-1121(6)	1684(6)	7730(40)	44(2)
C(8B)	-635(9)	1721(10)	7480(40)	44(2)
C(9A)	-474(5)	1351(6)	5340(30)	41(1)
C(10A)	-99(5)	1503(6)	4070(30)	41(1)
C(11A)	137(4)	1107(5)	2780(20)	41(1)
C(12A)	-2(3)	559(4)	2758(19)	41(1)
C(13A)	-376(3)	406(4)	4024(19)	41(1)
C(14A)	-612(4)	802(5)	5310(20)	41(1)
C(9B)	-456(6)	1342(8)	5480(40)	41(1)
C(10B)	-73(7)	1471(8)	4250(40)	41(1)
C(11B)	80(5)	1119(7)	2400(30)	41(1)
C(12B)	-149(4)	640(5)	1790(20)	41(1)
C(13B)	-532(4)	510(5)	3020(20)	41(1)
C(14B)	-685(5)	861(6)	4870(30)	41(1)

C(15)	-2275(3)	562(3)	12801(14)	50(2)
C(16)	-2613(2)	234(3)	14179(13)	47(2)
C(17)	-2867(3)	574(3)	16055(15)	54(2)
C(18)	-3202(3)	233(3)	17423(14)	54(2)
C(19)	-3486(3)	565(3)	19178(15)	58(2)
C(20)	-3827(3)	230(3)	20487(15)	60(2)
C(21)	-4102(3)	545(4)	22316(17)	73(3)
C(22)	-4458(3)	207(4)	23500(19)	92(3)
C(23)	553(3)	1620(3)	-221(13)	44(2)
C(24)	955(2)	1543(3)	-1676(13)	39(2)
C(25)	1211(2)	1074(3)	-1436(13)	41(2)
C(26)	1570(2)	1004(3)	-2896(14)	44(2)
C(27)	1680(2)	1400(3)	-4677(13)	39(2)
C(28)	1430(2)	1869(3)	-4920(13)	42(2)
C(29)	1064(2)	1938(3)	-3446(13)	43(2)
C(30)	2188(2)	1654(3)	-7951(13)	47(2)
C(31)	2545(2)	1360(3)	-9301(14)	46(2)
C(32)	2781(2)	1711(3)	-11184(13)	44(2)
C(33)	3122(2)	1386(3)	-12581(13)	45(2)
C(34)	3405(2)	1724(3)	-14326(13)	46(2)
C(35)	3735(2)	1386(3)	-15749(13)	47(2)
C(36)	4025(3)	1724(3)	-17444(14)	53(2)
C(37)	4351(3)	1377(3)	-18884(15)	58(2)

C(38)	4649(3)	1726(4)	-20509(16)	65(2)
C(39)	4978(3)	1390(4)	-21953(17)	75(3)
C(40)	5287(3)	1735(4)	-23520(20)	95(3)
O(1WA)	-2218(8)	1962(10)	5040(60)	77(7)
O(1WB)	-2313(8)	1904(9)	6390(60)	73(7)
O(1WC)	-2298(13)	2074(16)	3500(80)	102(13)
O(1WD)	-2404(11)	1958(14)	8140(80)	89(10)
O(2WA)	6424(10)	2892(15)	-22520(70)	196(14)
O(2WB)	6486(17)	2340(30)	-20920(130)	196(14)
O(2WC)	6475(19)	2280(30)	-24300(150)	196(14)

Table 3. Bond lengths [\AA] and angles [$^\circ$] for vs21.

O(1A)-C(7A)	1.411(16)
O(1A)-H(1AA)	0.8400
O(2A)-C(8A)	1.436(18)
O(2A)-H(2AA)	0.8400
O(1B)-C(7B)	1.40(2)
O(1B)-H(1BA)	0.8400
O(3)-C(3A)	1.374(18)
O(3)-C(3B)	1.39(2)
O(3)-C(15)	1.412(8)

O(4)-C(23)	1.350(8)
O(4)-C(11A)	1.363(14)
O(4)-C(11B)	1.413(18)
O(5)-C(23)	1.188(8)
O(6)-C(27)	1.362(8)
O(6)-C(30)	1.430(8)
C(1A)-C(6A)	1.376(11)
C(1A)-C(2A)	1.377(11)
C(1A)-H(1AB)	0.9500
C(2A)-C(3A)	1.377(11)
C(2A)-H(2AB)	0.9500
C(3A)-C(4A)	1.376(11)
C(4A)-C(5A)	1.376(11)
C(4A)-H(4AA)	0.9500
C(5A)-C(6A)	1.377(11)
C(5A)-C(7A)	1.474(16)
C(6A)-C(14A)	1.517(19)
C(1B)-C(2B)	1.386(15)
C(1B)-C(6B)	1.386(15)
C(1B)-H(1BB)	0.9500
C(2B)-C(3B)	1.386(15)
C(2B)-H(2BB)	0.9500
C(3B)-C(4B)	1.386(15)

C(4B)-C(5B)	1.386(15)
C(4B)-H(4BA)	0.9500
C(5B)-C(6B)	1.386(15)
C(5B)-C(7B)	1.47(2)
C(6B)-C(14B)	1.48(3)
C(7A)-C(8A)	1.48(2)
C(7A)-H(7AA)	1.0000
C(8A)-C(9A)	1.47(2)
C(8A)-H(8AA)	1.0000
C(7B)-C(8B)	1.48(4)
C(7B)-H(7BA)	1.0000
C(8B)-C(9B)	1.51(3)
C(8B)-H(8BA)	1.0000
C(9A)-C(14A)	1.382(9)
C(9A)-C(10A)	1.382(9)
C(10A)-C(11A)	1.382(9)
C(10A)-H(10A)	0.9500
C(11A)-C(12A)	1.382(9)
C(12A)-C(13A)	1.382(9)
C(12A)-H(12A)	0.9500
C(13A)-C(14A)	1.382(9)
C(13A)-H(13A)	0.9500
C(9B)-C(10B)	1.380(12)

C(9B)-C(14B)	1.380(11)
C(10B)-C(11B)	1.380(11)
C(10B)-H(10B)	0.9500
C(11B)-C(12B)	1.380(12)
C(12B)-C(13B)	1.380(12)
C(12B)-H(12B)	0.9500
C(13B)-C(14B)	1.380(11)
C(13B)-H(13B)	0.9500
C(15)-C(16)	1.497(9)
C(15)-H(15A)	0.9900
C(15)-H(15B)	0.9900
C(16)-C(17)	1.511(9)
C(16)-H(16A)	0.9900
C(16)-H(16B)	0.9900
C(17)-C(18)	1.504(10)
C(17)-H(17A)	0.9900
C(17)-H(17B)	0.9900
C(18)-C(19)	1.510(10)
C(18)-H(18A)	0.9900
C(18)-H(18B)	0.9900
C(19)-C(20)	1.494(10)
C(19)-H(19A)	0.9900
C(19)-H(19B)	0.9900

C(20)-C(21)	1.499(11)
C(20)-H(20A)	0.9900
C(20)-H(20B)	0.9900
C(21)-C(22)	1.500(11)
C(21)-H(21A)	0.9900
C(21)-H(21B)	0.9900
C(22)-H(22A)	0.9800
C(22)-H(22B)	0.9800
C(22)-H(22C)	0.9800
C(23)-C(24)	1.469(10)
C(24)-C(25)	1.371(9)
C(24)-C(29)	1.380(9)
C(25)-C(26)	1.360(9)
C(25)-H(25A)	0.9500
C(26)-C(27)	1.385(9)
C(26)-H(26A)	0.9500
C(27)-C(28)	1.362(9)
C(28)-C(29)	1.381(9)
C(28)-H(28A)	0.9500
C(29)-H(29A)	0.9500
C(30)-C(31)	1.487(9)
C(30)-H(30A)	0.9900
C(30)-H(30B)	0.9900

C(31)-C(32)	1.503(9)
C(31)-H(31A)	0.9900
C(31)-H(31B)	0.9900
C(32)-C(33)	1.504(9)
C(32)-H(32A)	0.9900
C(32)-H(32B)	0.9900
C(33)-C(34)	1.514(9)
C(33)-H(33A)	0.9900
C(33)-H(33B)	0.9900
C(34)-C(35)	1.503(9)
C(34)-H(34A)	0.9900
C(34)-H(34B)	0.9900
C(35)-C(36)	1.510(9)
C(35)-H(35A)	0.9900
C(35)-H(35B)	0.9900
C(36)-C(37)	1.512(10)
C(36)-H(36A)	0.9900
C(36)-H(36B)	0.9900
C(37)-C(38)	1.515(10)
C(37)-H(37A)	0.9900
C(37)-H(37B)	0.9900
C(38)-C(39)	1.507(11)
C(38)-H(38A)	0.9900

C(38)-H(38B)	0.9900
C(39)-C(40)	1.513(12)
C(39)-H(39A)	0.9900
C(39)-H(39B)	0.9900
C(40)-H(40A)	0.9800
C(40)-H(40B)	0.9800
C(40)-H(40C)	0.9800
C(7A)-O(1A)-H(1AA)	109.5
C(8A)-O(2A)-H(2AA)	109.5
C(7B)-O(1B)-H(1BA)	109.5
C(3A)-O(3)-C(3B)	6.0(13)
C(3A)-O(3)-C(15)	118.5(8)
C(3B)-O(3)-C(15)	121.1(9)
C(23)-O(4)-C(11A)	124.1(7)
C(23)-O(4)-C(11B)	116.7(7)
C(11A)-O(4)-C(11B)	10.6(9)
C(27)-O(6)-C(30)	120.8(5)
C(6A)-C(1A)-C(2A)	120.0
C(6A)-C(1A)-H(1AB)	120.0
C(2A)-C(1A)-H(1AB)	120.0
C(3A)-C(2A)-C(1A)	120.0
C(3A)-C(2A)-H(2AB)	120.0

C(1A)-C(2A)-H(2AB)	120.0
O(3)-C(3A)-C(4A)	126.8(10)
O(3)-C(3A)-C(2A)	113.1(10)
C(4A)-C(3A)-C(2A)	120.0
C(5A)-C(4A)-C(3A)	120.0
C(5A)-C(4A)-H(4AA)	120.0
C(3A)-C(4A)-H(4AA)	120.0
C(4A)-C(5A)-C(6A)	120.0
C(4A)-C(5A)-C(7A)	120.8(9)
C(6A)-C(5A)-C(7A)	119.2(9)
C(1A)-C(6A)-C(5A)	120.0
C(1A)-C(6A)-C(14A)	122.4(10)
C(5A)-C(6A)-C(14A)	117.5(10)
C(2B)-C(1B)-C(6B)	120.0
C(2B)-C(1B)-H(1BB)	120.0
C(6B)-C(1B)-H(1BB)	120.0
C(1B)-C(2B)-C(3B)	120.0
C(1B)-C(2B)-H(2BB)	120.0
C(3B)-C(2B)-H(2BB)	120.0
C(4B)-C(3B)-C(2B)	120.0
C(4B)-C(3B)-O(3)	122.6(13)
C(2B)-C(3B)-O(3)	117.4(13)
C(5B)-C(4B)-C(3B)	120.0

C(5B)-C(4B)-H(4BA)	120.0
C(3B)-C(4B)-H(4BA)	120.0
C(6B)-C(5B)-C(4B)	120.0
C(6B)-C(5B)-C(7B)	117.5(12)
C(4B)-C(5B)-C(7B)	122.3(12)
C(5B)-C(6B)-C(1B)	120.0
C(5B)-C(6B)-C(14B)	121.1(13)
C(1B)-C(6B)-C(14B)	118.8(13)
O(1A)-C(7A)-C(5A)	109.1(11)
O(1A)-C(7A)-C(8A)	114.3(11)
C(5A)-C(7A)-C(8A)	110.6(12)
O(1A)-C(7A)-H(7AA)	107.5
C(5A)-C(7A)-H(7AA)	107.5
C(8A)-C(7A)-H(7AA)	107.5
O(2A)-C(8A)-C(9A)	111.2(15)
O(2A)-C(8A)-C(7A)	112.0(12)
C(9A)-C(8A)-C(7A)	109.9(13)
O(2A)-C(8A)-H(8AA)	107.9
C(9A)-C(8A)-H(8AA)	107.9
C(7A)-C(8A)-H(8AA)	107.9
O(1B)-C(7B)-C(5B)	112.1(14)
O(1B)-C(7B)-C(8B)	112.2(17)
C(5B)-C(7B)-C(8B)	111.3(15)

O(1B)-C(7B)-H(7BA)	106.9
C(5B)-C(7B)-H(7BA)	106.9
C(8B)-C(7B)-H(7BA)	106.9
C(7B)-C(8B)-C(9B)	113.6(18)
C(7B)-C(8B)-H(8BA)	107.8
C(9B)-C(8B)-H(8BA)	107.8
C(14A)-C(9A)-C(10A)	120.0
C(14A)-C(9A)-C(8A)	118.3(11)
C(10A)-C(9A)-C(8A)	121.7(11)
C(11A)-C(10A)-C(9A)	120.0
C(11A)-C(10A)-H(10A)	120.0
C(9A)-C(10A)-H(10A)	120.0
O(4)-C(11A)-C(12A)	113.0(8)
O(4)-C(11A)-C(10A)	127.0(8)
C(12A)-C(11A)-C(10A)	120.0
C(11A)-C(12A)-C(13A)	120.0
C(11A)-C(12A)-H(12A)	120.0
C(13A)-C(12A)-H(12A)	120.0
C(14A)-C(13A)-C(12A)	120.0
C(14A)-C(13A)-H(13A)	120.0
C(12A)-C(13A)-H(13A)	120.0
C(13A)-C(14A)-C(9A)	120.0
C(13A)-C(14A)-C(6A)	121.8(9)

C(9A)-C(14A)-C(6A)	118.2(9)
C(10B)-C(9B)-C(14B)	120.0
C(10B)-C(9B)-C(8B)	121.2(15)
C(14B)-C(9B)-C(8B)	118.8(15)
C(9B)-C(10B)-C(11B)	120.0
C(9B)-C(10B)-H(10B)	120.0
C(11B)-C(10B)-H(10B)	120.0
C(12B)-C(11B)-C(10B)	120.0
C(12B)-C(11B)-O(4)	118.2(10)
C(10B)-C(11B)-O(4)	121.1(10)
C(11B)-C(12B)-C(13B)	120.0
C(11B)-C(12B)-H(12B)	120.0
C(13B)-C(12B)-H(12B)	120.0
C(14B)-C(13B)-C(12B)	120.0
C(14B)-C(13B)-H(13B)	120.0
C(12B)-C(13B)-H(13B)	120.0
C(13B)-C(14B)-C(9B)	120.0
C(13B)-C(14B)-C(6B)	121.7(12)
C(9B)-C(14B)-C(6B)	117.9(12)
O(3)-C(15)-C(16)	107.8(6)
O(3)-C(15)-H(15A)	110.1
C(16)-C(15)-H(15A)	110.1
O(3)-C(15)-H(15B)	110.1

C(16)-C(15)-H(15B)	110.1
H(15A)-C(15)-H(15B)	108.5
C(15)-C(16)-C(17)	113.8(6)
C(15)-C(16)-H(16A)	108.8
C(17)-C(16)-H(16A)	108.8
C(15)-C(16)-H(16B)	108.8
C(17)-C(16)-H(16B)	108.8
H(16A)-C(16)-H(16B)	107.7
C(18)-C(17)-C(16)	112.6(6)
C(18)-C(17)-H(17A)	109.1
C(16)-C(17)-H(17A)	109.1
C(18)-C(17)-H(17B)	109.1
C(16)-C(17)-H(17B)	109.1
H(17A)-C(17)-H(17B)	107.8
C(17)-C(18)-C(19)	114.3(7)
C(17)-C(18)-H(18A)	108.7
C(19)-C(18)-H(18A)	108.7
C(17)-C(18)-H(18B)	108.7
C(19)-C(18)-H(18B)	108.7
H(18A)-C(18)-H(18B)	107.6
C(20)-C(19)-C(18)	114.5(7)
C(20)-C(19)-H(19A)	108.6
C(18)-C(19)-H(19A)	108.6

C(20)-C(19)-H(19B)	108.6
C(18)-C(19)-H(19B)	108.6
H(19A)-C(19)-H(19B)	107.6
C(19)-C(20)-C(21)	115.5(7)
C(19)-C(20)-H(20A)	108.4
C(21)-C(20)-H(20A)	108.4
C(19)-C(20)-H(20B)	108.4
C(21)-C(20)-H(20B)	108.4
H(20A)-C(20)-H(20B)	107.5
C(20)-C(21)-C(22)	114.5(8)
C(20)-C(21)-H(21A)	108.6
C(22)-C(21)-H(21A)	108.6
C(20)-C(21)-H(21B)	108.6
C(22)-C(21)-H(21B)	108.6
H(21A)-C(21)-H(21B)	107.6
C(21)-C(22)-H(22A)	109.5
C(21)-C(22)-H(22B)	109.5
H(22A)-C(22)-H(22B)	109.5
C(21)-C(22)-H(22C)	109.5
H(22A)-C(22)-H(22C)	109.5
H(22B)-C(22)-H(22C)	109.5
O(5)-C(23)-O(4)	122.6(7)
O(5)-C(23)-C(24)	127.2(7)

O(4)-C(23)-C(24)	110.1(6)
C(25)-C(24)-C(29)	118.8(7)
C(25)-C(24)-C(23)	122.0(6)
C(29)-C(24)-C(23)	119.1(6)
C(26)-C(25)-C(24)	120.5(7)
C(26)-C(25)-H(25A)	119.8
C(24)-C(25)-H(25A)	119.8
C(25)-C(26)-C(27)	120.8(7)
C(25)-C(26)-H(26A)	119.6
C(27)-C(26)-H(26A)	119.6
O(6)-C(27)-C(28)	125.3(6)
O(6)-C(27)-C(26)	115.4(6)
C(28)-C(27)-C(26)	119.3(7)
C(27)-C(28)-C(29)	119.8(7)
C(27)-C(28)-H(28A)	120.1
C(29)-C(28)-H(28A)	120.1
C(24)-C(29)-C(28)	120.8(7)
C(24)-C(29)-H(29A)	119.6
C(28)-C(29)-H(29A)	119.6
O(6)-C(30)-C(31)	106.4(6)
O(6)-C(30)-H(30A)	110.4
C(31)-C(30)-H(30A)	110.4
O(6)-C(30)-H(30B)	110.4

C(31)-C(30)-H(30B)	110.4
H(30A)-C(30)-H(30B)	108.6
C(30)-C(31)-C(32)	114.7(6)
C(30)-C(31)-H(31A)	108.6
C(32)-C(31)-H(31A)	108.6
C(30)-C(31)-H(31B)	108.6
C(32)-C(31)-H(31B)	108.6
H(31A)-C(31)-H(31B)	107.6
C(31)-C(32)-C(33)	112.4(6)
C(31)-C(32)-H(32A)	109.1
C(33)-C(32)-H(32A)	109.1
C(31)-C(32)-H(32B)	109.1
C(33)-C(32)-H(32B)	109.1
H(32A)-C(32)-H(32B)	107.9
C(32)-C(33)-C(34)	115.4(6)
C(32)-C(33)-H(33A)	108.4
C(34)-C(33)-H(33A)	108.4
C(32)-C(33)-H(33B)	108.4
C(34)-C(33)-H(33B)	108.4
H(33A)-C(33)-H(33B)	107.5
C(35)-C(34)-C(33)	114.3(6)
C(35)-C(34)-H(34A)	108.7
C(33)-C(34)-H(34A)	108.7

C(35)-C(34)-H(34B)	108.7
C(33)-C(34)-H(34B)	108.7
H(34A)-C(34)-H(34B)	107.6
C(34)-C(35)-C(36)	114.4(6)
C(34)-C(35)-H(35A)	108.7
C(36)-C(35)-H(35A)	108.7
C(34)-C(35)-H(35B)	108.7
C(36)-C(35)-H(35B)	108.7
H(35A)-C(35)-H(35B)	107.6
C(35)-C(36)-C(37)	113.7(6)
C(35)-C(36)-H(36A)	108.8
C(37)-C(36)-H(36A)	108.8
C(35)-C(36)-H(36B)	108.8
C(37)-C(36)-H(36B)	108.8
H(36A)-C(36)-H(36B)	107.7
C(36)-C(37)-C(38)	112.8(7)
C(36)-C(37)-H(37A)	109.0
C(38)-C(37)-H(37A)	109.0
C(36)-C(37)-H(37B)	109.0
C(38)-C(37)-H(37B)	109.0
H(37A)-C(37)-H(37B)	107.8
C(39)-C(38)-C(37)	113.9(7)
C(39)-C(38)-H(38A)	108.8

C(37)-C(38)-H(38A)	108.8
C(39)-C(38)-H(38B)	108.8
C(37)-C(38)-H(38B)	108.8
H(38A)-C(38)-H(38B)	107.7
C(38)-C(39)-C(40)	114.4(8)
C(38)-C(39)-H(39A)	108.7
C(40)-C(39)-H(39A)	108.7
C(38)-C(39)-H(39B)	108.7
C(40)-C(39)-H(39B)	108.7
H(39A)-C(39)-H(39B)	107.6
C(39)-C(40)-H(40A)	109.5
C(39)-C(40)-H(40B)	109.5
H(40A)-C(40)-H(40B)	109.5
C(39)-C(40)-H(40C)	109.5
H(40A)-C(40)-H(40C)	109.5
H(40B)-C(40)-H(40C)	109.5

Symmetry transformations used to generate equivalent atoms:

Table 4. Anisotropic displacement parameters ($\text{\AA}^2 \times 10^3$) for vs21. The anisotropic displacement factor exponent takes the form: $-2 \left[h^2 a^{*2} U^{11} + \dots + 2 h k a^* b^* U^{12} \right]$

	U11	U22	U33	U23	U13	U12
O(1A)	76(3)	18(2)	54(3)	-1(2)	1(2)	1(2)
O(2A)	76(3)	18(2)	54(3)	-1(2)	1(2)	1(2)
O(1B)	76(3)	18(2)	54(3)	-1(2)	1(2)	1(2)
O(2B)	76(3)	18(2)	54(3)	-1(2)	1(2)	1(2)
O(3)	68(3)	32(3)	48(3)	2(2)	11(3)	-2(2)
O(4)	62(3)	36(3)	56(3)	11(2)	10(3)	6(2)
O(5)	78(4)	31(3)	55(3)	6(2)	8(3)	11(3)
O(6)	61(3)	30(3)	56(3)	0(2)	5(3)	-3(2)
C(1A)	59(2)	23(2)	40(2)	2(1)	-2(2)	0(2)
C(2A)	59(2)	23(2)	40(2)	2(1)	-2(2)	0(2)
C(3A)	59(2)	23(2)	40(2)	2(1)	-2(2)	0(2)
C(4A)	59(2)	23(2)	40(2)	2(1)	-2(2)	0(2)
C(5A)	59(2)	23(2)	40(2)	2(1)	-2(2)	0(2)
C(6A)	59(2)	23(2)	40(2)	2(1)	-2(2)	0(2)
C(1B)	59(2)	23(2)	40(2)	2(1)	-2(2)	0(2)
C(2B)	59(2)	23(2)	40(2)	2(1)	-2(2)	0(2)
C(3B)	59(2)	23(2)	40(2)	2(1)	-2(2)	0(2)

C(4B)	59(2)	23(2)	40(2)	2(1)	-2(2)	0(2)
C(5B)	59(2)	23(2)	40(2)	2(1)	-2(2)	0(2)
C(6B)	59(2)	23(2)	40(2)	2(1)	-2(2)	0(2)
C(7A)	62(8)	17(4)	53(8)	-3(4)	5(5)	-6(4)
C(8A)	62(8)	17(4)	53(8)	-3(4)	5(5)	-6(4)
C(7B)	62(8)	17(4)	53(8)	-3(4)	5(5)	-6(4)
C(8B)	62(8)	17(4)	53(8)	-3(4)	5(5)	-6(4)
C(9A)	56(2)	24(2)	42(2)	2(2)	-2(2)	0(2)
C(10A)	56(2)	24(2)	42(2)	2(2)	-2(2)	0(2)
C(11A)	56(2)	24(2)	42(2)	2(2)	-2(2)	0(2)
C(12A)	56(2)	24(2)	42(2)	2(2)	-2(2)	0(2)
C(13A)	56(2)	24(2)	42(2)	2(2)	-2(2)	0(2)
C(14A)	56(2)	24(2)	42(2)	2(2)	-2(2)	0(2)
C(9B)	56(2)	24(2)	42(2)	2(2)	-2(2)	0(2)
C(10B)	56(2)	24(2)	42(2)	2(2)	-2(2)	0(2)
C(11B)	56(2)	24(2)	42(2)	2(2)	-2(2)	0(2)
C(12B)	56(2)	24(2)	42(2)	2(2)	-2(2)	0(2)
C(13B)	56(2)	24(2)	42(2)	2(2)	-2(2)	0(2)
C(14B)	56(2)	24(2)	42(2)	2(2)	-2(2)	0(2)
C(15)	66(5)	43(4)	41(5)	0(4)	5(4)	2(4)
C(16)	57(5)	41(4)	43(5)	2(4)	0(4)	-1(4)
C(17)	63(5)	46(5)	54(5)	3(4)	6(4)	1(4)
C(18)	69(6)	51(5)	42(5)	4(4)	1(4)	1(4)

C(19)	61(5)	64(5)	50(5)	0(4)	3(4)	3(4)
C(20)	64(6)	65(5)	50(5)	5(4)	-1(4)	-1(4)
C(21)	67(6)	78(6)	75(7)	6(5)	5(5)	11(5)
C(22)	87(7)	98(8)	93(8)	-5(6)	29(6)	-1(6)
C(23)	64(5)	25(4)	41(5)	-1(3)	-11(4)	-5(4)
C(24)	50(4)	23(4)	42(4)	-12(3)	-4(4)	-6(3)
C(25)	58(5)	31(4)	33(4)	3(3)	-4(4)	-4(3)
C(26)	55(5)	25(4)	53(5)	-3(3)	-4(4)	-3(3)
C(27)	50(5)	27(4)	39(4)	-7(3)	-2(4)	-10(3)
C(28)	62(5)	24(4)	40(4)	0(3)	-4(4)	-2(3)
C(29)	59(5)	22(4)	47(5)	-4(3)	0(4)	-2(3)
C(30)	60(5)	32(4)	47(5)	-3(3)	-6(4)	-5(4)
C(31)	50(5)	34(4)	54(5)	-5(4)	-1(4)	-6(3)
C(32)	58(5)	37(4)	37(4)	-1(3)	-5(4)	-6(3)
C(33)	58(5)	32(4)	44(4)	-1(3)	-3(4)	-5(3)
C(34)	61(5)	40(4)	37(4)	-3(3)	-6(4)	-3(4)
C(35)	57(5)	48(4)	36(4)	4(4)	-7(4)	1(4)
C(36)	65(5)	51(5)	43(5)	3(4)	-4(4)	-5(4)
C(37)	58(5)	58(5)	56(5)	4(4)	-2(4)	3(4)
C(38)	68(6)	69(6)	57(5)	-7(5)	5(5)	-4(5)
C(39)	66(6)	81(7)	77(7)	2(5)	9(5)	13(5)
C(40)	85(7)	95(8)	106(9)	-15(7)	30(7)	-6(6)

Table 5. Hydrogen coordinates ($\times 10^4$) and isotropic displacement parameters ($\text{\AA}^2 \times 10^3$) for vs21.

	x	y	z	U(eq)
H(1AA)	-991	2165	11008	74
H(2AA)	-679	2547	6580	74
H(1BA)	-1063	2206	10306	74
H(2BA)	-739	2464	6561	74
H(1AB)	-1157	-89	5096	49
H(2AB)	-1761	-304	7542	49
H(4AA)	-1599	1140	11328	49
H(1BB)	-1075	-104	5361	49
H(2BB)	-1660	-369	7887	49
H(4BA)	-1751	1210	10486	49
H(7AA)	-629	1434	10087	53
H(8AA)	-1014	1840	5540	53

H(7BA)	-1257	1835	6139	53
H(8BA)	-494	1611	9134	53
H(10A)	-4	1880	4089	49
H(12A)	161	286	1871	49
H(13A)	-471	29	4008	49
H(10B)	85	1801	4667	49
H(12B)	-44	398	522	49
H(13B)	-690	180	2601	49
H(15A)	-2414	890	11974	60
H(15B)	-2041	695	13995	60
H(16A)	-2464	-77	15081	57
H(16B)	-2825	71	12933	57
H(17A)	-2656	739	17302	65
H(17B)	-3019	883	15157	65
H(18A)	-3045	-59	18411	65
H(18B)	-3396	44	16161	65
H(19A)	-3292	745	20467	70
H(19B)	-3636	864	18198	70
H(20A)	-3676	-78	21404	72
H(20B)	-4026	61	19193	72
H(21A)	-4240	866	21426	88
H(21B)	-3905	696	23670	88
H(22A)	-4620	441	24676	138

H(22B)	-4325	-108	24414	138
H(22C)	-4662	68	22182	138
H(25A)	1138	797	-242	49
H(26A)	1748	680	-2692	53
H(28A)	1506	2149	-6100	50
H(29A)	885	2261	-3653	51
H(30A)	2304	2000	-7163	56
H(30B)	1943	1751	-9136	56
H(31A)	2414	1034	-10188	55
H(31B)	2764	1219	-8039	55
H(32A)	2928	2027	-10296	53
H(32B)	2563	1867	-12412	53
H(33A)	2969	1094	-13587	54
H(33B)	3318	1197	-11331	54
H(34A)	3210	1921	-15556	55
H(34B)	3566	2010	-13319	55
H(35A)	3573	1107	-16788	56
H(35B)	3925	1182	-14519	56
H(36A)	4191	2000	-16405	63
H(36B)	3836	1932	-18665	63
H(37A)	4186	1110	-19971	69
H(37B)	4536	1161	-17670	69
H(38A)	4463	1942	-21722	78

H(38B)	4811	1996	-19418	78
H(39A)	4815	1129	-23082	89
H(39B)	5157	1165	-20741	89
H(40A)	5487	1488	-24416	142
H(40B)	5460	1984	-22412	142
H(40C)	5114	1957	-24742	142

Table 6. Torsion angles [$^{\circ}$] for vs21.

C(6A)-C(1A)-C(2A)-C(3A)	0.0
C(3B)-O(3)-C(3A)-C(4A)	123(13)
C(15)-O(3)-C(3A)-C(4A)	5.7(13)
C(3B)-O(3)-C(3A)-C(2A)	-59(12)
C(15)-O(3)-C(3A)-C(2A)	-175.7(6)
C(1A)-C(2A)-C(3A)-O(3)	-178.7(10)
C(1A)-C(2A)-C(3A)-C(4A)	0.0
O(3)-C(3A)-C(4A)-C(5A)	178.5(11)
C(2A)-C(3A)-C(4A)-C(5A)	0.0
C(3A)-C(4A)-C(5A)-C(6A)	0.0
C(3A)-C(4A)-C(5A)-C(7A)	-178.5(11)
C(2A)-C(1A)-C(6A)-C(5A)	0.0
C(2A)-C(1A)-C(6A)-C(14A)	177.1(10)
C(4A)-C(5A)-C(6A)-C(1A)	0.0
C(7A)-C(5A)-C(6A)-C(1A)	178.5(11)

C(4A)-C(5A)-C(6A)-C(14A)	-177.2(9)
C(7A)-C(5A)-C(6A)-C(14A)	1.2(12)
C(6B)-C(1B)-C(2B)-C(3B)	0.0
C(1B)-C(2B)-C(3B)-C(4B)	0.0
C(1B)-C(2B)-C(3B)-O(3)	-176.8(13)
C(3A)-O(3)-C(3B)-C(4B)	-71(12)
C(15)-O(3)-C(3B)-C(4B)	-4.5(16)
C(3A)-O(3)-C(3B)-C(2B)	106(12)
C(15)-O(3)-C(3B)-C(2B)	172.2(8)
C(2B)-C(3B)-C(4B)-C(5B)	0.0
O(3)-C(3B)-C(4B)-C(5B)	176.7(14)
C(3B)-C(4B)-C(5B)-C(6B)	0.0
C(3B)-C(4B)-C(5B)-C(7B)	174.9(16)
C(4B)-C(5B)-C(6B)-C(1B)	0.0
C(7B)-C(5B)-C(6B)-C(1B)	-175.1(15)
C(4B)-C(5B)-C(6B)-C(14B)	-178.0(13)
C(7B)-C(5B)-C(6B)-C(14B)	6.9(17)
C(2B)-C(1B)-C(6B)-C(5B)	0.0
C(2B)-C(1B)-C(6B)-C(14B)	178.1(13)
C(4A)-C(5A)-C(7A)-O(1A)	-17.5(14)
C(6A)-C(5A)-C(7A)-O(1A)	164.0(8)
C(4A)-C(5A)-C(7A)-C(8A)	-144.1(12)
C(6A)-C(5A)-C(7A)-C(8A)	37.5(15)

O(1A)-C(7A)-C(8A)-O(2A)	54.1(19)
C(5A)-C(7A)-C(8A)-O(2A)	177.7(11)
O(1A)-C(7A)-C(8A)-C(9A)	178.2(12)
C(5A)-C(7A)-C(8A)-C(9A)	-58.2(18)
C(6B)-C(5B)-C(7B)-O(1B)	-167.0(12)
C(4B)-C(5B)-C(7B)-O(1B)	18(2)
C(6B)-C(5B)-C(7B)-C(8B)	-40(2)
C(4B)-C(5B)-C(7B)-C(8B)	144.6(15)
O(1B)-C(7B)-C(8B)-C(9B)	176.2(14)
C(5B)-C(7B)-C(8B)-C(9B)	50(2)
O(2A)-C(8A)-C(9A)-C(14A)	166.9(9)
C(7A)-C(8A)-C(9A)-C(14A)	42.4(16)
O(2A)-C(8A)-C(9A)-C(10A)	-16.0(15)
C(7A)-C(8A)-C(9A)-C(10A)	-140.5(11)
C(14A)-C(9A)-C(10A)-C(11A)	0.0
C(8A)-C(9A)-C(10A)-C(11A)	-177.0(13)
C(23)-O(4)-C(11A)-C(12A)	134.9(7)
C(11B)-O(4)-C(11A)-C(12A)	87(6)
C(23)-O(4)-C(11A)-C(10A)	-43.5(10)
C(11B)-O(4)-C(11A)-C(10A)	-92(6)
C(9A)-C(10A)-C(11A)-O(4)	178.3(9)
C(9A)-C(10A)-C(11A)-C(12A)	0.0
O(4)-C(11A)-C(12A)-C(13A)	-178.6(8)

C(10A)-C(11A)-C(12A)-C(13A)	0.0
C(11A)-C(12A)-C(13A)-C(14A)	0.0
C(12A)-C(13A)-C(14A)-C(9A)	0.0
C(12A)-C(13A)-C(14A)-C(6A)	-179.0(9)
C(10A)-C(9A)-C(14A)-C(13A)	0.0
C(8A)-C(9A)-C(14A)-C(13A)	177.1(12)
C(10A)-C(9A)-C(14A)-C(6A)	179.0(9)
C(8A)-C(9A)-C(14A)-C(6A)	-3.8(12)
C(1A)-C(6A)-C(14A)-C(13A)	-17.5(11)
C(5A)-C(6A)-C(14A)-C(13A)	159.7(7)
C(1A)-C(6A)-C(14A)-C(9A)	163.5(8)
C(5A)-C(6A)-C(14A)-C(9A)	-19.4(11)
C(7B)-C(8B)-C(9B)-C(10B)	152.6(14)
C(7B)-C(8B)-C(9B)-C(14B)	-27(2)
C(14B)-C(9B)-C(10B)-C(11B)	0.0
C(8B)-C(9B)-C(10B)-C(11B)	-179.3(16)
C(9B)-C(10B)-C(11B)-C(12B)	0.0
C(9B)-C(10B)-C(11B)-O(4)	-169.8(11)
C(23)-O(4)-C(11B)-C(12B)	115.2(9)
C(11A)-O(4)-C(11B)-C(12B)	-108(6)
C(23)-O(4)-C(11B)-C(10B)	-74.8(9)
C(11A)-O(4)-C(11B)-C(10B)	62(6)
C(10B)-C(11B)-C(12B)-C(13B)	0.0

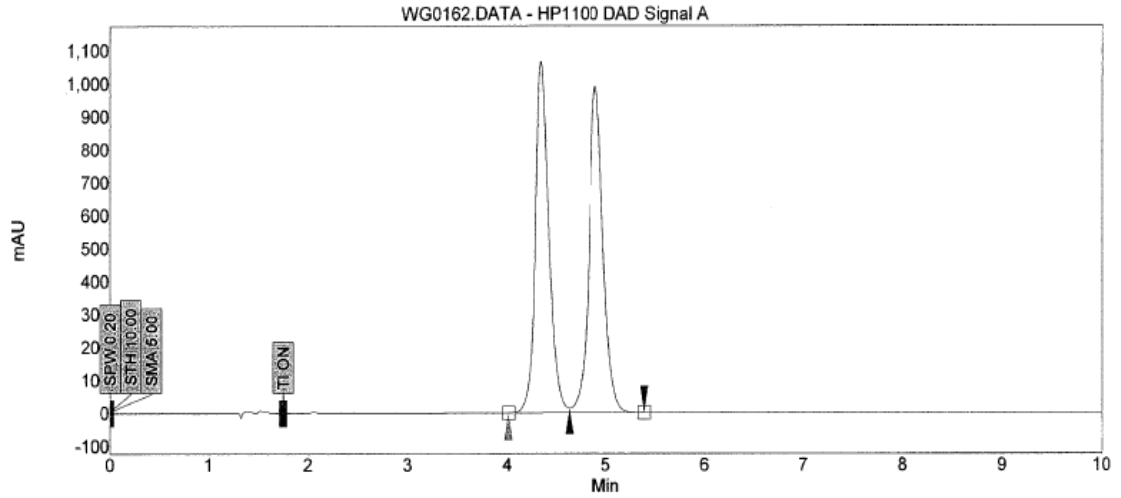
O(4)-C(11B)-C(12B)-C(13B)	170.1(10)
C(11B)-C(12B)-C(13B)-C(14B)	0.0
C(12B)-C(13B)-C(14B)-C(9B)	0.0
C(12B)-C(13B)-C(14B)-C(6B)	-173.2(12)
C(10B)-C(9B)-C(14B)-C(13B)	0.0
C(8B)-C(9B)-C(14B)-C(13B)	179.3(16)
C(10B)-C(9B)-C(14B)-C(6B)	173.5(11)
C(8B)-C(9B)-C(14B)-C(6B)	-7.2(15)
C(5B)-C(6B)-C(14B)-C(13B)	-168.4(9)
C(1B)-C(6B)-C(14B)-C(13B)	13.6(15)
C(5B)-C(6B)-C(14B)-C(9B)	18.3(15)
C(1B)-C(6B)-C(14B)-C(9B)	-159.8(10)
C(3A)-O(3)-C(15)-C(16)	-172.8(8)
C(3B)-O(3)-C(15)-C(16)	-179.0(10)
O(3)-C(15)-C(16)-C(17)	-175.1(6)
C(15)-C(16)-C(17)-C(18)	-179.6(7)
C(16)-C(17)-C(18)-C(19)	-175.8(7)
C(17)-C(18)-C(19)-C(20)	178.4(7)
C(18)-C(19)-C(20)-C(21)	177.8(7)
C(19)-C(20)-C(21)-C(22)	176.8(8)
C(11A)-O(4)-C(23)-O(5)	10.9(11)
C(11B)-O(4)-C(23)-O(5)	19.8(12)
C(11A)-O(4)-C(23)-C(24)	-171.3(7)

C(11B)-O(4)-C(23)-C(24)	-162.5(8)
O(5)-C(23)-C(24)-C(25)	-178.5(7)
O(4)-C(23)-C(24)-C(25)	3.9(9)
O(5)-C(23)-C(24)-C(29)	-2.4(11)
O(4)-C(23)-C(24)-C(29)	-180.0(6)
C(29)-C(24)-C(25)-C(26)	0.8(10)
C(23)-C(24)-C(25)-C(26)	177.0(6)
C(24)-C(25)-C(26)-C(27)	-1.0(10)
C(30)-O(6)-C(27)-C(28)	0.4(10)
C(30)-O(6)-C(27)-C(26)	-179.6(6)
C(25)-C(26)-C(27)-O(6)	-178.5(6)
C(25)-C(26)-C(27)-C(28)	1.5(10)
O(6)-C(27)-C(28)-C(29)	178.1(6)
C(26)-C(27)-C(28)-C(29)	-1.9(10)
C(25)-C(24)-C(29)-C(28)	-1.2(10)
C(23)-C(24)-C(29)-C(28)	-177.5(6)
C(27)-C(28)-C(29)-C(24)	1.8(10)
C(27)-O(6)-C(30)-C(31)	-172.8(6)
O(6)-C(30)-C(31)-C(32)	-173.5(6)
C(30)-C(31)-C(32)-C(33)	-177.2(6)
C(31)-C(32)-C(33)-C(34)	-174.2(6)
C(32)-C(33)-C(34)-C(35)	-178.5(6)
C(33)-C(34)-C(35)-C(36)	-178.6(6)

C(34)-C(35)-C(36)-C(37)	-179.3(6)
C(35)-C(36)-C(37)-C(38)	-178.2(7)
C(36)-C(37)-C(38)-C(39)	179.7(7)
C(37)-C(38)-C(39)-C(40)	-178.1(8)

Symmetry transformations used to generate equivalent atoms:

Appendix 2. Resolution analysis data for 2.36



Index	Name	Start Time [Min]	Time [Min]	End [Min]	RT Offset [Min]	Quantity [% Area]	Height [μV]	Area [μV.Min]	Area [%]
1	UNKNOWN	4.01	4.33	4.63	0.00	49.81	1066.1	168.0	49.815
2	UNKNOWN	4.63	4.89	5.39	0.00	50.19	989.5	169.3	50.185
Total						100.00	2055.7	337.3	100.000

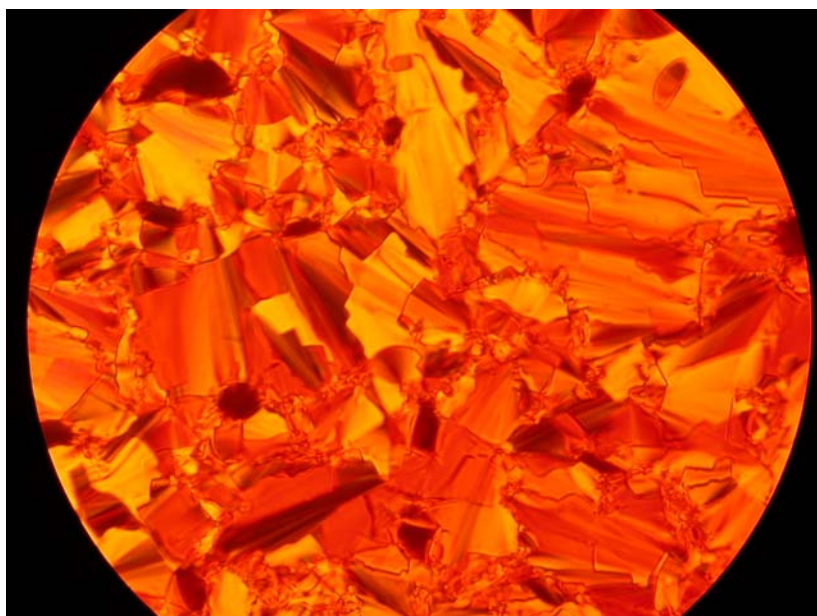
Method: AD-H20%MeOH

Appendix 3 The Texture of Compounds 3.30a-e in Polarized Microscopy

2.30a SmC phase



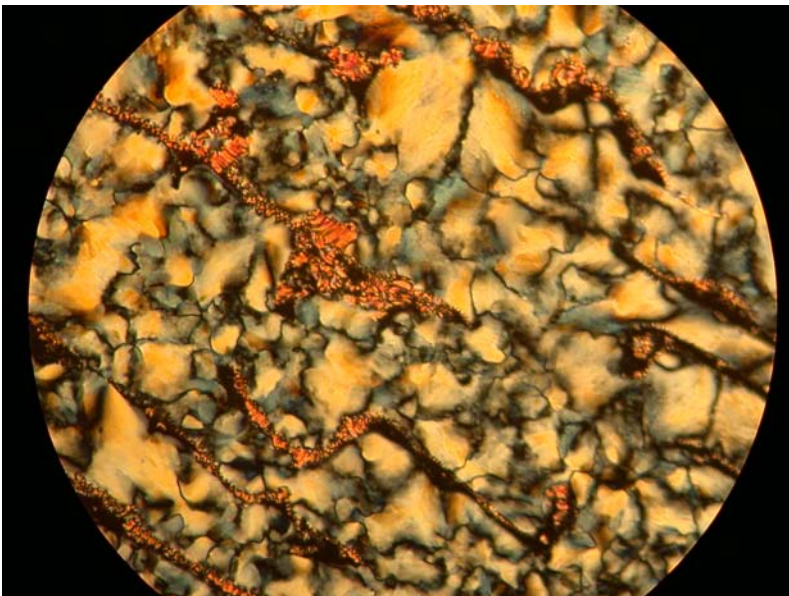
2.30b SmC phase



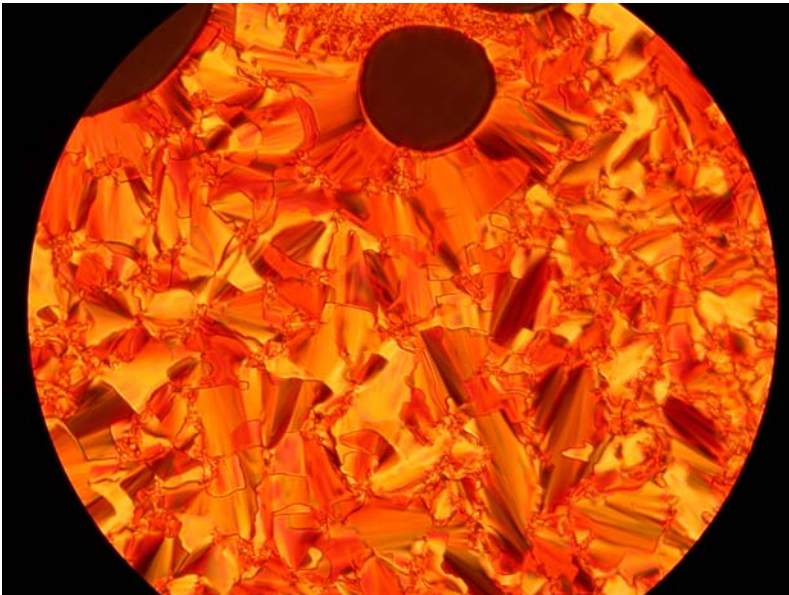
2.30c SmC phase



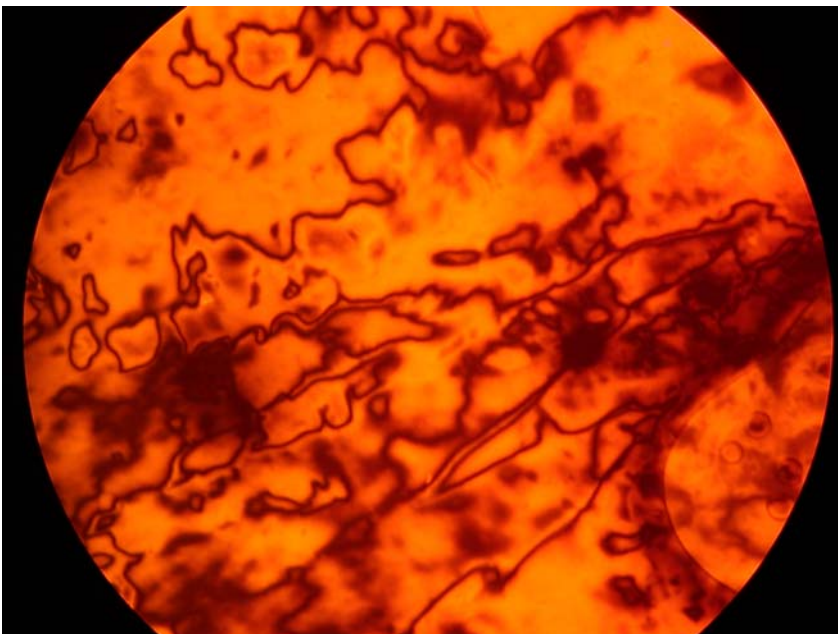
2.30d N phase



2.30d SmC phase



2.30e N phase



2.30e SmC phase

